

## ABSTRACT

CLARK IV, JOE BOAZ. The Synthesis and Characterization of Ester-Bearing Polycarbodiimides. (Under the direction of Bruce M. Novak.)

Over the last decade and a half, research in the Novak Group has focused predominantly on a class of helical macromolecules known as polycarbodiimides. As a group, our earliest works focused on the living polymerization of carbodiimides with both early- and late-transition metal catalysts. The extensive studies that followed probed the cooperativity of the helix with various pendant, catalytic, or ionically-associated chiral entities. Investigations into the optical properties of these materials identified liquid crystalline behavior, as well as an optical switching phenomenon, in association with certain architectural features. The vast majority of the polycarbodiimides that have been synthesized and studied to date bore simple aliphatic or aromatic pendant groups. Though they have proven highly stable under both acidic and basic conditions, and relatively stable at elevated temperatures, few efforts have been made to develop structures capable of utilizing these properties for subsequent pendant group modifications. The efforts described herein recount the ordeal of synthesizing a new subclass of polycarbodiimides, bearing ester pendant groups, and chronicle what the reactivity of these novel structures has taught us about the fundamental properties of the polycarbodiimide structure. The ester-bearing carbodiimides polymerized in the following studies fall into two divisions, those that bear an enolizable proton, and those that do not. The ones bearing an enolizable proton are derived from L-alanine, while the others were made from p-

aminobenzoic acid. While carbodiimides of the latter division can be polymerized with titanium (IV) catalysts, those of the former are polymerized most cleanly by heating alone. Though copper (I) butanethiolate rapidly accelerates such thermally-driven polymerizations, it also catalyzes the formation of small molecules, predominantly dimers, thus creating a trade-off of small molecule contaminants in exchange for a workable polymerization rate and a measure of molecular weight control afforded by the monomer-to-initiator ratio. Through trial and error, a procedure for removing such small molecule contaminants was developed to isolate these ester-bearing polycarbodiimides in high molecular weight. Stability studies find ester-bearing polycarbodiimides are categorically unstable under strongly basic conditions. While polycarbodiimides derived from L-alanine prove unstable with respect to strong acids too, those derived from p-aminobenzoic acid can be tailored for robustness under acidic conditions, though such structures also prove resistant to pendant group modification. Ester-bearing polycarbodiimides prove to be relatively unstable with respect to elevated temperatures. Through studies of various structural derivatives, the source of instability with respect to acids, bases, and elevated temperatures was identified to be the electron-withdrawing effect of the ester pendant group, thus revealing, for the first time, that polycarbodiimides are not inherently stable structures, that their stability is directly correlated to predictable electronic influences.

The Synthesis and Characterization of  
Ester-Bearing Polycarbodiimides

by  
Joe B. Clark IV

A dissertation submitted to the Graduate Faculty of  
North Carolina State University  
in partial fulfillment of the  
requirements for the degree of  
Doctor of Philosophy

Chemistry

Raleigh, North Carolina

2010

APPROVED BY:

---

Lin He

---

Marian G. McCord

---

Tatyana I. Smirnova

---

Bruce M. Novak  
Chair of Advisory Committee

## **DEDICATION**

This book is dedicated to my parents, Joe B. Clark III and Joan W. Clark, who have provided unwavering support in my academic studies, to my two mentors, Dr. Robert Morrison and Dr. Robert Bereman, each of whom inspired me to strive for higher academic achievement and provided sage advice to this end, to my academic advisor, Dr. Novak, who afforded me with this incredible learning experience, to my brother, Thomas Clark, who has enriched my soul with his music, and to my fiancée Erin, who made the last three years of graduate school the best in life. Thank you all for your support. I am humbled by your selfless contributions to my life and honored to know each of you.

## BIOGRAPHY

The author first matriculated at North Carolina State University in 1994, completing a B.S. Degree in Chemistry in 1999. Over the next four years, he worked as a chemist in a variety of industrial settings, first as a GC/MS Chemist for CompuChem in Cary, NC; then as a Quality Assurance Chemist at B.O.C. Gases in RTP; and finally as an Associate Scientist at Vector Research in Durham, NC. While working in industry, he began taking graduate level chemistry classes part time. In 2004, he matriculated as a full time graduate student at N.C. State University with the intention of merely earning a Master's Degree. After developing an affinity for teaching, and then research, he decided to pursue a PhD instead. The document that follows is the culmination of those efforts. In his time in graduate school at N.C. State, he made an effort to develop beyond the mere academic requirements for the doctorate by participating in a variety of leadership development opportunities. Within the Chemistry Department, he served as the Vice President of the Phi Lambda Upsilon. He also served as the Departmental Representative in the University Graduate Student Association for two years. Within the University Graduate Student Association, he serves as the Chairman of the Social Committee for one year and as the Vice President of Internal Affairs for a year and a half. Finally, in his last two and a half years at N.C. State, he served on the Student Conduct Board. Upon graduation, he will continue his love of learning through the pursuit of a Pharm.D. at the University of Wisconsin School of Pharmacy.

## ACKNOWLEDGEMENTS

First, I'd like to thank Jan Singhass, who employed her glassblowing skills to turn the vacuum manifold I had initially abused into the high vacuum system on which I relied so heavily in my research. I would like to thank her for her kindness and for teaching me the essentials of vacuum manifold maintenance. I'd like to thank Dr. S. Sankar, who trained me extensively on the NMR and mentored me in the writing of our department's first Varian NMR User's Manual. I'd like to thank former Novak Group members Keitaro Seto and Hyun-Su Lee for taking the time to mentor me on laboratory techniques. I'd like to thank Justin Kennemur for collaborating with me on our (his) first publication. I'd like to thank Januka Budhathoki-Uprety for the positive attitude she has brought to the group. I'd also like to thank other members of the Novak Group, past and present, who, each in their own unique way, have taught me invaluable lessons about the importance of courtesy when sharing a work environment, of professionalism in attitude and behavior, and of considering how what we say of others affects their reputation as well as our own. I'd like to thank my teaching mentors, Dr. Sandberg, Dr. Brown, Dr. Gallardo-Williams, and Dr. Warren, who have each taught me valuable lessons on the instruction of chemistry students. I'd like to thank my academic committee members, Dr. He, Dr. Smirnova, and Dr. McCord. I am honored by their service. Finally, I'd like to thank my advisor Dr. Novak, who has funded my research and has patiently mentored with me for many years, not only to make me a better teacher and researcher, but also to guide the development of my character and perseverance.

## TABLE OF CONTENTS

LIST OF TABLES.....	ix
LIST OF FIGURES .....	x
CHAPTER 1: THE HISTORY OF POLYCARBODIIMIDES	
1.1. Introduction .....	1
1.2. Early Studies on Carbodiimide Polymerization.....	4
1.3. Living Polymerization of Carbodiimides.....	6
1.4. Thermal Decomposition of Polycarbodiimides .....	10
1.5. Polycarbodiimide Microstructure: The Role of Regiochemistry .....	13
1.6. Polycarbodiimide Macrostructure: From Worms to Rigid Rods .....	16
1.7. Concepts of Cooperativity .....	17
1.7.1. The Kinetics and Thermodynamics of Homochiral Polycarbodiimide Helicity .....	20
1.7.2. Too Many Chiefs, Not Enough Indians: An Optimum Sergeant/Soldier Ratio .....	22
1.7.3. The Helix-Directing Authority of the Chiral Majority.....	23
1.7.4. Protons and Polycarbodiimides: The Chaperoning of Orderly Affairs .....	26
1.7.5. Gods of Helicity: The Search for an Omnipotent Chiral Center .....	31
1.8. Optical Switching with a Helical Polycarbodiimide Nanoshutter .....	35
1.9. Liquid Crystalline Properties of Polycarbodiimides.....	37
1.10. References.....	40

## CHAPTER 2: POLYMERIZATION OF NOVEL ESTER-BEARING CARBODIIMIDES

2.1.	Introduction .....	44
2.2.	Syntheses of Novel Ester-Bearing Carbodiimides.....	45
2.2.1.	Standard Dehydration of 1,3-Disubstituted Ureas .....	45
2.2.2.	Standard Desulfurization of 1,3-Disubstituted Thioureas.....	47
2.2.3.	Alternative Strategies for Carbodiimide Synthesis .....	48
2.3.	Polymerization of Novel Ester-Bearing Carbodiimides.....	51
2.3.1.	Studies with Traditional Polymerization Catalysts .....	51
2.3.2.	Thermally-Induced Carbodiimide Polymerization .....	58
2.3.3.	Thiolate-Initiated, Thermal Polymerizations .....	60
2.4.	The Dilemma of Dimers and Troublesome Trimers .....	64
2.4.1.	Raising the Roof: What's Going Down Above $T_C$ . .....	64
2.4.2.	Fractional Precipitation and Extraction: The Disposal of Disorderly Dimers.....	69
2.5.	Conclusions .....	71
2.6.	Experimental Section .....	72
2.6.1.	General Procedures and Equipment .....	72
2.6.2.	Experimental Procedures and Characterizations .....	74
2.7	References.....	91

## CHAPTER 3: THE STABILITY AND REACTIVITY OF ESTER-BEARING

### POLYCARBODIIMIDES

3.1.	Introduction .....	94
3.2.	Base-Catalyzed Hydrolysis of a New Ester-Bearing Polycarbodiimide ....	95
3.3.	Transesterification Studies on a New Ester-Bearing Polycarbodiimide....	97
	3.3.1. News Flash: Novel Polycarbodiimide Sour on PTSA! .....	98
	3.3.2. Transesterification Studies Under Mild Conditions .....	98
3.4.	Follow-Up Studies on an Old Ester-Bearing Polycarbodiimide.....	101
3.5.	Regioselectivity Study on Carbodiimide Polymerization Catalysts .....	106
3.6.	Descendants of an Old Ester-Bearing Polycarbodiimide .....	109
3.7.	Polycarbodiimide Regiochemistry: Microstructural Determination via <sup>13</sup> C NMR .....	113
3.8.	Conclusions .....	119
3.9.	Experimental Section .....	121
	3.9.1. General Procedures and Equipment .....	121
	3.9.2. Experimental Procedures and Characterizations .....	123
3.10.	References.....	148
	APPENDICES.....	149
	Appendix 1: Filter Paper-Covered, Vacuum-Needle Assembly Instructions .....	150
	Appendix 2: Guide to Vacuum Manifold Maintenance .....	159
	Appendix 3: Creating an Improvised Holding Device for Molecular Sieves.....	181
	Appendix 4: Varian NMR User's Manual.....	185

Section 1: Essential Operations for Basic 1D Spectra .....	186
Section 2: Optional Operations for Basic 1D Spectra Enhancement .....	190
Section 3: Glide Program Operations for Advanced 1D & 2D Spectra.....	192
Section 4: Manual Setup Operations for Advanced 1D Experiments .....	196
Section 5: Operations for Collecting Spectra at Variable Temperatures .....	200
Table 1: Freezing & Boiling Point of Deuterated Solvents.....	203
Table 2: Commands for Access to Standard Solvent Parameters .....	204
Table 3: Comprehensive Reference Chart of Solvent Chemical Shifts .....	205
List of Useful Varian NMR Software Commands .....	206

## LIST OF TABLES

Table 1.1. Optical rotation data of poly(N,N'-di-n-hexylcarbodiimides) prepared with chiral initiators, measured in chloroform at the sodium-D line, 598 nm .....	3
---	---

## LIST OF FIGURES

- Figure 1.1. Examples of polymers containing carbodiimide units: Polyhexamethylenecarbodi-imide was obtained by the stepwise decarboxylation of 1,6-di-isocyanate hexane with 3-methyl-1-phenyl-3-phospholene 1-oxide catalyst in N-methyl-2-pyrrolidone solvent. Crosslinked polystyrene, presenting 2.4 mmol pendant carbodiimide per gram, was obtained from chloromethylated crosslinked polystyrene via Gabriel Synthesis, followed by reaction with isopropylisocyanate, and subsequent dehydration with p-toluenesulfonyl chloride and triethylamine in refluxing methylene chloride.....2
- Figure 1.2. 1-Dimensional representation of atom connectivity within the polymer obtained via polymerization of a carbodiimide.....3
- Figure 1.3. Ball-and-stick model of the 3-dimensional helical arrangement of carbon and nitrogen atoms within the polycarbodiimide backbone, colored black and blue respectively, and substituents, colored gray.. .....3
- Figure 1.4. Titanium catalysts first found to initiate the living polymerization of carbodiimides. ....7
- Figure 1.5. Copper (I) and Copper (II) catalysts incorporating amidinate initiating groups as coordinating ligands.....8
- Figure 1.6. Illustration of initiation, propagation, and termination steps of carbodiimide polymerization with a titanium alkoxide complex. These

living polymerizations are typically terminated by precipitating a hydrocarbon solution of the polymer in methanol, though exchangeable protons from any source terminate propagation in an analogous manner .....	9
Figure 1.7. Thermally-induced, free radical depolymerization mechanism .....	11
Figure 1.8. Structure of the dicarbodiimides 1,4-di(N'-methylcarbodiimido)butane and 1,4-di(N'-methylcarbodiimido)hexane utilized for the crosslinking of poly(N,N'-di-n-hexylcarbodiimide).....	12
Figure 1.9. Two regiochemistries of an asymmetrically-substituted repeat unit...	13
Figure 1.10. Illustration of depolymerization product(s) resulting from scissions across original monomer units for regiospecific versus non-regiospecific microstructures (irregularly-inserted monomer shown in red). The alternative, scissions between the original monomer units, would return the original monomer exclusively in either case.....	14
Figure 1.11. Pyramid of Cooperativity. The hierarchy of the pyramid illustrates the lengths to which a given polymer system cooperates with the predominant chiral entity by adopting a preferred helical sense. The pinnacle of cooperativity is the induction of a single-handed helix by a single chiral entity, either by a chiral catalyst exercising its influence on the active site during polymerization or through perturbation from a chiral endgroup at the chain's terminus .....	18

- Figure 1.12. The schematic on top depicts the stereoisomeric relationships among right- and left-handed helices of polymers bearing chiral pendant groups. The schematic beneath illustrates the energy difference between the diastereomeric interactions of the right- and left-handed helical conformations with a given chiral entity ..... 19
- Figure 1.13. The respective exo- and endo-resonance forms of the amidinium ion, resulting from protonation of the polycarbodiimide backbone..... 27
- Figure 1.14. Pendant groups on adjacent imine nitrogens may orient in either a trans-cis or trans-trans arrangement. In theory, protonation of the backbone would facilitate transformations into trans-trans orientations through the free rotation of pendant entities in the endo-resonance form of the amidinium ion, inadvertently lowering the activation energy of the helical inversion process ..... 28
- Figure 1.15. Normalized specific rotation in chloroform of poly(N,N'-di-n-hexylcarbodiimide) as a function of champhorsulfonic acid concentration ((R) = hollow boxes, (S) = solid dots)..... 30
- Figure 1.16. Titanium (IV) catalysts with chiral amide initiators, shown in color, utilized to polymerize N,N'-di-n-hexylcarbodiimide for chiral end group studies ..... 32
- Figure 1.17. The (R-BINOL)Ti(O-*i*Pr)<sub>2</sub> catalyst. When polymerizing the achiral N-hexyl-N'-phenylcarbodiimide, this catalyst preferentially induces a right-handed (P) helix as assigned by comparing the spectrum observed via

vibrational circular dichroism (VCD) with the one simulated by theoretical modeling calculations. Curiously, replacing the isopropoxides with tert-butoxides reverses the helical selectivity, dictating preferential induction of the left-handed (M) helix instead .....34

Figure 1.18. Two states resulting from shutter-like motions of 1-naphthyl substituents .....35

Figure 1.19. Anisotropic changes in the aromatic region among variable temperature <sup>1</sup>H NMR spectra of poly(N-(1-naphthyl)-N'-octadecylcarbodiimide) in THF-d<sub>8</sub>. The most noteworthy trend with increasing temperature is the disappearance of the signals for two protons from the region of broad overlap centered at 7.0 ppm corresponding with their re-emergence upfield at approximately 6.5 ppm .....36

Figure 1.20. Schematic representations of four prominent liquid crystalline phases. A common feature shared by all liquid crystal phases is an orderly orientation of the molecules. The distinguishing feature of phases that are nematic is a lack of positional order. When the mesogens in a nematic phase are chiral, they adopt a twisted orientation with respect to one another, creating what is referred to as a chiral nematic or cholesteric phase. Smectic phases are characterized by the restricted layering of molecules. In the smectic A phase, the orientation of the

	molecules is perpendicular to the layering. In the smectic C phase, the molecules are tilted relative to the layering.....	35
Figure 1.21.	Schematic representation of (A) the smectic phase of poly(N,N'-di-n-hexylcarbodiimide) versus (B) the nematic phase of poly(n-hexyl isocyanate).....	39
Figure 2.1.	The two polycarbodiimides bearing an ester pendant group synthesized by Jeonghan Kim. Each of these structures was synthesized via living polymerization with a titanium catalyst. A noteworthy feature, later proven essential for the utilization of titanium catalysts, is the lack of enolizable protons.....	44
Figure 2.2.	Illustration of four methyl ester-bearing carbodiimide structures derived by reacting L-alanine methyl ester hydrochloride with various aliphatic or aromatic isocyanates in pyridine solvent and dehydrating the resulting 1,3-disubstituted ureas with triphenylphosphine dibromide in methylene chloride and triethylamine .....	46
Figure 2.3.	Synthesis of an L-alanine methyl ester-bearing carbodiimide via desulfurization of a 1,3-disubstituted thiourea generated in situ. Mercuric oxide, the classical metal oxide utilized for this method, is coupled with the dehydrating reagent magnesium sulfate, used to remove the H <sub>2</sub> O byproduct. HgS is also generated and can be easily removed by filtering through diatomaceous earth.....	47

- Figure 2.4. The reaction of N,N'-di-t-butylthiourea with DCC leads to N,N'-di-t-butyl carbodiimide and N,N','-dicyclohexylthiourea. Curiously, the reaction of DCC with N,N'-dimethylthiourea under the same conditions is reported to produce dimethyl cyanamide,  $\text{Me}_2\text{NC}\equiv\text{N}$ , instead ..... 49
- Figure 2.5. Phosphorus pentachloride is a highly reactive reagent. In this experiment, not only did it generate the chloroformamidine hydrochloride intermediate, which reacted with base to form the carbodiimide, it also chlorinated the benzylic position of the 4-methylphenyl substituent ..... 50
- Figure 2.6.  $^1\text{H}$  NMR spectrum of the product resulting from carbodiimide **III** reacted with  $\text{CpTiCl}_2\text{OCH}_2\text{CF}_3$ . The profile indicates high molecular weight materials, characterized by broad signals, mixed with a comparable quantity of low molecular weight materials, characterized by sharp signals ..... 54
- Figure 2.7. The polymerization of N,N'-bis(4-n-butylphenyl)carbodiimide fails at room temperature due to the heightened activation energy resulting from the steric hindrance of the bulky pendant groups and ligand, respectively, on the carbodiimide and catalyst. Gentle heating provides sufficient energy to facilitate polymerization ..... 55
- Figure 2.8.  $^1\text{H}$  NMR spectrum of the product resulting from carbodiimide **III** reacted with  $\text{CuCl}_2$  for 1 month at  $60\text{ }^\circ\text{C}$ . The profile indicates primarily high

molecular weight material, as evidenced by the predominance of broad, versus sharp, signals.....57

Figure 2.9.  $^1\text{H}$  NMR spectrum of the thermal polymerization product resulting from heating carbodiimide **III** at 60 °C for 4 weeks in the absence of catalyst. When compared with the spectrum of the polycarbodiimide formed under the same conditions in the presence of  $\text{CuCl}_2$ , Figure 2.8, this spectrum has fewer and less intense sharp signals, suggesting that thermal polymerization in the absence of  $\text{CuCl}_2$  proceeds more cleanly, and that rather than facilitating polymerization,  $\text{CuCl}_2$  actually catalyzes the formation of small molecules, such as dimers and trimers .....59

Figure 2.10.  $^1\text{H}$  NMR spectrum of the product resulting from heating carbodiimide **III** with copper (I) butanethiolate. Though the spectrum consists predominately of broad, polymer signals, the intensity of sharp signals indicates greater contamination from small molecules than when the polymer is formed upon heating in the absence of catalyst, Figure 2.9. It seems that greater diversion of carbodiimide, down byproduct pathways leading to dimers and trimers, is an unavoidable cost of utilizing copper (I) butanethiolate to accelerate these heated polymerization reactions.....63

Figure 2.11. Four of the many conceivable stereoisomers that may be formed from the dimerization of N-phenyl-N'-(L-alanine methyl ester)carbodiimide. Others could have one phenyl substituent in an imine position while the

other occupies an amine position. The pair at the top are referred to as E,E-isomers, while the pair beneath are referred to as Z,Z-isomers. Theoretical considerations are said to favor the formation of Z,Z-isomers.....67

Figure 2.12. Extracted Ion Chromatograph of the 409 m/z ratio, corresponding to twice the mass of N-phenyl-N'-(L-alanine methyl ester)carbodiimide. The Total Ion Chromatograph indicates the dimer eluted at 15.2 min as the predominant small molecule.....68

Figure 2.13. Extracted Ion Chromatograph of the 613 m/z ratio, corresponding to three times the mass of N-phenyl-N'-(L-alanine methyl ester)carbodiimide. The profile of the plot indicates at least seven trimeric stereoisomers, two predominant, four trace.....68

Figure 2.14. <sup>1</sup>H NMR spectrum of a clean polymer isolated by precipitation of a single heavy fraction, followed by washing away a single light fraction. The relative absence of sharp signals in this spectrum, compared with the spectrum of the unclean polymer, Figure 2.10, showcases the success of precipitating and extracting fractions in sequence to remove small molecule contaminants .....70

Figure 3.1. The quantitative conversion of poly-III to a urea structure is the first case in which a polycarbodiimide has been observed to hydrolyze under basic conditions.....95

- Figure 3.2.  $^1\text{H}$  NMR spectra before and after base-catalyzed hydrolysis of poly(N-phenyl-N'-(L-alanine methyl ester)carbodiimide). Both the pendant methyl ester and the polymer backbone are hydrolyzed under strongly basic conditions..... 96
- Figure 3.3.  $^1\text{H}$  NMR spectra of poly-III before and after 1 week of reaction with 2-methoxyethanol in the presence of p-toluenesulfonic acid (2.1 equivalents / repeat) in chloroform solvent. The most prominent change in the spectra is the replacement of broad proton signals with sharp signals, consistent with decomposition of the polymer into smaller molecules. Increasing the reaction temperature greatly accelerates the decomposition process..... 99
- Figure 3.4. Expanded view of the region of interest on the  $^1\text{H}$  NMR spectra of a relatively light fraction of poly-III, before and after transesterification with 2-methoxyethanol, catalyzed by mercury (II) acetate. The notable absence of a signal for the hydroxyl proton of the free alcohol, highlighted in red, from the spectrum of the transesterified polymer, indicates that the additional proton signals are from newly-placed, 2-methoxyethyl substituents on the pendant group. The relative broadness of the aforementioned signals is also consistent with polymer attachment ..... 100
- Figure 3.5. Outline of the multi-step synthetic route to the ester-bearing polycarbodiimide first developed by Jeonghan Kim. The initial step,

synthesis of t-butyl p-aminobenzoate, was first reported by Taylor, Fletcher, and Sabb. The original polymer synthesized by Kim was made with an achiral titanium catalyst,  $\text{CpTiCl}_2\text{N}(\text{CH}_3)_2$ , rather than the chiral (S)-Binol titanium catalyst utilized for the follow-up studied of this work.....102

Figure 3.6.  $^1\text{H}$  NMR spectra of poly-VI before and after sonicating in a simple 4:1 mixture of acetone and deionized water for 1 week. The replacement of broad proton signals with sharp signals indicates decomposition of the polymer into smaller molecules. In contrast to poly-VI's instability, poly(N-benzyl-N'-(4-n-butylphenyl)carbodiimide) does not decompose under analogous conditions..... 103

Figure 3.7.  $^1\text{H}$  NMR spectra of poly-VI before and after stirring or sonicating in a 4:1 mixture of acetone and 2.5 wt% aqueous sodium hydroxide for 1 week. Both stirring and sonicating in the presence of aqueous base lead to hydrolysis of the polymer backbone, as evidenced by the replacement of broad polymer signals with sharp small molecule signals. When compared with the ratio of broad-to-sharp signals in Spectrum B of Figure 3.6, the relatively lower intensity of broad signals in the bottom spectrum here indicates that sonicating in the presence of sodium hydroxide significantly accelerates the breakdown of the polymer..... 104

- Figure 3.8.  $^1\text{H}$  NMR spectra of poly-VI before and after stirring or sonicating in a 4:1 mixture of acetone and 2.0 wt% aqueous p-toluenesulfonic acid. When compared with the ratio of broad-to-sharp signals in the Figure 3.7 spectra, it is clear from the relatively lower intensity of broad signals here that the polymer backbone hydrolyzes more rapidly under acidic conditions than under basic conditions. Hydrolysis occurs most rapidly with sonication under acidic conditions, leading to more complete dissolution of the insoluble polymer in 12 hours than within 1 week of simply stirring ..... 105
- Figure 3.9. Aliphatic region of poly(N-hexyl-N'-phenylcarbodiimide) made with copper versus chiral titanium catalyst. The sharper carbon signals of the latter are a consequence of both its higher regioselectivity and its more singular helicity..... 107
- Figure 3.10. Expanded view of the signals for the alpha methylene carbons. Notice that the minor regiochemistry, having the hexyl substituent in the imine position, is significantly more prevalent from the copper-catalyzed polymerization ..... 108
- Figure 3.11. Four new derivatives of the old ester-bearing carbodiimide design by Jeonghan Kim. Monomer VIII and IX were made by dehydrating the corresponding urea precursor, while VII and X were made from the corresponding thiourea..... 110

- Figure 3.12. Hybrid design crossing Kim's ester-bearing polycarbodiimide – which is unstable under conditions that are strongly acidic or basic and even decomposes upon mere sonication – with a structure proven to be robust even when sonicated under strongly acidic or basic conditions for 1 week.....112
- Figure 3.13. Infrared spectrum of poly-X. The only observable imine absorption is at  $1635\text{ cm}^{-1}$ , suggesting the aromatic pendant group occupies the imine position. The infrared spectrum does not provide any indication of the alternative regiochemistry, thus allowing observers to speculate that the structure is regioregular.....115
- Figure 3.14.  $^{13}\text{C}$  NMR spectra of poly-X before and after applying 30 Hz (0.40 ppm) of line broadening to the data. Notice the latter provides much greater detail, such as the signal of the carbonyl carbon at 166 ppm and that of the quaternary t-butyl carbon, just downfield of the solvent signal, at 80.9 ppm. ....117
- Figure 3.15. Highlighted and expanded views of the benzylic methylene carbon signals. Even with merely 5 Hz of line broadening, a signal clearly stands out from the noise. Further application of line broadening reveals two, slightly overlapping signals corresponding to each anticipated regiochemistry.....118

## Chapter 1: The History of Polycarbodiimides

### 1.1. Introduction

Carbodiimides are an important class of compounds having the structure  $R-N=C=N-R'$ . The substituents R and R' are commonly carbon-attached structures, typically aliphatic or aromatic hydrocarbon substituents. But there are a variety of other atoms through which the carbodiimide functional group may be substituted. Silicon<sup>1,2</sup>, nitrogen<sup>3,4</sup>, phosphorus<sup>5,6</sup>, and sulfur<sup>7,8</sup> substituted carbodiimides constitute diverse architectural subclasses. There are also a variety of salts, loosely referred to as metal-substituted carbodiimides<sup>9</sup>, having  $[NCN]^{2-}$  anions paired with cations ranging from alkali<sup>10,11</sup>, alkali earth<sup>12</sup>, and transition<sup>13,14</sup> metals to a variety of rare earth elements.<sup>15</sup>

The reactivity of carbodiimides bearing inorganic substituents differs fundamentally from that of organically-substituted carbodiimides. The latter have proven exceedingly useful in organic synthesis, while the former are of increasing interest as ceramic material precursors.<sup>9</sup> For instance, bis-trimethylsilylcarbodiimide is used to obtain silicon carbonitride films by RF plasma-enhanced chemical vapor deposition.<sup>16</sup>

Perhaps the most prominent application of a carbodiimide in organic chemistry is the Merrifield Method – the standard for automated peptide synthesis – which utilizes dicyclohexylcarbodiimide to promote amide bond formation by activating the carbonyl group for condensation with an amine.<sup>17</sup> Having such an ability to facilitate the formation of amide bonds between molecules, without

becoming a part of the bonds themselves, carbodiimides are referred to as ‘zero-link’ crosslinking agents.<sup>18</sup>

The utility of carbodiimides as dehydrating agents in the Merrifield Method and others, such as the “Reverse Merrifield”<sup>19</sup>, led to the development of polymers containing carbodiimide units as solid-phase dehydrating agents, Figure 1.1. One such polymer is polyhexamethylenecarbodi-imide, which incorporates the carbodiimide unit as a part of the polymer backbone.<sup>20</sup> Another polymer developed for these applications places the carbodiimide unit as a pendant group, rather than as part of the polymer backbone.<sup>21</sup> Though these materials consist of repeat units that are not derived from the polymerization of a carbodiimide monomer, and are thus not polycarbodiimides in this customary sense, the fact that they contain ‘many’ carbodiimides has led to their description as “polycarbodiimides.”

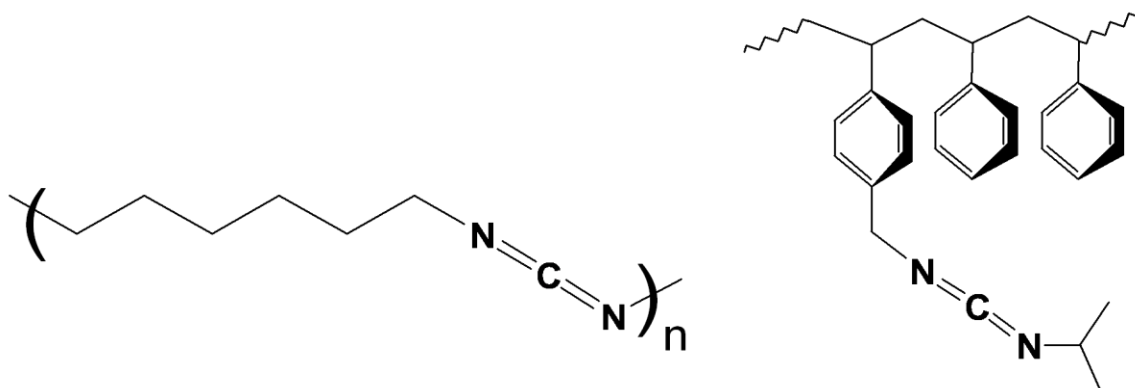


Figure 1.1: Examples of polymers containing carbodiimide units: Polyhexamethylenecarbodi-imide was obtained by the stepwise decarboxylation of 1,6-di-isocyanate hexane with 3-methyl-1-phenyl-3-phospholene 1-oxide catalyst in N-methyl-2-pyrrolidone solvent. Crosslinked polystyrene, presenting 2.4 mmol pendant carbodiimide per gram, was obtained from chloromethylated crosslinked polystyrene via Gabriel Synthesis, followed by reaction with isopropylisocyanate, and subsequent dehydration with p-toluenesulfonyl chloride and triethylamine in refluxing methylene chloride.

On the other hand, authentic polycarbodiimides, i.e. those obtained via polymerization of carbodiimides, are often referred to as polyguanidines. Glancing at a 1-dimensional representation, Figure 1.2, the structure might appear to showcase repeating guanidine units, but the dihedral angle between one amidine unit and the next is approximately  $60^\circ$ , breaking the planarity that is a defining feature of the guanidine unit.

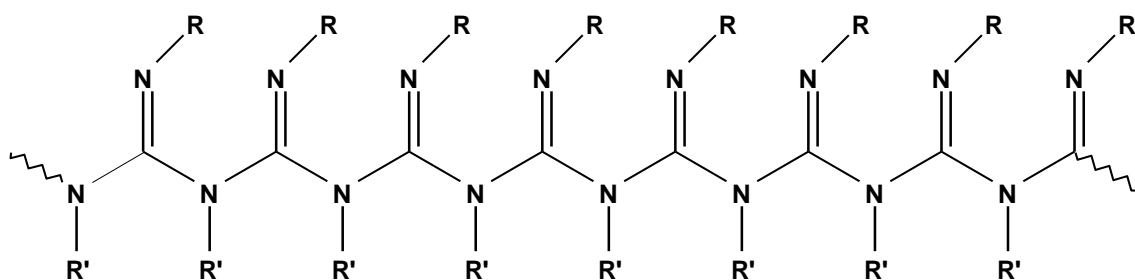


Figure 1.2: 1-Dimensional representation of atom connectivity within the polymer obtained via polymerization of a carbodiimide.

The result is a polymer that adopts a 6/1 helix, Figure 1.3, in the solid state as suggested by molecular modeling and confirmed by X-ray scattering studies.<sup>22</sup>

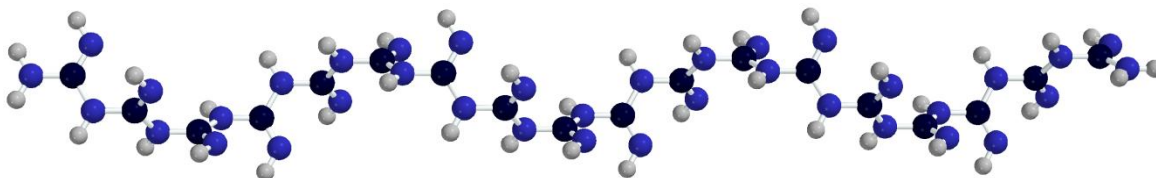


Figure 1.3: Ball-and-stick model of the 3-dimensional helical arrangement of carbon and nitrogen atoms within the polycarbodiimide backbone, colored black and blue respectively, and substituents, colored gray.

The persistence of the helical conformation in solution, suggested by viscosity and light scattering data,<sup>22</sup> led to chiro-optic experiments probing the cooperativity of polycarbodiimides with various chiral entities towards induction of right- or left-handed biases between helical conformations.<sup>23</sup> These studies culminated in the helix-sense selective polymerization of achiral carbodiimides with chiral catalysts,<sup>24</sup> while also leading to publications on polycarbodiimides displaying liquid crystalline properties<sup>25,26</sup> and a chiroptical switching phenomenon.<sup>27-29</sup>

Unpublished works that have been the subject of dissertation research within the Novak Group include the exploration of polycarbodiimide absorption properties at solution-solid interfaces;<sup>30</sup> efforts to develop photoswitchable chiral pendant groups;<sup>31</sup> preparation of polycarbodiimide-coated nanoparticles ;<sup>32</sup> development of cross-linked, cholesteric, polycarbodiimide gels;<sup>33</sup> and the synthesis and characterization of water soluble polycarbodiimides.<sup>34</sup> The focus of this dissertation is the synthesis and characterization of polycarbodiimides presenting ester-bearing pendant groups.

## 1.2. Early Studies on Carbodiimide Polymerization

The first publication on the polymerization of carbodiimides was authored by G.C. Robinson in 1964.<sup>35</sup> Upon testing several anionic and cationic initiators under a variety of conditions, the only combination that proved even a qualified success was n-butyllithium in hydrocarbon solvents, reported to yield low molecular weight polymer regardless of the solvent, temperature, or monomer-to-initiator ratio.

Conditions that failed to facilitate polymerization include sodium dispersion in dimethylformamide at -20 or -40 °C, anhydrous aluminum bromide in toluene at 25 °C, methyl iodide in xylene at 25 °C, and p-bromobenzenesulfonyl chloride in toluene at 25 °C. Monomers successfully polymerized by n-butyllithium in hydrocarbon solvent include diethylcarbodiimide, di-n-butylcarbodiimide, di-n-hexylcarbodiimide, diphenylcarbodiimide, and diallylcarbodiimide. While methylisopropylcarbodiimide, having one secondary alkyl substituent, also proved capable of anionic polymerization, monomers of greater steric hindrance, such as methyl-t-butylcarbodiimide, dicyclohexylcarbodiimide, and diisopropylcarbodiimide, were not.

Robinson also investigated the autopolymerization of diethylcarbodiimide in the absence of catalyst, identifying an optimal temperature range. Autopolymerization was reportedly slow at 25 °C. 100 °C proved sub-optimal, converting approximately 1% of diethylcarbodiimide to polymer in 8 hours. Heating at 115 to 125 °C converted 50% of the carbodiimide to polymer in 30 hours, while heating at 150 °C resulted in less complete polymerization, likely a consequence of convergence on the ceiling temperature of poly(N,N'-diethylcarbodiimide).

### 1.3. Living Polymerization of Carbodiimides

Living polymerization is most simply defined as a polymerization reaction lacking chain-terminating or chain-transferring side reactions.<sup>36</sup> Practically speaking, side reactions that terminate chains prematurely, and those that transfer reactivity to other species – such as monomers, solvent molecules, or previously terminated chains – lead to polymers of lower molecular weight and higher chain-length variability.

Polymerizations of a living nature promote the synthesis of higher molecular weight materials through an exclusive reaction in which all of the monomer is consumed through growth of the originally-initiated polymer chains. The absence of chain-terminating or chain-transferring reactions significantly reduces chain-length variability, while also facilitating the synthesis of polymers having a targeted molecular weight, pre-determined by the ratio of monomer to initiator.

The first publication on the living polymerization of carbodiimides was authored by Andrew Goodwin and Bruce Novak in 1994.<sup>37</sup> Building on earlier success with the living polymerization of isocyanates,<sup>38</sup> which are isoelectronic with carbodiimides, they found that covalent titanium amide and alkoxide complexes, Figure 1.4, promoted living polymerization of carbodiimides having a variety of aliphatic and aromatic substituents.

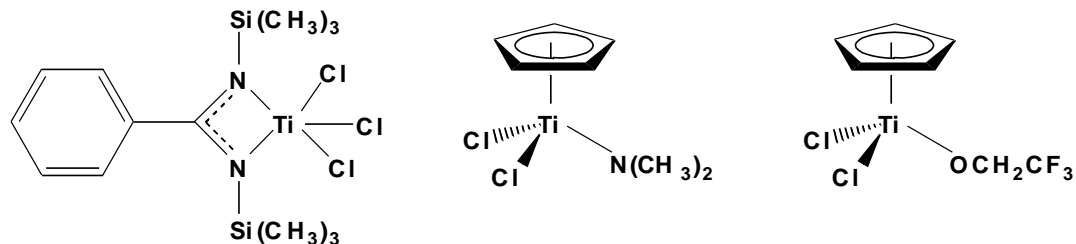


Figure 1.4: Titanium catalysts first found to initiate the living polymerization of carbodiimides.

Among carbodiimides bearing aliphatic substituents, the degree of substitution at the site of attachment proved essential in determining whether, and at what rate, polymerization occurs. Carbodiimides bearing two primary substituents polymerize rapidly, while those bearing one each of a primary and a secondary substituent do so at a relatively sluggish rate. A carbodiimide having one each of a methyl and tertiary substituent, as well as those bearing two secondary substituents, proved incapable of polymerization with titanium catalysts.

Solvents that proved suitable for these polymerizations included aromatic hydrocarbons (benzene and toluene), halogenated hydrocarbons (chloroform), aliphatic hydrocarbons (hexanes), ethers (THF and diethyl ether), and pyridine. The only appreciable difference among polymerization rates in these solvents was observed with the strongly-coordinating pyridine, for which the rate of polymerization is reported to be substantially slower.<sup>39</sup>

The salient drawback of these titanium complexes is their high degree of sensitivity to atmospheric impurities, namely oxygen and water. The search for a

more robust alternative led to the discovery that simple copper salts (CuCl and CuCl<sub>2</sub>) also initiate living polymerizations of carbodiimides, culminating in the design of the air- and moisture-tolerant copper (I) and copper (II) amidinate complexes shown in Figure 1.5.<sup>40</sup> Furthermore, these copper complexes proved capable of polymerizing carbodiimides in enolizable solvents – such as acetone and ethyl acetate – that were problematic for the more reactive titanium initiators.

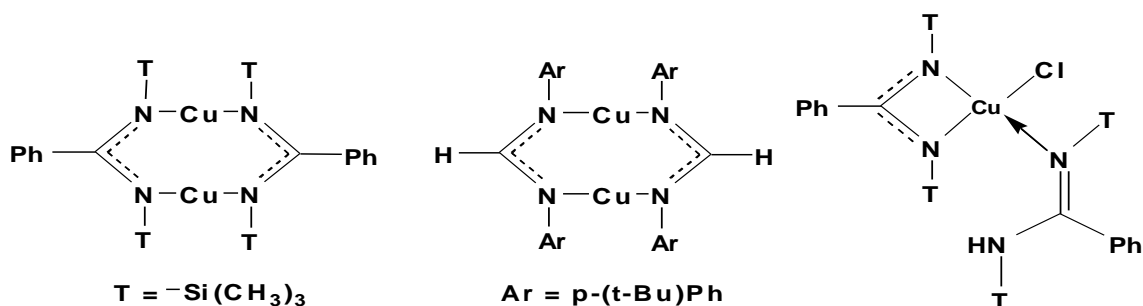
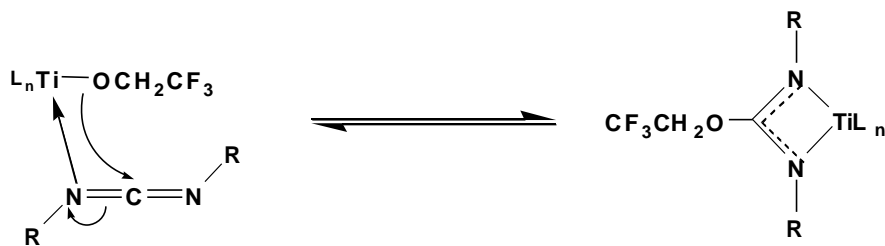


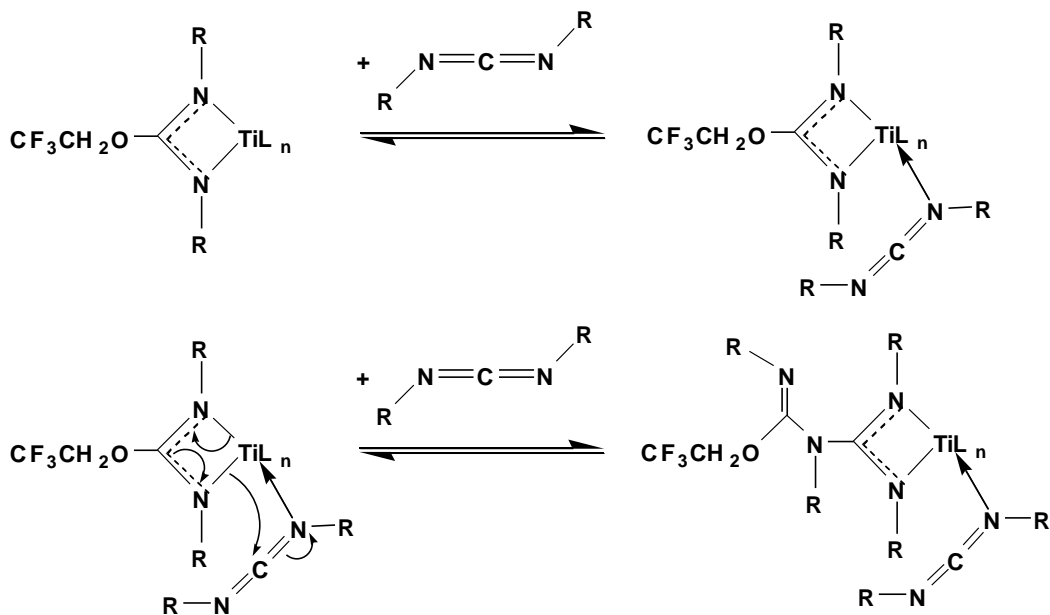
Figure 1.5: Copper (I) and Copper (II) catalysts incorporating amidinate initiating groups as coordinating ligands.

As with the aforementioned titanium (IV) complexes, these copper (I) and copper (II) catalysts initiate polymerization through insertion of the carbodiimide into the bond between the metal and the initiating group, forming an intermediate amidinate complex through which subsequent carbodiimide insertions propagate chain growth. The analogous process for a titanium (IV) alkoxide complex is illustrated in Figure 1.6. In each case, the first carbodiimide insertion transfers the initiating group from the metal to the electrophilic carbodiimide carbon where it terminates the inactive end of the subsequently-propagated chain.

### Initiation



### Propagation



### Termination

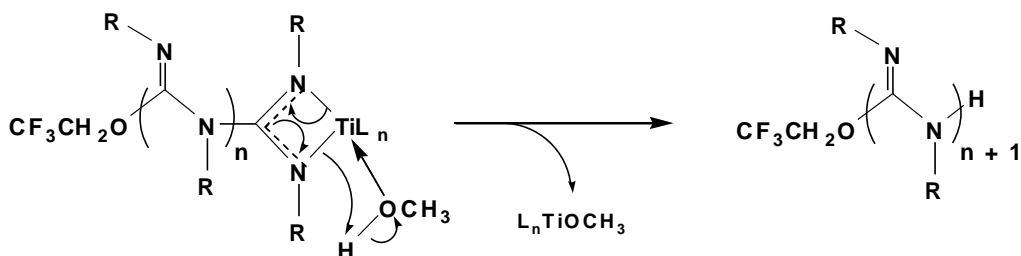


Figure 1.6: Illustration of initiation, propagation, and termination steps of carbodiimide polymerization with a titanium alkoxide complex. These living polymerizations are typically terminated by precipitating a hydrocarbon solution of the polymer in methanol, though exchangeable protons from any source terminate propagation in an analogous manner.

#### 1.4. Thermal Decomposition of Polycarbodiimides

The thermally-induced decomposition of polycarbodiimides was first studied by Robinson, who noted that it appeared to be an unzipping process given that no fragments, other than monomer, were detected in the pyrolyzate.<sup>35</sup> Subsequent research by Goodwin found that mixing a polycarbodiimide with a radical initiator, 2,2'-azobisisobutyronitrile (AIBN), facilitated the onset of decomposition at a lower temperature, while mixing with a radical scavenger, 2,6-di-*t*-butyl-4-methylphenol (BHT), extended the range of thermal stability.<sup>39</sup> These results suggest a radical chain-scission mechanism, Figure 1.7, through which homolytic bond cleavages on the backbone yield imidoyl and amidinate radicals that propagate along the chain, unzipping the carbodiimide units.

Such chain scissions are not necessarily random, which is why the thermal stability of polycarbodiimides, made from a racemic mixture of monomer, is significantly less than that of their homochiral analogues. The heightened steric repulsions, between adjacent pendant groups of opposite handedness, create weak points between such repeats along the backbone. This explains why the onset of thermal decomposition for poly(*rac*)-*N*-methyl-*N'*-( $\alpha$ -methylbenzyl)carbodiimide) is 30 °C lower than that of poly(*R*)-(+)-*N*-methyl-*N'*-( $\alpha$ -methylbenzyl)carbodiimide).<sup>39</sup>

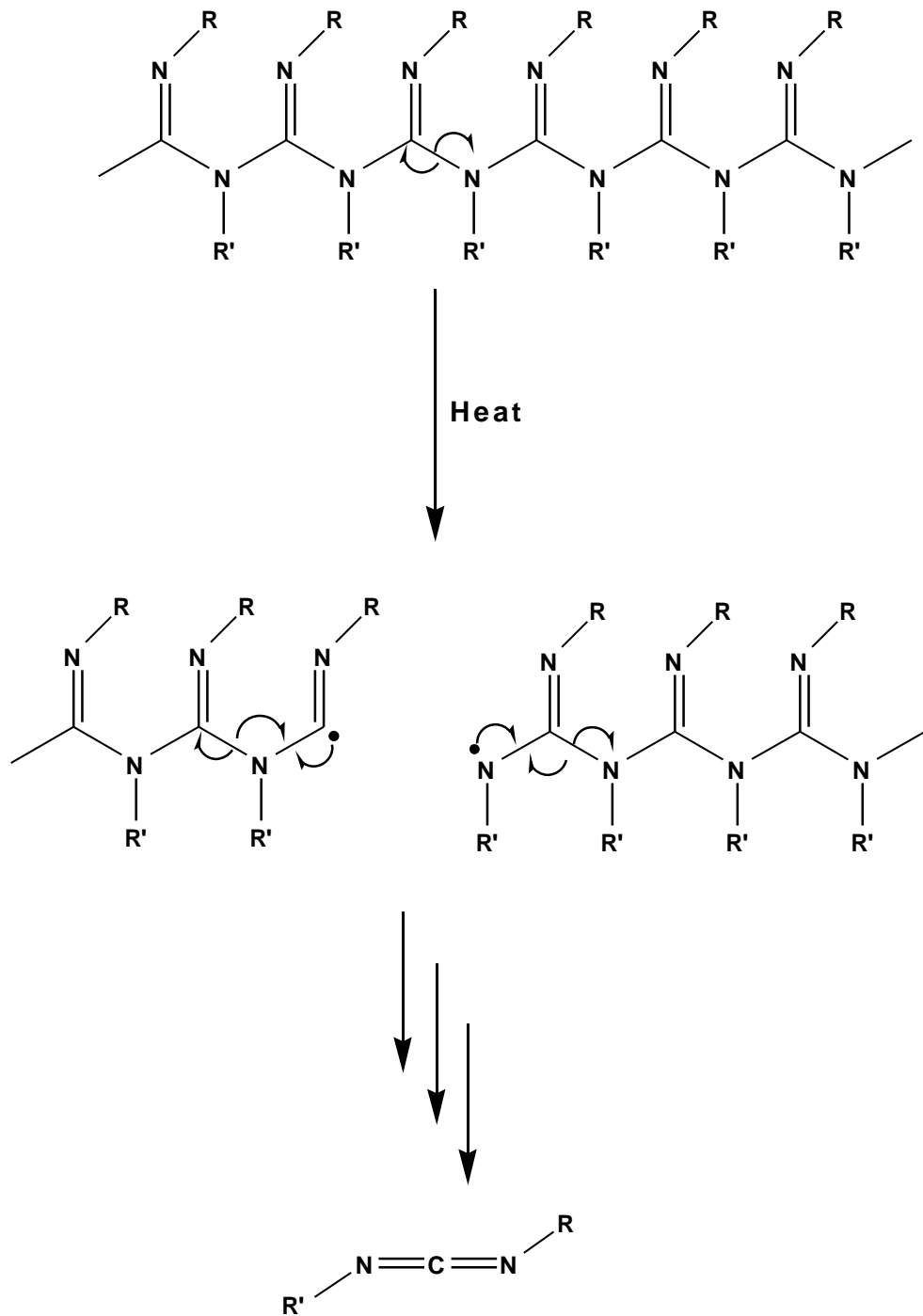


Figure 1.7: Thermally-induced, free radical depolymerization mechanism.

Efforts to improve the thermal stability of polycarbodiimides via structural modification have thus far proven impotent. Semiladder architectures, incorporating cyclic ring systems along the backbone, often enhance the thermal stability of polymer structures relative to linear analogues.<sup>41</sup> For instance, poly(cyclo-1,2-diisocyanateodecane) exhibits an onset of decomposition at 276 °C, nearly one hundred degrees higher than that of poly(n-hexyl isocyanate) at 180 °C.<sup>42</sup> Unfortunately, various cyclopolymers made from 1,2-dicarbodiimides proved no more thermally robust than linear polymers derived from monocarbodiimides.<sup>33</sup>

Crosslinking is another strategy often utilized to improve the thermal stability of polymer structures.<sup>43</sup> Two examples include the crosslinking of polystyrene and poly(methyl methacrylate) with 0.5% of  $Zr_6O_4(OH)_4(\text{methacrylate})_{12}$  clusters, which is reported to elevate the onset of thermal decomposition by 49 °C and 113 °C respectively.<sup>44</sup> Sadly, improvements in the thermal stability of polycarbodiimides via crosslinking prove negligible. When poly(N,N'-di-n-hexylcarbodiimide) is crosslinked to varying degrees with either of two dicarbodiimides, Figure 1.8, elevations of the thermal decomposition onset range from merely 1 to 10 °C.

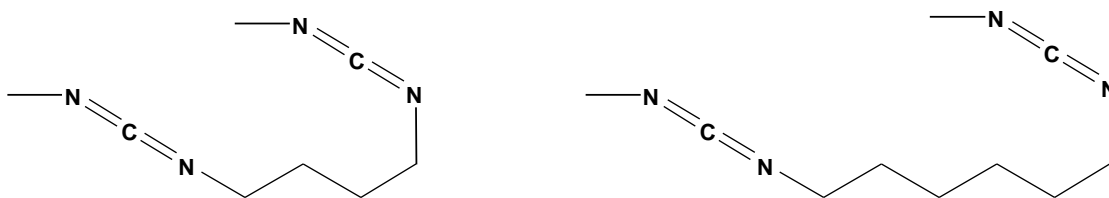


Figure 1.8: Structure of the dicarbodiimides 1,4-di(N'-methylcarbodiimidio)butane and 1,4-di(N'-methylcarbodiimidio)hexane utilized for the crosslinking of poly(N,N'-di-n-hexylcarbodiimide).

### 1.5. Polycarbodiimide Microstructure: The Role of Regioselectivity

For any asymmetrically-substituted carbodiimide, there are potentially two regiochemistries for the pendant groups on a given polycarbodiimide repeat. Consider the case of the N-hexyl-N'-phenylcarbodiimide, illustrated in Figure 1.9. Hypothetically, either the hexyl or the phenyl substituent might occupy the amine or the imine position. The extent to which a polymerization dictates which substituent is placed in which position is referred to as the regiospecificity of the reaction.

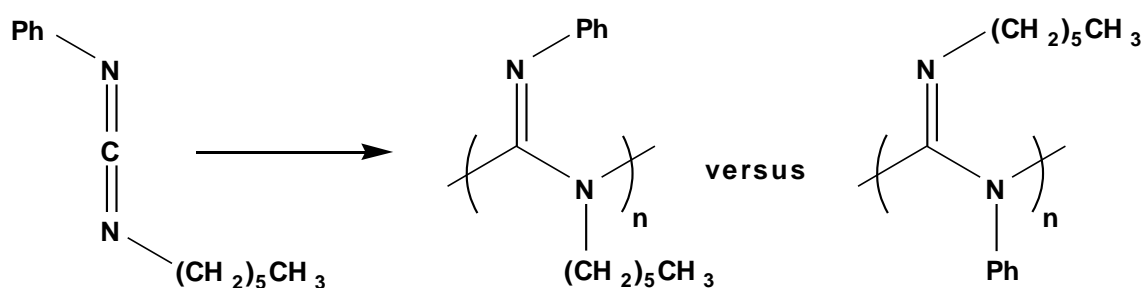


Figure 1.9: Two regiochemistries of an asymmetrically-substituted repeat unit.

Early efforts to quantify the regioselectivity of carbodiimide polymerizations relied on thermal degradation studies.<sup>39</sup> If thermally-induced scissions were random, scissions across the original monomer units would be as likely as scissions between them. Scissions between the original monomers yield the original monomers regardless. But for cases in which adjacent repeat units have opposite regiochemistries, scissions across the original monomers lead to metathesis monomers, Figure 1.10. However, such scissions are not random. When a polycarbodiimide microstructure entails structural irregularities, all bonds are not created equal. Some are cleaved more easily than others, biasing the degradation pathways, and thus precluding quantitative interpretations.

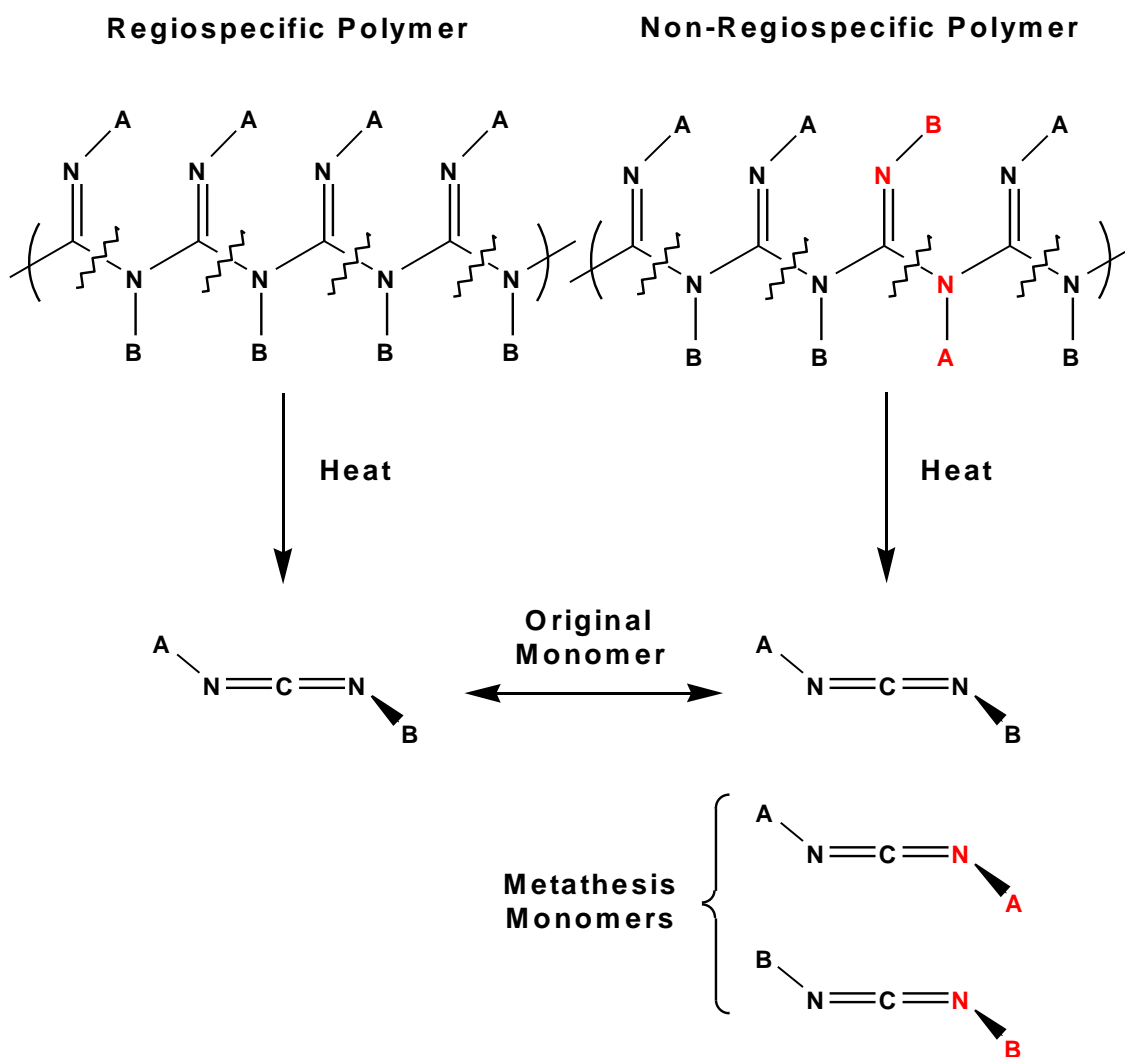


Figure 1.10: Illustration of depolymerization product(s) resulting from scissions across original monomer units for regiospecific versus non-regiospecific microstructures (irregularly-inserted monomer shown in red). The alternative, scissions between the original monomer units, would return the original monomer exclusively in either case.

Given that adjacent repeat units, paired in a less-stable regiochemical orientation, may favor cleavage between the original monomers, the absence of metathesis monomers alone does not prove regioregularity. Nevertheless, the presence of metathesis monomers is a certain indicator of regioirregularity. Hence these studies found that regiospecific polymerizations of carbodiimides are the exception, rather than the rule, as metathesis monomers are commonly observed.

The two exceptions that degrade exclusively to yield the original monomers suggest that extreme differences between the asymmetric substituents may be required to achieve highly regioselective polymerization. The first, poly(N-methyl-N'-( $\alpha$ -methylbenzyl)carbodiimide),<sup>39</sup> exhibits the largest steric difference that is achievable, as carbodiimides pairing a methyl substituent with one that is tertiary, rather than secondary, are not polymerizable. The second, poly(N-hexyl-N'-pentafluorophenylcarbodiimide),<sup>45</sup> is facilitated by extreme electronic effects. The strongly electron-withdrawing, pentafluorophenyl substituent heavily biases the regioselectivity of the propagation pathway by a synergy of inductive and resonance influences on the metal-amidinate complex.

Aside from the aforementioned limitations, thermal degradation is also incapable of indicating which of the two possible regiochemistries may be preferred. Peak broadening precludes use of <sup>1</sup>H NMR to address such questions, and the utility of infrared analysis alone is limited. With respect to the microstructural determination of polycarbodiimides, <sup>13</sup>C NMR provides the greatest insights, which are addressed in detail in Section 3.7.

## 1.6. Polycarbodiimide Macrostructure: From Worms to Rigid Rods

The relationship between the size of a polymer and its macromolecular conformation in solution is often characterized by its radius of gyration,  $R_G$ . Simply put, the radius of gyration is the mean square distance of the repeating units from the polymer's center of gravity. This value is experimentally determined from measurements of the angular dissymmetry of light scattered by the polymer molecules in solution.<sup>46</sup> The radius of gyration is proportional to the weight average molecular weight raised to a scaling factor that is highly sensitive to the macromolecular conformation of the polymer chain,  $R_G \propto [M_w]^\nu$ .<sup>47</sup> The exponent  $\nu$  ranges from 1/3 for a solid sphere and 1/2 for a Gaussian coil (in a theta solvent) to 1.0 for a rigid rod.

Studies on polycarbodiimides indicate macromolecular conformations that range from worm-like chains to rigid rods, depending on the chirality of the substituents and the steric congestion they create around the backbone. The scaling factors of 0.78 for poly(N,N'-di-n-hexylcarbodiimide), 0.89 for poly((*rac*)-N-methyl-N'-( $\alpha$ -methylbenzyl)carbodiimide), and 1.0 for poly((*R*)-(+)-N-methyl-N'-( $\alpha$ -methylbenzyl)carbodiimide) roughly quantify the magnitude of these influences on the macromolecular conformation adopted by a given polycarbodiimide.<sup>37</sup>

## 1.7. Concepts of Cooperativity

The helical nature of polycarbodiimides affords preferential induction of right- or left-handed helical conformations via cooperation with chiral entities. The extent of this cooperation in a given system can be visualized on a continuum of hierarchical levels illustrated by the Pyramid of Cooperativity, Figure 1.11. In each case, the cooperative effect is a result of the energy difference in the diastereomeric interaction of the chiral entity with the right- and left-handed conformation of the helix, Figure 1.12.

Through nearest-neighbor interactions of identical chiral pendant groups on each repeat unit, homochiral polymers achieve their cooperative influence over the shortest length scale, i.e. those of the nearest neighbor. These represent the lowest level of cooperativity at the base of the pyramid. At the level of sergeants and soldiers, the interaction of a chiral pendant group on one repeat unit with the achiral pendant groups on repeat units to either side can be thought of as cascading down the chain to influence helicity in a cooperative fashion. Majority Rules probes a slightly higher level of cooperativity due to the fact that in spite of its competing helical preference, repeat units having the less prevalent pendant enantiomer defer, with respect to conformation, to repeat units influenced by the excess pendant enantiomer to adopt a predominant handedness.

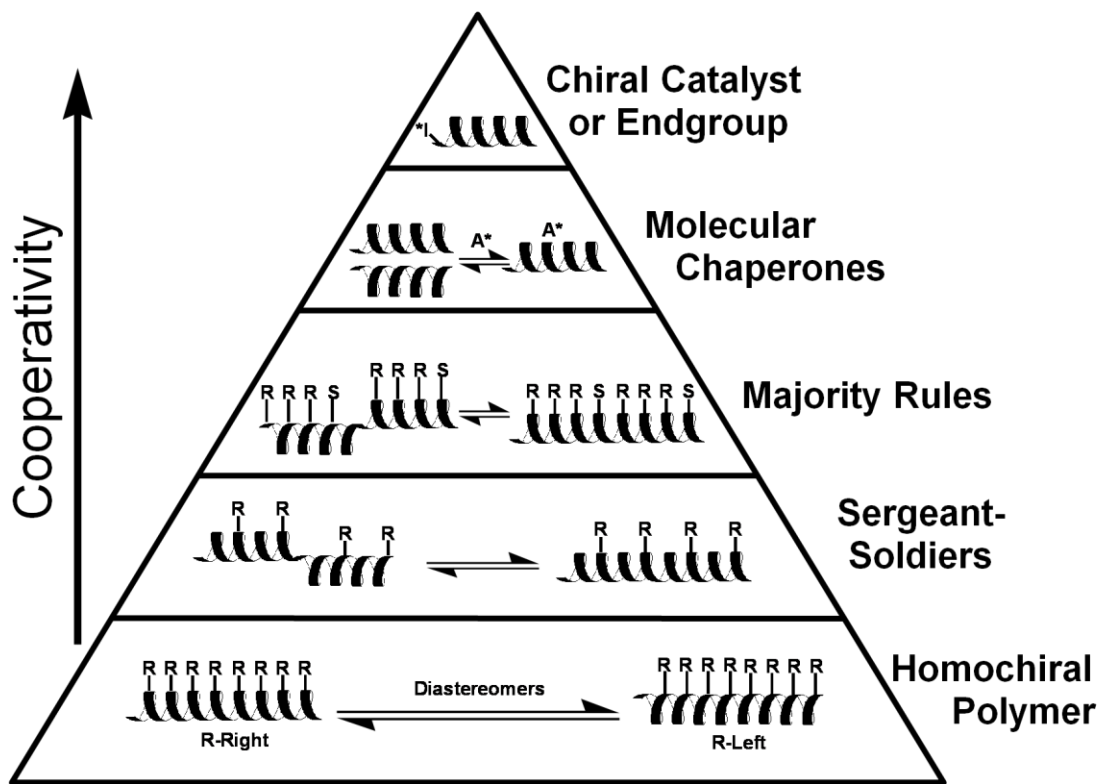


Figure 1.11: Pyramid of Cooperativity. The hierarchy of the pyramid illustrates the lengths to which a given polymer system cooperates with the predominant chiral entity by adopting a preferred helical sense. The pinnacle of cooperativity is the induction of a single-handed helix by a single chiral entity, either by a chiral catalyst exercising its influence on the active site during polymerization or through perturbation from a chiral endgroup at the chain's terminus.

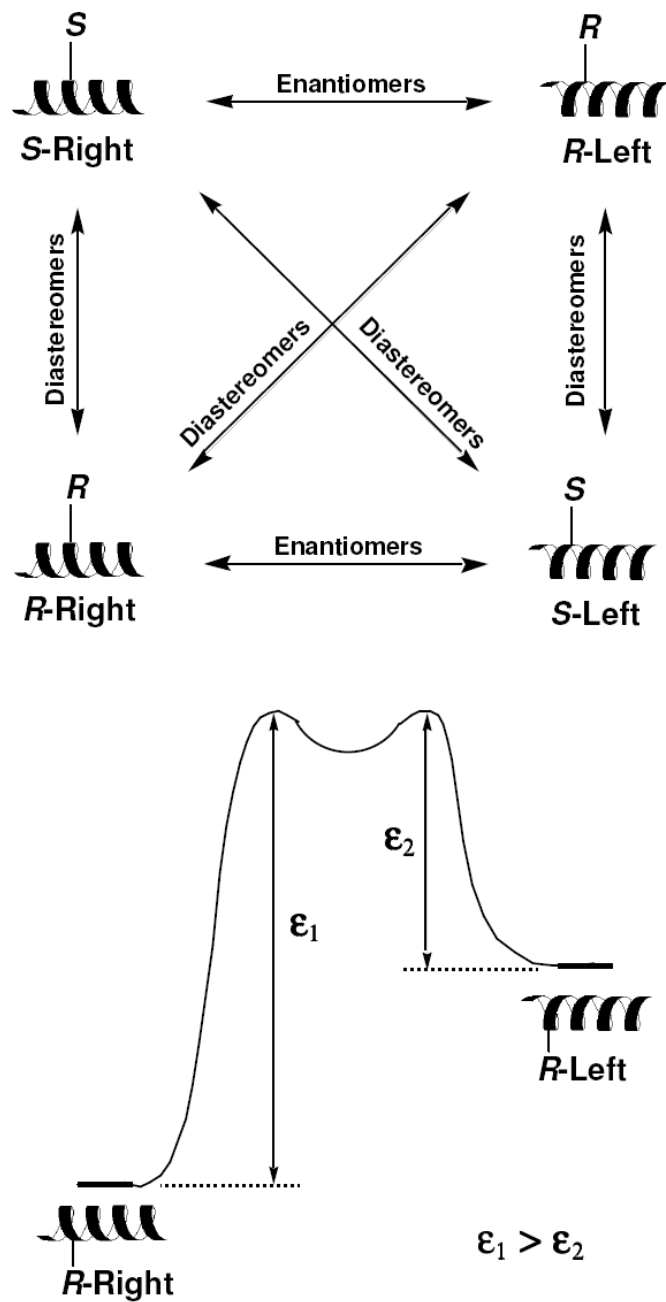


Figure 1.12: The schematic on top depicts the stereoisomeric relationships among right- and left-handed helices of polymers bearing chiral pendant groups. The schematic beneath illustrates the energy difference between the diastereomeric interactions of the right- and left-handed helical conformations with a given chiral entity.

While all three of the aforementioned levels of cooperativity rely on chiral entities that are covalently attached to the polymer structure, molecular chaperoning involves non-covalent interactions between small chiral molecules and the polymer. These may range from subtle, van der Waals forces to strong, hydrogen-bonding or ionic-pairing interactions. By generating a preferred diastereomeric complex, molecular chaperons induce a preferred helical conformation on the host polymer.

Finally, the pinnacle of cooperativity is the induction of a single-handed helix by a single chiral entity. There are two common manifestations of this phenomenon. In one, a chiral end group exerts a conformational influence from the terminus of the chain. In the other, a chiral catalyst exercises its influence on the propagating chain end during polymerization, leaving a single-handed helix in its wake. Unlike the covalently-attached chiral end group, which has a persistent effect on the polymer following work up, single-handed helical polymers made with a chiral catalyst can be thought of as inheriting their conformation, as the original chiral perturbant is removed when the chain is terminated.

#### 1.7.1. The Kinetics and Thermodynamics of Homochiral Polycarbodiimide Helicity

Any effort to fathom the means by which a polycarbodiimide cooperates with a pendant chiral entity must begin with an appreciation of the two distinct manners in which the helical conformation may be biased. The first is via the effect that the pendant chiral entity has on the conformation adopted by the subsequent repeat unit during the polymerization process. When chiral monomers approach the site of

chain propagation, steric interactions with the chiral entity on the previously inserted monomer dictate the rate at which a given monomer orientation and angle of approach are utilized. Insertions from some orientations and angles are more facile than those from others, resulting in chain conformations that are controlled by the kinetics of these chiral interactions. In this manner, a polycarbodiimide adopts what is referred to as a kinetically-controlled conformation.

However, such conformations are not necessarily the most stable. Indeed, the most stable conformation is occasionally the exact opposite of the one dictated by kinetics. Poly(N-(R)-2,6-(dimethylheptyl)-N'-phenylcarbodiimide), for instance, adopts a kinetically-controlled conformation exhibiting an optical rotation,  $[\alpha]_{435}$ , of  $-209^\circ$ . However, when annealed at temperatures between 50 and 85 °C, the optical rotation changes to  $+255^\circ$ .<sup>24</sup> Given that the original monomer had a rotation of merely  $-0.32^\circ$ , the magnitudes of these measurements are due almost exclusively to the chirality of the helix. The sign change in this case is consistent with a reversal of the handedness of the helix. Thus, through an annealing process, a polycarbodiimide may irreversibly adopt what is referred to as a thermodynamically-controlled conformation.

### 1.7.2. Too Many Chiefs, Not Enough Indians: An Optimum Sergeant/Soldier Ratio

The relationships among chiral entities, the helices they induce, and the resulting optical properties of cooperative systems are occasionally quite complicated, as the first sergeants and soldiers experiment utilizing a polycarbodiimide curiously illustrates.<sup>39</sup>

In experiments of this type, the optical activity of a co-polymer system is studied as a function of varying compositions of chiral and achiral repeats, i.e. sergeants and soldiers, respectively. The typical cooperative effect is an increase in optical activity, corresponding with increasing relative amounts of chiral units, converging into a plateau of optical activity upon exceeding the concentration of “sergeants” needed to fully compel the achiral “soldiers” to adopt the preferred helix.

*However*, in the first study of this kind involving carbodiimide co-polymers, what was observed instead is optical activity reaching a maximum at a certain optimum composition, after which subsequent increases in the ratio of sergeants to soldiers *sharply* decrease the optical rotation! Though a *subtle* trend of this sort has been observed before,<sup>48</sup> where rotational influences of the chiral pendant group and the helix are also in opposition, the scale of the effect seen here is unparalleled.

The origins of this anomalous behavior lie in the intricate manner in which the two substituents paired on the chiral monomer effect the optical rotation of the polymers into which they are incorporated. (R)-(+)-N-methyl-N'-( $\alpha$ -methylbenzyl)carbodiimide polymerizes into a preferred helical conformation exhibiting an optical rotation,  $[\alpha]_{598}$ , of *merely*  $-10.8^\circ$ . Such an attenuated rotation is

typical of a homochiral polycarbodiimide also bearing a miniscule methyl substituent. The monomer itself rotates the sodium-D line by  $+25.8^\circ$ . In this system, the contributions to the optical rotation by the chiral pendant group and that of the helix it preferentially induces are comparable in magnitude and opposite in sign.

When co-polymerized with the decreasing amounts of the achiral N,N'-di-n-hexylcarbodiimide, the optical rotation of the kinetically-controlled conformation increases rapidly as the composition approaches a chiral monomer content of 20%. The trend is less pronounced, but continues to a content of approximately 40%, where the optical rotation reaches a maximum value of  $-52.2^\circ$ , beyond which it gradually declines – due to the opposing optical influence of the pendant chiral entity – until it matches that of the homochiral polymer.

### 1.7.3. The Helix-Directing Authority of the Chiral Majority

In the land of polymers, it is occasionally the case that a particular democratic process rules in “societies” that are “well-integrated,” so to speak. Here we are talking about random co-polymers, in which dissimilar monomers are incorporated randomly within a polymer chain. More specifically, when a chiral mixture of repeat units is interspersed in a random fashion, they may interact cooperatively to determine the helical conformation that is adopted.

Studies of this type, which involve the polymerization of chiral monomers in varying enantiomeric ratios, are referred to as Majority Rules experiments. The typical cooperative effect observed in these studies is an increase in optical rotation,

corresponding with increasing enantiomeric excess, converging on a plateau of optical activity following the excess needed to fully compel the minority to adopt the helical sense favored by the majority.<sup>49,50</sup>

The optical effects observed in the first Majority Rules experiment on a polycarbodiimide are more elaborate. Rather than exhibiting an optical rotation that plateaus as the enantiomeric excess approaches purity, this system displays optical activity reaching a maximum at a certain optimum enantiomeric excess, after which subsequent increases in chiral purity modestly decrease the optical rotation.<sup>45</sup>

A decrease in optical rotation, upon approaching enantiomeric purity, has also been reported elsewhere in a similar case where the optical influence of the pendant chiral entity opposes that of the helix it favors.<sup>51</sup> At an enantiomeric excess of 80%, co-polymers of (R)- and (S)-2,6-dimethylheptyl isocyanate exhibit a maximum optical rotation in chloroform that is approximately  $640^\circ$  in magnitude, which is roughly  $140^\circ$  greater than that of a homochiral composition.

The chiral pendant group, on the terpene precursor from which those isocyanates are derived, rotates the sodium-D line merely  $7.0^\circ$  in the opposite direction in chloroform. But the scale of that influence is doubled in the Majority Rules experiment in that every incremental increase in chiral purity not only adds chiral pendant groups having an opposing rotational influence, but also removes groups that were reinforcing the dominant rotational influence of the helix.

Given this report, it was not surprising when an analogous optical trend was observed in the first Majority Rules experiment on a polycarbodiimide. When

varying enantiomeric ratios of (R)- and (S)- N-methyl-N'-( $\alpha$ -methylbenzyl) carbodiimide are co-polymerized, an enantiomeric excess of 65% proves optimum, yielding an optical rotation,  $[\alpha]_{385}$ , in chloroform of  $-135^\circ$  for excess (R). As the enantiomeric excess approaches purity, the rotation declines modestly, settling at roughly  $-85^\circ$ .<sup>45</sup>

In terms of the percentage change in optical rotations, this trend is significantly greater in magnitude than the one observed among the aforementioned polyisocyanates. However, in absolute terms, the magnitude of this trend is not as dramatic as the numbers alone might intimate, considering that the measurements were taken at 365 nm, which magnifies the scale of the rotations compared with those at the more customarily utilized sodium D-line. For instance, consider the optical rotations of (R)-(+)-N-methyl-N'-( $\alpha$ -methylbenzyl)carbodiimide for which  $[\alpha]_{598}$  is  $-10.8^\circ$ , while  $[\alpha]_{365}$  measures  $-72.0^\circ$ .

Nevertheless, it is clear from the data that co-polymerizations of enantiomeric mixtures of (R)- and (S)-N-methyl-N'-( $\alpha$ -methylbenzyl)carbodiimide do cooperate in establishing the helical sense preferred by the majority. The moderate intensity of this effect affords confident deduction that the co-polymerization of these enantiomers is not stereoselective. In other words, these chiral monomers do not polymerize into separate homochiral chains or segregated stereoblocks. Were they to do so, each block or chain would adopt its own preferred helical sense, resulting in a decidedly linear optical response to variations in the enantiomeric ratio, the very definition of non-cooperative behavior.

The atypical optical response to enantiomeric excess observed in the first study of a polycarbodiimide proves the exception, rather than the rule, and is a consequence of the relatively low optical rotation, compared with that of the pendant chiral entity, of a polycarbodiimide helix presenting, as the other pendant group, a miniscule methyl substituent. A subsequent study revealed that annealed copolymers composed of enantiomeric mixtures of N-2,6-dimethylheptyl-N-hexylcarbodiimide manifest a more typical cooperative optical response, plateauing at an enantiomeric excess of 60%.<sup>45</sup> With respect to the apparent trend, the magnitude of the  $[\alpha]_{365} = +7.6^\circ$  influence of the chiral pendant group<sup>23</sup>, measured on the monomer in hexane, contributes negligibly to the  $-170^\circ$  rotation of the annealed (R)-homochiral polymer in chloroform.<sup>45</sup>

#### 1.7.4. Protons & Polycarbodiimides: The Chaperoning of Orderly Affairs

Upon polymerization of a carbodiimide, the  $60^\circ$  dihedral angle, between one repeat unit and the next, partitions the chain into amidine units. Amidines are organic bases. Protonation occurs at the imino nitrogen, leading to the resonance stabilized amidinium ion, Figure 1.13, that, depending on the substituents, has a pKa value ranging from 5 to 13.<sup>52</sup> Upon protonation, the solubility of a polycarbodiimide often changes remarkably. For instance, poly(N,N'-diethylcarbodiimide) becomes water soluble when protonated by hydrochloric acid, and precipitates when deprotonated with sodium hydroxide.<sup>35</sup>

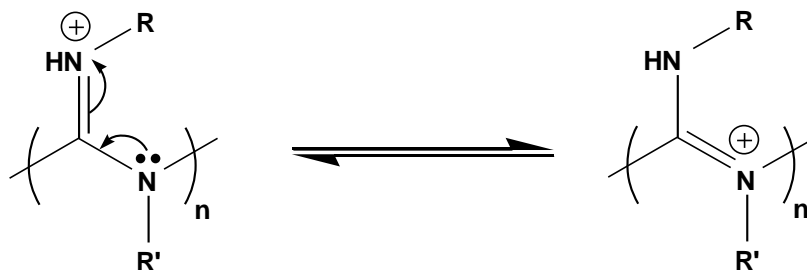


Figure 1.13: The respective exo- and endo-resonance forms of the amidinium ion, resulting from protonation of the polycarbodiimide backbone.

Aside from altering the solubility, protonating a polycarbodiimide also facilitates transformation into the most thermodynamically-stable conformation. For instance, poly(N-(R)-2,6-dimethylhexyl)-N'-hexylcarbodiimide is reported to adopt a kinetically-controlled conformation having an  $[\alpha]_{365} = +7.5^\circ$  in hexanes. The monomer itself has an  $[\alpha]_{365} = +7.6^\circ$ , which suggests that the optical rotation exhibited by the polymer is essentially contributed by the chiral pendant group. In this case, the kinetically-controlled conformation features a random distribution of right- and left-handed helices, separated by helical reversals within the chain. Reaching the thermodynamically-stable conformation, having an  $[\alpha]_{365} = -157.5^\circ$  in hexanes, requires slow annealing at elevated temperatures. However, protonation with five equivalents of benzoic acid effectively catalyzes this transformation at room temperature, immediately resulting in  $[\alpha]_{365} = -144^\circ$  in chloroform.<sup>23</sup> Current speculation is that protonating the imine positions catalyzes the re-orientation of pendant group arrangements that typically hinder inversion of the backbone into the energetically-favored helix, Figure 1.14.

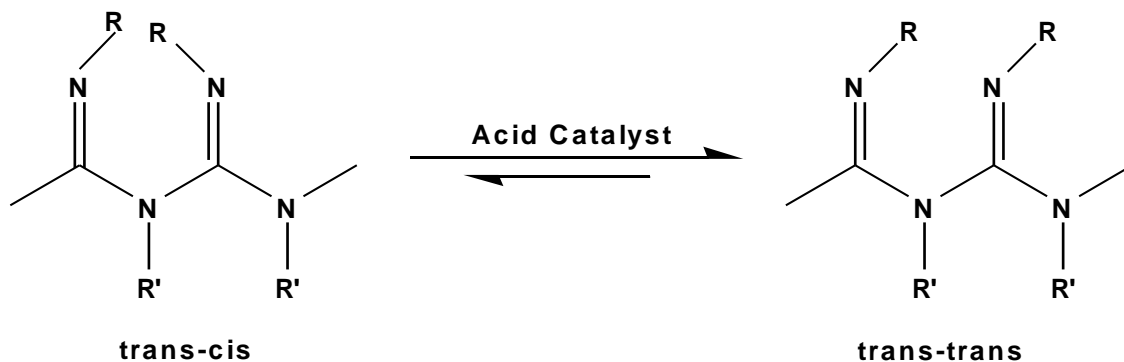


Figure 1.14: Pendant groups on adjacent imine nitrogens may orient in either a trans-cis or trans-trans arrangement. In theory, protonation of the backbone would facilitate transformations into trans-trans orientations through the free rotation of pendant entities in the endo-resonance form of the amidinium ion, inadvertently lowering the activation energy of the helical inversion process.

While protonating the polycarbodiimide backbone does enable a chiral pendant group to induce its thermodynamically-preferred helical sense, a study with enantiomerically-pure camphorsulfonic acids finds that a tightly-bound chiral counteranion, favoring the opposite helical sense, can exert an even greater conformational influence.<sup>45</sup> When virgin poly(N-(R)-2,6-dimethylhexyl)-N'-hexylcarbodiimide ( $[\alpha]_{365} = +7.5^\circ$ ) is protonated with (R)-CSA in chloroform, the net optical rotation of the polymer measures  $-300^\circ$ . However, when protonated with (S)-CSA, the net rotation measures  $+24^\circ$ . When dissolved in tetrahydrofuran, rather than chloroform, this chiral counteranion effect is essentially negated by the more distanced ion-pairing, resulting in net rotations of  $-123^\circ$  and  $-102^\circ$ , following protonation with (R)- and (S)-CSA respectively.

This chiral counteranion has also proven capable of chaperoning the induction of a single-handed helix from a racemic mixture of helices on a

polycarbodiimide bearing achiral substituents. When poly(N,N'-di-n-hexylcarbodiimide) is protonated with increasing amounts of (S)-CSA, an exponential increase in the net specific rotation is observed, Figure 1.15.<sup>23</sup> Here too, an essential element in the efficacy of helical induction is a tight pairing of the chiral counteranion with the protonated polycarbodiimide backbone. When protonated with 4.25 equivalents of (S)-CSA in chloroform, the net rotation of the polymer is 250°, but when equivalently protonated in tetrahydrofuran, the more distanced ion pairing mitigates the helix-inducing potency of the chaperone, resulting in a rotation of merely 55°.

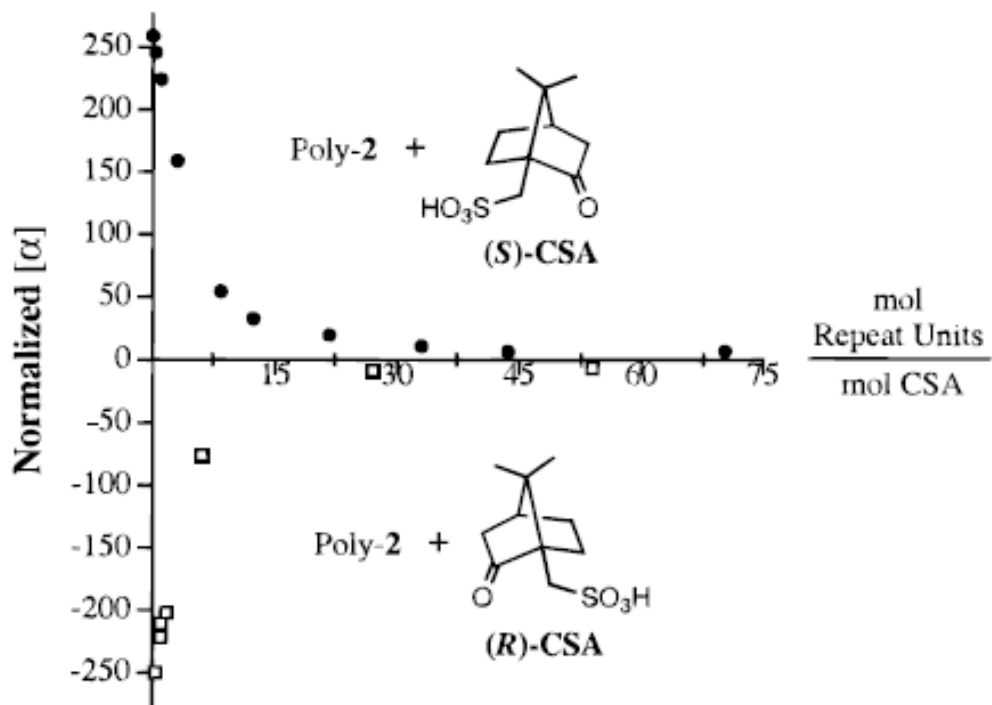


Figure 1.15: Normalized specific rotation in chloroform of poly(N,N'-di-n-hexylcarbodiimide) as a function of champhorsulfonic acid concentration ((R) = hollow boxes, (S) = solid dots).

### 1.7.5. Gods of Helicity: The Search for an Omnipotent Chiral Center

Speaking philosophically, as an intensive property of a system, chiral purity represents order. A random distribution, of right- and left-handed forms, possesses greater entropy. Regarding helical polymers, a racemic mixture of right- and left-handed helices is favored by the second law of thermodynamics. To take such a system, in which opposite helices are mirror images of one another, and seek to impose such order that only one form exists, is a godly endeavor. A theologian would argue that such an act requires the intelligent design of a supreme being. A chemist, on the other hand, would simply formulate an “intelligent design,” aiming to employ a “supreme being,” an *omnipotent* chiral center so to speak, and run reactions to explore the truth of it.

One such design employs a chiral end group exerting a conformational influence from the terminus of the chain. Due to the cascade of steric interactions, the right- and left-handed helices are merely pseudoequivalent, differing ever so slightly in energy. The diastereomeric interactions manifest most sharply at reduced temperatures, where, thermodynamically, the lower-energy helix is favored. To a limited extent, the magnitude of the effect is proportional to the scale of the steric interactions, the bulkier the chiral end group, the greater its conformational influence. Limitations also arise from the fact that, statistically speaking, the further from the chiral terminus a repeat unit is, the more entropic “free will” it exercises in the way it rolls, literally!

Chiroptic studies on polycarbodiimides bearing chiral end groups, Figure 1.16, find that they precisely embody these anticipated attributions.<sup>39</sup> Judging from changes in the sign and magnitude of optical rotation, Table 1.1, it appears that at room temperature, entropy favors a relatively equal distribution of the two helices. Comparing two chains of different length bearing the same chiral end group, the longer one presents a rotation of lesser magnitude at the lowest temperature, thus exhibiting the limitations of conformational influence with increasing distance from the chiral terminus. Also, comparing analogous polymers of relatively equal length, the one bearing the bulkier chiral end group displays greater rotations at reduced temperatures, revealing magnitudes of influence directly proportional to the scale of the steric interactions.

Table 1.1: Optical rotation data of poly(N,N'-di-n-hexylcarbodiimides) prepared with chiral initiators, measured in chloroform at the sodium-D line, 598 nm.

Initiator	Monomer:Initiator	$[\alpha]_D^{25}$	$[\alpha]_D^{0.0}$	$[\alpha]_D^{-10}$	$[\alpha]_D^{-30}$
<b>I</b>	<b>84:1</b>	<b>+1.2°</b>	<b>-1.9°</b>	<b>-2.4°</b>	<b>-3.0°</b>
<b>II</b>	<b>98:1</b>	<b>0.0°</b>	<b>-1.2°</b>	<b>-3.6°</b>	<b>-5.2°</b>
<b>II</b>	<b>41:1</b>	<b>+0.3°</b>	<b>-0.8°</b>	<b>-3.6°</b>	<b>-6.8°</b>

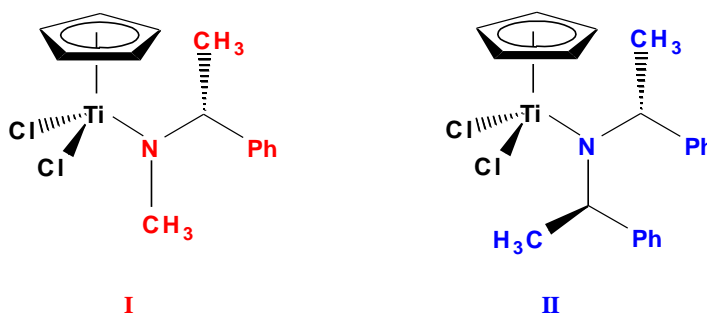


Figure 1.16: Titanium (IV) catalysts with chiral amide initiators, shown in color, utilized to polymerize N,N'-di-n-hexylcarbodiimide for chiral end-group studies.

So as a means of utilizing a single chiral entity to impose a transcendent helical order, to selectively synthesize one of two perfectly-equivalent helices, the chiral end group strategy falls short here in two respects. First, placing a chiral terminus on the chain means that the right- and left-handed helices are no longer perfectly equivalent. Indeed, it is the subtle energy difference between the two that is the source of preferential helical induction, which leads to the second shortcoming: the magnitude of the ordering, even when manifest most sharply at reduced temperature, is meager. Limitations arise from the activation energy of the helical inversion process, whose increasing inaccessibility at reduced temperatures inhibits expression of the inherent thermodynamic preference.

In essence, the incompatible thermal energy requirements of preferential helical induction and the activation energy needed to achieve it preclude utilization of chiral end groups to effect the formation of exclusive right- or left-handed helices on a polycarbodiimide. Thus placement of the chiral center on the initiating ligand, from which it becomes the end group, proves suboptimal. Instead, the more intelligent design utilizes chirality on the persistent ligand sphere of the metallic coordination-insertion catalyst. From the transient vantage of the active site, this single chiral entity dictates the helical conformation of the incipient polymer from beginning to end, as if it were the proverbial hand of god.

The prototype design that has proven most successful in this endeavor is the (BINOLate)Ti(O-*i*Pr)<sub>2</sub> catalyst, Figure 1.17. 2,2'-binaphthol and its derivatives are among the most widely used chiral ligands in asymmetric catalysis.<sup>53</sup>

(BINOLate)TiX<sub>2</sub> catalysts alone have been utilized to effect high enantioselectivity in many systems, including carbonyl-ene reactions,<sup>54</sup> Mukaiyama aldol condensations,<sup>55</sup> and the allylation of aldehydes<sup>56</sup> and ketones,<sup>57</sup> to name a few.

When carbodiimides pairing a hexyl substituent with either an isopropyl, hexyl, or phenyl substituent are polymerized with the (S-BINOL)Ti(O-*i*Pr)<sub>2</sub> catalyst, the optical rotations, [α]<sub>435</sub>, of the resulting polymers, measured in toluene, are -15°, -44°, and -753° respectively.<sup>24</sup> Quantitatively, the enantiomeric excess of the preferred helix in each case remain uncertain. Qualitative comparisons of poly(N,N'-di-*n*-hexylcarbodiimides) made with the chiral catalyst, versus chiral initiators, are problematic in that the optical rotation measurements were made at different wavelengths, in different solvents. Nevertheless, given that the optical rotations of poly(N,N'-di-*n*-hexylcarbodiimides) bearing a chiral end group are approximately zero at room temperature, it is clear from the data that helix-sense selective polymerization via chiral catalyst is superior by at least an order of magnitude.

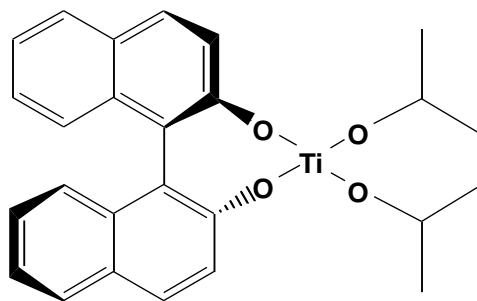


Figure 1.17: The (R-BINOL)Ti(O-*i*Pr)<sub>2</sub> catalyst. When polymerizing the achiral N-hexyl-N'-phenylcarbodiimide, this catalyst preferentially induces a right-handed (P) helix as assigned by comparing the spectrum observed via vibrational circular dichroism (VCD) with the one simulated by theoretical modeling calculations.<sup>58</sup> Curiously, replacing the isopropoxides with tert-butoxides reverses the helical selectivity, dictating preferential induction of the left-handed (M) helix instead.

## 1.8. Optical Switching with a Helical Polycarbodiimide Nanoshutter

Having reached the pinnacle of cooperativity, with the helix-sense selective polymerization of carbodiimides, subsequent optical studies uncovered an intriguing switching phenomenon. It turns out that many pendant polyaromatics, such as 1-naphthyl, 1-anthryl, and 1-pyrenyl substituents, behave as cylindrical nanoshutters with respect to their orientation on the polymer backbone.<sup>29</sup> Collectively occupying either of two positions, having dipole moments aligned with or against the helical director, these flap-like appendages often rearrange synchronously in response to changes in solvent polarity or temperature as illustrated in Figure 1.18.

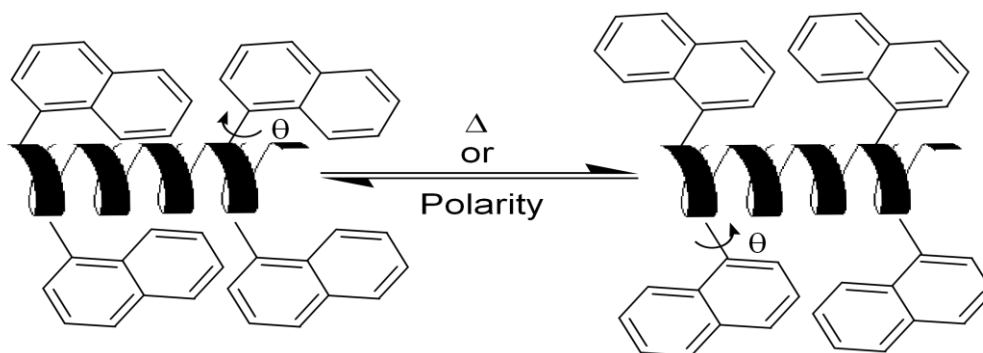


Figure 1.18: Two states resulting from shutter-like motions of 1-naphthyl substituents.

The specific optical rotation changes dramatically in response to these reversible rearrangements, ranging from  $+1300^\circ$  at  $0^\circ\text{C}$  to  $-400^\circ$  at  $50^\circ\text{C}$  for poly(N-(1-naphthyl)-N'-octadecylcarbodiimide) in THF, as an example. The rotation of the 1-naphthyl units changes their  $\Pi$ -electron interactions with the nitrogen lone-pairs on the backbone, leading to a switch observable via ECD and anisotropic changes among variable temperature  $^1\text{H}$  NMR spectra, Figure 1.19, while leaving the chirality of the backbone, sensed by the VCD absorption of the C=N bond, unchanged.

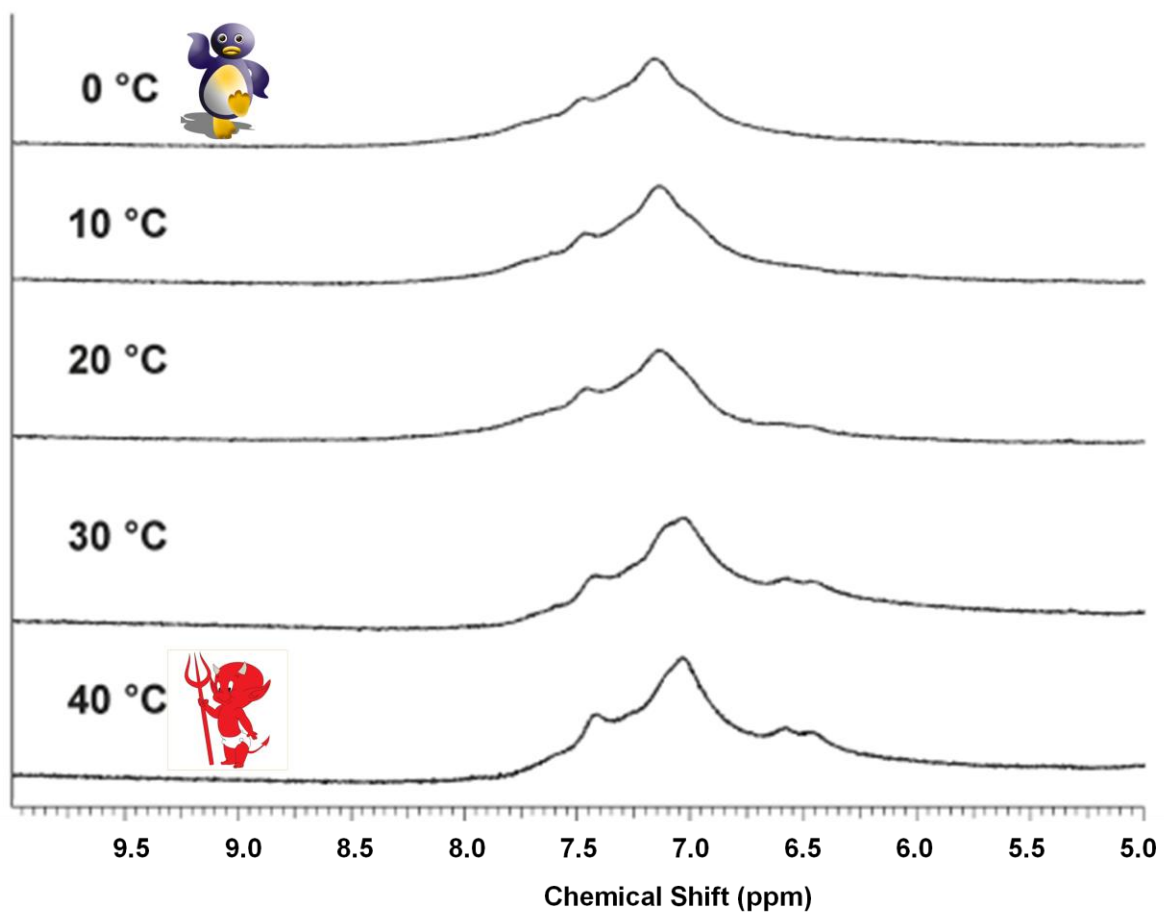


Figure 1.19: Anisotropic changes in the aromatic region among variable temperature <sup>1</sup>H NMR spectra of poly(N-(1-naphthyl)-N'-octadecylcarbodiimide) in THF-d<sub>8</sub>. The most noteworthy trend with increasing temperature is the disappearance of the signals for two protons from the region of broad overlap centered at 7.0 ppm corresponding with their re-emergence upfield at approximately 6.5 ppm.<sup>29</sup>

## 1.9. Liquid Crystalline Properties of Polycarbodiimides

The term liquid crystal is used to describe phases of matter in which the molecules exhibit oriented fluid motions, which, in many cases, are confined within layers. Liquid crystals are broadly divided into two categories, those exhibiting liquid crystalline behavior due to solvent effects, referred to as lyotropic, and those acting as liquid crystals over a certain temperature range, referred to as thermotropic. Perhaps the most common liquid crystals are those created by amphiphilic molecules that self-assemble into micelles, hexagonal arrays, and lamellar structures.<sup>59</sup> Other molecules that display liquid crystalline behavior typically have two elements in common, flexible components imparting fluidity and rigid components, referred to as mesogens, bestowing orientation and layering effects. Chirality may endow an additional level of molecular orientation.

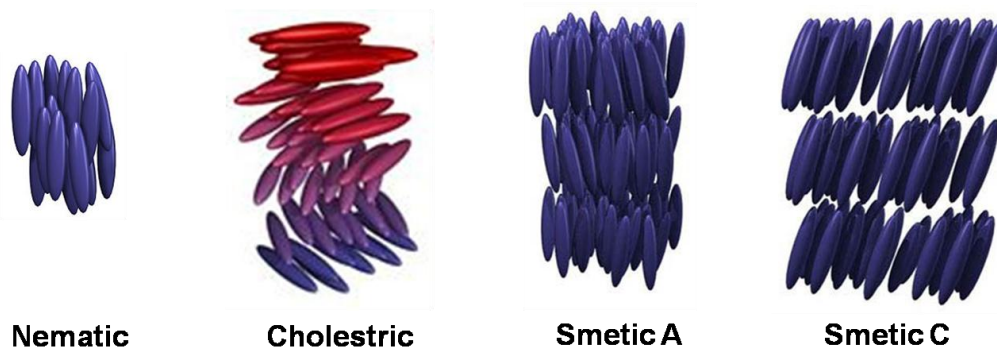


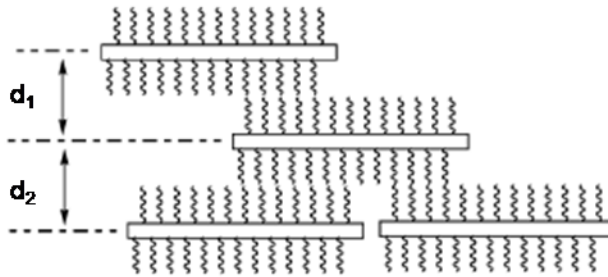
Figure 1.20: Schematic representations of four prominent liquid crystalline phases.<sup>59</sup> A common feature shared by all liquid crystal phases is an orderly orientation of the molecules. The distinguishing feature of phases that are nematic is a lack of positional order. When the mesogens in a nematic phase are chiral, they adopt a twisted orientation with respect to one another, creating what is referred to as a chiral nematic or cholestric phase. Smectic phases are characterized by the restricted layering of molecules. In the smectic A phase, the orientation of the molecules is perpendicular to the layering. In the smectic C phase, the molecules are tilted relative to the layering.

Combining side chains capable of imparting both fluidity and chirality with a helical backbone that acts as a mesogen, polycarbodiimides can be modified to induce a variety of lyotropic liquid crystalline phases. The versatility afforded by two side chains per repeat proves felicitous in this regard. When comparing poly(N,N'-di-n-hexylcarbodiimide) with its isocyanate analogue, poly(n-hexyl isocyanate), the former forms more highly ordered smectic textures,<sup>25</sup> while the latter adopts nematic phases.<sup>60-62</sup> Here the polycarbodiimide's higher side-chain density enhances the corona barrier, leading to more uniform separation of the helices, Figure 1.19.

By varying the length of the two side chains per repeat, polycarbodiimides can also be induced to form nematic liquid crystal phases.<sup>26</sup> Poly((*rac*)-N-methyl-N'-( $\alpha$ -methylbenzyl)carbodiimide) for instance, adopts a nematic texture. Its optically pure analogue, poly((*R*)-(+)-N-methyl-N'-( $\alpha$ -methylbenzyl)carbodiimide), exhibits a cholesteric phase. The latter also forms mesophases at lower concentrations, an observation that correlates with data from light scattering and thermal analyses suggesting that the optically-pure chains are more rigid.

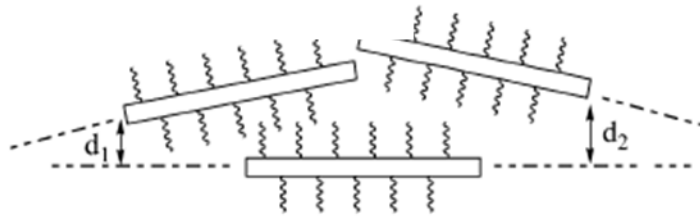
Since most polycarbodiimides decompose at relatively low temperatures (ca. 150 – 200 °C), thermotropic mesophases are uncommon. Two exceptions, poly(N,N'-di-n-dodecylcarbodiimide) and poly(N-12-((4'-methoxybiphenyl-4-oxy)dodecyl-N'-n-dodecylcarbodiimide), display thermotropic mesophases just below their decomposition temperature.<sup>26</sup> The mesophase behavior of the former can be described as helical rods aligning in molten paraffin, while latter forms a smectic layered texture due to the added influence of the mesogenic side chain entity.

**A. Poly(N,N'-di-n-hexylcarbodiimide)**



$$d_1 = d_2 \approx 13 \text{ \AA}$$

**B. Poly(n-hexyl isocyanate)**



$$d_1 \neq d_2$$

Figure 1.21: Schematic representation of (A) the smectic phase of poly(N,N'-di-n-hexylcarbodiimide) versus (B) the nematic phase of poly(n-hexyl isocyanate).<sup>25</sup>

## 1.10. References

- (1) Gordetsov, A. S.; Kozyukov, V. P.; Vostokov, I. A.; Sheludyakova, S. V.; Dergunov, Y. I.; Mironov, V. F. *Russian Chemical Reviews* **1982**, *51*, 485-469.
- (2) Razuvaev, G. A.; Gordetsov, A. S.; Kozina, A. P.; Brevnova, T. N.; Semenov, V. V.; Skoveleva, S. E.; Boxer, N. A.; Dergunov, Y. I. *Journal of Organometallic Chemistry* **1987**, *327*, 303-309.
- (3) Cooley, J. H.; Evain, E. J. *Journal of Organic Chemistry* **1989**, *54*, 1048-1051.
- (4) Wadsworth, W. S.; Emmons, W. D. *Journal of Organic Chemistry* **1964**, *29*, 2816-2820.
- (5) Palacios, F.; Ochoa De Retana, A. M.; Martinez de Margorta, E.; Rodriguez, M.; Pagalday, J. *Tetrahedron* **2003**, *59*, 2617-2623.
- (6) Rankin, D. W. H. *Journal of the Chemical Society - Dalton Transcriptions* **1972**, *7*, 869-873.
- (7) Gupta, R. K.; Stammer, C. H. *Journal of Organic Chemistry* **1968**, *33*, 4368-4371.
- (8) Thrasher, J. S.; Howell, J. L.; Clifford, A. F. *Inorganic Chemistry* **2008**, *21*, 1616-1622.
- (9) Ulrich, H. *Chemistry and Technology of Carbodiimides*; Wiley, 2007.
- (10) Down, M. G.; Haley, M. J.; Hubberstey, P.; Pulham, R. J.; Thunder, A. E. *Journal of the American Chemical Society - Dalton Transcriptions* **1978**, 1407-1411.
- (11) Becker, M.; Jansen, M. *Solid State Sciences* **2000**, *2*, 711-715.
- (12) Berger, U.; Schnick, W. *Journal of Alloys and Compounds* **1994**, *206*, 179-184.
- (13) Liu, X.; Krott, M.; Mller, P.; Hu, C.; Lueken, H.; Dronskowski, R. *Inorganic Chemistry* **2005**, *44*, 3001-3003.
- (14) Becker, M.; Jansen, M. *Acta Crystallographica* **2001**, *C57*, 347-348.

- (15) Hashimoto, Y.; Takahashi, M.; Kikkawa, S.; Kanamaru, F. *Journal of Solid State Chemistry* **1996**, *125*, 37-42.
- (16) Zhou, Y.; Probst, D.; Thissen, A.; Kroke, E.; Riedel, R.; Hauser, R.; Hoche, H.; Broszeit, E.; Kroll, P.; Stafast, H. *Journal of the European Ceramic Society* **2006**, *26*, 1325-1335.
- (17) Rebek, J.; Feitler, D. *Journal of the American Chemical Society* **1973**, *95*, 4052-4053.
- (18) Kunkel, G. R.; Mehrabian, M.; Martinson, H. G. *Molecular and Cellular Biochemistry* **1981**, *34*, 3-13.
- (19) Fridkin, M.; Patchornik, A.; Katchalski, E. *Journal of the American Chemical Society* **1966**, *88*, 3164-3165.
- (20) Wolman, Y.; Kivity, S.; Frankel, M. *Chemical Communications* **1967**, 629-630.
- (21) Weinshenker, N. M.; Shen, C. M. *Tetrahedron Letters* **1972**, *13*, 3281-3284.
- (22) Nieh, M.-P.; Goodwin, A.; Stewart, J.; Novak, B.; Hoagland, D. *Macromolecules* **1998**, *31*, 3151-3154.
- (23) Schlitzer, D.; Novak, B. *Journal of the American Chemical Society* **1998**, *120*, 2196-2197.
- (24) Tian, G.; Lu, Y.; Novak, B. *Journal of the American Chemical Society* **2004**, *126*, 4082-4083.
- (25) Kim, J.; Novak, B. *Macromolecules* **2004**, *37*, 1660-1662.
- (26) Kim, J.; Novak, B. *Macromolecules* **2004**, *37*, 8286-8292.
- (27) Tang, H.; Boyle, P.; Novak, B. *Journal of the American Chemical Society* **2005**, *127*, 2136-2142.
- (28) Tang, H.; Novak, B.; He, J.; Polavarapu, P. *Communications* **2005**, *44*, 7298-7301.
- (29) Kennemur, J.; Clark IV, J. B.; Tian, G.; Novak, B. *Macromolecules* **2010**, *43*, 1896-1873.
- (30) Larson, R. J., PhD Dissertation, University of Massachusetts Amherst, 2000.

- (31) Blackburn, J. L., PhD Dissertation, North Carolina State University, 2004.
- (32) Lu, Y., PhD Dissertation, North Carolina State University, 2005.
- (33) Zhang, Y., PhD Dissertation, North Carolina State University, 2008.
- (34) Li, H., PhD Dissertation, North Carolina State University, 2006.
- (35) Robinson, C. *Journal of Polymer Science: Part A* **1964**, 2, 3901-3908.
- (36) Szwarc, M.; Levy, M.; Milkovich, R. *Journal of the American Chemical Society* **1956**, 78, 2656-2657.
- (37) Goodwin, A.; Novak, B. *Macromolecules* **1994**, 27, 5520-5522.
- (38) Patten, T.; Novak, B. *Journal of the American Chemical Society* **1991**, 113, 5056-5066.
- (39) Goodwin, A., PhD Dissertation, University of California at Berkeley, 1996.
- (40) Shibayama, K.; Seidel, S.; Novak, B. *Macromolecules* **1997**, 30, 3159-3163.
- (41) Butler, G. *Cyclopolymerization and Cyclocopolymerization*; Marcel Dekker, Inc.: New York, 1992.
- (42) Patten, T., PhD Dissertation, University of California, Berkeley, 1994.
- (43) Madorsky, S. *Thermal Degradation of Organic Polymers*; John Wiles & Sons: New York, 1964.
- (44) Gao, Y.; Kogler, F.; Schubert, U. *Journal of Polymer Science: Part A* **2005**, 43, 6586-6591.
- (45) Schlitzer, D., PhD Dissertation, University of Massachusetts Amherst, 1998.
- (46) Debye, P. *Journal of Physical and Colloid Chemistry* **1947**, 51, 18-32.
- (47) Flory, P. *Principles of Polymer Chemistry*; Cornell University Press: Ithaca, 1953.
- (48) Green, M.; Reidy, M. *Journal of the American Chemical Society* **1989**, 111, 6452-6454.

- (49) Langeveld-Voss, B.; Waterval, R.; Meijer, E. *Macromolecules* **1999**, *32*, 227-230.
- (50) Jin, W.; Fukushima, T.; Niki, M.; Kosaka, A.; Ishii, N.; Aida, T. *Proceedings of the National Academy of Sciences of the United States of America* **2005**, *102*, 10801-10806.
- (51) Green, M.; Garetz, B.; Munoz, B.; Chang, H. *Journal of the American Chemical Society* **1995**, *117*, 4181-4182.
- (52) Aly, A.; Nour-El-Din, A. *ARKIVOC* **2008**, *2008*, 153-194.
- (53) Noyori, R. *Asymmetric Catalysis in Organic Synthesis*; Wiley: New York, 1994.
- (54) Mikami, K.; Terada, M.; Nakai, T. *Journal of the American Chemical Society* **1989**, *111*, 1940-1941.
- (55) Matsukawa, S.; Mikami, K. *Tetrahedron: Asymmetry* **1995**, *6*, 2571-2574.
- (56) Keck, G.; Geraci, L. *Tetrahedron Letters* **1993**, *34*, 7827-7828.
- (57) Casolari, S.; D'Addario, D.; Tagliavini, E. *Organic Letters* **1999**, *1*, 1061-1063.
- (58) Tang, H.; Garland, E.; Novak, B. *Macromolecules* **2007**, *40*, 3575-3580.
- (59) [http://barrett-group.mcgill.ca/teaching/liquid\\_crystal/LC01.htm](http://barrett-group.mcgill.ca/teaching/liquid_crystal/LC01.htm).
- (60) Aharoni, S. *Macromolecules* **1979**, *12*, 94-103.
- (61) Aharoni, S.; Walsh, E. *Macromolecules* **1979**, *12*, 271-276.
- (62) Bianchi, E.; Ciferri, A.; Krigbaum, W. *Macromolecules* **1984**, *17*, 856-861.

## Chapter 2: Polymerization of Novel Ester-Bearing Carbodiimides

### 2.1. Introduction

Since the first living polymerization of a carbodiimide, reported in 1994,<sup>1</sup> several dozen polycarbodiimide structures have been synthesized and characterized by the Novak Group. The vast majority of these structures have simple aliphatic or aromatic pendant groups as substituents. Only a handful of them have pendant groups containing a heteroatom and most of these are either halogens, attached to an aromatic ring, or oxygen, in the form of relatively inert ether groups. Prior to the work in this chapter, only two carbodiimides containing ester functionalities have been polymerized, Figure 2.1.<sup>2</sup>

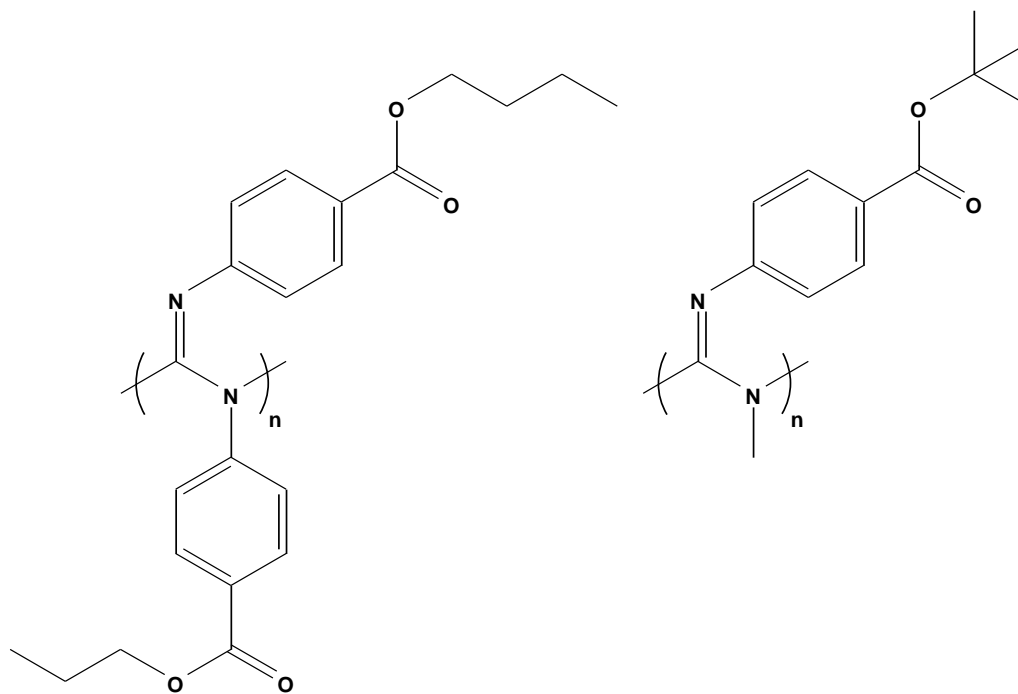


Figure 2.1: The two polycarbodiimides bearing an ester pendant group synthesized by Jeonghan Kim.<sup>2</sup> Each of these structures was synthesized via living polymerization with a titanium catalyst. A noteworthy feature, later proven essential for the utilization of titanium catalysts, is the lack of enolizable protons.

## 2.2. Syntheses of Novel Ester-Bearing Carbodiimides

Following the establishment of living polymerization methodologies for carbodiimides,<sup>1,3</sup> and prior to initiation of this work, the predominant focus of research has been the exploration of properties inherent in the polycarbodiimide structures themselves. The revelation that these polymers adopt a helical conformation in the solid state that persists in solution led to voluminous chiro-optic experiments on the induction of biases in the helical conformation via chiral catalysts or pendant entities.<sup>4-6</sup> Other works have explored the liquid crystalline properties of polycarbodiimides<sup>7,8</sup> or the mechanics of a chiroptical switching phenomenon associated with pendant 1-naphthyl or 1-anthryl substituents.<sup>9-11</sup> Only perfunctory efforts have been made to modify polycarbodiimide structures following polymerization,<sup>2,12</sup> predominantly in the interest of altering the solubility.<sup>12</sup> This being the case, there has been little effort to synthesize and polymerize carbodiimide structures bearing functionally-modifiable pendant groups, which is the motive behind the following efforts to develop novel ester-bearing polycarbodiimides.

### 2.2.1. Standard Dehydration of 1,3-Disubstituted Ureas

The class of precursors most commonly utilized in the Novak Group for the synthesis of carbodiimides is 1,3-disubstituted ureas. These precursors are synthesized, typically in quantitative yields, via reaction of amines with isocyanates.<sup>13</sup> Dehydration of a 1,3-disubstituted urea produces the carbodiimide.

While several alternative routes have been reported, the one that has become our standard utilizes triphenylphosphine dibromide in the presence of triethylamine.<sup>14,15</sup>

In an effort to access the rich world of peptide chemistry with the polycarbodiimide architecture, efforts to develop novel ester-bearing carbodiimides began with the methyl ester-substituted derivative of the simplest chiral amino acid, alanine. By reacting L-alanine methyl ester hydrochloride with various isocyanates, and dehydrating the resulting 1,3-disubstituted ureas, several methyl ester-bearing carbodiimides were synthesized for polymerization testing, Figure 2.2. The noteworthy feature shared by these carbodiimides is the presence of an enolizable proton. The synthesis of high molecular weight polymers from carbodiimides having enolizable protons proved to be a challenging synthetic endeavor.

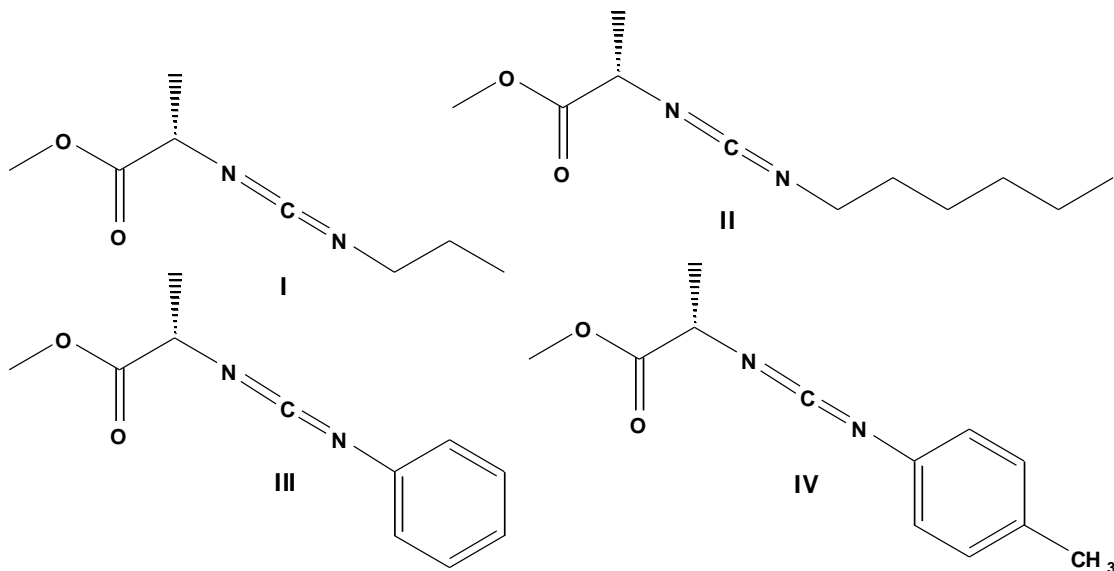


Figure 2.2: Illustration of four methyl ester-bearing carbodiimide structures derived by reacting L-alanine methyl ester hydrochloride with various aliphatic or aromatic isocyanates in pyridine solvent and dehydrating the resulting 1,3-disubstituted ureas with triphenylphosphine dibromide in methylene chloride and triethylamine.

## 2.2.2. Standard Desulfurization of 1,3-Disubstituted Thioureas

The second most commonly utilized class of carbodiimide precursors in the Novak Group is 1,3-disubstituted thioureas. These precursors are synthesized, typically in situ, via reaction of amines with isothiocyanates and are the fallback when the isocyanate needed to synthesize the analogous urea precursor is not commercially available. Desulfurization of a 1,3-disubstituted thiourea produces the carbodiimide. Though a variety of metal oxides, such as those of zinc,<sup>16</sup> arsenic,<sup>17</sup> lead, and silver<sup>18</sup> are reported to effect thiourea desulfurizations, and have been sporadically tested by our group members, the one that remains our standard is the classical method utilizing mercuric oxide in the presence of a dehydrating agent.<sup>19</sup>

In an effort to expand the library of novel ester-bearing carbodiimides for polymerization testing, L-alanine methyl ester hydrochloride was reacted with 4-fluorophenylisothiocyanate, which was then desulfurized in situ to afford an 83% yield of the corresponding carbodiimide, Figure 2.3.

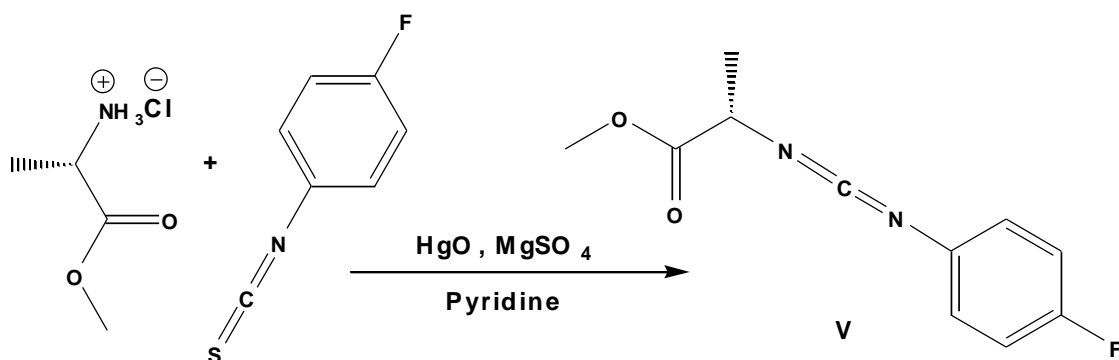


Figure 2.3: Synthesis of an L-alanine methyl ester-bearing carbodiimide via desulfurization of a 1,3-disubstituted thiourea generated in situ. Mercuric oxide, the classical metal oxide utilized for this method, is coupled with the dehydrating reagent magnesium sulfate, used to remove the H<sub>2</sub>O byproduct. HgS is also generated and can be easily removed by filtering through diatomaceous earth.

The 4-chlorophenyl analogue of this carbodiimide was synthesized via the alternate, urea precursor route. But the yield, 3%, was too low for subsequent polymerization studies, which leads to an important point. Beyond consideration of the commercial availability of isocyanate versus isothiocyanate starting materials, the choice of which route to utilize for a given synthesis is often dictated by the influence of the resulting carbodiimide's physical properties on purification efforts. Desulfurization of the thiourea proves to be the route of choice in cases such as these, where the resulting carbodiimides are very polar. Strong dipole-dipole interactions make the volatility of the carbodiimide comparable to that of the triphenylphosphine oxide byproduct of the urea precursor route, which precludes purification via vacuum distillation. Having a high polarity also complicated separation of the carbodiimide from triphenylphosphine oxide via column chromatography, where too little time on the column would have led to co-elution, while too much led to a greatly reduced recovery as a result of product degradation.

### 2.2.3. Alternative Strategies for Carbodiimide Synthesis

Aside from the aforementioned strategies, there are many others reported to effect the respective dehydration and desulfurization of 1,3-disubstituted ureas and thioureas. For instance, in addition to its use with bromine in the dehydration of ureas, triphenylphosphine is reported to effect the desulfurization of thioureas in the presence of triethylamine and carbon tetrachloride.<sup>20</sup> Reactive chlorine compounds, such as  $\text{SOCl}_2$ ,  $\text{SO}_2\text{Cl}_2$ ,  $\text{SCl}_2$ , or  $\text{S}_2\text{Cl}_2$ , are also reported to convert thioureas into

carbodiimides.<sup>21</sup> Another curious desulfurization strategy invokes one carbodiimide to form another, where dicyclohexylcarbodiimide, DCC, reacts with thiourea to equilibrate a new carbodiimide and N,N'-dicyclohexylthiourea, Figure 2.4.<sup>22</sup>

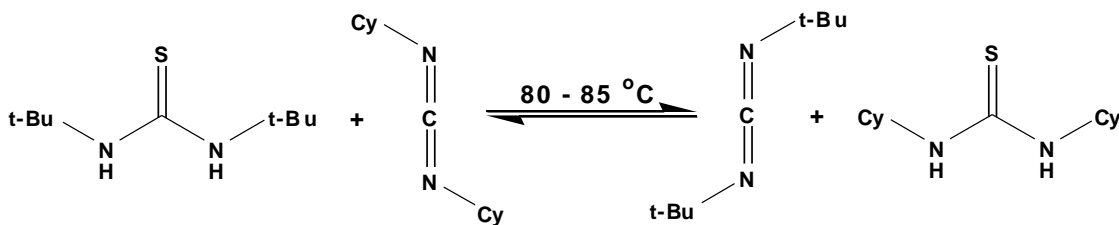


Figure 2.4: The reaction of N,N'-di-t-butylthiourea with DCC leads to N,N'-di-t-butyl carbodiimide and N,N'-dicyclohexylthiourea. Curiously, the reaction of DCC with N,N'-dimethylthiourea under the same conditions is reported to produce dimethyl cyanamide,  $\text{Me}_2\text{NC}\equiv\text{N}$ , instead.<sup>22</sup>

Of the alternative procedures for the dehydration of ureas, perhaps the one most self-touted is described in a Nutrasweet Patent, claiming to produce – in “high yield” no less – a carbodiimide of such immaculateness that “it may be used without further purification.” This patented, “Nutrasweet Method” of carbodiimide synthesis calls for dehydrating the urea with p-toluenesulfonyl chloride and pyridine in refluxing methylene chloride, followed by two aqueous washes, one with sodium bicarbonate, the other with aqueous acid. Subsequent removal of the methylene chloride is purported to afford the pure carbodiimide.<sup>23</sup> Multiple attempts, by several investigators within the Novak Group, to replicate the stellar success of this report have failed for a variety of 1,3-disubstituted ureas, including a pair derived from L-alanine methyl ester hydrochloride.

Another procedure for the dehydration of 1,3-disubstituted ureas utilizes reactive chlorine compounds. Both phosgene,  $\text{COCl}_2$ ,<sup>24</sup> and phosphorus

pentachloride,  $\text{PCl}_5$ ,<sup>25</sup> reportedly react with ureas, having secondary or tertiary alkyl substituents, to produce chloroformamidinium hydrochlorides, which, upon treatment with triethylamine, are said to generate carbodiimides.<sup>18</sup> One effort to employ the latter in our research led to a curious result. While dehydrating a urea derived from L-alanine methyl ester hydrochloride reacted with p-tolylisocyanate, not only did the phosphorus pentachloride facilitate dehydration, it also chlorinated the benzylic position of the 4-methylphenyl substituent, Figure 2.5. A search of literature on phosphorus pentachloride reactivity revealed a previous report of analogous chlorinations.<sup>26</sup> Though the product of this experiment was of synthetic interest, the cost of the starting materials, coupled with the meager reaction yield, 5%, precluded subsequent investigations.

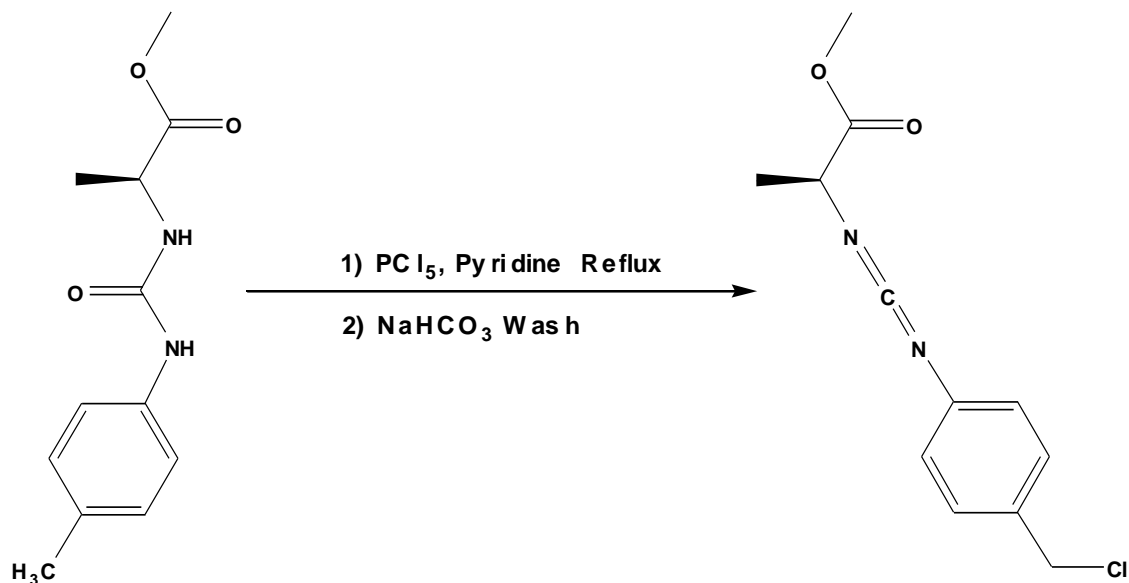


Figure 2.5: Phosphorus pentachloride is a highly reactive reagent. In this experiment, not only did it generate the chloroformamidinium hydrochloride intermediate, which reacted with base to form the carbodiimide, it also chlorinated the benzylic position of the 4-methylphenyl substituent.

### 2.3. Polymerization of Novel Ester-Bearing Carbodiimides

In the interest of developing functionally-modifiable polycarbodiimides, a variety of novel ester-bearing monomers were synthesized. Of primary interest were ester-protected amino acids, which, if incorporated as pendant groups, might open doors to the field of peptide chemistry for the polycarbodiimide architecture. Using the methods discussed in the previous section, approximately half a dozen designs – pairing methyl ester-protected L-alanine with various aliphatic and aromatic substituents – were synthesized for polymerization testing. The discussion that follows recounts the ordeal of developing an innovative methodology for polymerizing these novel carbodiimides and for removing the low molecular weight contaminants that are inevitable byproducts of this thermally-driven process.

#### 2.3.1. Studies with Traditional Polymerization Catalysts

As described in Chapter 1, there are two categories of catalysts developed by the Novak Group for the living polymerization of carbodiimides, those based on a titanium (IV) species,<sup>1</sup> and those based on a copper species in either a +1 or +2 oxidative state.<sup>3</sup> To those uninitiated in polycarbodiimide research, a cursory review of our literature might lead one to speculate that the copper catalyst systems are the superior choice.<sup>3</sup> Compared to those made with titanium, they are more tolerant of moisture and air. They tolerate a much larger array of functional groups, which allows them to polymerize carbodiimides in solvents – such as acetone and ethyl acetate – that are not compatible with titanium (IV) catalysts. The polydispersity of

polycarbodiimides, prepared with copper catalyst, is comparable to that of those prepared with titanium catalysts and the yields of these copper-catalyzed polymerizations are excellent, ranging from 70 to 100%.

In spite of the aforementioned advantages, copper catalysts have three salient drawbacks. First, copper catalysts often exhibit poor solubility. The simple CuCl and CuCl<sub>2</sub> salts are only sparingly soluble in low polarity solvents. Cu(OMe)Cl is even less soluble and has been suggested by others to exist as aggregated structures in which each methoxide bridges two copper cations.<sup>27</sup> Even with the copper-amidinate complexes, solubility limitations are sometimes an issue. The second problem with copper catalysts is that the copper-amidinate complexes were difficult to make or, more specifically, challenging to purify. Finally, polycarbodiimides made with copper catalysts were often colored, suggesting contamination of the sample with residual copper following the workup.<sup>28</sup>

In contrast, titanium catalysts exhibit good solubility in a variety of solvents, including benzene, toluene, methylene chloride, chloroform, diethyl ether, and tetrahydrofuran. The titanium metal is also easily removed by precipitating a hydrocarbon solution of the crude polymer in alcohol. And though titanium catalysts are moisture- and air-sensitive, they are not difficult to make or challenging to purify for researchers who are skilled in the art of Schlenk techniques. Furthermore, recent research, detailed in Section 3.5., indicates that polymerizations of asymmetric carbodiimides facilitated by titanium (IV) are more regioselective than those carried out in the presence of copper (II).

Nevertheless, it is the ability of copper catalysts to tolerate a larger array of functional groups that ultimately proved decisive in the quest to polymerize novel ester-bearing carbodiimides. Preliminary studies revealed titanium catalysts to have little or no compatibility with carbodiimides **I**, **II**, and **III**. Our most active titanium catalyst,  $\text{TiCl}_3\text{OCH}_2\text{CF}_3$ , failed to polymerize any of the three. A less active titanium catalyst,  $\text{CpTiCl}_2\text{OCH}_2\text{CF}_3$  also failed to polymerize carbodiimides **I** and **II**, but did polymerize carbodiimide **III** to a limited extent. The  $^1\text{H}$  NMR spectrum indicates the presence of both high and low molecular weight products, in comparable quantities, as evidenced, respectively, by the mixture of broad and sharp signals having relatively equal intensities, Figure 2.6.

Following reflection on these preliminary results, one salient feature of carbodiimides **I**, **II**, and **III** conceivably responsible for their incompatibility with titanium catalysts is the presence of an enolizable proton, a feature conspicuously absent on the structure of the pair of ester-bearing carbodiimides successfully polymerized by Jeonghan Kim with a titanium catalyst in earlier studies.<sup>2</sup> Anticipating that copper catalysts, capable of polymerizing carbodiimides in ethyl acetate,<sup>3</sup> would prove more compatible with these structures, polymerization feasibility studies on carbodiimides **I**, **II**, and **III** were initiated with copper (II) chloride. In contrast to their mixture with titanium catalysts, which resulted in decomposition characterized by darkening discoloration and a loss of intensity for the  $\text{N}=\text{C}=\text{N}$  infrared absorption, the mixture of these carbodiimides with copper (II) chloride resulted in no discernible reaction.

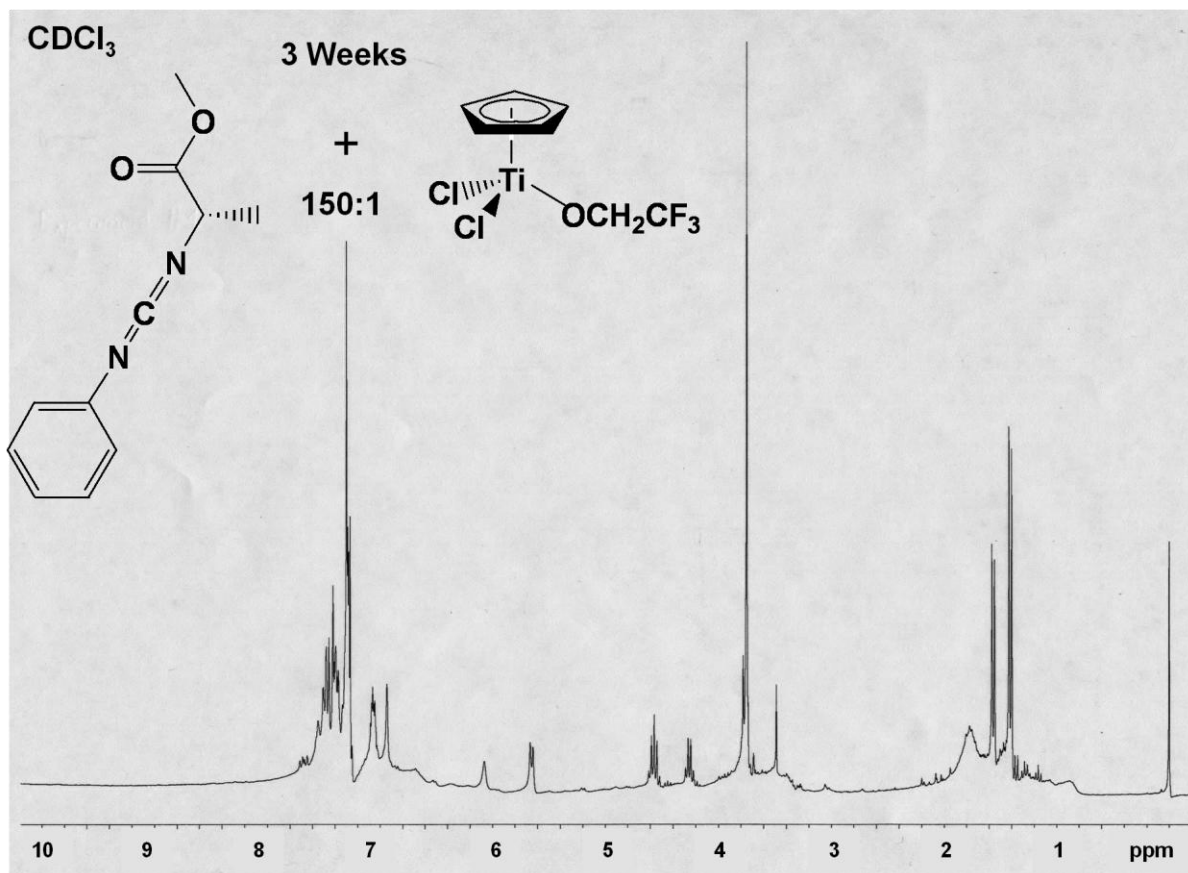


Figure 2.6:  $^1\text{H}$  NMR spectrum of the product resulting from carbodiimide **III** reacted with  $\text{CpTiCl}_2\text{OCH}_2\text{CF}_3$ . The profile indicates high molecular weight materials, characterized by broad signals, mixed with a comparable quantity of low molecular weight materials, characterized by sharp signals.

Considering the lack of reactivity between these carbodiimides and copper (II) chloride, a reasonable question to ask is whether the activation energies of these polymerizations were simply inaccessible at room temperature. Predicaments of this nature, observed by previous investigators in the Novak Group, have been successfully resolved on occasion by running polymerizations at an elevated temperature. Andrew Goodwin synthesized a pair of 1,2-dicarbodiimides that polymerized in high yield with  $\text{TiCl}_3\text{O-iPr}$  when heated to  $85\text{ }^\circ\text{C}$ , but failed to react appreciably at room temperature.<sup>4</sup> Jeoghan Kim successfully polymerized N,N'-bis(4-n-butylphenyl)carbodiimide at  $45\text{ }^\circ\text{C}$  with a chiral titanium catalyst, a reaction that also failed at room temperature, Figure 2.7.<sup>2</sup>

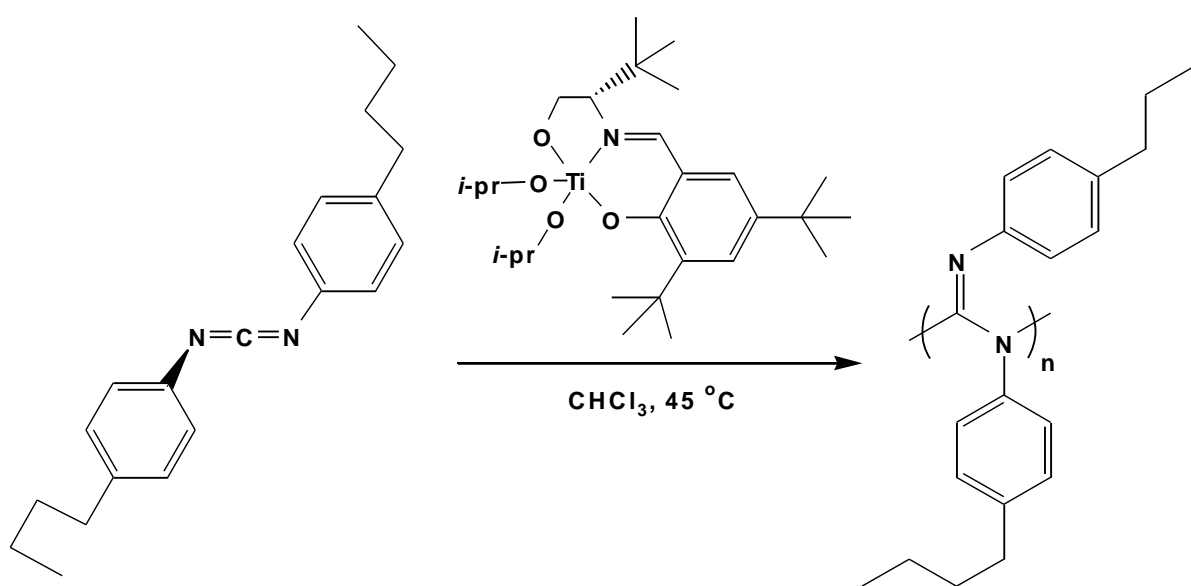


Figure 2.7: The polymerization of N,N'-bis(4-n-butylphenyl)carbodiimide fails at room temperature due to the heightened activation energy resulting from the steric hindrance of the bulky pendant groups and ligand, respectively, on the carbodiimide and catalyst. Gentle heating provides sufficient energy to facilitate polymerization.

Giving consideration to those precedents, follow-up experiments were conducted on carbodiimides **I**, **II**, and **III** with copper (II) chloride at 60 °C. At this elevated temperature, carbodiimides **I** and **II** became discolored in the presence of CuCl<sub>2</sub>, but again failed to polymerize. However the reaction of carbodiimide **III** with CuCl<sub>2</sub> gradually increased in viscosity over the course of one month, after which cooling to room temperature produced a solid black tar. The <sup>1</sup>H NMR spectrum following workup indicates a polymeric structure as the major product, evidenced by the predominance of broad, versus sharp, signals, Figure 2.8.

Following this discovery with carbodiimide **III**, a pair of derivatives, having either an electron-donating methyl group, **IV**, or an electron-withdrawing fluorine, **V**, on the para-position, were synthesized for polymerization testing. When heated with CuCl<sub>2</sub>, carbodiimide **IV** polymerized at a rate that was not appreciably different from the rate at which **III** did. This was not surprising given that the magnitude of electron donation, and hence the electronic distinction between **III** and **IV**, is mild. However, when carbodiimide **V** was heated to 60 °C with CuCl<sub>2</sub>, the reaction proceeded much faster, indicating that the strong electron-withdrawing fluorine accelerates polymerization. This result correlates with general observations from the field of carbodiimide chemistry that electron-withdrawing groups on aromatic substituents reduce the stability of carbodiimides, increasing their polymerization tendency, as noted in Henri Ulrich's book on the "*Chemistry and Technology of Carbodiimides*."<sup>18</sup>

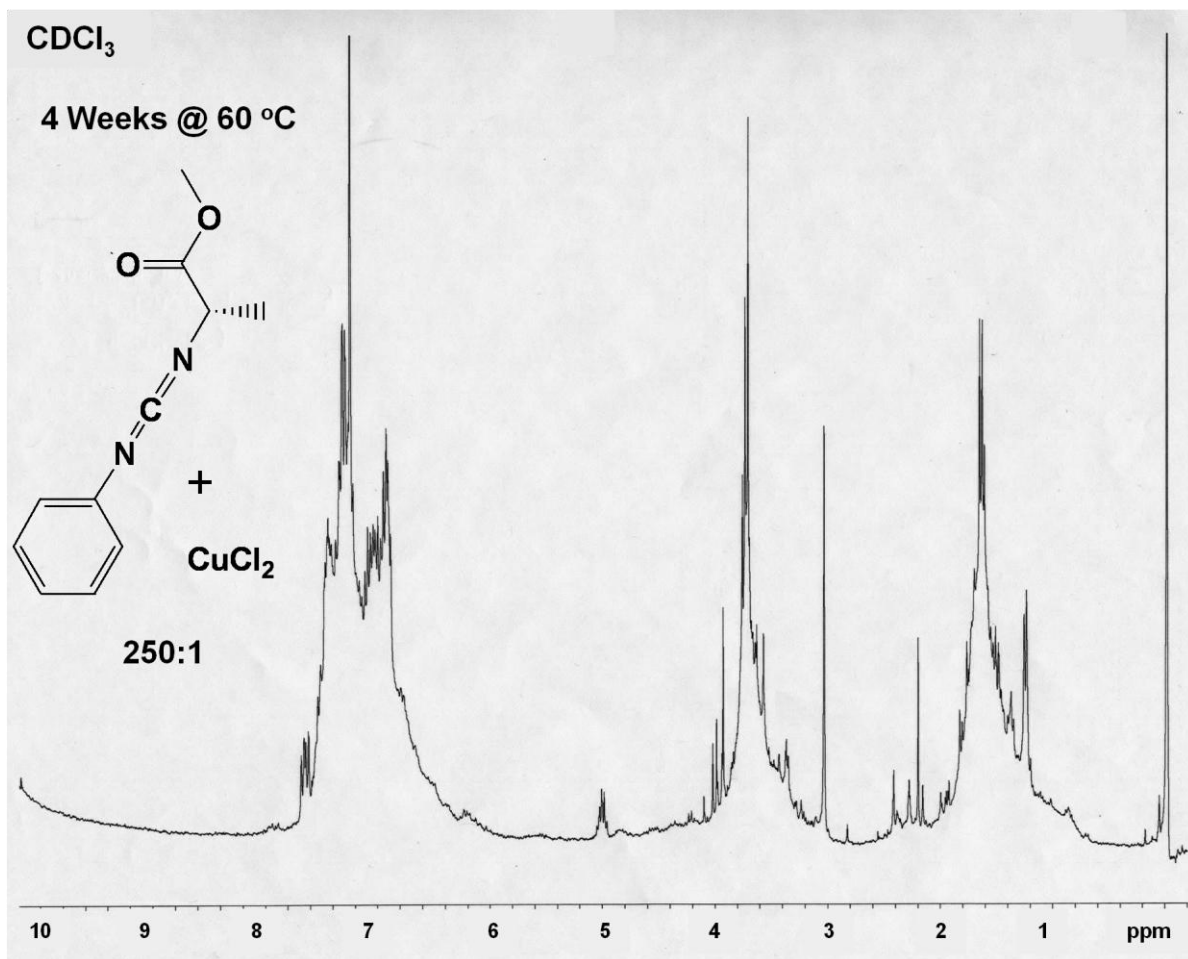


Figure 2.8: <sup>1</sup>H NMR spectrum of the product resulting from carbodiimide **III** reacted with CuCl<sub>2</sub> for 1 month at 60 °C. The profile indicates primarily high molecular weight material, as evidenced by the predominance of broad, versus sharp, signals.

### 2.3.2. Thermally-Induced Carbodiimide Polymerization

Given that the combination of copper (II) chloride with heat polymerizes carbodiimide **III**, where copper (II) chloride alone fails, we know that heat is an essential element in the polymerization process. The question that remains is whether the copper (II) chloride is also an essential element, whether heat alone is capable of facilitating polymerization. An experiment, heating carbodiimide **III** at 60 °C in the absence of any catalyst, revealed that heat alone does indeed facilitate polymerization, and it does so at a rate that is not distinguishable from that at which heat does so in the presence of various catalytic amounts of copper (II) chloride.

The discovery that copper (II) chloride does not accelerate the polymerization of carbodiimide **III** opens the question of what effect, if any, the presence of copper (II) chloride does have on the reaction process. A comparison of the <sup>1</sup>H NMR spectra of poly-**III** synthesized by heating in the presence of CuCl<sub>2</sub>, Figure 2.8, with poly-**III** made in the absence of CuCl<sub>2</sub>, Figure 2.9, reveals the latter to have fewer and less intense sharp signals, indicating that, rather than facilitating polymerization, the copper (II) chloride actually catalyzes the formation of small molecules, such as dimers and trimers. *Heating **III** in the absence of copper (II) chloride actually leads to a cleaner polymerization!*

This result correlates with the observation that heating in the absence of catalyst leads to a brittle, translucent, light-brown solid, while heating in the presence of CuCl<sub>2</sub> instead produces a sticky black tar. In the latter case, the dimer and trimer contaminants heavily discolor the product and function as plasticizers.

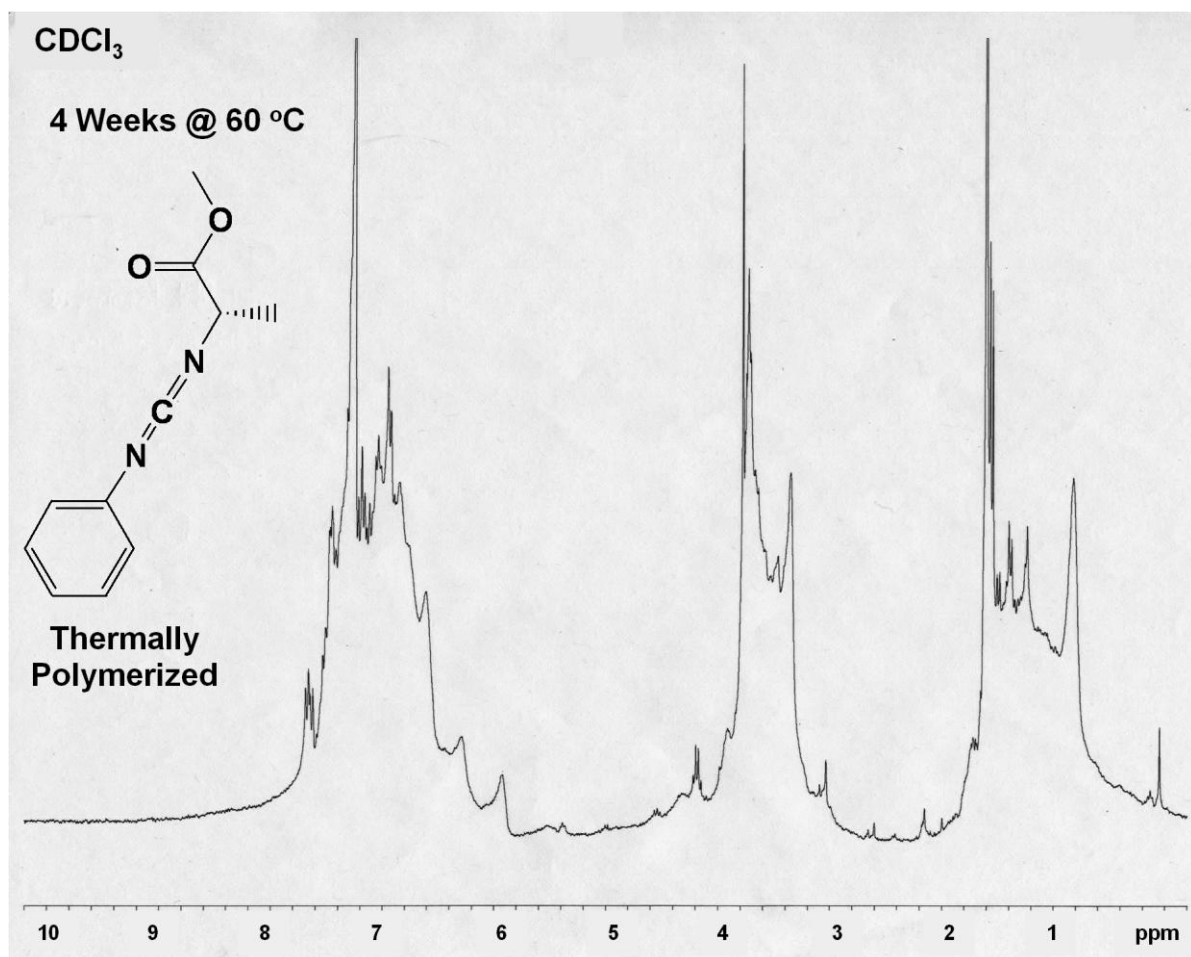


Figure 2.9: <sup>1</sup>H NMR spectrum of the thermal polymerization product resulting from heating carbodiimide **III** at 60 °C for 4 weeks in the absence of catalyst. When compared with the spectrum of the polycarbodiimide formed under the same conditions in the presence of CuCl<sub>2</sub>, Figure 2.8, this spectrum has fewer and less intense sharp signals, suggesting that thermal polymerization in the absence of CuCl<sub>2</sub> proceeds more cleanly, and that rather than facilitating polymerization, CuCl<sub>2</sub> actually catalyzes the formation of small molecules, such as dimers and trimers.

### 2.3.3. Thiolate-Initiated, Thermal Polymerizations

Since the polymerization of carbodiimides with catalysts based on copper (I) and (II), as well as those based on titanium (IV), is thought to be initiated via insertion of the carbodiimide into the bond between the metal and the initiating ligand, it is logical to ask whether limitations in this regard, for a given combination of carbodiimide and catalyst, relate to the nucleophilicity of the initiating ligand. The failure of copper (II) chloride to initiate the polymerization of carbodiimide **III** is a case in point. Given that chloride is generally considered a fair nucleophile, the question is whether a ligand that is a good nucleophile, such as cyanide or an alkoxide, or an excellent nucleophile, such as a thiolate, might succeed in initiating carbodiimide polymerizations, with copper (I) or (II), where chloride fails.

Earlier research on the polymerization of carbodiimides, with copper (I) and (II), explored the utility of two catalysts using alkoxide initiating ligands.<sup>3</sup> One, Cu(O-t-Bu), polymerized N,N'-di-n-hexylcarbodiimide within 1 week at room temperature, but the yield of the reaction, 54%, was relatively low compared with that of the analogous reaction using CuCl (96%). The other, Cu(OMe)Cl, polymerized N,N'-di-n-hexylcarbodiimide in much higher yield, 99%, a result that is more likely attributable to the enhanced oxidative state of the copper rather than to the reduced steric hindrance of the smaller methyl substituent. When compared with the 100% yield of the analogous reaction using CuCl<sub>2</sub>, again, there appears to be no inherent advantage from the use of an alkoxide initiating ligand.

The earlier studies also investigated three copper-amidinate complexes, Figure 1.5.<sup>3</sup> The good nucleophilicity of the amidinate ligand, coupled with the enhanced solubility of their copper complexes, did make the copper amidinates highly active polymerization catalysts for carbodiimides. However, as mentioned earlier, the challenges of synthesizing and purifying these copper-amidinate complexes discouraged their utilization in subsequent research. Given this consideration, efforts to find a superior copper catalyst for the polymerization of novel ester-bearing carbodiimides began with a search of commercially-available copper salts. A quick survey of the Aldrich catalogue revealed several candidates pairing copper with ligands having a nucleophilicity predictably greater than that of chloride, including CuBr, CuBr<sub>2</sub>, CuCN, and CuI.

Considering that thiolates are excellent nucleophiles, the two commercially-available salts that seemed most tantalizing were copper (I) butanethiolate and copper (I) thiophenolate. Since carbodiimides, and the solvents in which they are often polymerized, tend to be relatively non-polar, the alkyl and aryl chains respectively attached to these thiolates would enhance their carbodiimide solubility relative to that of the aforementioned, commercially-available copper salts. Preliminary experiments with these copper (I) thiolates, utilizing a 100:1 ratio of monomer to initiator, revealed butanethiolate to be superior, polymerizing N,N'-di-n-hexylcarbodiimide in 65% yield in 5 weeks at room temperature. Copper (I) thiophenolate, on the other hand, took 12 weeks to polymerized N,N'-di-n-hexylcarbodiimide, resulting in a yield of merely 29%.

Follow-up experiments revealed that heating carbodiimide **III** with copper (I) butanethiolate greatly accelerated polymerization at 60 °C. Whereas heating **III** in the absence of any catalyst produces a solid polymer in approximately 1 month, heating in the presence of copper (I) butanethiolate results in solid polymer within roughly a week. The rate of polymerization proves inversely proportional to the ratio of carbodiimide to catalyst. For instance, a ratio of 50:1 results in a highly viscous reaction mixture within 2 days, while ratios of 250:1 and 500:1 require 5 and 8 days, respectively, to produce mixtures of comparable viscosity. Sadly, these reactions prove not to be well-defined living polymerizations, as sharp signals, suggesting the presence of dimers and trimers, are clearly apparent in the <sup>1</sup>H NMR spectra of these thiolate-initiated, thermally-polymerized polycarbodiimides, Figure 2.10.

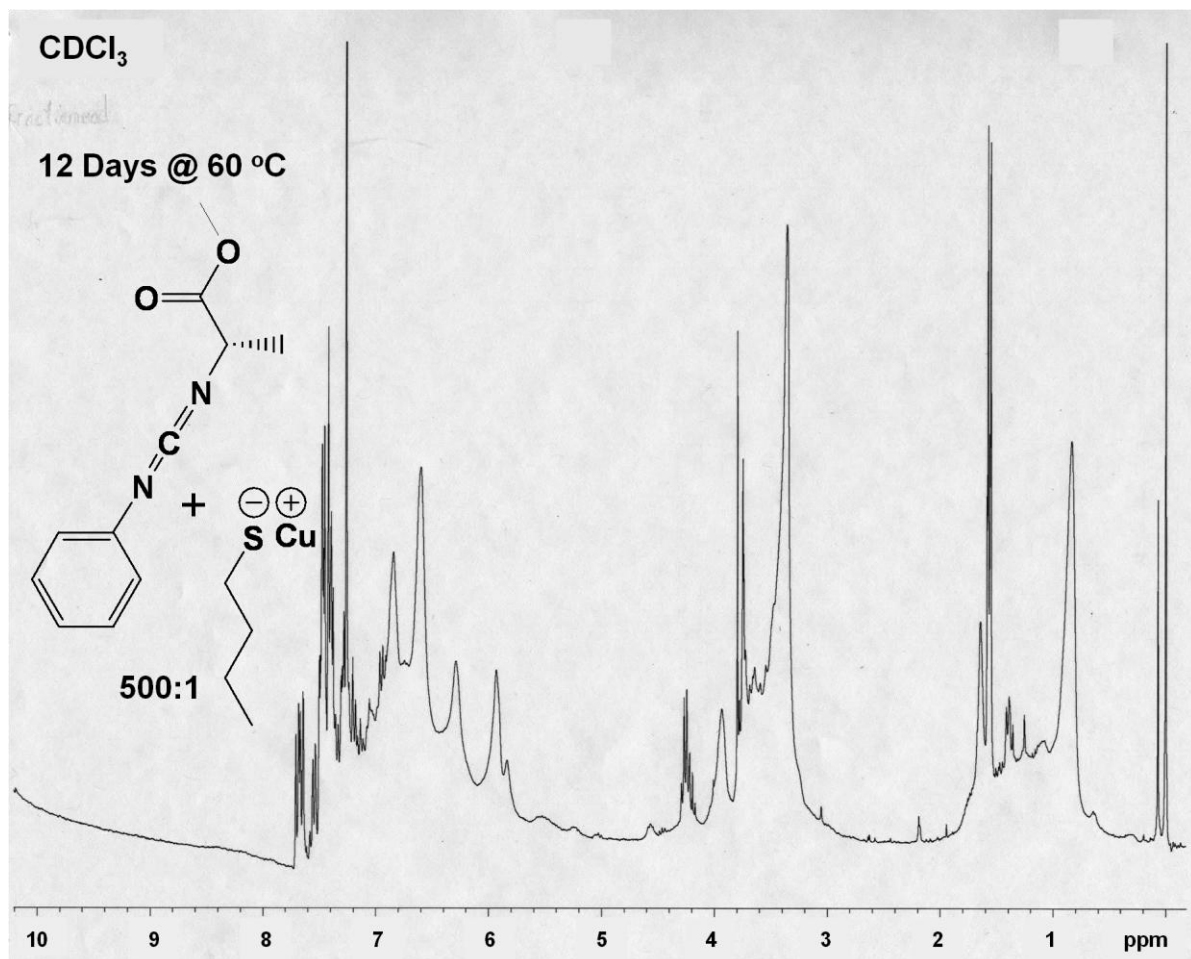


Figure 2.10: <sup>1</sup>H NMR spectrum of the product resulting from heating carbodiimide **III** with copper (I) butanethiolate. Though the spectrum consists predominately of broad, polymer signals, the intensity of sharp signals indicates greater contamination from small molecules than when the polymer is formed upon heating in the absence of catalyst, Figure 2.9. It seems that greater diversion of carbodiimide, down byproduct pathways leading to dimers and trimers, is an unavoidable cost of utilizing copper (I) butanethiolate to accelerate these heated polymerization reactions.

## 2.4 The Dilemma of Dimers and Troublesome Trimers

In our efforts to develop novel ester-bearing polycarbodiimides, we are faced with a dilemma. On one hand, heat alone facilitates relatively clean, thermal polymerization. But these uncatalyzed reactions take many weeks and afford no control of molecular weight. On the other, heating with copper (I) butanethiolate catalyzes polymerization within days and affords molecular weight control via carbodiimide-to-catalyst ratio. However, copper (I) lowers the activation energy of dimer and trimer formation more than it does for the rate limiting step of polymerization. Lastly, the prototype carbodiimide, **III**, proves unreactive with copper (I) butanethiolate at 25 °C, leading to our dilemma: dimers and trimers are inevitable byproducts of the optimum conditions for the polymerization of such carbodiimides.

### 2.4.1. Raising the Roof: What's Going Down Above $T_c$

For any reaction involving an equilibrium between monomer and polymer, the free energy of the polymerization can be expressed by the equation

$$\Delta G_p = \Delta H_p - T\Delta S_p \quad (3.1)$$

where  $\Delta G_p$ ,  $\Delta H_p$ , and  $\Delta S_p$  are the respective differences in free energy, enthalpy, and entropy between one mole of monomer and one mole of polymer repeat units.

A typical chain polymerization involves converting a monomer's higher energy  $\pi$ -bonds into the lower energy  $\sigma$ -bonds that bind the polymer's repeat units. Consequently, most chain polymerizations are highly exothermic, exhibiting a large,

negative  $\Delta H_p$ . Meanwhile, the act of binding monomers into repeat units typically reduces their degrees of freedom, leading to a mildly negative  $\Delta S_p$ .

Consequently, at low temperatures, the large, negative value of  $\Delta H_p$  dominates the free energy expression, resulting in spontaneous polymerization. However, at higher temperatures, the magnitude of the  $T\Delta S_p$  term increases, leading to a point at which its positive contribution to the free energy expression completely offsets the negative contribution of the  $\Delta H_p$  term. This point, when the free energy of polymerization equals zero, and equilibrium favors neither monomer nor polymer, is referred to as the ceiling temperature,  $T_c$ . Here, where  $\Delta G_p = 0$ , Eq. 3.1 simplifies to

$$T_c = \Delta H_p / \Delta S_p \quad (3.2)$$

Simply put, the ceiling temperature is the temperature above which spontaneous chain-growth polymerization does not occur for a given monomer. For carbodiimides, the ceiling temperatures that have been characterized range from 80 °C for N,N'-di-n-hexylcarbodiimide to 156 °C for ((R/S)-N-methyl-N'-( $\alpha$ -phenylethyl) carbodiimide.<sup>3</sup> At temperatures exceeding  $T_c$ , living polycarbodiimides unzip cleanly to monomer. But not all carbodiimides prove stable at elevated temperatures. For instance, N,N'-diphenylcarbodiimide forms dimer in 43% yield when heated at 165 to 170 °C for 16 hours.

Examples of carbodiimide dimerization abound in the literature. When catalyzed by tetrafluoroboric acid, aliphatic carbodiimides are reported to undergo rapid dimerization at room temperature, forming protonated dimeric salts that cleanly

afford the dimer upon neutralization with base.<sup>29</sup> Dimers of dibenzylcarbodiimide have been isolated in low yield from the distillation residue of the monomer.<sup>30</sup> Analogous dimerization reactions are suspected to account for much of our own loss of product while isolating carbodiimides via vacuum distillation.

Though less common, carbodiimide trimerizations have also been reported. For instance, heating N,N'-diphenylcarbodiimide with N-methylhexamethyldisilazane is reported to produce the diphenylcarbodiimide trimer.<sup>31</sup> Unheated, uncatalyzed reactions of this sort have also been observed, as in the case of N,N'-dimethylcarbodiimide, reported to undergo trimerization on standing at room temperature.<sup>32</sup>

When reacted with copper (I) butanethiolate above its ceiling temperature, carbodiimide **III** undergoes relatively clean dimerization. <sup>1</sup>H NMR reveals only sharp signals and suggests a single, low molecular weight product. Analysis by LC/MS reveals predominately dimer. Though there are many potential stereoisomers of such dimers, Figure 2.11, the extracted ion chromatograph of the 409 m/z ratio indicates a single, dominant stereoisomer along with three stereoisomers present in trace, Figure 2.12. An extracted ion chromatograph of the 613 m/z ratio picks up seven trimeric stereoisomers, two dominant, four trace, Figure 2.13. Though precise quantitative comparisons among the relative amounts of dimers and trimers cannot be made, it is clear from the near invisibility of peaks corresponding to the 613 m/z ratio on the total ion chromatograph, relative to that corresponding to the dominant 409 m/z peak, that one dimeric stereoisomer is the vastly predominant product.

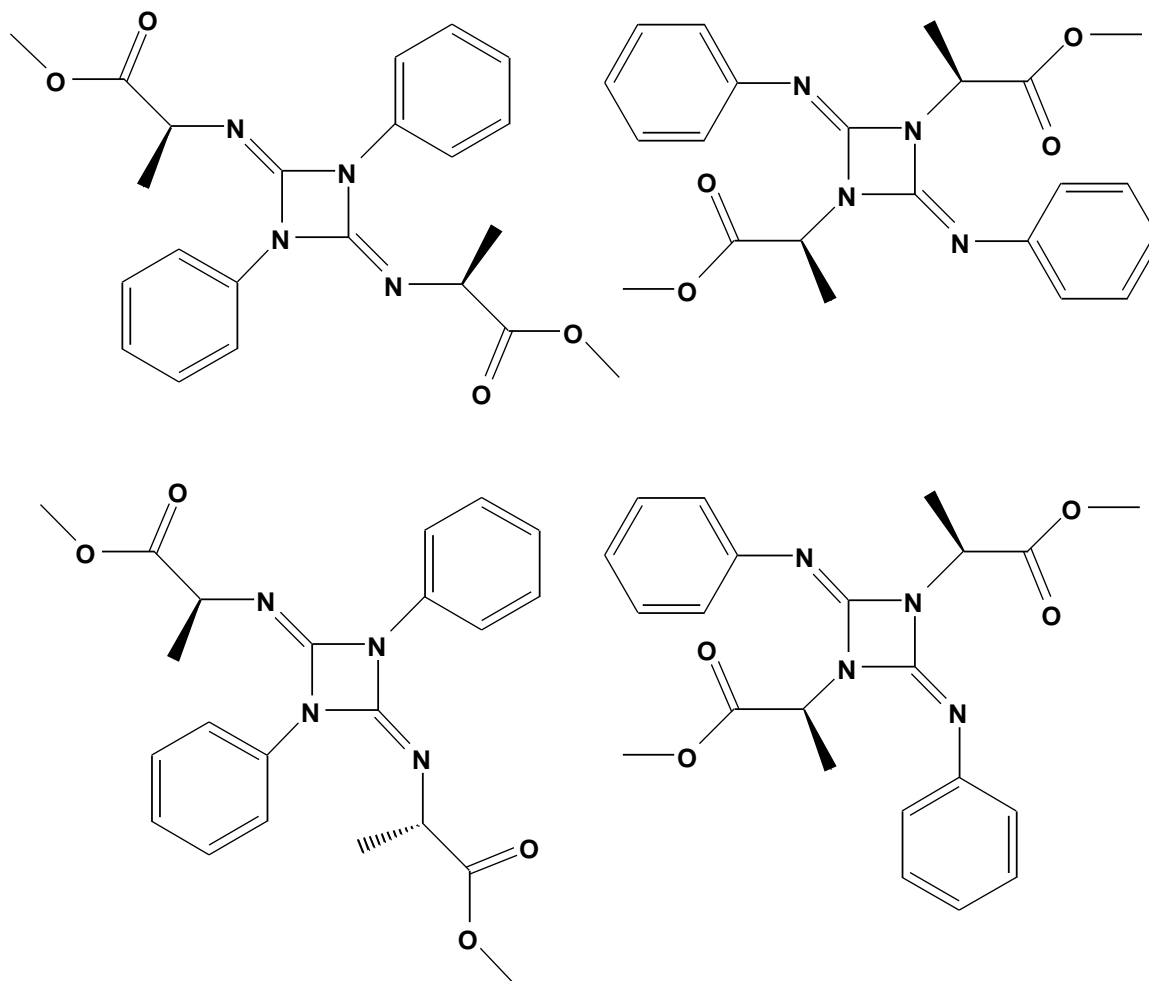


Figure 2.11: Four of the many conceivable stereoisomers that may be formed from the dimerization of N-phenyl-N'-(L-alanine methyl ester)carbodiimide. Others could have one phenyl substituent in an imine position while the other occupies an amine position. The pair at the top are referred to as E,E-isomers, while the pair beneath are referred to as Z,Z-isomers. Theoretical considerations are said to favor the formation of Z,Z-isomers.<sup>18</sup>

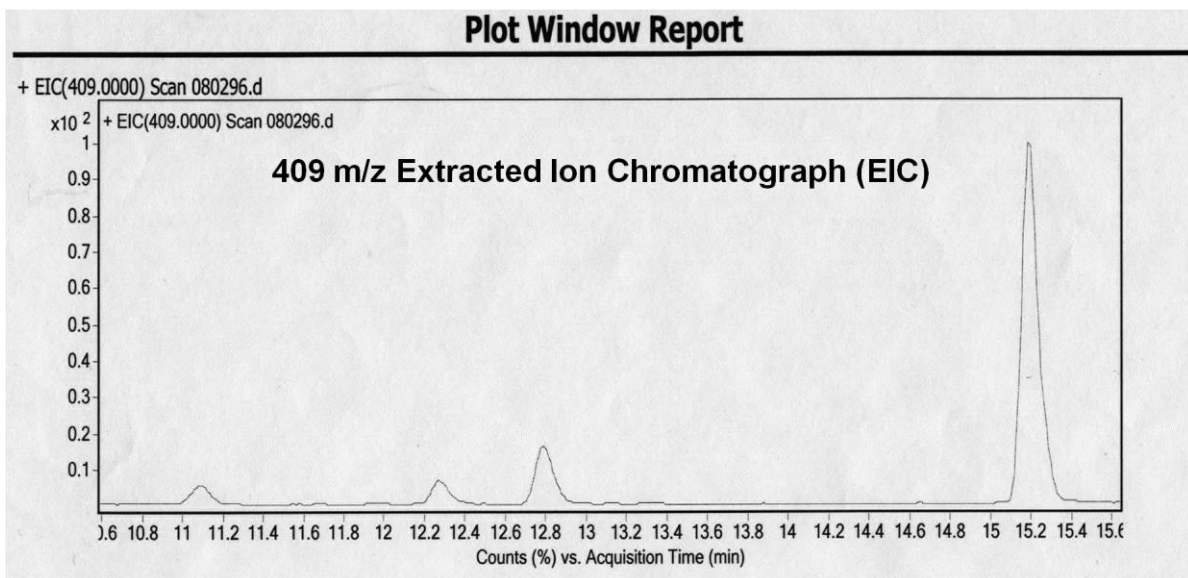


Figure 2.12: Extracted Ion Chromatograph of the 409 m/z ratio, corresponding to twice the mass of N-phenyl-N'-(L-alanine methyl ester)carbodiimide. The Total Ion Chromatograph indicates the dimer eluted at 15.2 min as the predominant small molecule.

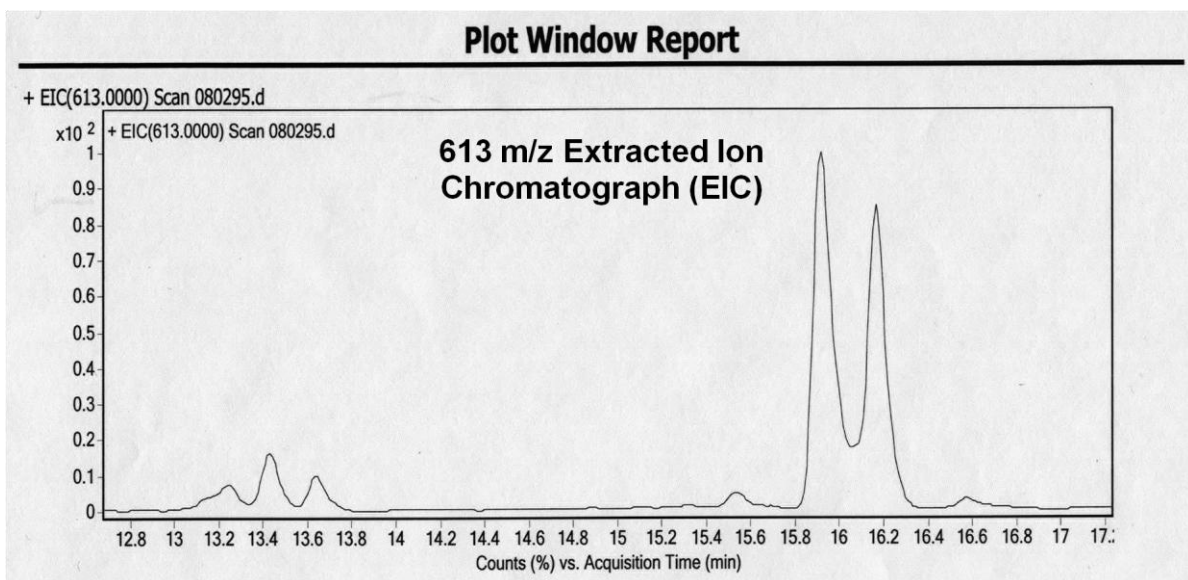


Figure 2.13: Extracted Ion Chromatograph of the 613 m/z ratio, corresponding to three times the mass of N-phenyl-N'-(L-alanine methyl ester)carbodiimide. The profile of the plot indicates at least seven trimeric stereoisomers, two predominant, four trace.

#### 2.4.2. Fractional Precipitation and Extraction: The Disposal of Disorderly Dimers

To review, the optimum polymerization conditions for our prototype ester-bearing carbodiimide, **III**, unavoidably produce small, stable molecules as well. Aside from facilitating polymerization, heating with copper (I) butanethiolate also catalyzes dimerization. The dimerization process becomes increasingly competitive at higher temperatures, where entropy disfavors polymerization, leading almost exclusively to dimers, with a trace of trimers, above the ceiling temperature.

Since the broad overlap of conditions catalyzing both polymerization and dimerization precludes exclusive polymer synthesis, the challenge becomes removing the dimers afterward. The standard approach to isolating high molecular weights utilizes the general principle that, with rare exception, a polymer's solubility decreases with increasing molecular weight. The two general methods of doing this are fractional precipitation, which progressively precipitates lighter fractions, and fractional extraction, which progressively extracts heavier fractions.<sup>33</sup>

Through a process of trial and error, following the synthesis of each batch of poly-**III**, a crude method was developed to successfully remove the vast majority of small molecule contaminants. The general procedure involves precipitating a single heavy fraction, followed by extracting a single light fraction from the heavy fraction. As a rule, the relative quantity of small molecules that remain is directly proportional to the total recovery. In other words, the higher the recovery, the higher the relative amount of contaminants. The <sup>1</sup>H NMR spectrum of a typical clean polymer reveals negligible amounts of dimer following a 33% recovery, Figure 2.14.

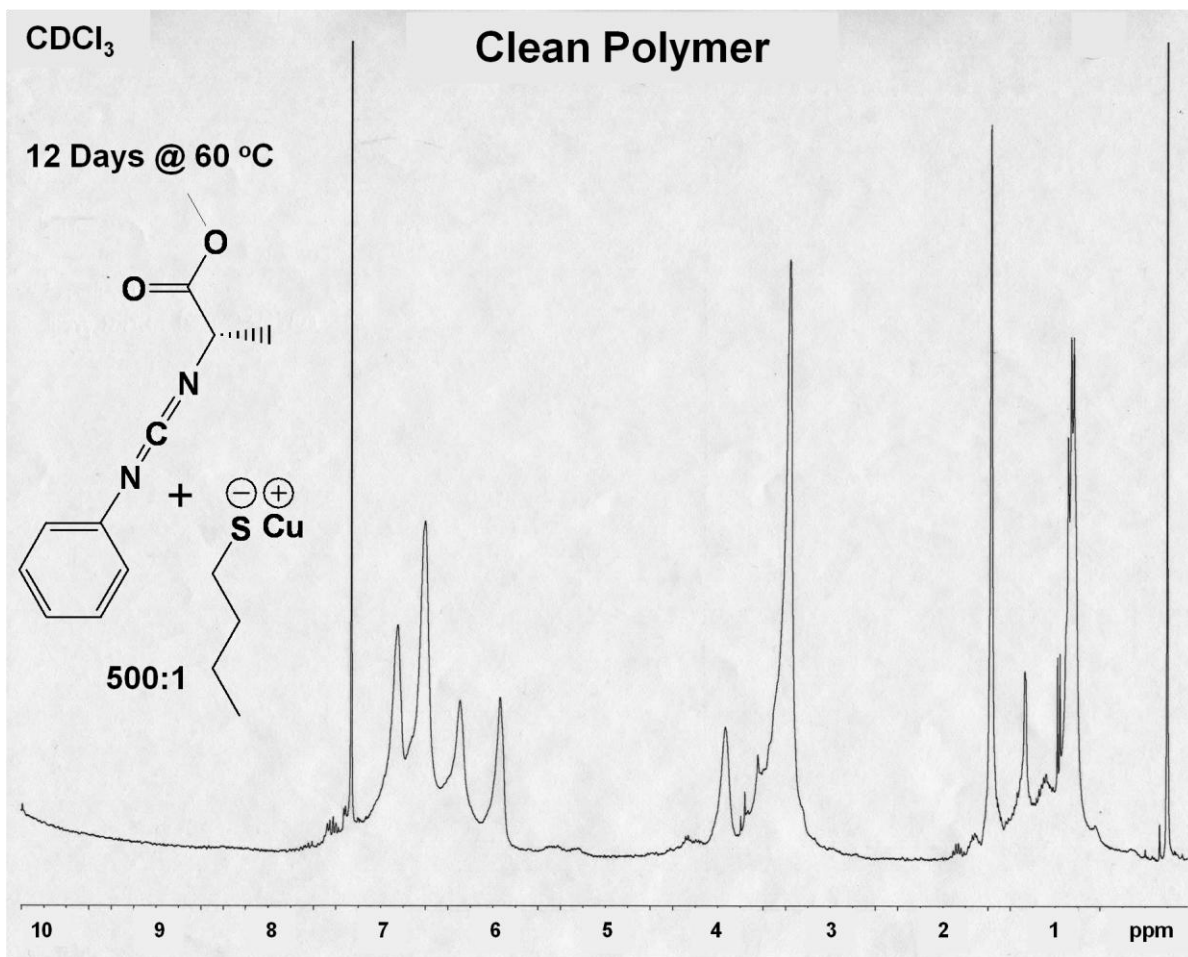


Figure 2.14: <sup>1</sup>H NMR spectrum of a clean polymer isolated by precipitation of a single heavy fraction, followed by washing away a single light fraction. The relative absence of sharp signals in this spectrum, compared with the spectrum of the unclean polymer, Figure 2.10, showcases the success of precipitating and extracting fractions in sequence to remove small molecule contaminants.

## 2.5. Conclusions

A series of novel ester-bearing carbodiimides have been synthesized from the simple, chiral amino acid, L-alanine. Research on the polymerization of these carbodiimides reveals all of them to be incompatible with the commonly used titanium (IV) catalysts. Investigations with copper catalysts led to the discovery that carbodiimides pairing an aryl substituent with the ester-bearing pendant group prove capable of polymerization, while those pairing an alkyl substituent with it do not. The presence of an electron-withdrawing group on the aryl substituent accelerates polymerization. Control reactions reveal the rate of heated polymerization to be unaffected by the presence of copper (II) chloride, that heat alone facilitates polymerization, and that  $\text{CuCl}_2$  merely catalyzes the formation of small molecules, such as dimers and trimers. Studies with copper (I) thiolates suggest that the nucleophilicity of the anion plays a vital role in determining its ability to initiate carbodiimide polymerizations exhibiting high activation energies. Copper (I) butanethiolate greatly accelerates the thermal polymerization of our prototype ester-bearing carbodiimide. The exploration of this carbodiimide's reactivity above the ceiling temperature reveals dimerization to be a thermally-favorable process. Since the broad overlap of conditions catalyzing both polymerization and dimerization precludes exclusive polymer synthesis, a general procedure – coupling a fractional precipitation with a fractional extraction – was developed to remove small molecule contaminants and isolate high molecular weights of these novel ester-bearing polycarbodiimides.

## 2.6. Experimental Section

### 2.6.1. General Procedures and Equipment

#### Instruments

All infrared spectra were recorded on a JASCO FT/IR-410 spectrometer. Characteristic absorptions are reported in wavenumbers ( $\text{cm}^{-1}$ ). All nuclear magnetic resonance spectra were recorded on Varian Mercury 300 or 400 MHz spectrometers. Chemical shifts are reported in  $\delta$  (ppm) relative to the assignment of solvent chemical shifts, referenced to tetramethylsilane, as listed in Table 3 of Appendix 4. Optical rotation measurements were recorded on a Jasco P-1010 Polarimeter at 589 nm. Solutions measured for optical rotation were prepared by dissolving 20 mg of sample overnight in 10 mL of solvent at room temperature. Thermogravimetric analyses were recorded on a TA Instruments Hi-Res TGA 2950 Thermogravimetric Analyzer. Differential Scanning Calorimetry analyses were performed with a TA Instruments DSC 2920 Modulated DSC.

#### Reagents

All reagents were obtained from a commercial supplier and used without further purification with the exception of solvents utilized for air- and moisture-sensitive procedures, which were purified under a nitrogen atmosphere via reflux over an appropriate drying agent,<sup>34</sup> followed by fractional distillation. 4A molecular sieves were oven-dried overnight at 215 °C, then cooled, and stored, in a desiccator. *The purity of commercially-supplied reagents was factored into all calculations in the sections that follow.*

## Inert Atmospheres

All air- and moisture-sensitive procedures were either conducted in a nitrogen-filled MBRAUN UNILab Dry Box or while utilizing Schlenk techniques facilitated by a Chemglass, CG-4441-03, 5-Port, Glass Stopcock, Inert Gas, Vacuum Manifold, coupled with a dual liquid nitrogen trap attached to a Welch Model Number 1402-01 Vacuum Pump. Vacuum pressures were observed with a Kurt J Lesker Company Millitorr Vacuum Gauge. Unopened, volatile-free, vacuum line pressures exceeding 50 mtorr were corrected by routine – typically weekly – vacuum line maintenance, which entailed Steps 12 through 16 of the more thorough “Guide to Vacuum Manifold Maintenance” procedure listed in Appendix 2. Glassware used for air- and moisture-sensitive procedures was dried overnight in an oven at 140 °C. Alternatively, glassware was flame-dried under vacuum (<100 mtorr). Stir bars utilized for air- and moisture-sensitive reactions were dried overnight, either in an oven at 140 °C or under vacuum (<100 mtorr). Alternatively, stir bars were retrieved from storage under nitrogen in the dry box. All septa were dried overnight in a vacuum chamber and stored under nitrogen in the dry box until used. All filter paper-covered, vacuum-needle assemblies utilized for air- and moisture-sensitive procedures were dried overnight in an oven at 140 °C.

## 2.6.2. Experimental Procedures and Characterizations

**N-phenyl-N'-(L-alanine methyl ester)urea.** L-alanine methyl ester hydrochloride, 99% (10.0 g, 70.9 mmol), a magnetic stir bar, and reagent grade pyridine (50 mL) were added to a 100 mL round bottom flask. Once the L-alanine methyl ester hydrochloride had dissolved, hexyl isocyanate, 98% (8.62 g, 70.9 mmol) was transferred into the flask by pipet. A pyridine rinse (1 mL) of the weighing vial was utilized to facilitate quantitative transfer. The reaction mixture was magnetically stirred overnight. The next day, pyridine was removed by rotovap at 50 °C followed by high vacuum for two days with the flask submerged in an oil bath heated to 50 °C. Chloroform (50 mL) and deionized water (50 mL) were added to the resulting goop. The flask was shook vigorously to achieve complete dissolution. Following separation, the chloroform extract was dried with a saturated sodium chloride wash (25 mL), followed by standing for 30 minutes over sodium sulfate. The solution was then added dropwise to refluxing hexanes (250 mL) to precipitate the urea. After cooling to room temperature, the flask containing the precipitated urea was placed in an ice-water bath. After cooling to 0 °C, a filter paper-covered, vacuum-needle assembly was utilized to remove the supernatant. [See Appendix 1 for filter paper-covered, vacuum-needle assembly instructions.] The remaining volatiles were removed by rotovap, followed by high vacuum to reveal 14.1 g of white powder (90% yield). IR (KBr Pellet) 3342 (s), 3093 (w), 3054 (w), 3027 (w), 2983 (m), 2959 (m), 2934 (m), 1735 (vs), 1638 (vs), 1227 (s), 640 (m)  $\text{cm}^{-1}$ ;  $^1\text{H}$  NMR (300 MHz, Acetone- $\text{d}_6$ )  $\delta$  (ppm) 8.09 (s, br, 1H), 7.46 (d,  $J = 8.4$  Hz, 2H), 7.22 (m,

2H), 6.92 (t, J = 7.5 Hz, 1H), 6.13 (d, br, J = 5.4 Hz, 1H), 4.41 (m, 1H), 3.69 (s, 3H), 1.36 (d, J = 7.2 Hz, 3H);  $^{13}\text{C}$  NMR (300 MHz,  $\text{CDCl}_3$ )  $\delta$  (ppm) 175, 156, 139, 129, 123, 120, 52.4, 48.9, 18.4.

**N-(4-methylphenyl)-N'-(L-alanine methyl ester)urea.** A procedure analogous to the one for the preparation of N-phenyl-N'-(L-alanine methyl ester) urea was employed. The quantities of reagents used were: 10.0 g (71.0 mmol) L-alanine methyl ester hydrochloride, 99%; 50 mL pyridine; and 9.54 g (71.0 mmol) p-tolyl isocyanate, 99%. Yield: 17.4 g White Powder (90%). IR (KBr Pellet) 3323 (s), 3098 (w), 3032 (w), 2992 (m), 2953 (m), 1740 (s), 1637 (vs), 1222 (s)  $\text{cm}^{-1}$ ;  $^1\text{H}$  NMR (300 MHz, Acetone- $d_6$ )  $\delta$  (ppm) 8.0 (s, br, 1H), 7.35 (d, J = 8.6 Hz, 2H), 7.04 (d, J = 8.6 Hz, 2H), 6.10 (d, br, J = 6.0 Hz, 1H), 4.39 (m, 1H), 3.68 (s, 3H), 2.23 (s, 3H), 1.35 (d, J = 7.2 Hz, 3H);  $^{13}\text{C}$  NMR (300 MHz,  $\text{CDCl}_3$ )  $\delta$  (ppm) 175, 156, 136, 133, 130, 121, 52.4, 48.9, 20.8, 18.5.

**N-(n-propyl)-N'-(L-alanine methyl ester)urea.** A procedure analogous to the one for the preparation of N-phenyl-N'-(L-alanine methyl ester)urea was employed. The quantities of reagents used were: 6.04 g (43.7 mmol) L-alanine methyl ester hydrochloride, 99%; 25 mL pyridine; and a 10% excess, 4.04 g (48.0 mmol) of propyl isocyanate, 99%. Yield 6.54 g Off-White Powder (80%). IR (KBr Pellet) 3334 (s), 2964 (w), 2876 (w), 1748 (s), 1634 (s), 1219 (s)  $\text{cm}^{-1}$ ;  $^1\text{H}$  NMR (300 MHz, Acetone- $d_6$ )  $\delta$  (ppm) 4.32 (q, 1H), 3.65 (s, 3H), 3.06 (t, 2H), 2.84 (s, br, 1H), 2.72 (2, br, 1H), 1.40 (m, 2H), 1.29 (d, 3H), 0.87 (t, 3H).

**N-(n-hexyl)-N'-(L-alanine methyl ester)urea.** A procedure analogous to the one for the preparation of N-phenyl-N'-(L-alanine methyl ester)urea was employed. The quantities of reagents used were: 5.01 g (35.5 mmol) L-alanine methyl ester hydrochloride, 99%; 25 mL pyridine; and an 8% excess, 5.02g (38.3 mmol) of hexyl isocyanate, 97%. Yield 6.07 g Tan Powder (74%). IR (KBr Pellet) 3336 (s), 2962 (w), 2875 (w), 1734 (s), 1633 (s), 1217 (s)  $\text{cm}^{-1}$ ;  $^1\text{H}$  NMR (300 MHz,  $\text{CDCl}_3$ )  $\delta$  (ppm) 5.29 (s, br, 1H), 4.84 (s, br, 1H), 3.99 (q, 1H), 3.78 (s, 3H), 3.25 (t, 2H), 1.45 (m, 2H), 1.42 (d, 3H), 1.22 (m, 6H), 0.87 (t, 3H).

**N-(4-chlorophenyl)-N'-(L-alanine methyl ester)urea.** A procedure analogous to the one for the preparation of N-phenyl-N'-(L-alanine methyl ester)urea was employed. The quantities of reagents used were: 10.0 g (70.9 mmol) L-alanine methyl ester hydrochloride, 99%; 50 mL pyridine; and 11.1 g (70.9 mmol) 4-chlorophenyl isocyanate, 98%. Yield 16.7 g White Powder (91%). IR (KBr Pellet) 3342 (s), 3093 (w), 2992 (m), 2954 (m), 1739 (vs), 1640 (vs), 1223 (s), 635 (m)  $\text{cm}^{-1}$ ;  $^1\text{H}$  NMR (300 MHz, Acetone- $d_6$ )  $\delta$  (ppm) 8.22 (s, br, 1H), 7.49 (d,  $J = 8.1$  Hz, 2H), 7.25 (d,  $J = 8.1$  Hz, 2H), 6.20 (d, br,  $J = 6.0$  Hz, 1H), 4.40 (m, 1H), 3.69 (s, 3H), 1.36 (d,  $J = 7.2$  Hz, 3H);  $^{13}\text{C}$  NMR (300 MHz,  $\text{CDCl}_3$ )  $\delta$  (ppm) 175, 156, 137, 129, 128, 121, 52.6, 48.9, 18.3.

**N,N'-di-n-hexylurea.** Hexyl isocyanate, 97% (6.11 g, 48.0 mmol), a magnetic stir bar, and reagent grade chloroform (30 mL) were added to a 100 mL round bottom flask. The flask was positioned in an ice-water bath to cool the solution to 0 °C. Over the next 30 minutes, a solution of hexylamine, 99% (4.86 g,

48.0 mmol) in chloroform (10 mL) was added to the reaction flask. The ice-water bath was removed and the reaction mixture was stirred overnight at room temperature. The solvent was then removed by rotovap, followed by high vacuum, to reveal 10.7 g of white powder (99% yield). IR (KBr Pellet) 3335 (m), 2961 (m), 2931 (m), 2857 (m), 1618 (vs), 1577 (vs)  $\text{cm}^{-1}$ ;  $^1\text{H}$  NMR (300 MHz,  $\text{CDCl}_3$ )  $\delta$  (ppm) 4.41 (t, br, 2H), 3.12 (m, 2H), 1.46 (m, 2H), 1.27 (m, 6H), 0.85 (t,  $J = 6.6$  Hz, 3H);  $^{13}\text{C}$  NMR (300 MHz,  $\text{CDCl}_3$ )  $\delta$  (ppm) 160, 40.5, 31.8, 30.6, 26.9, 22.8, 14.2.

**N-phenyl-N'-(L-alanine methyl ester)carbodiimide.** Triphenylphosphine, 99% (7.45 g, 28.1 mmol) was dissolved in reagent grade methylene chloride (50 mL) in a 250 mL round bottom flask. The flask was submerged in an ice-water bath. Bromine (4.60 g, 28.8 mmol), weighed in a 20 mL vial and diluted in methylene chloride (9 mL), was added to the flask at an approximate rate of 1 mL every 5 minutes. A rinse of methylene chloride (1 mL) was utilized to facilitate quantitative transfer of the bromine solution. 30 minutes after the final addition of bromine, triethylamine, 99% (8.0 mL, 57 mmol) was added to the reaction mixture at an approximate rate of 1 mL every 5 minutes. N-phenyl-N'-(L-alanine methyl ester)urea (5.00 g, 22.5 mmol) was dissolved in methylene chloride (30 mL). 30 minutes after the final addition of triethylamine, the urea solution was added to the reaction mixture at an approximate rate of 5 mL every 5 minutes. Following addition of the urea, the reaction was allowed to proceed overnight. The following morning, the product mixture was washed with deionized water (20 mL). The methylene chloride solution was dried with a saturated sodium chloride wash (20 mL), followed by

standing for 5 minutes over sodium sulfate. The product solution was decanted to a vacuum-dried, 100 mL round bottom flask. The methylene chloride was subsequently removed by rotovap. A vacuum-dried stir bar and approximately one spatula transfer of calcium hydride were added to the carbodiimide. 2.31 g of clear, yellow oil were collected by vacuum distillation of the carbodiimide at an oil bath temperature of up to 155 °C and a pressure of down to 80 mtorr (50% yield). IR (Neat) 3064 (w), 2988 (w), 2953 (w), 2905 (w), 2137 (vs), 1744 (s), 1213 (s), 604 (w)  $\text{cm}^{-1}$ ;  $^1\text{H}$  NMR (300 MHz,  $\text{CDCl}_3$ )  $\delta$  (ppm) 7.34 (m, 2H), 7.17 (m, 3H), 4.35 (q,  $J = 7.2$ , 1H), 3.77 (s, 3H), 1.51 (d,  $J = 7.2$  Hz, 3H).

**N-(4-methylphenyl)-N'-(L-alanine methyl ester) carbodiimide.** A procedure analogous to the one for the preparation of N-phenyl-N'-(L-alanine methyl ester) carbodiimide was employed, except that calcium hydride was not used. The quantities of reagents used were: 7.50 g (28.3 mmol) triphenylphosphine, 99% in 50 mL  $\text{CH}_2\text{Cl}_2$ ; 4.52 g (28.3 mmol) bromine in 10 mL  $\text{CH}_2\text{Cl}_2$ ; 8.0 mL (57 mmol) triethylamine, 99%; and 5.35 g (22.6 mmol) N-(4-methylphenyl)-N'-(L-alanine methyl ester)urea in 30 mL  $\text{CH}_2\text{Cl}_2$ . Vacuum distillation at an oil bath temperature of up to 173 °C, and pressures down to 180 mtorr, collected 2.23 g of clear, colorless oil (45% yield). IR (Neat) 3056 (w), 2990 (w), 2950 (w), 2131 (vs), 1743 (m), 1194 (s)  $\text{cm}^{-1}$ ;  $^1\text{H}$  NMR (300 MHz,  $\text{CDCl}_3$ )  $\delta$  (ppm) 7.14 (d,  $J = 8.4$  Hz, 2H), 7.07 (d,  $J = 8.4$  Hz, 2H), 4.31 (q,  $J = 7.0$  Hz, 1H), 3.75 (s, 3H), 1.50 (d,  $J = 7.0$  Hz, 3H).

**N-propyl-N'-(L-alanine methyl ester)carbodiimide.** A procedure analogous to the one for the preparation of N-phenyl-N'-(L-alanine methyl ester)carbodiimide was employed. The quantities of reagents used were 7.93 g (29.9 mmol) triphenylphosphine, 99% in 50 mL CH<sub>2</sub>Cl<sub>2</sub>; 4.62 g (30.3 mmol) bromine in 9 mL CH<sub>2</sub>Cl<sub>2</sub>; 8.4 mL (61 mmol) triethylamine; and 6.07 g (29.4 mmol) N-n-propyl-N-(L-alanine methyl ester)urea in 30 mL CH<sub>2</sub>Cl<sub>2</sub>. Two water washes (15 mL each) were utilized before drying over sodium sulfate. Vacuum distillation was performed at oil bath temperatures ranging from 64 to 95 °C and pressures between 180 and 120 mtorr. Yield: 2.62 g Clear, Colorless Oil (57%). IR (Neat) 2964 (w), 2132 (s), 1744 (s), 1215 (s) cm<sup>-1</sup>; <sup>1</sup>H NMR (300 MHz, CDCl<sub>3</sub>) δ (ppm) 4.01 (q, 1H), 3.80 (s, 3H), 3.26 (t, 2H), 1.59 (m, 2H), 1.44 (d, 3H), 0.88 (t, 3H).

**N-hexyl-N'-(L-alanine methyl ester)carbodiimide.** A procedure analogous to the one for the preparation of N-phenyl-N'-(L-alanine methyl ester)carbodiimide was employed. Quantities of reagents used were: 7.60 g (28.7 mmol) triphenylphosphine, 99% in 100 mL CH<sub>2</sub>Cl<sub>2</sub>; 4.62 g (28.9 mmol) bromine in 12 mL CH<sub>2</sub>Cl<sub>2</sub>; 9.0 mL (64 mmol) triethylamine, 99% ; and 6.07 g (26.4 mmol) of the urea in 50 mL CH<sub>2</sub>Cl<sub>2</sub>. Two water washes (50 mL each) were utilized before drying over sodium sulfate. Vacuum distillation was performed at oil bath temperatures ranging from 175 to 230 °C and a pressure of down to 500 mtorr. Yield: 2.65 g Clear, Colorless Oil (35%). IR (Neat) 2957 (w), 2876 (w), 2133 (s), 1744 (s), 1210 (s) cm<sup>-1</sup>; <sup>1</sup>H NMR (300 MHz, CDCl<sub>3</sub>) δ (ppm) 4.02 (q, 1H), 3.80 (s, 3H), 3.32 (t, 2H), 1.59 (m, 2H), 1.48 (d, 3H), 1.38 (m, 6H), 0.88 (t, 3H).

**N-(4-chlorophenyl)-N'-(L-alanine methyl ester) carbodiimide.** A procedure similar to the one for the preparation of N-phenyl-N'-(L-alanine methyl ester) carbodiimide was employed. Quantities of reagents used were: 4.53 g (17.1 mmol) triphenylphosphine, 99% in 50 mL CH<sub>2</sub>Cl<sub>2</sub>; 2.76 g (17.3 mmol) bromine in 10 mL CH<sub>2</sub>Cl<sub>2</sub>; 4.8 mL (34 mmol) triethylamine, 99%; and 4.30 g (16.8 mmol) of the urea in 30 mL CH<sub>2</sub>Cl<sub>2</sub>. After allowing the reaction to proceed overnight, the sample was washed with deionized water (210 mL), followed by saturated sodium chloride (30 mL). Purification by column chromatography, utilizing CH<sub>2</sub>Cl<sub>2</sub> developing solvent and silica stationary phase, isolated merely 113 mg of clear, brown oil (3% yield). IR (Neat) 2990 (w), 2954 (w), 2135 (vs), 1744 (m), 1215 (s) cm<sup>-1</sup>; <sup>1</sup>H NMR (300 MHz, CDCl<sub>3</sub>) δ (ppm) 7.34 (d, J = 8.7 Hz, 2H), 7.22 (d, J = 8.7 Hz, 2H), 4.39 (q, J = 6.9 Hz, 1H), 3.77 (s, 3H), 1.51 (d, J = 6.9 Hz, 3H).

**N-(4-fluorophenyl)-N'-(L-alanine methyl ester) carbodiimide.** L-alanine methyl ester hydrochloride, 99% (3.0 g, 21.3 mmol) was dissolved in reagent grade pyridine (40 mL) in a 100 mL round bottom flask. Mercury (II) oxide, 99% (6.58 g, 43.0 mmol) was added to the flask, followed by 4-fluorophenyl isothiocyanate, 98% (3.33 g, 21.3 mmol). Following addition of the isothiocyanate, the reaction was allowed to proceed overnight. The next morning, a clear, light-orange solution was obtained from the gray product mixture by filtering through diatomaceous earth. The product solution was dried over magnesium sulfate. Rotovaping the pyridine away revealed viscous oil mixed with gray, mercury (II) sulfide precipitate. The oil was diluted in methylene chloride (5 mL) and filtered into a 25 mL Schlenk flask,

revealing a dark, reddish brown solution. The methylene chloride was removed by purging to relative dryness with nitrogen followed by application of high vacuum overnight to reveal 3.92 g of viscous orange oil (83% yield). IR (Neat) 3071 (w), 2989 (w), 2955 (m), 2876 (w), 2133 (vs), 1745 (s), 1224 (s)  $\text{cm}^{-1}$ ;  $^1\text{H}$  NMR (300 MHz,  $\text{CDCl}_3$ )  $\delta$  (ppm) 7.13 (m, 2H), 6.96 (m, 2H), 4.16 (q,  $J = 6.9$ , 1H), 3.77 (s, 3H), 1.54 (d,  $J = 6.9$ , 3H).

**N-(4-chloromethylphenyl)-N'-(L-alanine methyl ester) carbodiimide.**

Phosphorus pentachloride, 95% (2.78 g, 12.7 mmol) was dissolved in reagent grade pyridine (10 mL) in a 50 mL round bottom flask. N-(4-methylphenyl)-N'-(L-alanine methyl ester)urea (3.00 g, 12.7 mmol), dissolved in pyridine (15 mL), was added to the flask. After refluxing for 1 hour, the pyridine was removed by rotovap, followed by high vacuum overnight, revealing a sticky black goop. Chloroform (140 mL), saturated sodium bicarbonate (100 mL), and deionized water (100 mL) were added to the goop. The mixture was so black that a distinction between layers could only be discerned by turning off the lights and shining a flashlight through the separatory funnel from behind. The aqueous layer appeared to have a more bubbly texture than the chloroform layer. Even still, the boundary between layers was not clear. After draining a large portion of the chloroform (~120 mL), additional chloroform (60 mL) was added to the separatory funnel. The newly transparent chloroform layer revealed black sediment. After draining all portions through filter paper to remove the sediment, the boundary between the chloroform and aqueous layers became clear. Following separation, the chloroform layer was dried over sodium sulfate and

rotovaped to reveal a dark solid. Short path distillation, utilizing a Buchi Glass Oven B-580 w/ a Buchi Drive Unit, at temperatures ranging from 195 to 210 °C and pressures down to 85 mtorr, isolated 170 mg of clear oil (5% yield). IR (Neat) 3025 (w), 2987 (w), 2954 (w), 2870 (w), 2132 (vs), 1739 (s), 1212 (s)  $\text{cm}^{-1}$ ;  $^1\text{H}$  NMR (300 MHz,  $\text{CDCl}_3$ )  $\delta$  (ppm) 7.14 (d,  $J = 8.7$ , 2H), 7.07 (d,  $J = 8.7$ , 2H), 4.19 (q,  $J = 5.7$ , 1H), 3.75 (s, 3H), 3.47 (s, 1H), 1.41 (d,  $J = 5.7$ , 3H).

**N,N'-di-n-hexylcarbodiimide.** Triphenylphosphine, 99% (14.5 g, 54.8 mmol) was dissolved in reagent grade methylene chloride (50 mL) in a 250 mL round bottom flask. The flask was submerged in an ice-water bath. Bromine (8.76 g, 54.8 mmol), weighed in a 20 mL vial and diluted in methylene chloride (9 mL), was added to the flask at an approximate rate of 1 mL every 5 minutes. A rinse of methylene chloride (1 mL) was utilized to facilitate quantitative transfer of the bromine solution. Triethylamine, 99% (15.6 mL, 111 mmol) was added at a rate of approximately 1 mL every 5 minutes. N,N'-di-n-hexylurea (10.0 g, 43.8 mmol) was dissolved in methylene chloride (20 mL). 30 minutes after the final addition of triethylamine, the urea solution was added to the reaction mixture at an approximate rate of 5 mL every 5 minutes. Following addition of the urea, the reaction was allowed to proceed overnight. The following morning, the product mixture was washed with deionized water (50 mL). The methylene chloride solution of the product was dried with a saturated sodium chloride wash (30 mL), followed by standing over sodium sulfate for 5 minutes. The product solution was decanted to a 250 mL round bottom flask and rotovaped to a volume of approximately 40 mL. Pentanes (240 mL) were added

to precipitate the triphenylphosphine oxide byproduct as a loose slurry. The solution was filtered into a 500 mL round bottom flask with several rinses of pentanes (totaling 80 mL) to facilitate transfer. The slurry was transferred to a Soxhlet Extractor thimble to which 100 mg calcium hydride was also added. A reflux condenser was attached. The setup was attached to a nitrogen line and the slurry was extracted via overnight reflux. The following day, the solvents were removed by rotovap. Short path distillation, utilizing a Buchi Glass Oven B-580 w/ a Buchi Drive Unit (30 mtorr, 154 °C) isolated a clear, colorless oil (6.64 g, 72% yield). IR (Neat) 2956 (m), 2930 (s), 2858 (m), 2130 (vs), 1467 (w), 1342 (w), 725 (vw)  $\text{cm}^{-1}$ ;  $^1\text{H}$  NMR (300 MHz,  $\text{CDCl}_3$ )  $\delta$  (ppm) 3.17 (t,  $J = 6.8$  Hz, 2H), 1.54 (m, 2H), 1.28 (m, 6H), 0.88 (t,  $J = 6.7$  Hz, 3H);  $^{13}\text{C}$  NMR (300 MHz,  $\text{CDCl}_3$ )  $\delta$  (ppm) 141, 47.9, 31.6, 31.5, 26.7, 22.8, 14.3.

**$\text{CpTiCl}_3$ .** In a dry box,  $\text{Cp}_2\text{TiCl}_2$  (10.0 g, 40.3 mmol) and a large magnetic stir bar were placed in a 250 mL 3-neck flask. A reflux condenser, topped with a joint-to-hose adapter having a stopcock, was attached to the center neck. Each side neck of the flask was sealed with a rubber septum. The assembly was removed from the dry box, attached to a Schlenk line, and opened to a positive pressure of nitrogen. Dry toluene (100 mL) was added to the flask via syringe. The flask was submerged in an ice-water bath on top of a magnetic stir plate. Titanium (IV) chloride (13.5 mL, 123 mmol) was added to the stirring contents of the flask via syringe. The flask was removed from the ice-water bath, wiped dry, and placed in an oil bath heated to 135 °C. The reaction mixture was refluxed for 6 hours and then

left to stir at room temperature overnight. The following day, the flask was submerged in an ice-water bath for 30 minutes. The solvent was removed with a filter paper-covered, vacuum-needle assembly. [See Appendix 1 for filter paper-covered, vacuum-needle assembly instructions.] Following removal of the solvent, the septa were replaced with glass stoppers lubricated with high-vacuum silicon grease. Vacuum drying overnight at pressures down to 50 mtorr revealed 11.6 g of grayish-orange powder (69% yield). The product was transferred to a large-scale sublimation apparatus. The apparatus was submerged in an oil bath heated 90 °C, while the cold finger was cooled with dry ice in isopropanol. After 3 days at a pressure of 25 mtorr, the sublimation apparatus was filled with nitrogen and transferred into a dry box. The product was rinsed from the cold finger, with anhydrous chloroform, into a 25 mL Schlenk flask. The Schlenk flask was sealed with a rubber septum and removed from the dry box. A syringe attached to a Schlenk line hose, opened to a positive pressure of nitrogen, was inserted into the septum. An oil flow indicator was attached via a rubber hose to the side arm of the Schlenk line, which was then opened to monitor the flow of nitrogen while isolating the system from the atmosphere. The product was dried to a paste via nitrogen purge. The side arm of the Schlenk flask was attached to a Schlenk line having a positive pressure of nitrogen. The rubber septum was replaced by a glass stopper, lubricated with high-vacuum silicon grease. The product was dried under high vacuum to reveal 435 mg of richly dark-orange powder (4% recovery).

**CpTiCl<sub>2</sub>OCH<sub>2</sub>CF<sub>3</sub>.** In a N<sub>2</sub>-filled dry box, CpTiCl<sub>3</sub> (3.16 mmol, 692 mg) was weighed and transferred to a 50 mL Schlenk flask. A magnetic stir bar was added. The flask was sealed with a rubber septum, removed from the dry box, attached to a nitrogen line, and placed under a positive pressure of nitrogen. Dry triethylamine (3.16 mmol, 0.440 mL) was added via syringe. 2,2,2-trifluoroethanol (3.16 mmol, 230 μL) was added via syringe. 2 hours later, the product solution was transferred to another 50 mL Schlenk flask with the use of a filter paper-covered, vacuum-needle assembly to separate the soluble product from the insoluble triethylammonium chloride precipitate. [See Appendix 1 for filter paper-covered, vacuum-needle assembly instructions.] The solvent was removed via a purge of nitrogen, followed by high vacuum (<50 mtorr), revealing 510 mg of a yellow solid (57% yield). 124 mg of pure yellow crystals were isolated via sublimation at 80 °C and 10 mtorr (24% recovery).

**TiCl<sub>3</sub>OCH<sub>2</sub>CF<sub>3</sub>.** This catalyst was synthesized via significant modification of two literature procedures.<sup>35,36</sup> Titanium tetrachloride (29.1 mmol, 3.20 mL) and methylene chloride (10 mL) were added via syringe to a nitrogen-filled, 25 mL Schlenk flask containing a stir bar and fitted with a reflux condenser. The flask was placed in an ice-water bath, set to mix with magnetic stirring, and 2,2,2-trifluoroethoxide (24.7 mmol, 1.80 mL) was added via syringe. Nitrogen gas was bubbled through the reaction mixture to facilitate removal of the hydrogen chloride byproduct. To avoid concentrating the reaction solution, the purge nitrogen was pre-saturated by bubbling it through an anhydrous methylene chloride reservoir (100 mL)

in route to the reaction flask. The flask was removed from the ice-water bath after 20 minutes. The reaction mixture was stirred at room temperature for the next 40 minutes, and then refluxed in a hot oil bath (43 °C) for 30 minutes. [30 minutes was judged to be the optimum reflux time based on the earliest perceptible observation of white titanium deposits on the reflux condenser, assumed to be a byproduct of catalyst decomposition.] The flask was removed from the hot oil bath, and a dry nitrogen purge was used to concentrate the reaction solution to a volume of approximately 5 mL. Anhydrous hexanes (10 mL) were added to the flask via syringe and the solution was again concentrated to approximately 5 mL via dry nitrogen purge. The flask was placed in an ice-water bath to more fully precipitate the product. An oven-dried, filter paper-covered, vacuum-needle assembly was inserted through the bottom of an appropriately-sized, vacuum-dried, rubber septum. [See Appendix 1 for filter paper-covered, vacuum-needle assembly instructions.] While maintaining a positive pressure of nitrogen in the reaction flask, the glass stopper was removed and the rubber septum containing the oven-dried, filter paper-covered, vacuum-needle assembly was inserted. The filter paper-covered hilt of the needle was then used to suction the solvent from the reaction flask into a 3-neck flask placed under vacuum. Anhydrous hexanes (5 mL) were added to the reaction flask via syringe. The precipitate and rinse were stirred for 10 minutes to facilitate washing while waiting on the hexanes to cool to the ice bath temperature. The hexanes were then removed as before, and this rinse procedure was repeated twice. Following removal of the last hexane rinse, the product was dried under vacuum,

with a slight flow of nitrogen, to reveal 1.22 g white powder having a faint-brown tint (20% yield).  $^1\text{H}$  NMR (300 MHz,  $\text{CDCl}_3$ ):  $\delta$  4.8 (br, major peak), 3.7 (br, minor peak). Catalytic activity was verified by mixing N,N'-di-n-hexylcarbodiimide in a 100:1 ratio with a small portion of the product. This test polymerization proceeded rapidly and exothermically, increasing viscosity immediately and forming solid polymer within seconds.

**Dimerization of N-phenyl-N'-(L-alanine methyl ester)carbodiimide.** N-phenyl-N'-(L-alanine methyl ester)carbodiimide (7.84 mmol, 1.60 g) was transferred to a 25 mL Schlenk flask in a  $\text{N}_2$ -filled dry box. Copper (I) butanethiolate (160  $\mu\text{mol}$ , 24 mg) and a small magnetic stir bar were added. The flask was sealed with a glass stopper, removed from the dry box, attached to a  $\text{N}_2$  line, opened to a positive pressure of  $\text{N}_2$ , and lowered into an oil bath heated to 155  $^\circ\text{C}$ . The reaction mixture became viscous and dark purple in color. After 2 hours and 30 minutes, the product was removed from heat. The next day, the product was dissolved in acetone (5 mL) and precipitated in deionized water (100 mL). An acetone rinse (1 mL) was utilized to facilitate quantitative transfer. The dimer was extracted with two portions of chloroform (25 mL each). The chloroform was dried with sodium sulfate and removed by rotovap, followed by high vacuum, revealing a crunchy black solid (1.49 g, 93% yield). IR (KBr Pellet) 3064 (w), 2987 (w), 2952 (w), 1749 (s), 1657 (s), 1620 (s)  $\text{cm}^{-1}$ ;  $^1\text{H}$  NMR (300 MHz,  $\text{CDCl}_3$ )  $\delta$  (ppm) 7.5 to 7.3 (m, 10H), 4.24 (q, 2H), 4.00 (s, 6H), 1.51 (d, 6H);  $^{13}\text{C}$  NMR (300 MHz,  $\text{CDCl}_3$ )  $\delta$  (ppm) 180, 158, 132, 129, 128, 126, 62.4, 55.8, 17.5.

**Overview of Carbodiimide Polymerization Procedures.** All polymerization were conducted under nitrogen as detailed under the heading “Inert Atmospheres,” in Section 2.6.1. All polymerizations discussed in this chapter were performed neat. With the exceptions of the polymer obtained via exclusively thermal polymerization of **III**, which was characterized in crude form, and the polymer of **V** catalyzed by  $\text{CuCl}_2$  and heat, which proved insoluble in every solvent tested, all polymers made from these ester-bearing carbodiimides were worked up by suspending the polymer, with the aid of gentle heating and a Thermolyne Type 16700 Mixer, in a minimum amount of acetone, precipitating in deionized water, and extracting the precipitated polymer with chloroform. The polymer solutions in chloroform were dried with a wash of saturated sodium chloride, followed by standing over sodium sulfate. The anhydrous chloroform was removed by rotovap, followed by high vacuum overnight, to reveal the ester-bearing polycarbodiimide. Poly(N,N'-di-n-hexylcarbodiimide), on the other hand, was worked up instead by dissolving in a minimum amount of chloroform and precipitating in methanol. Then the precipitated polymer was collected by filtering through Qualitative P8-Creped Fisherbrand Filter Paper and dried under high vacuum (<100 mtorr).

**Typical Procedure for the Isolation of a Clean Fraction.** The dark-brown product (2.15 g) obtained following workup of the heated reaction between N-phenyl-N'-(L-alanine methyl ester)carbodiimide) with copper (I) butanethiolate (500:1) was dissolved in chloroform (20 mL). The solution was evenly divided among 4 centrifuge tubes. Each tube was purged with nitrogen until the solution became

saturated. At this point, 10 mL of methanol were added to each tube, precipitating a heavy fraction, and the four samples were centrifuged at 3200 rpm and 19 °C for 20 minutes. The yellow supernatant was discarded. Methanol (20 mL) and chloroform (5 mL) were added to each tube to wash away a light fraction. The white suspension was centrifuged for 20 minutes at 3200 rpms and 4 °C. Again, the supernatant was discarded. Removal of the remaining volatiles by nitrogen purge, followed by high vacuum, revealed 716 mg of polymer having a discoloration that was merely light brown (33% recovery).

**Poly(N-phenyl-N'-(L-alanine methyl ester)carbodiimide).** Clean Fraction: IR (KBr Pellet) 3060 (w), 2989 (w), 2950 (w), 2871 (w), 2848 (w), 1739 (s), 1639 (s)  $\text{cm}^{-1}$ ;  $^1\text{H}$  NMR (300 MHz,  $\text{CDCl}_3$ )  $\delta$  (ppm) 6.85, 6.60, 6.29, 5.94, 3.93, 3.36, 1.57, 1.27, 0.86 (all broad) [Figure 2.14];  $^{13}\text{C}$  NMR (300 MHz,  $\text{CDCl}_3$ )  $\delta$  (ppm) 172.9, 146.8, 138.5, 130.3, 129.5, 128.2, 126.9, 126.3, 124.3, 55.7, 51.2, 20.6, 18.0.

**Poly(N-(4-methylphenyl)-N'-(L-alanine methyl ester)carbodiimide).** Un-Fractioned:  $^1\text{H}$  NMR (300 MHz,  $\text{CDCl}_3$ )  $\delta$  (ppm) 7.24, 7.09, 6.78, 5.94, 3.71, 3.36, 2.36, 2.29, 1.60 (broad signals).

**Poly(N-(4-fluorophenyl)-N'-(L-alanine methyl ester)carbodiimide).** Universally Insoluble: IR (KBr Pellet) 3058 (w), 2987 (w), 2954 (w), 2850 (w), 1735 (m), 1636 (s)  $\text{cm}^{-1}$ .

**Poly(N,N'-di-n-hexylcarbodiimide).** IR (KBr Pellet) 2956 (m), 2927 (m), 2858 (m), 1647 (m), 1467 (w), 1354 (w), 725 (w)  $\text{cm}^{-1}$ ;  $^1\text{H}$  NMR (300 MHz,  $\text{CDCl}_3$ )  $\delta$  (ppm) 4.2, 3.4, 3.1, 1.5, 1.3, 0.9 (all broad);  $^{13}\text{C}$  NMR (300 MHz,  $\text{CDCl}_3$ )  $\delta$  (ppm) 148, 49.0, 46.5, 32.6, 32.2, 29.9, 29.4, 28.0, 27.7, 23.2, 23.0, 14.4, 14.3.

## 2.7. References

- (1) Goodwin, A.; Novak, B. *Macromolecules* **1994**, *27*, 5520-5522.
- (2) Kim, J., PhD Dissertation, North Carolina State University, 2002.
- (3) Shibayama, K.; Seidel, S.; Novak, B. *Macromolecules* **1997**, *30*, 3159-3163.
- (4) Goodwin, A., PhD Dissertation, University of California at Berkley, 1996.
- (5) Schlitzer, D.; Novak, B. *Journal of the American Chemical Society* **1998**, *120*, 2196-2197.
- (6) Schlitzer, D., PhD Dissertation, University of Massachusetts Amherst, 1998.
- (7) Kim, J.; Novak, B. *Macromolecules* **2004**, *37*, 8286-8292.
- (8) Kim, J.; Novak, B. *Macromolecules* **2004**, *37*, 1660-1662.
- (9) Tang, H.; Boyle, P.; Novak, B. *Journal of the American Chemical Society* **2005**, *127*, 2136-2142.
- (10) Tang, H.; Novak, B.; He, J.; Polavarapu, P. *Communications* **2005**, *44*, 7298-7301.
- (11) Kennemur, J.; Clark IV, J. B.; Tian, G.; Novak, B. *Macromolecules* **2010**, *43*, 1896-1873.
- (12) Li, H., PhD Dissertation, North Carolina State University, 2006.
- (13) Vishnyakova, T.; Golubeva, I.; Glebova, E. *Usp. Khim.* **1985**, *54*, 429-449.
- (14) Bestmann, H.; Lienert, J.; Mott, L. *Justus Liebigs Ann. Chem.* **1968**, *718*, 24-32.
- (15) Palomo, C.; Mestres, R. *Synthesis* **1981**, 373-374.
- (16) Coles, R.; Levine, H. U.S. Pat. #2942025, 1960.
- (17) Herzog, I. *Angewandte Chemie* **1920**, *33*, 140.
- (18) *Chemistry and Technology of Carbodiimides*; Ulrich, H., Ed.; John Wiley & Sons, Ltd: West Sussex, 2007.

- (19) Weith, W. *Berichte der Deutschen Chemischen Gesellschaft* **1873**, 6, 1395.
- (20) Appel, R.; Kleinstueck, R.; Ziehe, K. *Chemische Berichte* **1971**, 104, 1335.
- (21) Eilingsfeld, H.; Seefelder, M.; Weidinger, H. *Angewandte Chemie* **1960**, 72, 836.
- (22) Wragg, R. *Tetrahedron Letters* **1970**, 45, 3931-3932.
- (23) Ager, D.; Froen, D. The Nutrasweet Company, World Intellectual Property Organization, WO/1991/004962, 1991.
- (24) Ulrich, H.; Tilley, J.; Saying, A. *Journal of Organic Chemistry* **1964**, 29, 2410-2404.
- (25) Ulrich, H.; Saying, A. *Journal of Organic Chemistry* **1965**, 30, 2779-2781.
- (26) Wyman, D.; Wang, J.; Freeman, J. *Journal of Organic Chemistry* **1963**, 28, 3173-3177.
- (27) Brubaker, C.; Wicholas, M. *Journal of Inorganic and Nuclear Chemistry* **1965**, 27, 59-62.
- (28) Novak, B., Electronic Correspondence.
- (29) Hartke, K.; Rossbach, F. *Angewandte Chemie* **1968**, 80, 83.
- (30) Zetzche, F.; Friedrich, A. *Chemische Berichte* **1940**, 73, 1114.
- (31) Ishii, I.; Ito, K.; Yasuda, K. Jap. Pat. 7,115,501, 1971.
- (32) Rapi, G.; Sbrana, G.; Gelsomini, N. *Journal of the Chemical Society C* **1971**, 3827.
- (33) Draun, D.; Cherdron, H.; Rehahn, M.; Ritter, H.; Voit, B. *Polymer Synthesis: Theory and Practice: Fundamentals, Methods, Experiments*, 2005.
- (34) *Purification of Laboratory Chemicals*; Perrin, D.; Armarego, W., Eds.; Pergamon Press: Oxford, 1988.
- (35) Paul, R.; Sharma, P.; Gupta, P.; Chadha, S. *Inorganica Chimica Acta* **1976**, 20, 7-9.

- (36) Patten, T.; Novak, B. *Journal of the American Chemical Society* **1996**, *118*, 1906-1916.

## Chapter 3: The Stability and Reactivity of Ester-Bearing Polycarbodiimides

### 3.1. Introduction

A common feature among the dozens of polycarbodiimide structures that have been synthesized and characterized by the Novak Group is their stability under both strongly acidic and strongly basic conditions. The stability of poly(N-benzyl-N'-(4-n-butylphenyl)carbodiimide), for instance, typifies the robustness of these structures vis-a-vis acids and bases. When stirred *or sonicated* in a mixture of acetone and either aqueous 2.5 wt% sodium hydroxide or 2.0 wt% paratoluenesulfonic acid, this polycarbodiimide proves completely inert. Comparisons by gel permeation chromatography before and after such treatments revealed no appreciable change in molecular weight estimates relative to polystyrene standards.

Another common feature of dead polycarbodiimides, bearing simple alkyl and aryl substituents, is their relative stability in solution at the elevated temperatures with which annealing studies are conducted, where racemization of single-handed helices are observed without appreciable polymer decomposition. The extensive investigations that follow suggest these properties – robustness vis-à-vis acids and bases as well as stability in solution at elevated temperatures – to be artifacts of the electron-donating ability of the alkyl or aryl substituents, rather than inherent properties of the polycarbodiimide backbone. The placement of an electron-withdrawing ester group in close proximity to the backbone easily undermines such felicitous properties, leading to thermally-unstable structures that hydrolyze at least as well, with acids or bases, as the ester groups themselves.

### 3.2. Base-Catalyzed Hydrolysis of a New Ester-Bearing Polycarbodiimide

The prototype of the novel ester-bearing polycarbodiimides discussed in Chapter 2 is poly-III. Attached to the polymer backbone through the alpha carbon, the inductive electron-withdrawing effect of the ester unit has a surprisingly powerful influence on the polycarbodiimide's stability. When sonicated in a 2:1 mixture of acetone and aqueous 2.5 wt% sodium hydroxide for five days, the initially insoluble polymer is hydrolyzed completely, leading to the urea structure illustrated in Figure 3.1. The contrast between the respective broad and sharp  $^1\text{H}$  NMR signals before and after, Figure 3.2 A & B, are consistent with the transition from polymer to small molecule. LC/MS analysis confirms the anticipated product structure, exhibiting  $m/z$  values of 209 and 231, corresponding respectively to the protonated urea and its sodium adduct, as the two most abundant peaks.

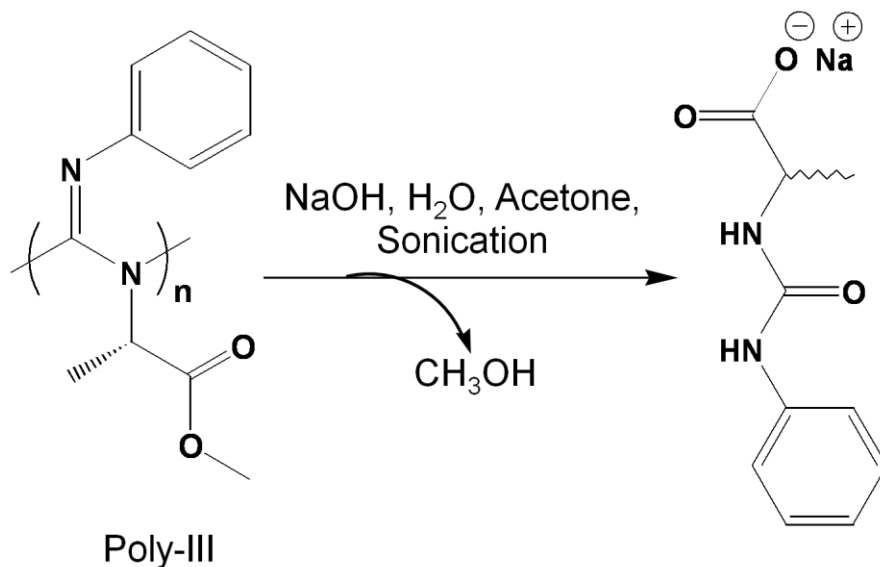


Figure 3.1: The quantitative conversion of poly-III to a urea structure is the first case in which a polycarbodiimide has been observed to hydrolyze under basic conditions.

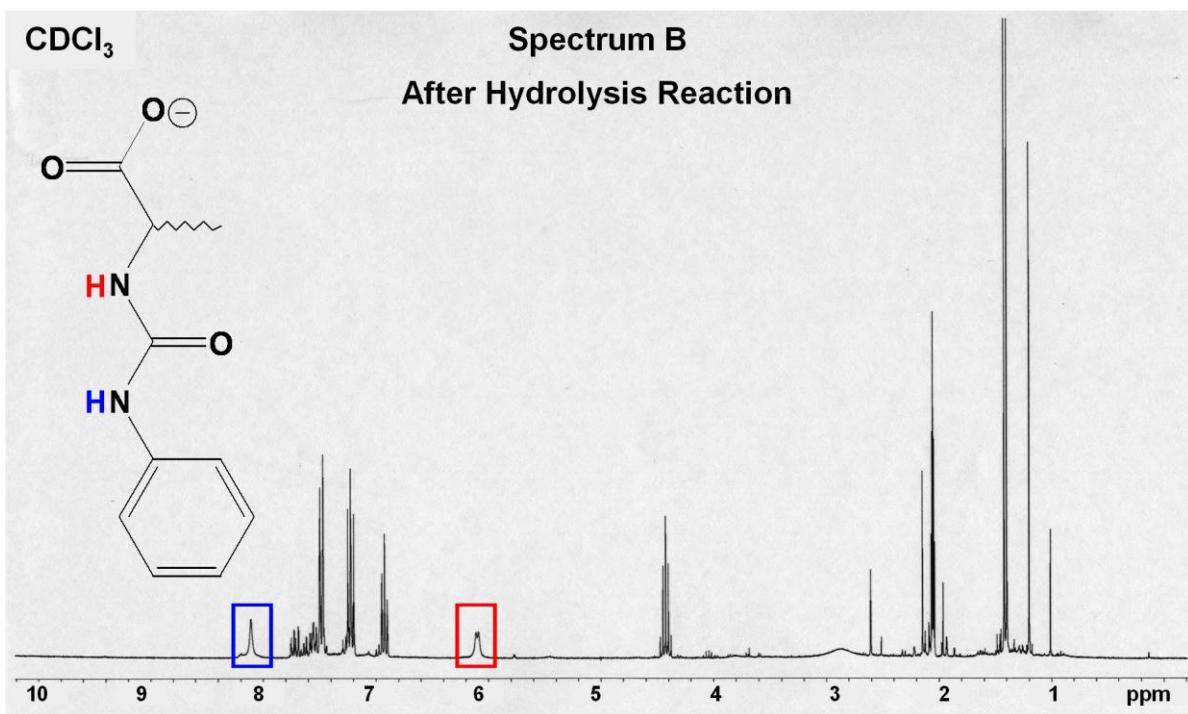
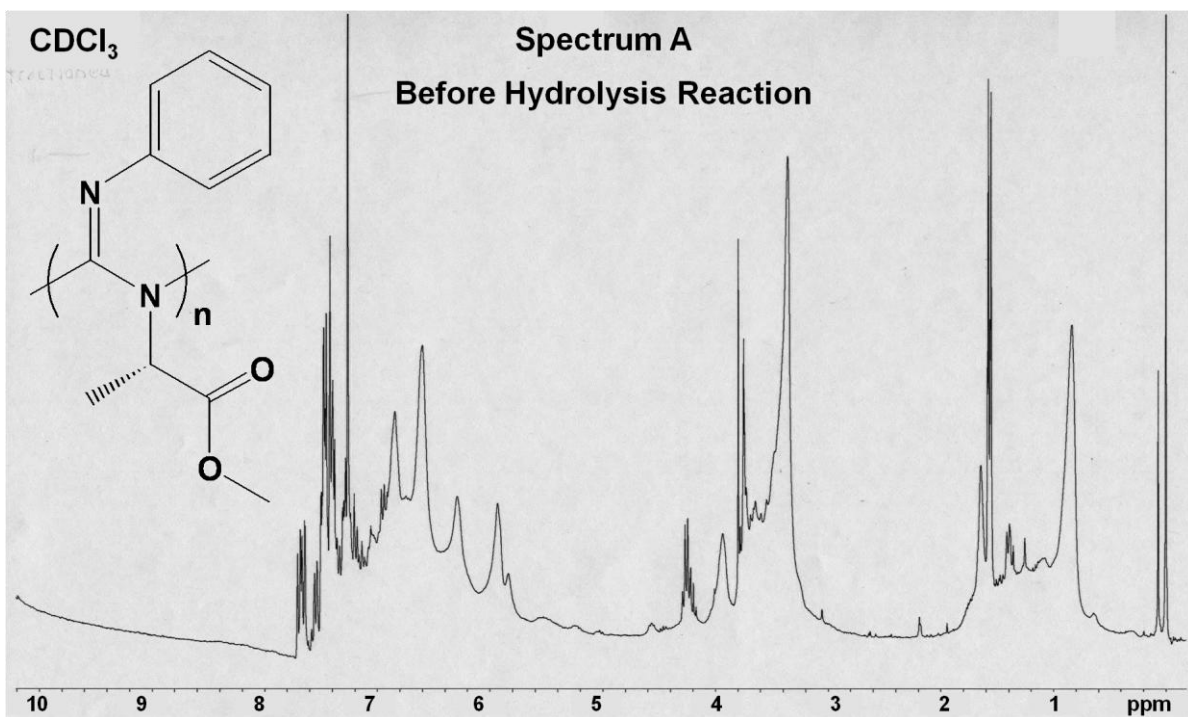


Figure 3.2: <sup>1</sup>H NMR spectra before and after base-catalyzed hydrolysis of poly(N-phenyl-N'-(L-alanine methyl ester)carbodiimide). Both the pendant methyl ester and the polymer backbone are hydrolyzed under strongly basic conditions.

### 3.3. Transesterification Studies on a New Ester-Bearing Polycarbodiimide

As mentioned in Chapter 2, the incentive for developing a novel class of ester-bearing polycarbodiimides is to provide these architectures with a modifiable pendant group. One route to modifying compounds having an ester group is to hydrolyze the ester and then react the resulting carboxylic acid or carboxylate with an alcohol or an amine to respectively create a new ester or amide linkage. But the susceptibility of the prototype to base catalyzed hydrolysis of the backbone precludes modifications in this manner. An alternative strategy is transesterification with an alcohol. Transesterification enzymes are often employed to facilitate such reactions. When compared with chemical catalysts, enzymes offer several advantages, such as milder reaction conditions. Enzymes are also capable of regio- and stereoselective transesterifications.

But for the purposes of modifying pendant esters, enzymes can exhibit one salient drawback, which is a complete lack of reactivity for ester groups located in close proximity to the backbone, as reported in the case of poly(styrene-co-methyl-2-(4-styryl) acetate).<sup>1</sup> This in spite of the fact that the monomer, methyl 2-(4-styryl acetate), is transesterified with alcohols by resin-bound *Candida Antarctica* Lipase B in high yields. When a diester derivative of the aforementioned polymer, incorporating five methylene spacers between the proximal and distal pendant esters, was reacted under these conditions, the distal ester is reported to transesterify extensively and exclusively, proving the limitation of this enzymatic transesterification to be an issue of pendant ester proximity to the backbone.

### 3.3.1. News Flash: Novel Polycarbodiimide Sour on PTSA!

Given the close proximity of the ester unit, derived from L-alanine, to the backbone of the prototype polycarbodiimide, the possibility of facilitating pendant ester transesterification with a chemical catalyst, rather than an enzyme, holds more promise. The traditional, most frequently used transesterification catalysts are acids, such as  $\text{H}_2\text{SO}_4$ ,  $\text{RSO}_2\text{OH}$ ,  $\text{H}_3\text{PO}_3$ , and  $\text{HCl}$ .<sup>2</sup> p-Toluenesulfonic acid, for instance, has been utilized to transesterify the pendant esters on poly(methyl acrylate) with optically active alcohols.<sup>3</sup> Unfortunately, the prototype ester-bearing polycarbodiimide, poly-III, decomposes on exposure to strong acid. In a pair of transesterification experiments on poly-III with p-toluenesulfonic acid, the most noticeable change over the course of the reaction was decomposition, as evidenced by changes in the  $^1\text{H}$  NMR spectra, Figure 3.3.

### 3.3.2. Transesterification Studies Under Mild Conditions

The instability of the prototype ester-bearing polycarbodiimide in the presence of strong acids or bases precludes modification under harsh conditions. Fortunately there are milder alternatives for the purpose of transesterification. Mercury (II) acetate,<sup>4</sup> potassium cyanide,<sup>5</sup> and 4-dimethylaminopyridine,<sup>6</sup> have each been reported to catalyze transesterifications, though none of these successfully facilitated transesterification of pendant esters on a heavy fraction of poly-III. When initially tested with a lower molecular weight fraction of the prototype,  $\text{Hg}(\text{OAc})_2$  did show some promise, as evidenced by changes in the  $^1\text{H}$  NMR spectra, Figure 3.4.

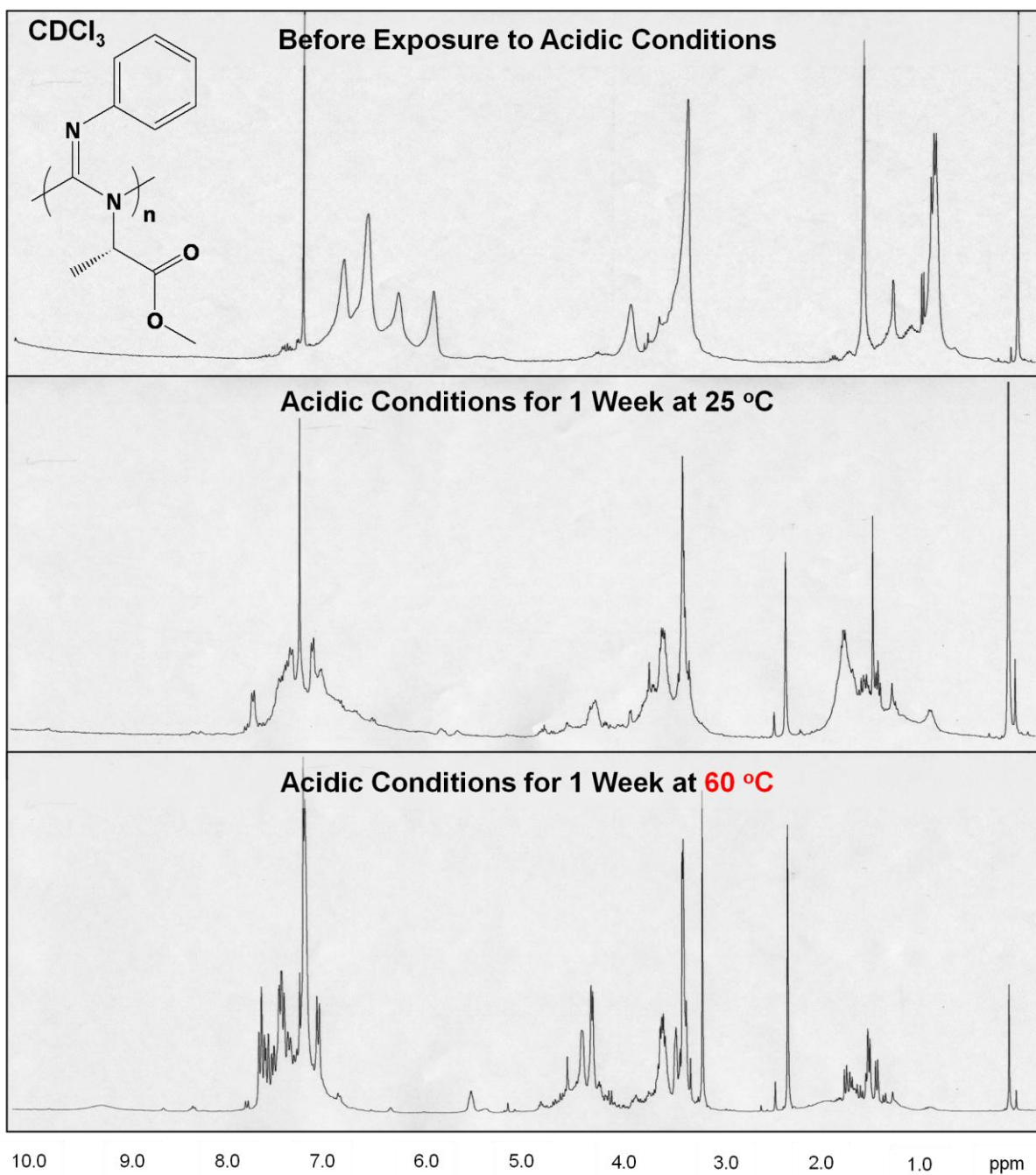


Figure 3.3:  $^1\text{H}$  NMR spectra of poly-III before and after 1 week of reaction with 2-methoxyethanol in the presence of p-toluenesulfonic acid (2.1 equivalents / repeat) in chloroform solvent. The most prominent change in the spectra is the replacement of broad proton signals with sharp signals, consistent with decomposition of the polymer into smaller molecules. Increasing the reaction temperature greatly accelerates the decomposition process.

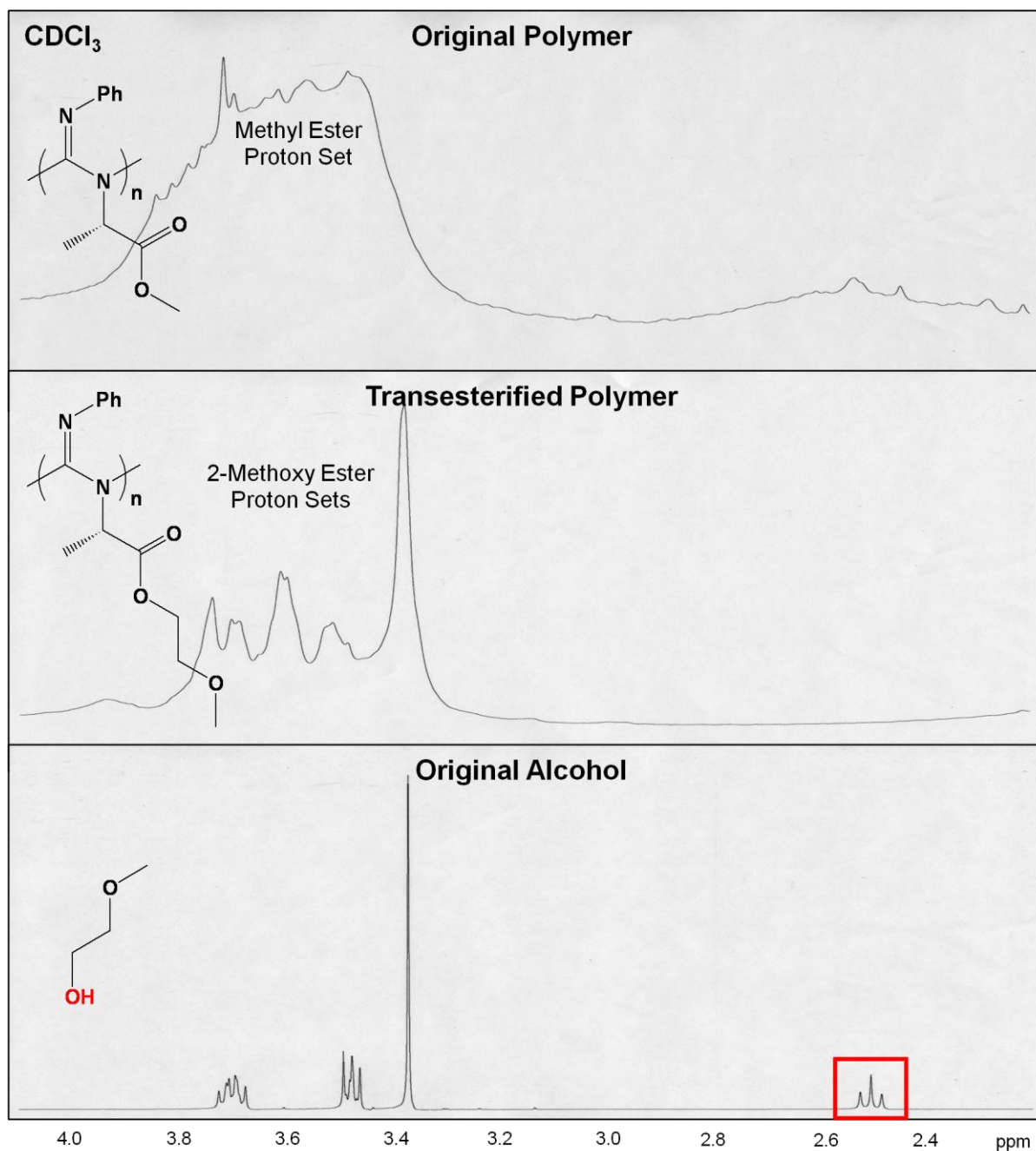


Figure 3.4: Expanded view of the region of interest on the  $^1\text{H}$  NMR spectra of a relatively light fraction of poly-III, before and after transesterification with 2-methoxyethanol, catalyzed by mercury (II) acetate. The notable absence of a signal for the hydroxyl proton of the free alcohol, highlighted in red, from the spectrum of the transesterified polymer, indicates that the additional proton signals are from newly-placed, 2-methoxyethyl substituents on the pendant group. The relative broadness of these signals is also consistent with polymer attachment.

### 3.4. Follow-Up Studies on an Old Ester-Bearing Polycarbodiimide

Having thoroughly explored the synthesis, stability, and reactivity of a polycarbodiimide derived from a simple, methyl ester-protected, chiral amino acid, and finding its potential for subsequent modification to be quite limited, our focus shifted to re-investigating an earlier ester-bearing design previously developed by Jeonghan Kim.<sup>7</sup> The multi-step synthesis is outlined in Figure 3.5. His pilot effort to free the acid with iodotrimethylsilane – renowned for mildly cleaving esters<sup>8,9</sup> – reportedly led to polymer decomposition<sup>7</sup> which, in hindsight, is likely to have been a consequence of the elevated temperature at which such deprotections are facilitated.

A more thorough investigation of this earlier design revealed that unlike polycarbodiimides bearing simple alkyl and aryl substituent – such as poly(N-benzyl-N'-(4-n-butylphenyl)carbodiimide), which proves stable when sonicated under strongly acidic or basic conditions for one week – the ester-bearing polycarbodiimide designed by Kim decomposes with mere sonication as evidenced by changes in the <sup>1</sup>H NMR spectra, Figure 3.6 A & B. Stirring or sonicating in aqueous base hydrolyzes the polymer backbone more rapidly than it cleaves the t-butyl group from the pendant ester, Figure 3.7. The polymer proves even less stable when stirred for the same amount of time in aqueous acid and it decomposes most rapidly when sonicated under strongly acidic conditions, Figure 3.8.

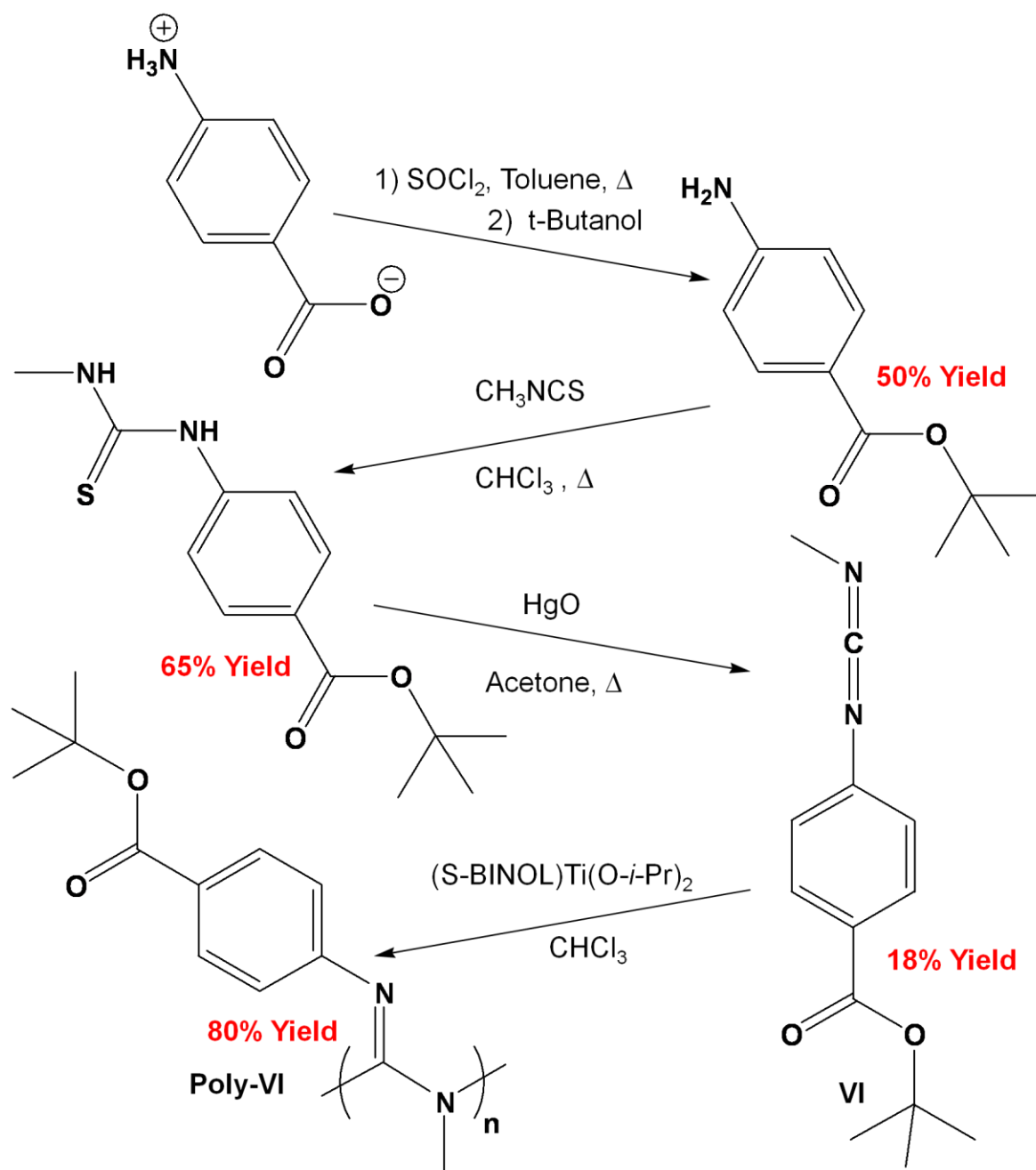


Figure 3.5: Outline of the multi-step synthetic route to the ester-bearing polycarbodiimide first developed by Jeonghan Kim.<sup>7</sup> The initial step, synthesis of t-butyl p-aminobenzoate, was first reported by Taylor, Fletcher, and Sabb.<sup>10</sup> The original polymer synthesized by Kim was made with an achiral titanium catalyst,  $\text{CpTiCl}_2\text{N}(\text{CH}_3)_2$ , rather than the chiral, (S)-BINOL titanium catalyst utilized for the follow-up studied of this work.

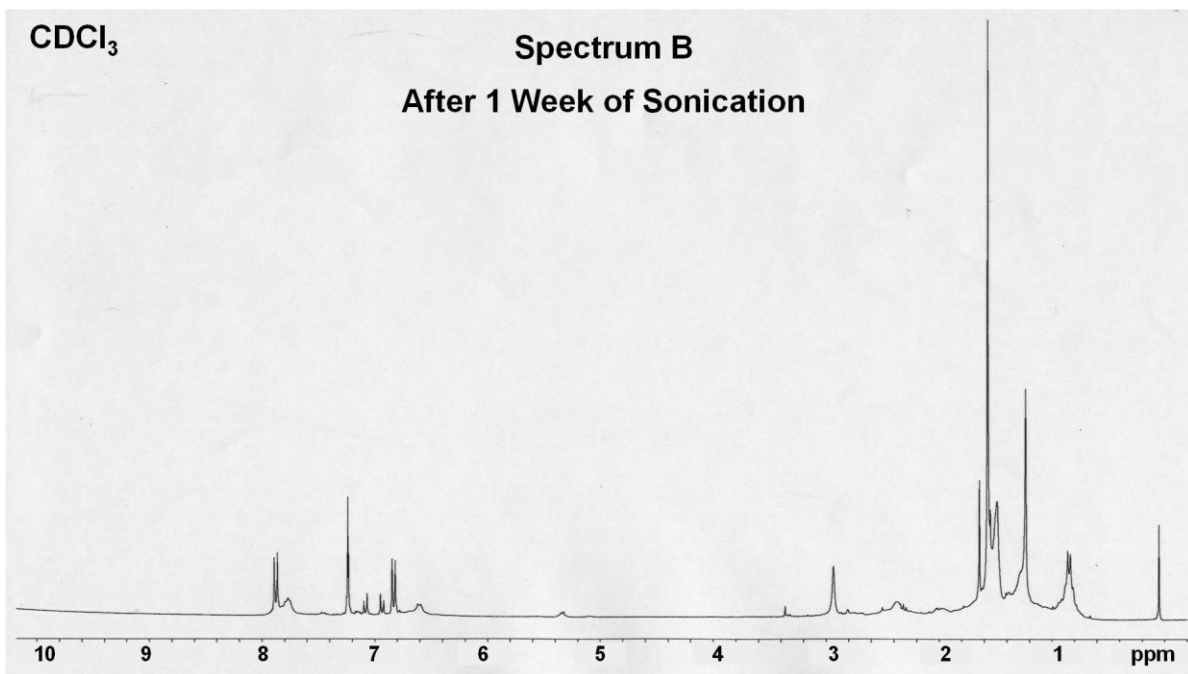
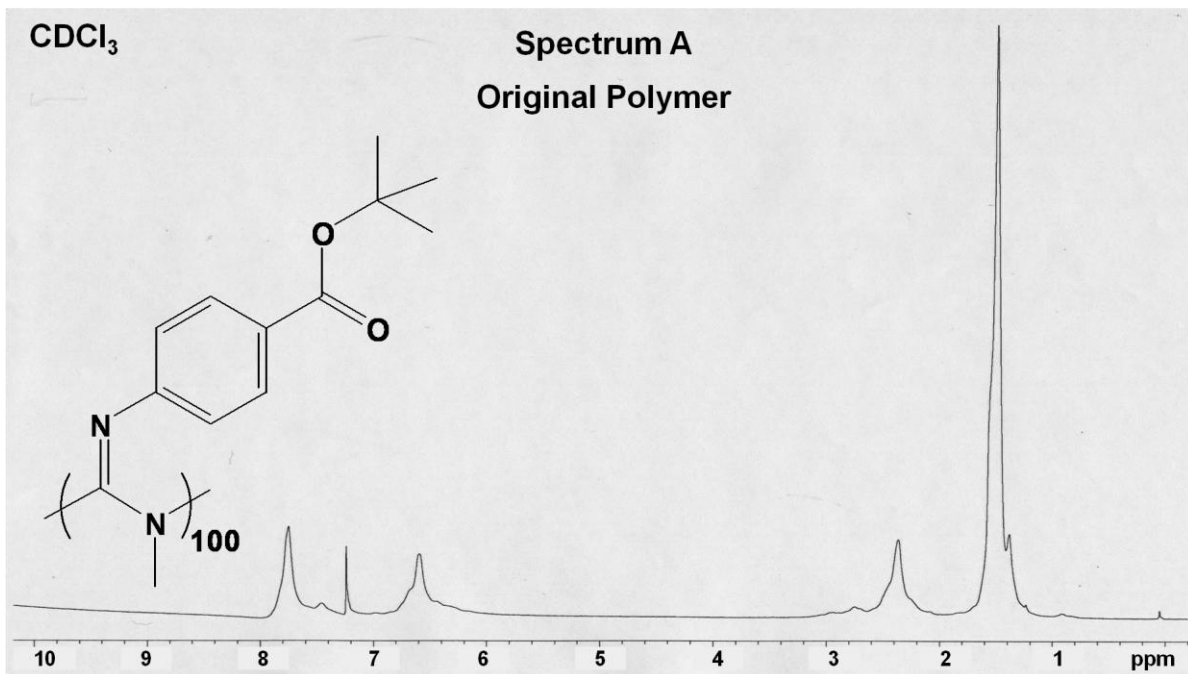


Figure 3.6: <sup>1</sup>H NMR spectra of poly-VI before and after sonicating in a simple 4:1 mixture of acetone and deionized water for 1 week. The replacement of broad proton signals with sharp signals indicates decomposition of the polymer into smaller molecules. In contrast to poly-VI's instability, poly(N-benzyl-N'-(4-n-butylphenyl)carbodiimide) does not decompose under analogous conditions.

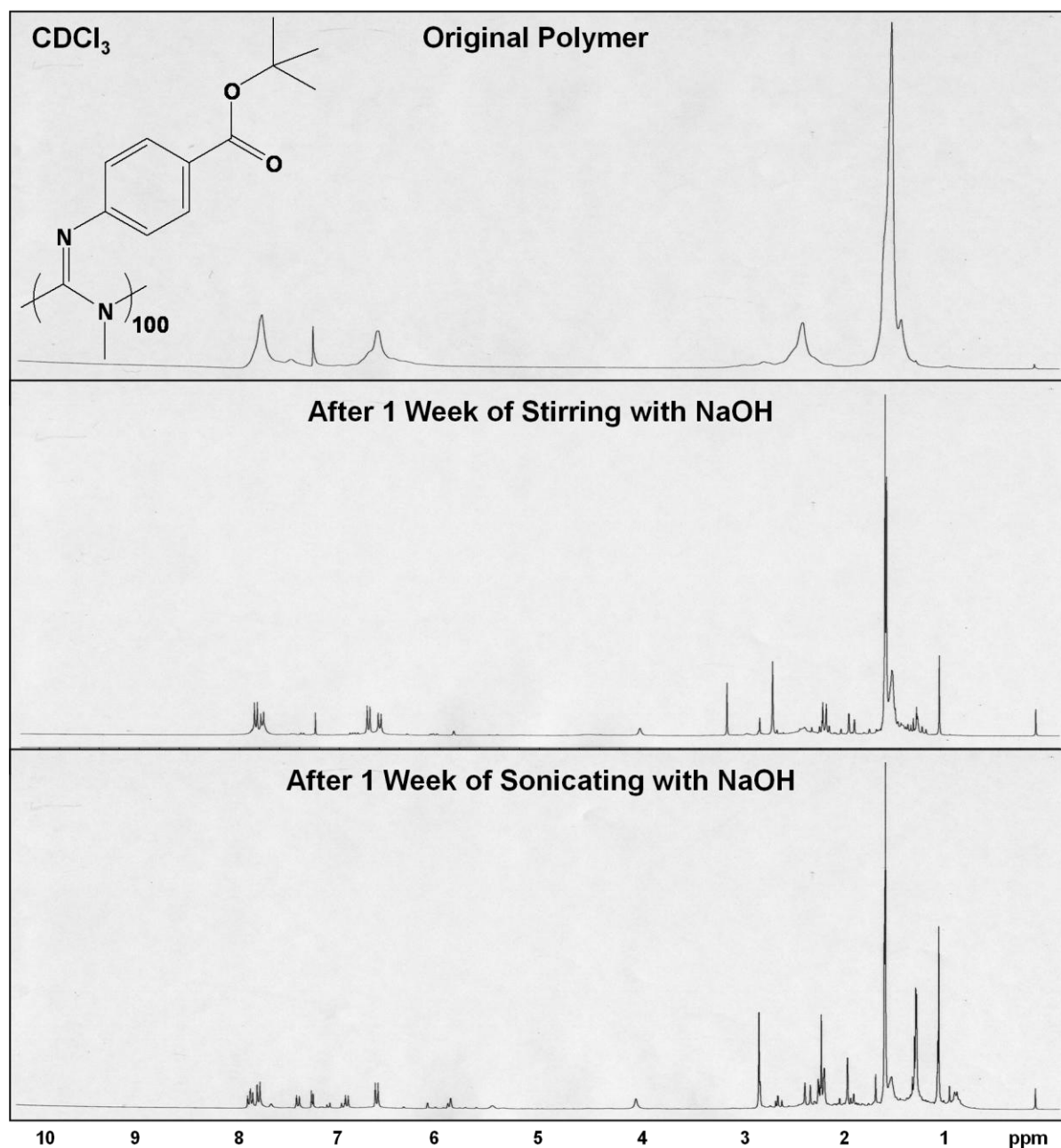


Figure 3.7:  $^1\text{H}$  NMR spectra of poly-VI before and after stirring or sonicating in a 4:1 mixture of acetone and 2.5 wt% aqueous sodium hydroxide for 1 week. Both stirring and sonicating in the presence of aqueous base lead to hydrolysis of the polymer backbone, as evidenced by the replacement of broad polymer signals with sharp small molecule signals. When compared with the ratio of broad-to-sharp signals in Spectrum B of Figure 3.6, the relatively lower intensity of broad signals in the bottom spectrum here indicates that sonicating in the presence of sodium hydroxide significantly accelerates the breakdown of the polymer.

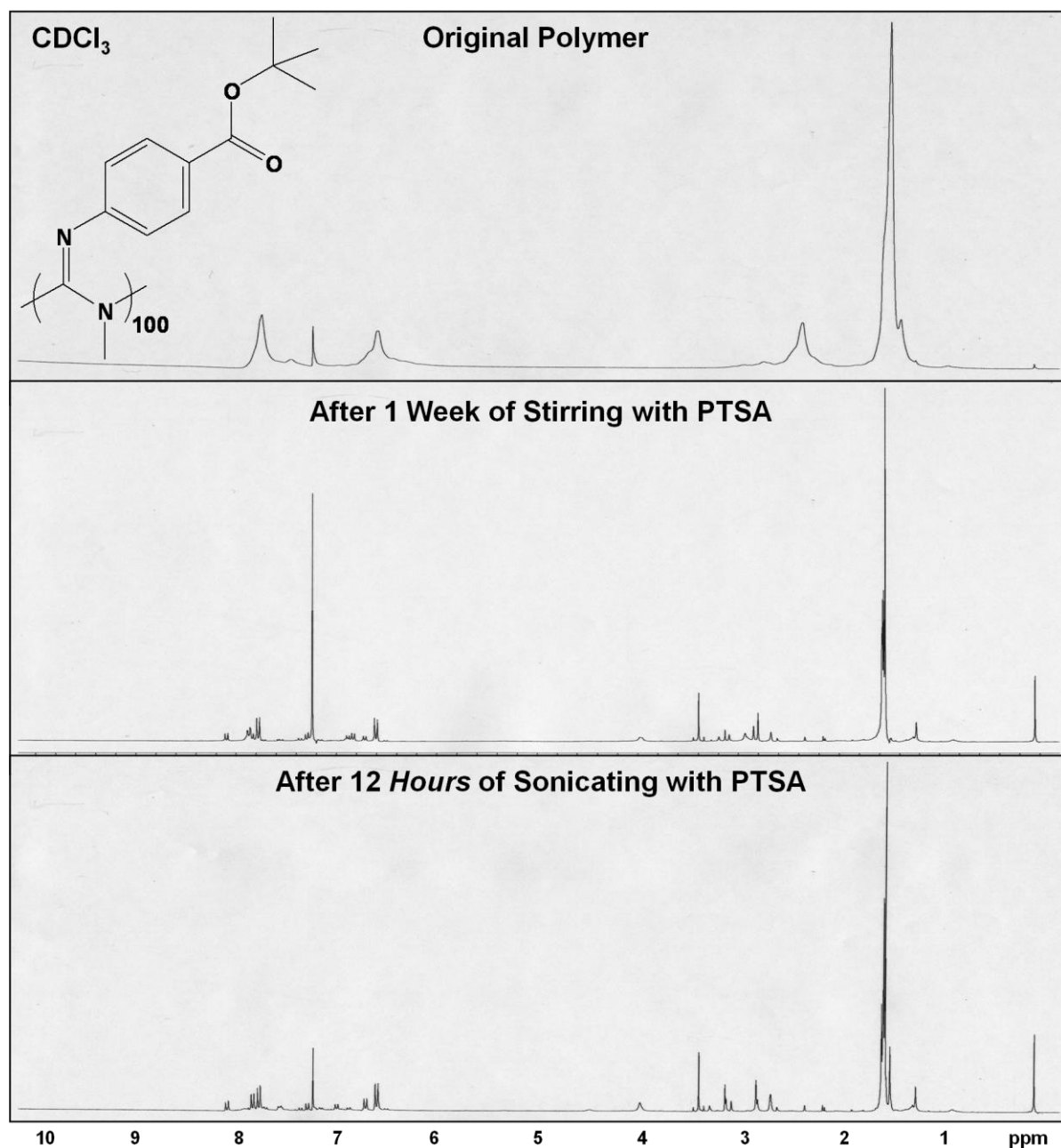


Figure 3.8:  $^1\text{H}$  NMR spectra of poly-VI before and after stirring or sonicating in a 4:1 mixture of acetone and 2.0 wt% aqueous p-toluenesulfonic acid. When compared with the ratio of broad-to-sharp signals in the Figure 3.7 spectra, it is clear from the relatively lower intensity of broad signals here that the polymer backbone hydrolyzes more rapidly under acidic conditions than under basic conditions. Hydrolysis occurs most rapidly with sonication under acidic conditions, leading to more complete dissolution of the insoluble polymer in 12 hours than within 1 week of simply stirring.

### 3.5. Regioselectivity Study on Carbodiimide Polymerization Catalysts

A key distinction between the structures of the older *t*-butyl ester-bearing carbodiimide designed by Kim and the newer ones derived from methyl ester-protected L-alanine is that due to the position of its ester unit on an aromatic ring, the former does not have any protons on the carbon that is alpha to the carbonyl. It is the enolizable proton on the alpha carbon of latter structures that precludes their polymerization with titanium catalysts. Thus titanium catalysts can be used to polymerize ester-bearing carbodiimides having structures analogous to the one designed by Kim, which is advantageous in that the chiral titanium catalyst proves to be more regioselective than copper catalysts.

The polymerization of N-hexyl-N'-phenylcarbodiimide with copper(I) butanethiolate versus the (S-BINOL)Ti(O-*i*Pr)<sub>2</sub> catalyst serves as a case in point. An expanded view of the aliphatic carbon region of the NMR spectra of this polycarbodiimide made with each catalyst, Figure 3.9 A & B respectively, finds the latter to have significantly sharper carbon signals, which is consistent with both a higher regioregularity and a predominance of one helical sense. A close inspection of the signals for the methylene carbons directly attached to the backbone, Figure 3.10, reveals not only sharper signals for the polymer made with chiral titanium catalyst, but also a greater relative intensity for the carbon signal of the dominant regiochemistry, which has the hexyl group on the amine position in either case.

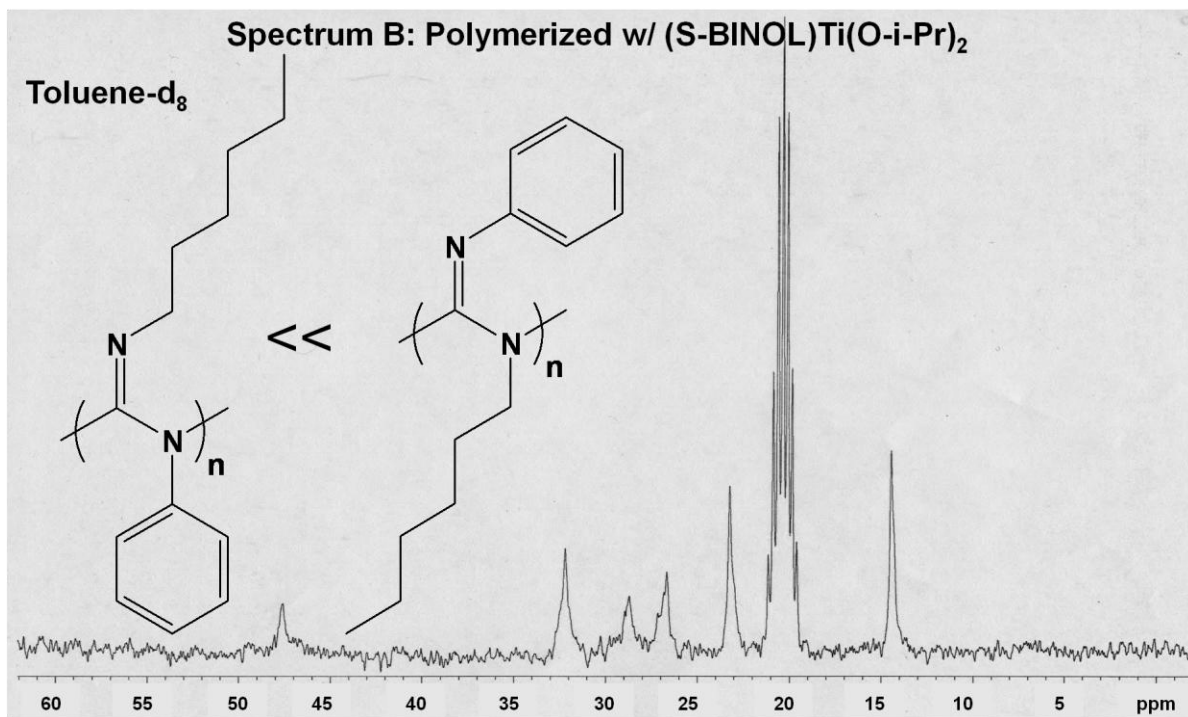
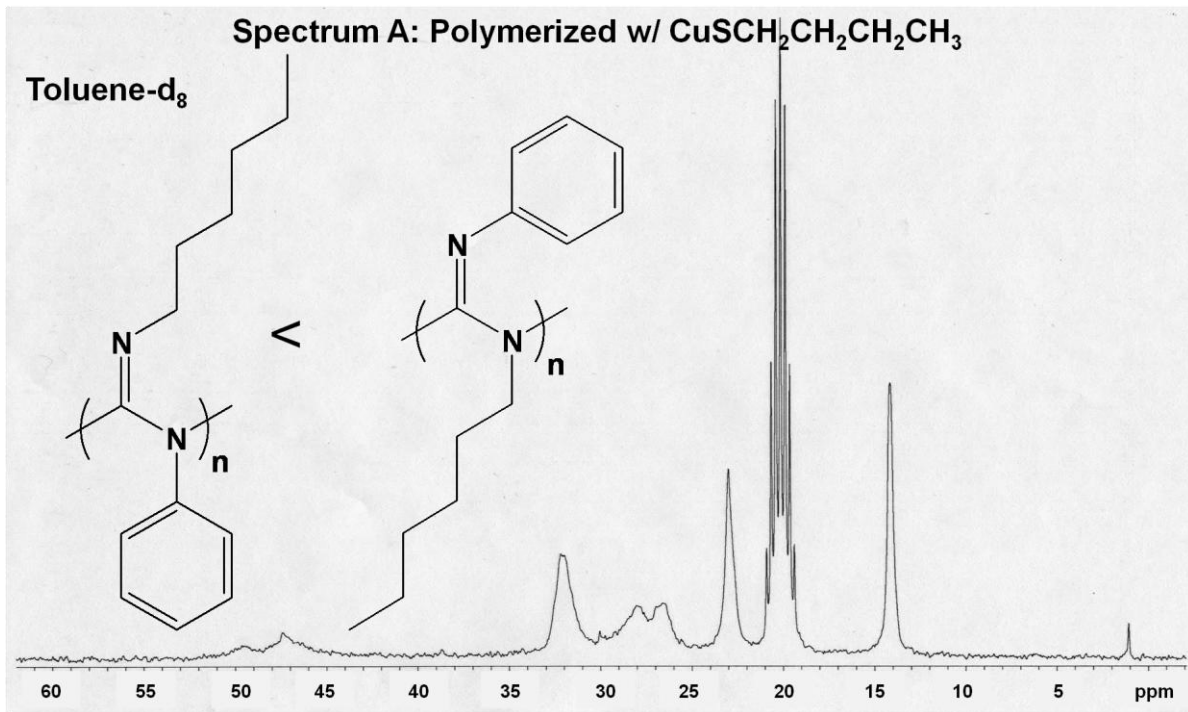


Figure 3.9: Aliphatic region of poly(N-hexyl-N'-phenylcarbodiimide) made with copper versus chiral titanium catalyst. The sharper carbon signals of the latter are a consequence of both its higher regioselectivity and its more singular helicity.

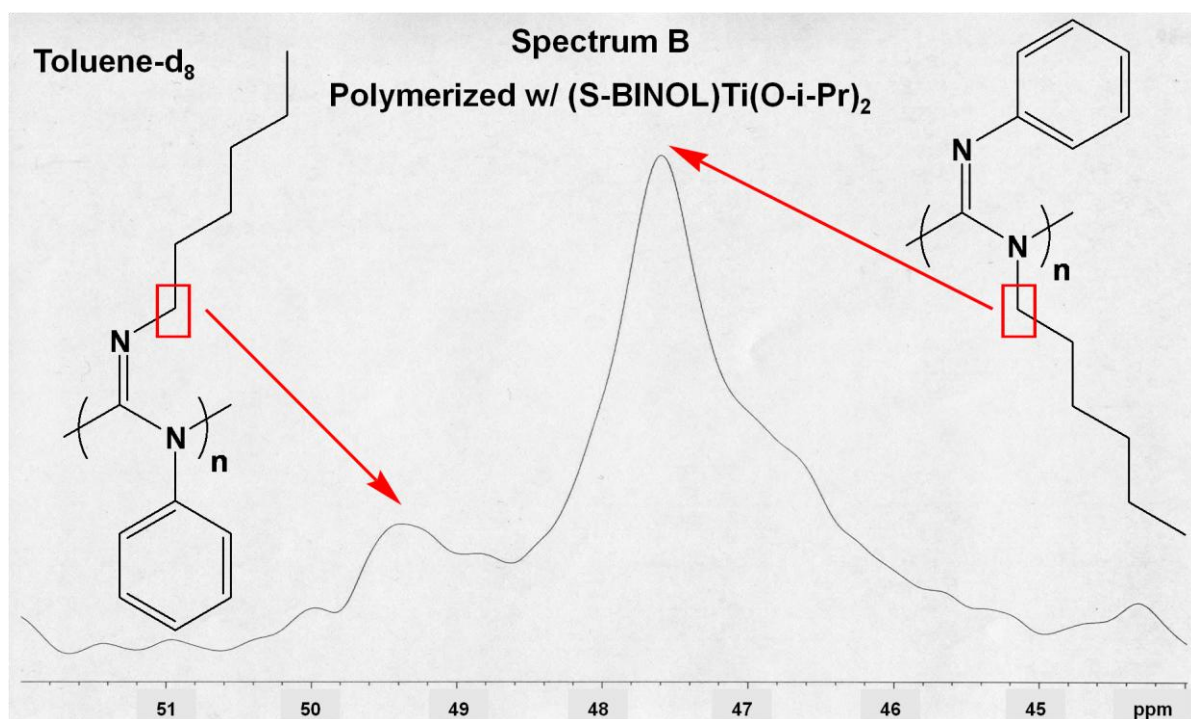
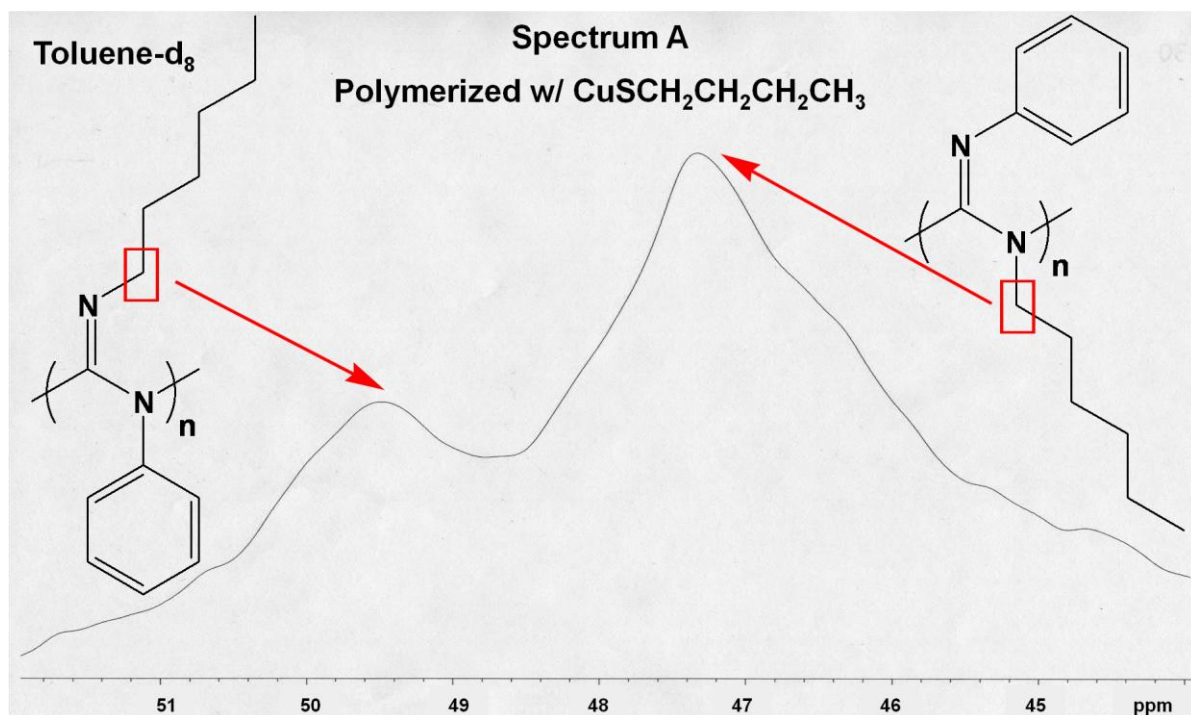


Figure 3.10: Expanded view of the signals for the alpha methylene carbons. Notice that the minor regiochemistry, having the hexyl substituent in the imine position, is significantly more prevalent from the copper-catalyzed polymerization.

### 3.6. Descendants of an Old Ester-Bearing Polycarbodiimide

In the interest of exploring the full potential of Kim's ester-bearing carbodiimide design, four derivatives were made, Figure 3.11. The first, VII, simply replaced the *t*-butyl substituent on the ester with a methyl group, with the aim of synthesizing a methyl ester-substituted polymer capable of modification via transesterification. Unlike most carbodiimides of comparable molecular weight, which are typically a clear viscous oil at room temperature, VII is a white solid. The only suitable solvent with which it can be dissolved is pyridine and the subsequent polymerization attempt unfortunately led to a low molecular weight product.

The second derivative, VIII, differed from the first in that the non-ester pendant group was an *n*-hexyl group rather than a methyl group. The aim of this modification was to alter the solubility of the monomer to facilitate polymerization in chloroform solvent. This strategy proved successful, leading to a chloroform-soluble carbodiimide, which was polymerized in high molecular weight with (S-BINOL)Ti(O-*i*-Pr)<sub>2</sub>.

The third derivative, IX, differed from the second in that the methyl substituent of the ester was replaced with a 2,2,2-trifluoroethyl group, which would, in theory, provide a better leaving group for transesterification. This carbodiimide too proved chloroform-soluble and was successfully polymerized in high molecular weight with the same chiral titanium catalyst.

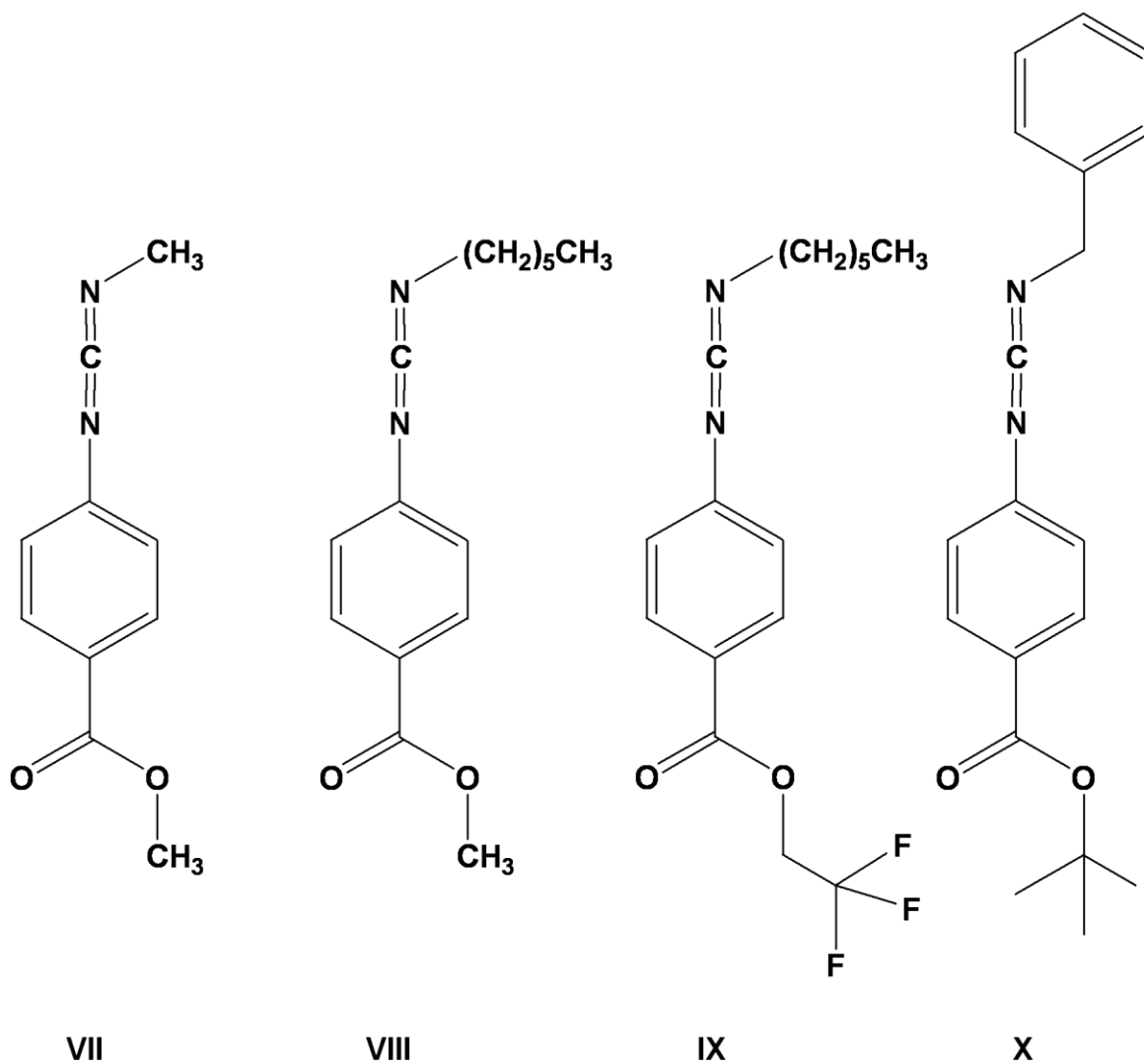


Figure 3.11: Four new derivatives of the old ester-bearing carbodiimide design by Jeonghan Kim. Monomer VIII and IX were made by dehydrating the corresponding urea precursor, while VII and X were made from the corresponding thiourea.

Unfortunately, neither poly-VIII nor poly-IX proved capable of transesterification. Both were tested with 250 equivalents per repeat of 2-methoxyethanol in the presence of appropriate catalytic amounts of either mercury (II) acetate<sup>4</sup> or potassium cyanide<sup>5</sup> with 18-crown-6, in chloroform, at both room temperature for 3 days in one set of experiments and at 60 °C overnight in another.

The most remarkable observation from these experiments was the thermal instability exhibited by poly-VIII and poly-IX. Both polymers decomposed appreciably in all reactions in which they were heated, as evidenced on the <sup>1</sup>H NMR spectra by the replacement of broad polymer signals with the sharp signals characteristic of small molecules. This thermally-induced decomposition was observed even in control reactions lacking catalyst, indicating that both poly-VIII and poly-IX are inherently unstable with respect to elevated temperatures. In either case, the instability appears to be a consequence of the electron-withdrawing effect of the ester unit on the phenyl pendant group, as the 2,2,2-trifluoroethyl ester of poly-IX exacerbated this instability, leading to decomposition at an accelerated rate.

The fourth derivative of Kim's ester-bearing carbodiimide, X, differs from the original in that the pendant methyl is replaced with a benzyl group. The aim was to develop a more robust structure on which the t-butyl ester substituent could be hydrolyzed without compromising the polycarbodiimide backbone. By replacing the pendant methyl with a benzyl group, the resulting polycarbodiimide would hybridize Kim's design with one proven to be stable in strong acid or base, Figure 3.12.

## Hybridization of Unstable & Stable Polycarbodiimide Designs

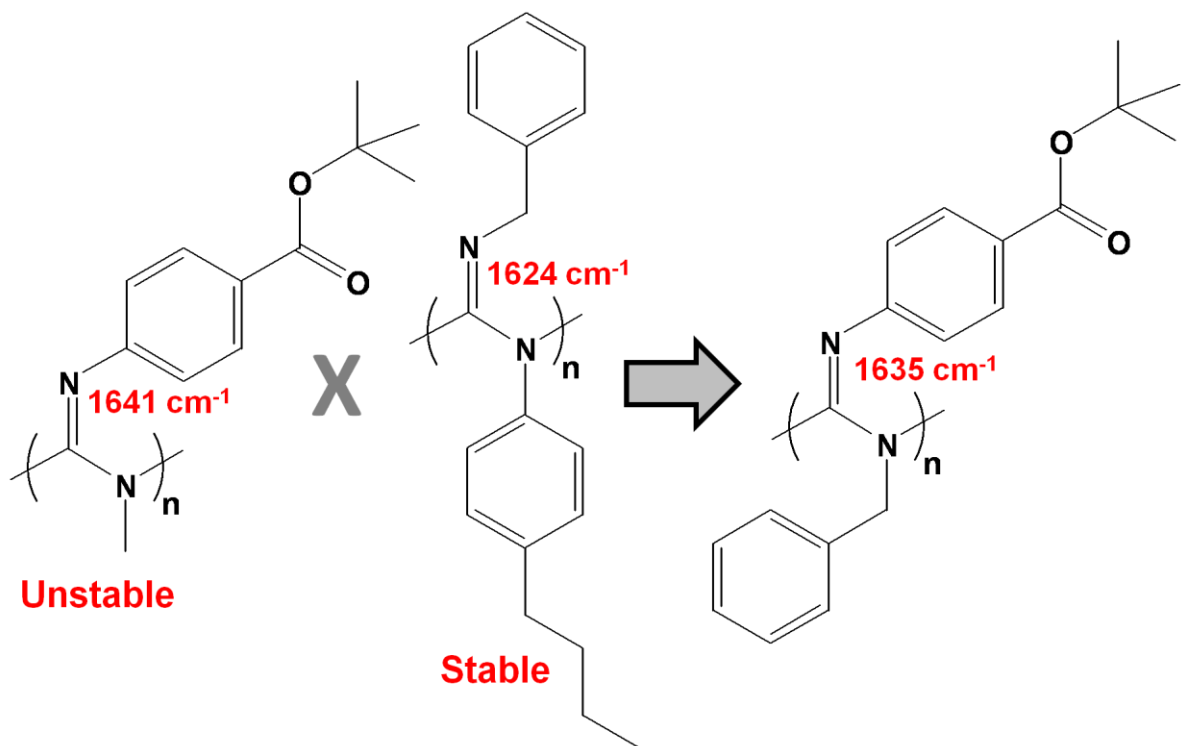


Figure 3.12: Hybrid design crossing Kim's ester-bearing polycarbodiimide – which is unstable under conditions that are strongly acidic or basic and even decomposes upon mere sonication – with a structure proven to be robust even when sonicated under strongly acidic or basic conditions for 1 week.

Curiously, poly-X exhibited the instability of Kim's design with respect to sonication and aqueous base, but it inherited the robustness of poly(N-benzyl-N'-(4-n-butylphenyl)carbodiimide) with respect to aqueous acid. Unfortunately, the t-butyl ester substituent proved to be just as stable under acidic conditions when presented from this structure, thus precluding subsequent polycarbodiimide modifications via coupling of alcohols or amides with a pendant free acid.

### 3.7. Polycarbodiimide Regiochemistry: Microstructural Determination via $^{13}\text{C}$ NMR

As mentioned in Section 1.5, for any asymmetrically-substituted carbodiimide, there are potentially two regiochemistries for the pendant groups on a given polycarbodiimide repeat. The earliest efforts to understand the regioselectivity of carbodiimide polymerizations relied on thermal degradation studies.<sup>11</sup> Based on the nearly ubiquitous observation of metathesis monomers following thermal degradation, these studies concluded that quantitatively regioselective polymerizations of asymmetric carbodiimides are exceptionally rare, requiring either an extreme difference in the size of the two pendant groups, as in the case of poly(N-methyl-N'-( $\alpha$ -methylbenzyl)carbodiimide),<sup>11</sup> or an extraordinary electronic influence, such as the one in poly(N-hexyl-N'-pentafluorophenylcarbodiimide).<sup>12</sup>

In recent years, the Novak Group has increasingly relied on the relative intensity of aliphatic- versus aromatic-imine absorptions on the infrared spectrum as a qualitative measure of which regiochemistry is preferred for a given polycarbodiimide pairing aliphatic and aromatic pendant groups. These estimates

are based on assignments of approximately 1620 and 1640  $\text{cm}^{-1}$ , respectively, for aliphatic- and aromatic-imine absorptions on such polycarbodiimides, following respective observations of 1640 and 1660  $\text{cm}^{-1}$  for imine absorptions on polycarbodiimides having only aliphatic or only aromatic pendant groups.

Assuming these assignments to be valid, the limitation of this practice is that in cases where the two regiochemistries are not present in comparable quantities, the close proximity of these imine absorptions precludes observing both since the higher intensity signal of the predominant imine absorption overlaps the lower intensity signal from the imine of the lesser regiochemistry. In situations such as these, it is easy to assume the polymer to be regioregular,<sup>13</sup> when such assumptions seem unlikely to be valid in light of the aforementioned thermal degradation studies.

The infrared spectrum of poly-X, Figure 3.13, is a case in point. As the only observable imine signal, the absorption at 1635  $\text{cm}^{-1}$ , indicating the aromatic group to occupy the imine position, would appear to suggest a single regiochemistry, a regioregular polycarbodiimide in other words. However, a thorough investigation via  $^{13}\text{C}$  NMR indicates a structure that is more regiochemically complex.

As an analytical technique for polycarbodiimide analysis, the use of  $^{13}\text{C}$  NMR has fallen into disfavor over the years. The quality of a spectrum, collected overnight, is typically insufficient to provide useful information in standard form, as illustrated by the  $^{13}\text{C}$  NMR spectrum of poly-X. The only signal that can be distinguished from the noise is the one for the three methyl carbons of the t-butyl group, Figure 3.14 A.

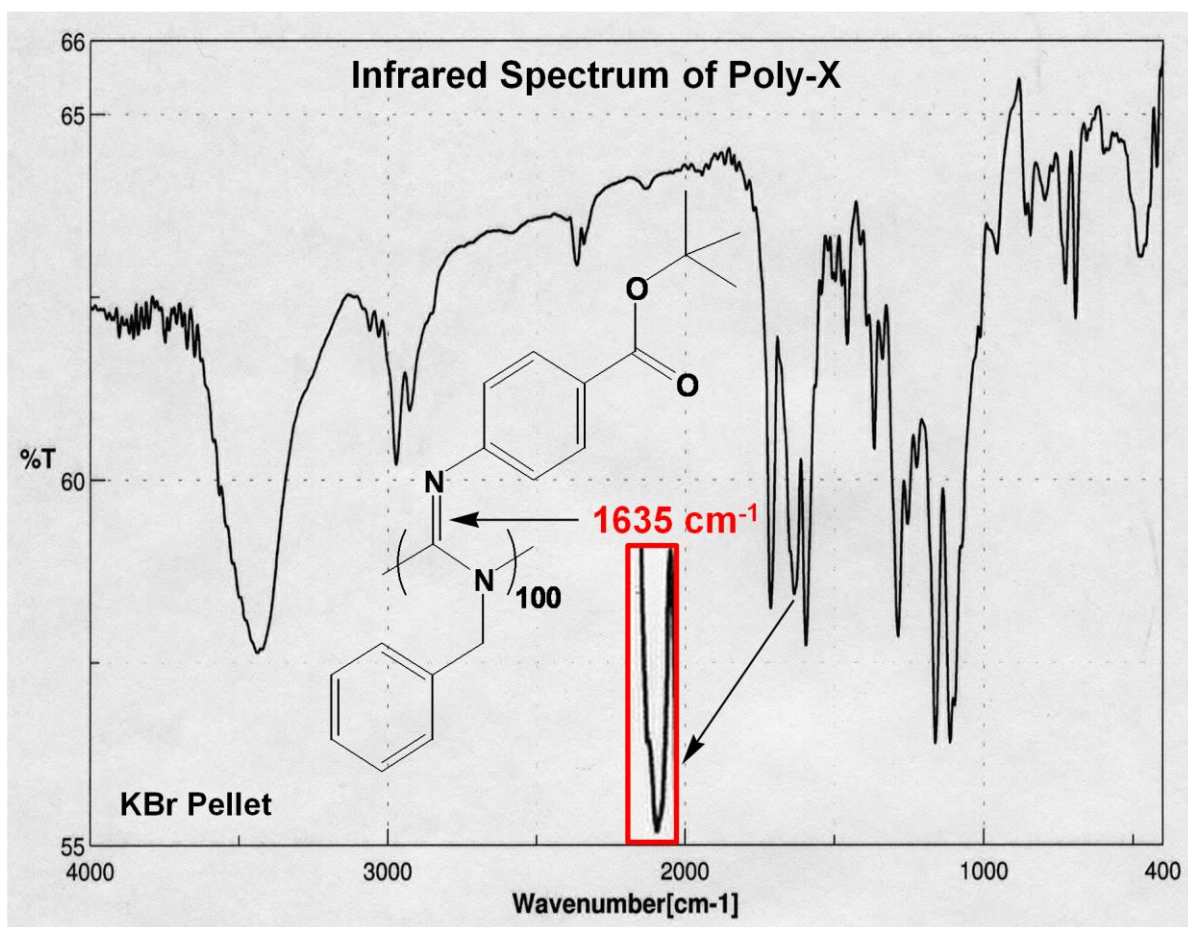


Figure 3.13: Infrared spectrum of poly-X. The only observable imine absorption is at  $1635\text{ cm}^{-1}$ , suggesting the aromatic pendant group occupies the imine position. The infrared spectrum does not provide any indication of the alternative regiochemistry, thus allowing observers to speculate that the structure is regioregular.

There are, however, a variety of ways to improve the NMR signal-to-noise ratio. The most obvious is to simply increase the number of scans. But a greater number of scans requires a lengthier analysis. A better compromise, given the time constraints on instrument availability, is to sacrifice some of the resolution to improve the signal-to-noise ratio through the application of line broadening. The greater separation of signals on the  $^{13}\text{C}$  NMR scale, versus those on the  $^1\text{H}$  NMR scale, provides a lot of room to sacrifice resolution without a loss of pertinent information.

When line broadening of 30 Hz – which is merely 0.40 ppm on the chemical shift scale – is applied to the  $^{13}\text{C}$  NMR spectrum of poly-X, what initially appeared to be relatively useless data, having only one distinguishable signal, Figure 3.14 A, reveals information on even the faintest signals of the structure, Figure 3.14 B. Even with a mere 5 Hz (0.067 ppm) of line broadening, a faint benzylic methylene carbon signal is apparent, Figure 3.15 A. A closer inspection of this region, with the application of 125 Hz (1.9 ppm) of line broadening, reveals two, slightly overlapping, methylene carbon signals, thus indicating two regiochemistries, Figure 3.15 B.

The relative intensities of the two benzylic methylene carbon signals agree with the predominant regiochemistry assignment via infrared imine absorption, namely that the benzyl group predominantly occupies the amine position. However, unlike the infrared spectrum, where only one regiochemistry is observable, here, through the application of line broadening to  $^{13}\text{C}$  NMR data, both are apparent, confirming as anticipated that the polycarbodiimide is indeed regioirregular.

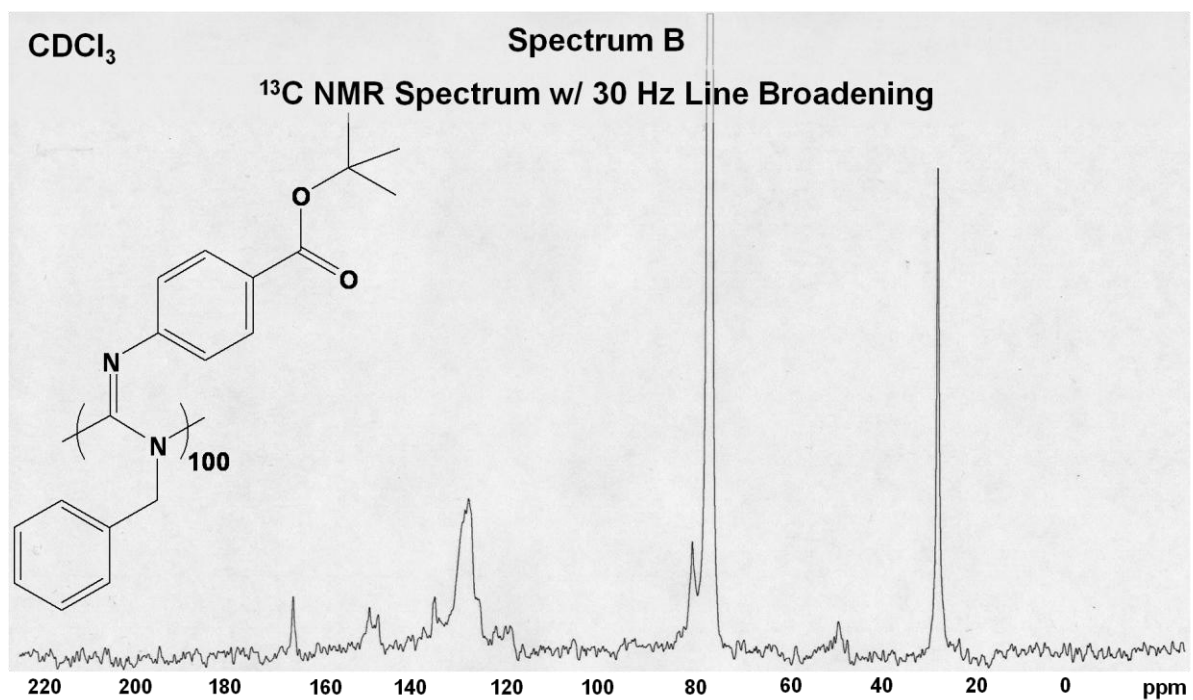
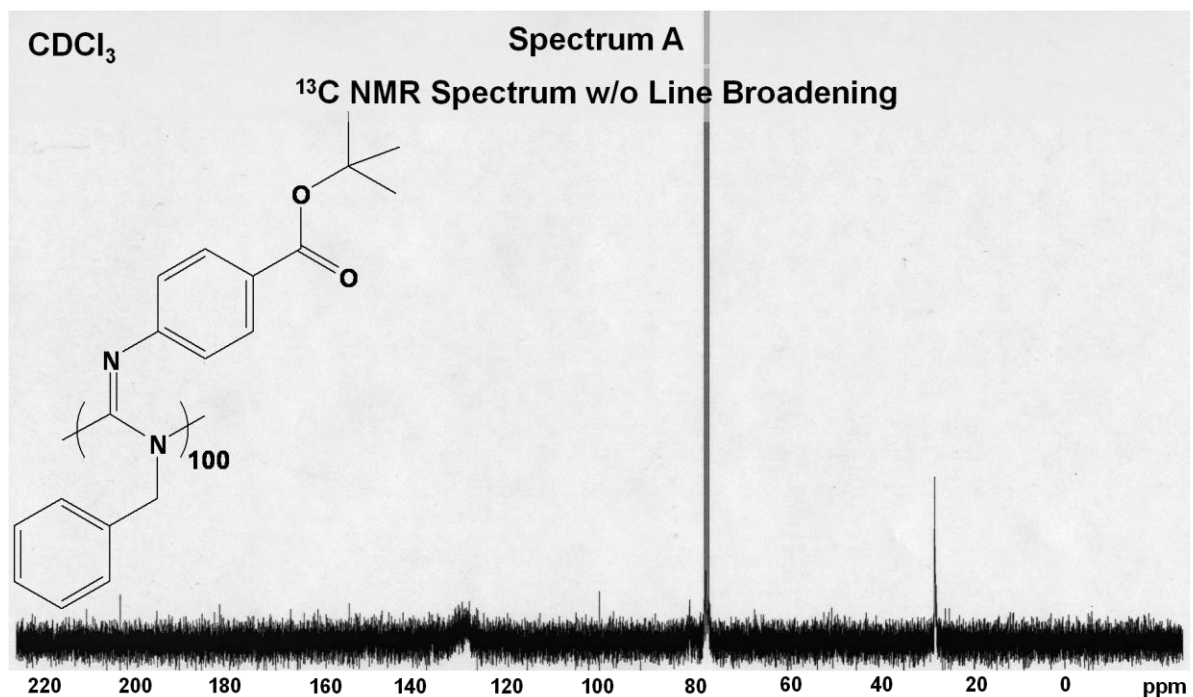


Figure 3.14: <sup>13</sup>C NMR spectra of poly-X before and after applying 30 Hz (0.40 ppm) of line broadening to the data. Notice the latter provides much greater detail, such as the signal of the carbonyl carbon at 166 ppm and that of the quaternary t-butyl carbon, just downfield of the solvent signal, at 80.9 ppm.

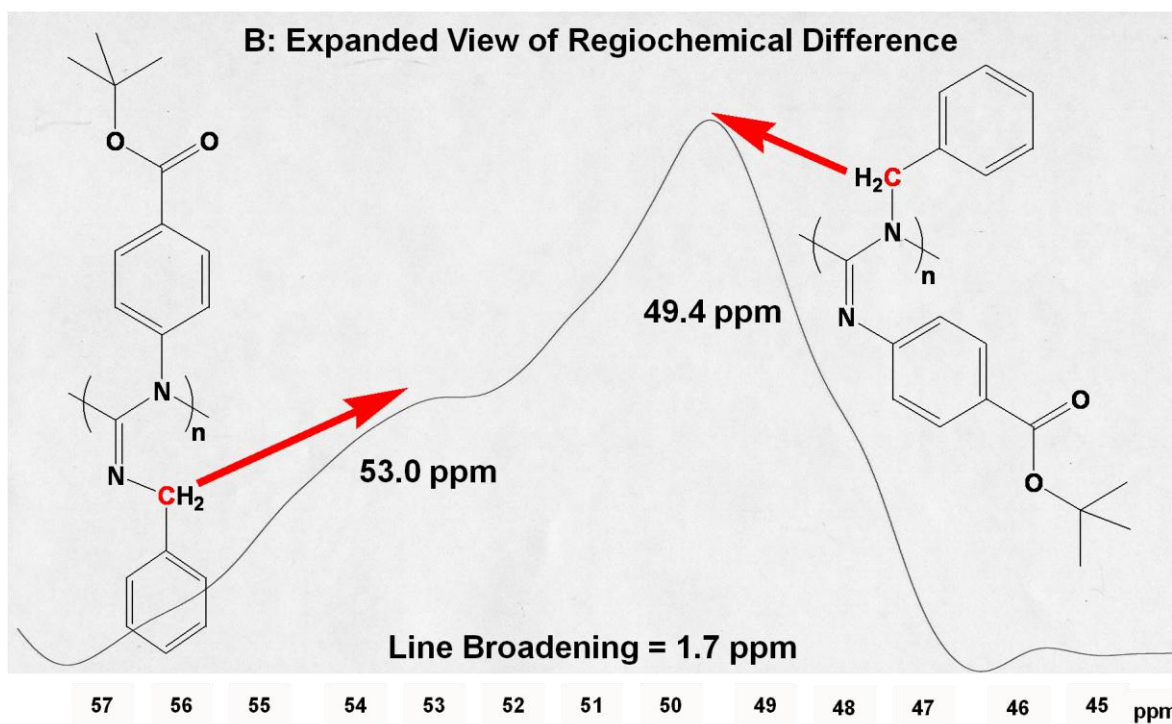
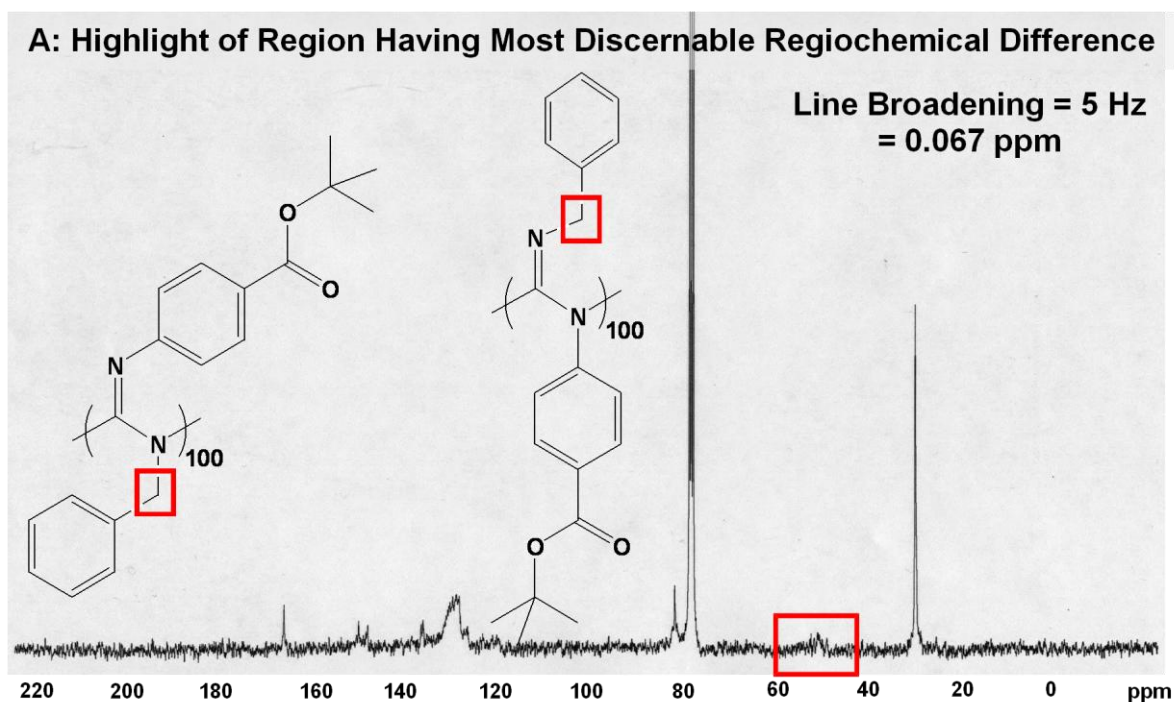


Figure 3.15: Highlighted and expanded views of the benzylic methylene carbon signals. Even with merely 5 Hz of line broadening, a signal clearly stands out from the noise. Further application of line broadening reveals two, slightly overlapping signals corresponding to each anticipated regiochemistry.

### 3.8. Conclusions

The stability of our latest model ester-bearing polycarbodiimide, synthesized from the chiral amino acid L-alanine, has been investigated under both strongly acidic and basic conditions. Efforts to transesterify the methyl ester substituent, in the presence of para-toluenesulfonic acid, reveal the polymer to decompose under strongly acidic conditions, doing so at an accelerated rate if heated. Base-catalyzed hydrolysis of the pendant ester substituent, with sodium hydroxide, hydrolyzes the polycarbodiimide backbone as well, leading to a well-characterized urea structure. Efforts to utilize mercury (II) acetate, potassium cyanide, or 4-dimethylaminopyridine to catalyze transesterification of the methyl ester pendant group with an alcohol were generally unsuccessful, though mercury (II) acetate did show promise with a sample of low molecular weight.

Re-opening our study of an earlier ester-bearing polycarbodiimide design, previously synthesized by Jeonghan Kim, a thorough investigation indicates the polymer to be unstable under conditions that are strongly basic or strongly acidic, revealing the polymer to decompose most rapidly when sonicated in the presence of a strong acid. The absence of enolizable protons allows ester-bearing carbodiimides of this earlier design to be polymerized with chiral, BINOL-titanium catalysts, which polymerize achiral carbodiimides with higher regioselectivity than does copper (I) butanethiolate.

Four derivatives of this earlier, ester-bearing carbodiimide were made, three of which were successfully polymerized in high molecular weight. One of these

three presented a methyl ester substituent, another a 2,2,2-trifluoroethyl ester substituent. Neither of these prove capable of transesterification catalyzed by mercury (II) acetate or potassium cyanide. Experiments in which these polymers are heated under refluxing conditions exhibit significant decomposition overnight, even in the absence of catalyst, an unprecedented level of instability when compared with well-studied polycarbodiimides bearing simple alkyl and aryl substituents. The electron-withdrawing effect of the 2,2,2-trifluoroethyl substituent exacerbates this instability.

Blending Kim's unstable ester-bearing polycarbodiimide design with that of poly(N-benzyl-N'-(4-n-butylphenyl)carbodiimide) – found to be highly stable under both acidic and basic conditions – the instability of the resulting hybrid, featuring a benzyl pendant group coupled with the ester-bearing aromatic one, indicates the original ester-bearing design to be inherently unstable with respect to sonication or basic conditions, though the auxiliary pendant group can be tailored to improve stability under acidic conditions. While the single imine absorption on the infrared spectrum of this hybrid polymer suggests a predominance of one regiochemistry, enhancement of the  $^{13}\text{C}$  NMR signal-to-noise ratio via line broadening reveals both regiochemistries to be present, facilitating new insights into the microstructure of such polycarbodiimide architectures.

### 3.9. Experimental Section

#### 3.9.1. General Procedures and Equipment

##### Instruments

All infrared spectra were recorded on a JASCO FT/IR-410 spectrometer. Characteristic absorptions are reported in wavenumbers ( $\text{cm}^{-1}$ ). All nuclear magnetic resonance spectra were recorded on Varian Mercury 300 or 400 MHz spectrometers. Chemical shifts are reported in  $\delta$  (ppm) relative to the assignment of solvent chemical shifts, referenced to tetramethylsilane, as listed in Table 3 of Appendix 4. Optical rotation measurements were recorded on a Jasco P-1010 Polarimeter at 589 nm. Solutions measured for optical rotation were prepared by dissolving 20 mg of sample overnight in 10 mL of solvent at room temperature. Thermogravimetric analyses were recorded on a TA Instruments Hi-Res TGA 2950 Thermogravimetric Analyzer. Differential Scanning Calorimetry analyses were performed with a TA Instruments DSC 2920 Modulated DSC.

##### Reagents

All reagents were obtained from a commercial supplier and used without further purification with the exception of solvents utilized for air- and moisture-sensitive procedures, which were purified under a nitrogen atmosphere via reflux over an appropriate drying agent,<sup>14</sup> followed by fractional distillation. 4A molecular sieves were oven-dried overnight at 215 °C, then cooled, and stored, in a desiccator. *The purity of commercially-supplied reagents was factored into all calculations in the sections that follow.*

## Inert Atmospheres

All air- and moisture-sensitive procedures were either conducted in a nitrogen-filled MBRAUN UNILab Dry Box or while utilizing Schlenk techniques facilitated by a Chemglass, CG-4441-03, 5-Port, Glass Stopcock, Inert Gas, Vacuum Manifold, coupled with a dual liquid nitrogen trap attached to a Welch Model Number 1402-01 Vacuum Pump. Vacuum pressures were observed with a Kurt J Lesker Company Millitorr Vacuum Gauge. Unopened, volatile-free, vacuum line pressures exceeding 50 mtorr were corrected by routine – typically weekly – vacuum line maintenance, which entailed Steps 12 through 16 of the more thorough “Guide to Vacuum Manifold Maintenance” procedure listed in Appendix 2. Glassware used for air- and moisture-sensitive procedures was dried overnight in an oven at 140 °C. Alternatively, glassware was flame-dried under vacuum (<100 mtorr). Stir bars utilized for air- and moisture-sensitive reactions were dried overnight, either in an oven at 140 °C or under vacuum (<100 mtorr). Alternatively, stir bars were retrieved from storage under nitrogen in the dry box. All septa were dried overnight in a vacuum chamber and stored under nitrogen in the dry box until used. All filter paper-covered, vacuum-needle assemblies utilized for air- and moisture-sensitive procedures were dried overnight in an oven at 140 °C.

### 3.9.2. Experimental Procedures and Characterizations

**t-Butyl p-Aminobenzoate.** p-Aminobenzoic acid (13.7 g, 99.9 mmol) was weighed and transferred to a 1000 mL round bottom flask. Toluene (200 mL), dried by standing over calcium hydride, and a magnetic stir bar were added. Thionyl chloride (55 mL, 89.7 g, 753 mmol), a 650% excess, was added to the reaction flask. The reaction mixture was refluxed overnight under an atmosphere of nitrogen. Removal of the volatiles by rotovap the next day revealed an amber oil. [Note: Oil-free, water-cooled, vacuum aspirators, such as the Brinkman Model B-169 Vacuum Aspirator, that are designed to be corrosive resistance, are the correct type to use for rotovaping samples containing thionyl chloride. Not even a liquid nitrogen-cooled, cold trap can prevent thionyl chloride from damaging an oil-lubricated vacuum pump attached to a rotovap.] t-Butyl alcohol (250 mL, 194 g, 2.61 mol), a 2,500% excess, and a magnetic stir bar were placed in a 500 mL round bottom flask. The amber oil, p-aminobenzoyl chloride, was transferred by pipet to the flask. The exotherm did not increase the temperature of the reaction above 40 °C. Following complete addition of the p-aminobenzoyl chloride, the reaction mixture was refluxed for 1 hour, 20 minutes. 143 mL of t-butyl alcohol were removed by rotovap at 65 °C. [Note: the freezing point of t-butyl alcohol is 23 to 26 °C. Hence a large quantity of it will freeze to the cold finger in the rotovap. Of the 143 mL of t-butyl alcohol recovered, 88 mL were initially recovered in liquid from the receiving flask and 55 mL were recovered from the receiving flask the next day after all of the alcohol that had frozen to the cold finger had melted.] Upon rotovaping to this concentration, the

alcohol solution was saturated. Saturated sodium carbonate (120 mL) was added to crushed ice (2000 mL) and room temperature water (500 mL). The reaction mixture was transferred to a separatory funnel, which was used to deliver the mixture in a steady stream to the cold, sodium carbonate slurry. A very large spatula was used to thoroughly mix the slurry while adding the reaction mixture. The product formed yellow clumps when added to the aqueous sodium carbonate mix. The resulting slurry was divided into two 1000 mL separatory funnels. The product was extracted with five, successive portions of chloroform (100 mL each). Each chloroform portion was poured first through one funnel, then the other, where they were shaken vigorously in each case. These extractions were performed while the water was still ice cold. The chloroform collected from these extractions formed two layers, the top layer of which is suspected to be predominately tert-butyl alcohol. Both layers were poured into a clean, 1000 mL separatory funnel. Saturated sodium chloride (500 mL) was added and the contents of the flask were shaken vigorously. Allowed to stand for 30 minutes, two layers appeared. The bottom, chloroform layer was slowly drained and then dried over sodium sulfate. [Note: Upon standing overnight, more chloroform separated from the salt water wash. This chloroform layer was collected as well.] The chloroform solution was initially cloudy in appearance. Upon standing overnight, the substance responsible for the cloudy appearance had clumped together, separating from the clear yellow solution to create a white cloud-like suspension. The solution was filtered through 18.5 cm diameter, Q8 filter paper. Because the white suspension clogs the filter paper, three filters were needed to

complete the filtration process as each filter was discarded upon clogging to the point of restricting the flow to a slow drip. Subsequent removal of the chloroform by rotovap revealed 12.9 g of yellow solid. The solid powder was loaded onto a chloroform-soaked column (95 g silica (60-200 particle size)) with chloroform (50 mL). Chloroform was used as the developing solvent and the column was developed under a positive air pressure. The first 185 mL, preceding the discolored band, were discarded. The next 1000 mL were collected. Removal of the chloroform by rotovap revealed 9.68 g of off-white powder (50% yield). IR (KBr Pellet) 3350 (s), 3238 (m), 3071 (vw), 3043 (vw), 3009 (w), 2974 (m), 2932 (w), 1686 (vs), 1638 (m), 1602 (s)  $\text{cm}^{-1}$ ;  $^1\text{H}$  NMR (300 MHz,  $\text{CDCl}_3$ )  $\delta$  (ppm) 7.78 (d,  $J = 8.9$  Hz, 2H), 6.60 (d,  $J = 8.9$  Hz, 2H), 3.98 (s, br, 2H), 1.55 (s, 9H).

**Methyl p-Aminobenzoate.** The first step, conversion of p-aminobenzoic acid to p-aminobenzoyl chloride, was performed exactly as described for t-Butyl p-Aminobenzoate. The second step, reaction of the acid chloride with an alcohol, differed as follows: anhydrous methanol (250 mL, 198 g, 6.17 mol), a 6000% excess, and a magnetic stir bar were placed in a 500 mL round bottom flask. The amber oil, p-aminobenzoyl chloride, was transferred by pipet to the flask. Following complete addition of the p-aminobenzoyl chloride, the reaction mixture was refluxed for 2 hours. 55 mL of methanol were removed by rotovap. Saturated sodium carbonate (140 mL) was added to crushed ice (2000 mL) and room temperature water (500 mL). The reaction mixture was transferred to a separatory funnel, which was used to deliver the mixture in a steady stream to the cold, sodium carbonate

slurry. A very large spatula was used to thoroughly mix the slurry while adding the reaction mixture. The product formed a fine precipitate when added to the aqueous sodium carbonate mix. The aqueous suspension was divided into two 1000 mL separatory funnels. Four chloroform extractions were performed by sending the extract through one funnel, then the other. The volumes of the five extracts were 250 mL, 100 mL, 100 mL, and then 50 mL. A goop-like substance, present at the bottom of the separatory funnel, was removed and discarded by filtering the extracts through 18.5 cm diameter, Q8 filter paper. Approximately half a dozen filters of this size were needed to collect all of this goop as the filter papers became clogged and needed replacing. The combined chloroform extracts (500 mL total) were pre-dried with a wash of saturated sodium chloride (500 mL) and then dried over sodium sulfate. Removal of the chloroform by rotovap revealed 9.89 g of off-white powder (65% yield). IR (KBr Pellet) 3370 (s), 3248 (m), 3066 (vw), 3032 (vw), 2996 (vw), 2947 (w), 1682 (s), 1656 (m) 1602 (vs)  $\text{cm}^{-1}$ ;  $^1\text{H NMR}$  (300 MHz,  $\text{CDCl}_3$ )  $\delta$  (ppm) 7.83 (d,  $J = 8.6$  Hz, 2H), 6.62 (d,  $J = 8.6$  Hz, 2H), 4.03 (s, br, 2H), 3.83 (s, 3H).

**2,2,2-Trifluoroethyl p-Aminobenzoate.** The first step, conversion of p-aminobenzoic acid to p-aminobenzoyl chloride, was performed exactly as described for t-Butyl p-Aminobenzoate. The second step, reaction of the acid chloride with an alcohol, differed as follows: 2,2,2-trifluoroethanol (100 mL, 139 g, 1.39 mol), a 1300% excess, and a stir bar were placed in a 500 mL round bottom flask. The amber oil, p-aminobenzoyl chloride, was transferred by pipet to the flask. The mixture formed a solid within a minute. Additional alcohol (100 mL, 139 g, 1.39 mol)

was added and the flask was lowered into an oil bath heated to 85 °C. Saturated sodium carbonate (120 mL) was added to crushed ice (2000 mL) and room temperature water (500 mL). The reaction mixture was transferred to a separatory funnel, used to deliver the mixture in a steady stream to the cold, sodium carbonate slurry. A very large spatula was used to mix the slurry while adding the reaction mixture. The product formed a fine, white precipitate in the sodium carbonate slurry. The slurry was divided into two 1000 mL separatory funnels. The product was extracted with five, successive chloroform portions (100 mL each). Each chloroform portion was poured first through one funnel, shaken vigorously, and then through the other. These extractions were performed while the water was still ice cold. The chloroform extracts were combined, dried over sodium sulfate, and filtered through P8 filter paper. The chloroform was removed by rotovap, leaving a brown liquid that solidified on standing. Attempts to recrystallize the product from chloroform proved unsuccessful. The product was dissolved in hot chloroform (50 mL) and transferred to a separatory funnel, which was used to transfer the solution dropwise into a flask of magnetically-stirred pentanes (300 mL). The supernatant was removed with a filter paper-covered, vacuum-needle assembly. [See Appendix 1 for filter paper-covered, vacuum-needle assembly instructions.] The remaining volatiles were removed under vacuum, revealing 13.7 g of slightly yellow powder (91% yield). IR (KBr Pellet) 3350 (s), 3242 (s), 3062 (vw), 3043 (vw), 3022 (vw), 2983 (w), 1707 (vs), 1647 (s), 1599 (vs)  $\text{cm}^{-1}$ ;  $^1\text{H}$  NMR (300 MHz,  $\text{CDCl}_3$ )  $\delta$  (ppm) 7.86 (d,  $J = 8.7$  Hz, 2H), 6.63 (d,  $J = 8.7$  Hz, 2H), 4.62 (q,  $J = 8.4$  Hz, 2H), 4.13 (s, 2H).

**N-methyl-N'-(p-(t-butoxy)carbonylphenyl)thiourea.**

t-Butyl-p-

aminobenzoate (9.68 g, 50.0 mmol) was weighed and transferred to a 250 mL round bottom flask. Chloroform (100 mL) and a magnetic stir bar were added. Methyl isothiocyanate, 97% (18.9 g, 251 mmol), a 400% excess, was added and the reaction mixture was heated for 1 week at 60 °C. The reaction mixture was rotovaped at 60 °C until saturated, as judged by the appearance of precipitation. The amount of chloroform that had been removed, measured by recovery from the collection flask of the rotovap, was approximately 45 mL. Upon cooling to room temperature, the relatively large quantity of precipitate resulted in a slurry. Removal of the remaining chloroform from the slurry, by vacuum filtration with a filter paper-covered, vacuum-needle assembly, was a slow, tedious process. [See Appendix 1 for filter paper-covered, vacuum-needle assembly instructions.] Upon removing the majority of the remaining chloroform, a wash of hexanes (5 mL) was used to facilitate purification. A total of 53.8 mL of supernatant were removed. Removal of the remaining volatiles by vacuum revealed 9.36 g of white powder, verified by <sup>1</sup>H NMR to be the desired thiourea in high purity as evidenced by the absence of the signal for the amine proton set of the starting material (70 % yield). IR (KBr Pellet) 3383 (s), 3165 (m), 3049 (vw), 3003 (w), 2978 (w), 2933 (w), 1693 (s), 1529 (s), 1161 (m), 1124 (m) cm<sup>-1</sup>; <sup>1</sup>H NMR (300 MHz, CDCl<sub>3</sub>) δ (ppm) 8.01 (d, J = 8.7 Hz, 2H), 7.88 (s, br, 1H), 7.21 (d, J = 8.7 Hz, 2H), 6.21 (s, br, 1H), 3.14 (d, J = 4.5, 3H), 1.57 (s, 9H).

**N-benzyl-N'-(p-(t-butoxy)carbonylphenyl)thiourea.**

t-Butyl-p-

aminobenzoate (6.20 g, 32.1 mmol) was weighed and transferred to a 100 mL round bottom flask. Chloroform (50 mL) and a magnetic stir bar were added. Benzyl isothiocyanate, 97% (14.8 g, 96.2 mmol), a 200% excess, was added to the flask. The reaction mixture was refluxed for 7 days. The flask was removed from heat and rotovaped until the product had a paste-like consistency. Since hexanes and benzyl isothiocyanate are miscible, hexanes (25 mL) were added, producing a fine, white precipitate. The supernatant was removed. After two subsequent hexane rinses (25 mL each), the product was dried under high vacuum, revealing 10.6 g of white powder. <sup>1</sup>H NMR analysis revealed contamination. The product was washed with three portions of hexanes (25 mL) and dried again under high vacuum to reveal 10.3 g of white powder (93% yield, which is approximately a 1% loss per hexane rinse). IR (KBr Pellet) 3302 (m), 3032 (vw), 3001 (w), 2974 (w), 2925 (w), 1695 (vs), 1525 (vs), 1304 (vs), 1157 (m), 1124 (m) cm<sup>-1</sup>; <sup>1</sup>H NMR (300 MHz, Acetone-d<sub>6</sub>) δ (ppm) 9.24 (s, br, 1H), 7.91 (d, J = 9.0 Hz, 2H), 7.84 (s, br, 1H), 7.67 (d, J = 8.7 Hz, 2H), 7.4 to 7.2 (m, 5H), 4.89 (d, J = 5.1, 2H), 1.57 (s, 9H).

**N-methyl-N'-(p-methoxycarbonylphenyl)thiourea.**

Methyl p-

aminobenzoate (6.00 g, 39.7 mmol) was weighed and transferred to a 250 mL round bottom flask. Chloroform (100 mL) and a magnetic stir bar were added. Methyl isothiocyanate, 97% (2.99 g, 199 mmol), a 400% excess, was added and the reaction mixture was heated for 6 days at 60 °C. The product, a light-brown solid, was suspended in the chloroform at the time the reaction was removed from heat.

After cooling to room temperature, the flask was stoppered and placed in the refrigerator for 2 hours. The cold supernatant was removed by use of a filter paper-covered, vacuum-needle assembly. [See Appendix 1 for filter paper-covered, vacuum-needle assembly instructions.] Removal of the remaining volatiles by high vacuum revealed 8.84 g light-brown powder (99% yield). IR (KBr Pellet) 3448 (s), 3386 (s), 3026 (w), 2945 (w), 1707 (s), 1533 (s), 1173 (m), 1111 (m)  $\text{cm}^{-1}$ ;  $^1\text{H}$  NMR (300 MHz,  $\text{CDCl}_3$ )  $\delta$  (ppm) 8.06 (d,  $J = 8.7$  Hz, 2H), 7.95 (s, br, 1H), 7.25 (d,  $J = 8.7$  Hz, 2H), 6.26 (s, br, 1H), 3.90 (s, 3H), 3.16 (s,  $J = 4.5$ , 3H).

**N-hexyl-N'-(p-methoxycarbonylphenyl)urea.** Methyl p-aminobenzoate (5.25 g, 34.7 mmol) was added to chloroform (50 mL) in a 100 mL round bottom flask. Hexyl isocyanate, 97% (9.11 g, 70.9 mmol) a 100% excess, was added and the reaction mixture was heated for 5 days at 60 °C. The chloroform solvent was removed by rotovap. Chloroform (15 mL) was added to re-dissolve the product. The product was then precipitated in magnetically-stirred pentanes (80 mL). Collection and drying of the precipitate revealed 7.60 g of white powder (79% yield). IR (KBr Pellet) 3346 (s), 3016 (vw), 2951 (m), 2929 (m), 2866 (m), 1716 (s), 1668 (s)  $\text{cm}^{-1}$ ;  $^1\text{H}$  NMR (300 MHz, Acetone- $d_6$ )  $\delta$  (ppm) 8.22 (s, br, 1H), 7.87 (d,  $J = 9.0$  Hz, 2H), 7.60 (d,  $J = 9.0$  Hz, 2H), 5.91 (t, br, 1H), 3.82 (s, 3H), 3.21 (m, 2H), 1.52 (m, 2H), 1.31 (m, br, 6H), 0.88 (t,  $J = 6.8$ , 3H).

**N-hexyl-N'-(p-(2,2,2-trifluoroethoxy)carbonylphenyl)urea.** Chloroform (50 mL) and t-(2,2,2-trifluoroethyl)-p-aminobenzoate (4.60 g, 30.4 mmol) were added to a 100 mL round bottom flask. Hexyl isocyanate, 97% (3.99 g, 30.4 mmol) was

added. The flask was placed in an oil bath heated to 60 °C to facilitate the reaction. 10 days later, the flask was removed from heat. The insoluble crude product was collected by filtration. The crude product was dissolved in acetone (40 mL) and then precipitated from the solution in ice-cold hexanes (200 mL). The solid white product was collected on filter paper. Drying of the product under high vacuum revealed 1.05 g of white flakes (10% yield). Concentrating the supernatant collected 3.48 g of white crystals (an additional 33% yield (bringing the total yield to 43%)). IR (KBr Pellet) 3440 (s), 3062 (vw), 2960 (m), 2933 (m), 2860 (w), 1732 (s), 1647 (s), 1171 (s)  $\text{cm}^{-1}$ ;  $^1\text{H}$  NMR (300 MHz,  $\text{CDCl}_3$ )  $\delta$  (ppm) 8.35 (2, br, 1H), 7.93 (d, J = 8.9 Hz, 2H), 7.65 (d, J = 8.9 Hz, 2H), 5.98 (t, br, 1H), 4.87 (q, J = 8.7, 2H), 3.21 (m, 2H), 1.51 (m, 2H), 1.30 (m, br, 6H), 0.88 (t, J = 6.6 Hz, 3H).

**N-methyl-N'-(p-(t-butoxy)carbonylphenyl)carbodiimide.** Acetone (150 mL), dried over sodium sulfate, was added to a 250 mL round bottom flask. N-methyl-N'-(p-(t-butoxy)carbonylphenyl)thiourea (9.68 g, 36.3 mmol) and a magnetic stir bar were added. A reflux condenser was attached and the flask was positioned in a hot oil bath heated to 75 °C. Mercury (II) oxide, 99% (11.9 g, 54.4 mmol) was added at a rate of approximately 2 g every 10 minutes. After the last addition, the reaction was refluxed for 3 hours. The product was removed from heat, allowed to cool for 1 hour, and then filtered, under pressure, through a column, pre-soaked with acetone, consisting, from top to bottom, of 2 mm sand, 5 mm diatomaceous earth (Celite<sup>TM</sup> – 545 Filter Aid), 2 mm sand, and 6.5 mm silica gel (60-200 Mesh – Grade 62). Acetone (300 mL) was used to rinse the product from the column. The total

volume of solution collected from the column was 473 mL. The solution was dried over magnesium sulfate. Upon transferring to another flask, the magnesium sulfate was rinsed with enough acetone to bring the total solution volume to 500 mL. Removal of the acetone by rotovap revealed 8.16 g of crude yellow oil. The oil was dissolved in 10 mL of chloroform for column chromatography. 163 g of silica (60-200 Mesh – Grade 62) which is approximately 20 g per 1 g of oil, were used in this column. [Subsequent consultation with other members of the Novak Group, who utilize column chromatography routinely for carbodiimide purification, suggests that using 20 g of silica per gram of carbodiimide may be far too much. Best estimates are that the optimum range is from 6 to 12 g of silica per gram of carbodiimide.] 2.5 L of chloroform were used to develop the column. The first fraction (400 mL) was discarded. The pure carbodiimide was isolated from the next fraction (300 mL). Removal of the chloroform by rotovap, followed by high vacuum, revealed 1.5 g of clear, slightly viscous, nearly colorless oil (18% yield). The much greater weight of crude oil loaded onto the column, 8.16 g, which would be 97% of the anticipated yield, suggests that this reaction resulted in a very high yield but that the majority of the product was lost on the column. IR (Neat) 3037 (w), 2978 (m), 2935 (m), 2144 (s), 1709 (s), 1599 (s), 1292 (s)  $\text{cm}^{-1}$ ;  $^1\text{H}$  NMR (300 MHz,  $\text{CDCl}_3$ )  $\delta$  (ppm) 7.90 (d, J = 8.4 Hz, 2H), 7.07 (d, J = 8.4 Hz, 2H), 3.20 (s, 3H), 1.58 (s, 9H).

**N-benzyl-N'-(p-(t-butoxy)carbonylphenyl)carbodiimide.** Acetone (100 mL), dried over sodium sulfate, was added to a 250 mL round bottom flask. N-benzyl-N'-(p-(t-butoxy)carbonylphenyl)thiourea (5.00 g, 12.6 mmol) and a magnetic

stir bar were added. A reflux condenser was attached and the flask was positioned in a hot oil bath heated to 70 °C. Mercury (II) oxide, 99% (4.79 g, 21.9 mmol) was added at a rate of approximately 1 g every 12 minutes. After the last addition, the reaction was refluxed for 4 hours. Immediately upon removing the flask from heat, the supernatant was recovered with a filter paper-covered, vacuum-needle assembly. [See Appendix 1 for filter paper-covered, vacuum-needle assembly instructions.] The mercury sulfide precipitate was rinsed with two portions of acetone (5 mL each) to facilitate transfer of the carbodiimide. The acetone was removed by rotovap, revealing 4.63 g of yellow oil. The oil was dissolved in chloroform (10 mL) for column chromatography. 46.2 g of silica (60-200 particle size – 62 Grade) which is approximately 10 g per 1 g of oil, topped with 2 cm of sand were used in the column. The sample was loaded onto the chloroform-soaked column and developed with chloroform. The structure of the column was compromised somewhat from the force of pouring in the developing solvent with less than appropriate care. The first, 100 mL fraction was discarded. The carbodiimide was isolated from the next 350 mL. Removal of the chloroform by rotovap, followed by high vacuum, revealed 2.30 g of clear oil (49% yield). IR (Neat) 3087 (vw), 3064 (w), 3030 (w), 3005 (w), 2978 (m), 2931 (m), 2870 (w), 2135 (vs), 1709 (s), 1296 (s)  $\text{cm}^{-1}$ ;  $^1\text{H}$  NMR (300 MHz, Acetone- $\text{d}_6$ )  $\delta$  (ppm) 7.87 (d,  $J = 8.7$  Hz, 2H), 7.5 to 7.2 (m, 5H), 7.08 (d,  $J = 8.7$  Hz, 2H), 4.71 (s, 2H), 1.56 (s, 9H).

**N-methyl-N'-(p-methoxycarbonylphenyl)carbodiimide.** Acetone

(100 mL), dried over sodium sulfate, was added to a 250 mL round bottom flask. N-methyl-N'-(p-methoxycarbonylphenyl)thiourea (4.20 g, 18.7 mmol) and a magnetic stir bar were added. A reflux condenser was attached and the flask was positioned in a hot oil bath heated to 75 °C. Mercury (II) oxide, 99% (6.14 g, 28.1 mmol), a 50% excess, was added at a rate of approximately 1 to 1.5 g every 12 minutes. After the last addition, the reaction was refluxed for 3 hours. Immediately upon removing the flask from heat, the supernatant was recovered with a filter paper-covered, vacuum-needle assembly. [See Appendix 1 for filter paper-covered, vacuum-needle assembly instructions.] This worked well: only a trace of the mercury sulfide byproduct transferred with the supernatant. The mercury sulfide precipitate was rinsed with two portions of acetone (5 mL each) to facilitate transfer of the carbodiimide. The acetone solution was concentrated to approximately 20 mL and loaded onto a column consisting of 2 cm sand and 35.0 g silica gel (60-200 Mesh – Grade 62). The column was developed with chloroform (300 mL). The first fraction (50 mL) was discarded. The second fraction (50 mL), characterized by a strong yellow discoloration, was isolated for further purification and dried with magnesium sulfate. IR and <sup>1</sup>H NMR analyses of the fractions that followed revealed comparable quantities of the carbodiimide product and thiourea reactant, so those were discarded. Removal of the acetone from the second fraction revealed a yellow oily paste. This fraction was dissolved in ethyl acetate (20 mL) and loaded onto a column consisting of 2 cm sand and 35.0 g silica gel (60-200 Mesh – Grade 62).

The column was developed with ethyl acetate. The first, 75 mL fraction was discarded. The next, 50 mL fraction exhibited a strong yellow discoloration. Removal of the ethyl acetate revealed a viscous, yellow oil. IR analysis revealed the asymmetric N=C=N stretch to be the dominant absorption on the spectrum.  $^1\text{H}$  NMR revealed the sample to be predominantly carbodiimide. The dominant contaminant signals were identified as  $\text{H}_2\text{O}$  and HOD, most likely from the un-dried acetone- $\text{d}_8$  NMR solvent. No exchangeable protons, characteristic of the thiourea precursor, were present. The sample was placed under high vacuum, down to 25 mtorr, for 2 hours. As the volatile ethyl acetate boiled away, the carbodiimide began to solidify, forming white specks within the viscous, yellow oil. The flask, containing 1.90 g (53% yield). IR (Neat) 3068 (vw), 3033 (vw), 2993 (w), 2951 (m), 2143 (vs), 1718 (s), 1277 (s)  $\text{cm}^{-1}$ ;  $^1\text{H}$  NMR (300 MHz, Acetone- $\text{d}_6$ )  $\delta$  (ppm) 7.94 (d, J = 8.6 Hz, 2H), 7.17 (d, J = 8.6 Hz, 2H), 3.83 (s, 3H), 3.25 (s, 3H).

**N-hexyl-N'-(p-methoxycarbonylphenyl)carbodiimide.**

Dibromotriphenylphosphorane salt, 98% (6.89 g, 16.0 mmol), a 25% excess, was dissolved in methylene chloride (20 mL) in a 100 mL round bottom flask. A magnetic stir bar was added and the flask was placed in an ice-water bath. Triethylamine, 99% (4.8 mL, 3.45 g, 34.1 mmol), a 30% excess, was added to the reaction at a rate of approximately 1 mL every 5 minutes. N-hexyl-N'-(p-methoxycarbonylphenyl)urea (3.56 g, 12.8 mmol) was dissolved in methylene chloride (30 mL). 1 hour after the last addition of triethylamine, the urea solution was added to the reaction at a rate of approximately 5 mL every 5 minutes. The next day, the product was washed with

deionized water (50 mL), followed by saturated sodium chloride (50 mL). The methylene chloride extract was dried by standing over sodium sulfate for 15 minutes. The methylene chloride was removed by rotovap. The carbodiimide was extracted from the remaining solids with pentanes (50 mL). The solid, triphenylphosphine oxide precipitate was rinsed with several portions of pentanes (5 mL each) to facilitate quantitative carbodiimide extraction. The pentane extract was dried over magnesium sulfate. Removal of the pentanes by rotovap, followed by high vacuum, revealed 3.01 g of yellow oil. Relative integration ratios of the  $^1\text{H}$  NMR spectrum indicates a 94% purity of the carbodiimide (85% yield), with 6% triphenylphosphine oxide contaminate. IR (Neat) 3053 (vw), 3018 (vw), 2952 (m), 2929 (m), 2858 (w), 2141 (vs), 1720 (s), 1275 (s)  $\text{cm}^{-1}$ ;  $^1\text{H}$  NMR (300 MHz, Acetone- $\text{d}_6$ )  $\delta$  (ppm) 7.95 (d,  $J = 8.7$  Hz, 2H), 7.17 (d,  $J = 8.7$  Hz, 2H), 3.86 (s, 3H), 3.55 (t,  $J = 6.8$  Hz, 2H), 1.73 (m, 2H), 1.46 (m, 2H), 1.33 (m, 4H), 0.88 (t,  $J = 7.0$  Hz, 3H).

**N-hexyl-N'-(p-(2,2,2-trifluoroethoxy)carbonylphenyl)carbodiimide.**

Dibromotriphenylphosphorane salt, 98% (7.04 g, 16.3 mmol), a 25% excess, was dissolved in methylene chloride (40 mL) in a 100 mL round bottom flask. A magnetic stir bar was added and the flask was placed in an ice-water bath. Triethylamine, 99% (4.8 mL, 3.45 g, 34.1 mmol), a 33% excess, was added to the reaction at a rate of approximately 1 mL every 5 minutes. N-hexyl-N'-(p-(2,2,2-trifluoroethoxy)carbonylphenyl)urea (4.53 g, 13.1 mmol) was suspended in methylene chloride (50 mL). The suspension of urea was added at a rate of approximately 6 mL every 5 minutes. The next day, the product solution was washed with deionized water (100

mL), followed by two, successive washes of saturated sodium chloride (100 mL each). Then the solution was dried by standing over sodium sulfate for 30 minutes. The solution was filtered into a 100 mL graduated cylinder and the sodium sulfate was rinsed with sufficient methylene chloride to bring the total volume of the solution to 100 mL. The solution was divided into two equal portions. 30 g of silica gel, Davisil, Grade 644, 100-200 mesh, was loaded onto a 4 cm diameter column. [Davisil, Grade 644 is an expensive, neutral grade of silica gel. Neutrality is a desirable feature in that acidic or basic gels are anticipated to react with carbodiimides, reducing column recovery.] The column was topped with approximately 2 cm of Ottawa Sand, Standard 20 – 30 Mesh. The methylene chloride was removed from one of the two aforementioned portions by rotovap. The crude product was then dissolved in chloroform (10 mL) and loaded onto the chloroform-soaked column. The column was developed with chloroform (843 mL). The first fraction (93 mL) was discarded. 1.90 g of opaque yellow oil was isolated from the next fraction (50 mL). The four, subsequent fractions (50 mL each) were included in the workup as described later, while the rest were ultimately discarded. The opaque, yellow oil was analyzed by  $^1\text{H}$  NMR. The relative integration ratios on the spectrum revealed a 68% purity of the carbodiimide, with 32% triphenylphosphine oxide contaminate, indicating a mass of 1.29 g carbodiimide, a 60% yield for the first, column-purified portion. Upon removing the methylene chloride from the aforementioned second portion by rotovap, the carbodiimide was extracted from the triphenylphosphine oxide byproduct with two, successive portions

of pentanes (50 mL each). Removal of the pentanes by rotovap, followed by high vacuum revealed 1.91 g of clear, yellow oil. The relative integration ratios of the  $^1\text{H}$  NMR spectrum revealed an 89% purity of the carbodiimide, with 11% triphenylphosphine oxide contaminate, indicating a mass of 1.70 g carbodiimide, a 79% yield for the second portion. Upon discovering that extraction with pentanes isolates the carbodiimide in higher purity, the carbodiimide isolated from the second, 50 mL fraction developed from the first portion was combined with subsequent 200 mL from the column, which had higher concentrations of triphenylphosphine oxide contaminant, and rotovaped to remove the chloroform. Extraction with two, successive portions of pentanes (50 mL each), followed by removal of the pentanes by rotovap and high vacuum, revealed 1.10 g of viscous, opaque, yellow oil. The relative integration ratios of the  $^1\text{H}$  NMR spectrum revealed a 62% purity of the carbodiimide, with 38% triphenylphosphine oxide contaminate, indicating a mass of 682 mg carbodiimide, a 32% yield, ultimately, for the first portion. IR (Neat) 3057 (vw), 2958 (m), 2931 (m), 2860 (w), 2145 (vs), 1736 (s), 1275 (s), 1157 (s)  $\text{cm}^{-1}$ ;  $^1\text{H}$  NMR (300 MHz, Acetone- $d_6$ )  $\delta$  (ppm) 8.00 (d,  $J = 8.6$  Hz, 2H), 7.23 (d,  $J = 8.6$  Hz, 2H), 4.91 (q, 2H), 3.57 (t,  $J = 6.6$  Hz, 2H), 1.73 (m, 2H), 1.46 (m, 2H), 1.34 (m, 4H), 0.89 (t,  $J = 6.9$  Hz, 3H).

**(S)-(-)-1,1'-Binaphth-2,2'-ol Titanium(IV) Diisopropoxide.** In a nitrogen-filled dry box, (S)-(-)-1,1'-Binaphthol-2,2'-ol (524 mg, 1.83 mmol) was weighed in a 20 mL vial. A magnetic stir bar and anhydrous toluene (2 mL) were added. A 3% excess of titanium tetraisopropoxide (536 mg, 1.89 mmol) was weighed in a

separate 20 mL vial. The titanium tetraisopropoxide was transferred by pipet to the vial containing the alcohol. A toluene rinse (1 mL) was utilized to facilitate quantitative transfer. After 4 hours of stirring in the vial, the reaction mixture and stir bar were transferred to a Schlenk flask. The flask was sealed, removed from the dry box, and attached to a Schlenk line. Using Schlenk technique, the flask was placed under a positive pressure of nitrogen. Removing the toluene solvent from the product, while not contaminating the sample with moisture and oxygen, is an art that is difficult to put into words and takes considerable practice. Basically, the first step was to ensure that the glass stopper used to seal the flask is properly greased in order to make an effective seal. While maintaining a positive outflow of nitrogen, the stopper was temporarily removed. Vacuum grease was applied to the stopper, which was then returned to the flask and twisted back and forth to ensure a uniform distribution. The flask was placed in an ice-water bath positioned on top of a magnetic stir plate. Magnetic stirring was applied, both to facilitate cooling and to avoid violent bumping of the solvent upon application of vacuum. Two of the five ports on the inert gas, vacuum manifold system were connected with a rubber hose. One port was opened to a positive pressure of nitrogen, the other was cracked slightly open to vacuum as needed to adjust the pressure in the vacuum manifold to approximately 500 mtorr. At this point, the reaction flask was opened to vacuum. The flask was shook vigorously to prevent the contents from bumping violently. The toluene evaporated rapidly as the nitrogen leak was gradually closed in stages over a period of 20 minutes. Following the point at which only a solid remained, the flask

was removed from the ice-water bath. Once the pressure had dropped to 80 mtorr, the flask was filled with nitrogen, the glass stopper was temporarily removed, under a positive outflow of nitrogen, and a flame-dried spatula was used to crush the dark-orange product into a powder. Vacuum was re-applied. Once the pressure reached 45 mtorr, the flask was filled with nitrogen and returned to the dry box. A test of the catalyst product with N,N'-di-n-hexylcarbodiimide (100:1), formed polymer within minutes, proving the batch to be active.

**Poly(N-methyl-N'-(p-(t-butoxy)carbonylphenyl)carbodiimide). (S)-(-)-**  
1,1'-Binaphth-2,2'-ol titanium(IV) diisopropoxide (26.8 mg, 59.5  $\mu$ mol) and a magnetic stir bar were added to a 10 mL glass vial containing N-methyl-N'-(t-butyl p-aminocarbonylphenyl)carbodiimide (1.46 g, 6.24 mmol) in a nitrogen-filled dry box. The catalyst appeared to be sparingly soluble in the carbodiimide, so after approximately 5 minutes, anhydrous chloroform (0.75 mL) was added. Following solvation in chloroform, the viscosity quickly increased. Within 5 minutes, the magnet stir bar was frozen in place. The vial was noticeably warm when removed from the dry box, indicating that the reaction was significantly exothermic. 24 hours later, anhydrous chloroform (3 mL) was added and the vial was placed on an orbital shaker. The following day, the viscous chloroform solution was further diluted with additional chloroform (4 mL). This solution was then added dropwise to magnetically-stirred methanol (100 mL), resulting in the appearance of a fine white precipitate in yellow supernatant. The clear yellow supernatant was removed with a filter paper-covered, vacuum-needle assembly. [See Appendix 1 for filter paper-

covered, vacuum-needle assembly instructions.] This was a very slow process, requiring approximately 30 min or so as the fine precipitate hindered the flow of supernatant through the filter paper. The precipitate was washed with four successive portions of methanol (25 mL). Removal of the methanol from the first wash revealed only a few milligrams of material, indicating that the polymer was not significantly soluble in methanol. Removal of the remaining volatiles from the precipitate by high vacuum revealed 1.17 g of white powder having a slightly yellow tint (80% yield). IR (KBr Pellet) 3041 (vw), 2978 (m), 2933 (w), 1712 (s), 1641 (s), 1594 (s), 1292 (s), 1157 (s)  $\text{cm}^{-1}$ ;  $^1\text{H}$  NMR (300 MHz,  $\text{CDCl}_3$ )  $\delta$  (ppm) 7.79 (s, br, 2H), 6.63 (s, br, 2H), 2.39 (s, br, 3H), 1.50 (s, br, 9H);  $^{13}\text{C}$  NMR (300 MHz,  $\text{CDCl}_3$ )  $\delta$  (ppm) 166, 152, 148, 131, 127, 121, 80.9, 34.1, 28.4; 185.8 °C Decomposition Temperature (5% Loss of Mass);  $T_g$  absent from Differential Scanning Calorimetry Analysis; Specific Optical Rotation measured  $-22.7^\circ \pm 0.5^\circ$ .

**Poly(N-benzyl-N'(p-(t-butoxy)carbonylphenyl)carbodiimide).** (S)-(-)-1,1'-Binaphth-2,2'-ol titanium(IV) diisopropoxide (31.7 mg, 70.4  $\mu\text{mol}$ ) and a magnetic stir bar were added to a 10 mL glass vial containing N-benzyl-N'-(t-butyl p-aminocarbonylphenyl)carbodiimide (2.29 g, 7.06 mmol) in a nitrogen-filled dry box. A chloroform rinse (0.25 mL) was utilized to facilitate transfer of the catalyst. Additional chloroform solvent (1 mL) was added at this point. The viscosity of the reaction solution increased gradually. The polymer reaction formed a solid within 4 to 5 days. On day 5, chloroform (3 mL) was added. Re-dissolving was facilitated via agitation with a vortexer. On day 7, the polymer was diluted with additional

chloroform (37 mL) and precipitated in magnetically-stirred methanol (200 mL). The precipitate was left stirring overnight. The next day, the supernatant was removed with a filter paper-covered, vacuum-needle assembly. [See Appendix 1 for filter paper-covered, vacuum-needle assembly instructions.] This was a very, very slow process, requiring approximately 3 hours as the fine precipitate hindered the flow of supernatant through the filter paper. The precipitate was rinsed with methanol (10 mL). The remaining volatiles were removed by vacuum, revealing 1.06 g of yellow flakes (46% yield). IR (KBr Pellet) 3064 (vw), 3035 (vw), 2976 (m), 2929 (w), 1713 (s), 1635 (s), 1592 (s), 1288 (s), 1163 (s), 1115 (s)  $\text{cm}^{-1}$ ;  $^1\text{H}$  NMR (300 MHz,  $\text{CDCl}_3$ )  $\delta$  (ppm) 7.86, 7.49, 7.14, 7.02, 6.89, 6.61, 6.44, 6.24, 6.09, 5.79, 5.79, 4.86, 3.46, 2.50, 1.56, 1.30, 0.95 (all broad);  $^{13}\text{C}$  NMR (300 MHz,  $\text{CDCl}_3$ )  $\delta$  (ppm) 166, 150, 148, 136, 128, 120, 80.8, 50.0, 48.3, 28.6; 182.2  $^\circ\text{C}$  Decomposition Temperature (5% Loss of Mass);  $T_g$  absent from Differential Scanning Calorimetry Analysis; Specific Optical Rotation measured  $-879^\circ \pm 0.8^\circ$ .

**Poly(N-methyl-N'(p-methylcarbonylphenyl)carbodiimide.** (S)-(-)-1,1'-Binaphth-2,2'-ol titanium(IV) diisopropoxide (45.0 mg, 99.9  $\mu\text{mol}$ ) and a magnetic stir bar were added to a 10 mL glass vial in a nitrogen-filled dry box. N-methyl-N'-(p-methylcarbonylphenyl)carbodiimide (1.90 g, 9.99 mmol) was dissolved in anhydrous pyridine (2 mL). After the carbodiimide fully dissolved, the pyridine solution was transferred by pipet to the vial containing the catalyst. The progress of the reaction was monitored by IR. Measurements at 12 hrs, 40 hrs, and 64 hrs revealed a progressive reduction in the intensity of the  $\text{N}=\text{C}=\text{N}$  absorption at  $2143 \text{ cm}^{-1}$ .

Absence of the carbodiimide absorption after 64 hours of reaction indicated reaction completion. Workup experiments indicated that the polymer does not precipitate from methanol, or hexanes with trace methanol, but does precipitate from water. The pyridine solution was transferred by pipet into a flask containing deionized water (120 mL) and methanol (30 mL). The product initially precipitated as globular collections, but developed into a fine powder upon stirring for several hours. The product was collected on P8 filter paper and rinsed from the paper with four, successive portions of acetone (50 mL each). Removal of the acetone by rotovap, followed by high vacuum, revealed 1.60 g of yellow powder (84% yield). Though the  $^1\text{H}$  NMR spectrum does exhibit some signal broadening, splitting in the aromatic region indicates a predominance of relatively low molecular weights. IR (KBr Pellet) 3063 (vw), 3035 (vw), 2993 (vw), 2951 (w), 2845 (vw), 1720 (s), 1635 (s), 1589 (s), 1275 (s)  $\text{cm}^{-1}$ ;  $^1\text{H}$  NMR (300 MHz,  $\text{CDCl}_3$ )  $\delta$  (ppm) 7.93 (d,  $J = 8.4$ , 2H), 6.86 (d,  $J = 8.4$ , 2H), 3.88 (s), 2.94 (s).

**Poly(N-hexyl-N'(p-methoxycarbonylphenyl)carbodiimide).** (S)-(-)-1,1'-Binaphth-2,2'-ol titanium(IV) diisopropoxide (46.5 mg, 103  $\mu\text{mol}$ ) and a magnetic stir bar were added to a 10 mL glass vial in a nitrogen-filled dry box. N-hexyl-N'-(p-methylcarbonylphenyl)carbodiimide, 94% (3.01 g, 10.9 mmol) was dissolved in anhydrous chloroform (2 mL). The chloroform solution was transferred by pipet to the vial containing the catalyst and stir bar. Three chloroform rinses (1 mL) were utilized to facilitate quantitative transfer. 4 days later, the chloroform solution was added to magnetically-stirred methanol (50 mL) to precipitate the polymer. Removal

of the methanol by filtration, followed by high vacuum, revealed 2.28 g of fine, yellow powder (81% yield). IR (KBr Pellet) 3068 (vw), 2952 (m), 2931 (m), 2858 (w), 1722 (s), 1631 (s), 1591 (s), 1275 (s), 1113 (s)  $\text{cm}^{-1}$ ;  $^1\text{H}$  NMR (300 MHz,  $\text{CDCl}_3$ )  $\delta$  (ppm) 7.80, 6.74, 6.47, 5.61, 4.21, 3.82, 3.64, 3.44, 3.16, 3.06, 2.88, 2.52, 1.58, 1.03, 0.72, 0.4 (all broad); 169.6  $^\circ\text{C}$  Decomposition Temperature (5% Loss of Mass); Specific Optical Rotation measured  $-31.2^\circ \pm 0.4^\circ$ .

**Poly(N-hexyl-N'-(p-(2,2,2-trifluoroethoxy)carbonylphenyl)carbodiimide).**

(S)-(-)-1,1'-Binaphth-2,2'-ol titanium(IV) diisopropoxide (682 mg) was dissolved in anhydrous chloroform (2.0 mL) in a nitrogen-filled dry box. N-hexyl-N'-(p-(2,2,2-trifluoroethoxy)carbonylphenyl)carbodiimide, 89% (1.91 g, 5.18 mmol) was dissolved in anhydrous chloroform (1 mL) in a separate 10 mL glass vial. A magnetic stir bar was added. 0.50 mL of the catalyst solution (25.5 mg, 52.0  $\mu\text{mol}$ ) was transferred to the vial containing the carbodiimide. IR analysis after 3 days revealed only a trace of remaining carbodiimide. Following failure of microscale workup experiments, the reaction mixture was transferred to a 100 mL round bottom flask. Several methylene chloride rinses were utilized to facilitate quantitative transfer. Removal of the volatiles by rotovap, followed by high vacuum, revealed a crunchy, orange powder. The characterization data that follow are for the crude polymer: IR (KBr Pellet) 3055 (vw), 2958 (m), 2931 (m), 2860 (w), 1736 (s), 1633 (s), 1589 (s), 1252 (s), 1169 (s), 1113 (s)  $\text{cm}^{-1}$ ;  $^1\text{H}$  NMR (300 MHz,  $\text{CDCl}_3$ )  $\delta$  (ppm) 7.93, 6.85, 4.66, 3.88, 3.73, 3.51, 3.45, 3.17, 2.62, 1.59, 1.04, 0.74 (all broad); 164.8  $^\circ\text{C}$  Decomposition Temperature (5% Loss of Mass); Specific Optical Rotation measured  $-12.5^\circ \pm 0.8^\circ$ .

**Poly(N-benzyl-N'-(4-n-butylphenyl)carbodiimide).** Courteously supplied by Joe Desousa.

**Poly(N-hexyl-N'-phenylcarbodiimide) made with Chiral Titanium Catalyst.** Courteously supplied by Januka Budhathoki-Uprety.

**Poly(N-hexyl-N'-phenylcarbodiimide) made with Copper Catalyst.** Copper (I) butanethiolate (15.2 mg, 98.9  $\mu\text{mol}$ ) was transferred to a Schlenk flask. N-hexyl-N'-phenylcarbodiimide (1.00 g, 4.94 mmol), courteously supplied by Januka Budhathoki-Uprety, and a stir bar were added to the flask. The flask was sealed, removed from the dry box, and attached to a nitrogen line. The reaction was run under a positive pressure of nitrogen while submerged in an oil bath heated to 60  $^{\circ}\text{C}$ . The reaction mixture became viscous within two days, solid within five. On day six, the reaction was removed from heat. Three days later a vortex mixer and a heat gun were employed to facilitate dissolving the polymer in three, successive portions of toluene (5 mL each). The polymer was then precipitated from toluene solution in magnetically-stirred methanol (90 mL). When an attempt to collect the polymer by filtration through P8 filter paper failed, the polymer was centrifuged at 3500 rpm for 20 minutes at room temperature. The supernatant was decanted and the polymer was dissolved with toluene and transferred into a 100 mL round bottom flask. Removal of the toluene by rotovap, followed by high vacuum, revealed 636 mg of brown polymer (64% yield).  $^1\text{H}$  NMR (300 MHz,  $\text{CDCl}_3$ )  $\delta$  (ppm) 7.00, 6.76, 3.46, 2.59, 1.54, 1.23, 1.06, 0.73 (all broad).

### **Hydrolysis of Poly(N-Phenyl-N'-(L-Alanine Methyl Ester)Carbodiimide).**

A heavy fraction of poly(N-methyl-N'-(L-alanine methyl ester)carbodiimide) (504 mg), synthesized with copper (I) butanethiolate (500:1) at 60 °C, was weighed and transferred to a 100 mL round bottom flask. Sodium hydroxide (250 mg) was dissolved in deionized water (10 mL). The sodium hydroxide solution and acetone (20 mL) were added to the reaction flask. The flask was submerged in a FS30H Ultrasonic Bath for 5 days. On the fifth day, the solution was neutralized with concentrated HCl to a pH of approximately 7. The product formed a sticky black mass at this pH. The pH was adjusted to approximately 1 in an effort to fully protonate any carboxylate units on the polymer. The product was extracted from the aqueous mixture with five, successive portions of ethyl acetate (150 mL X 2, then 50 mL X 3). Removal of the volatiles by rotovap, followed by high vacuum, revealed 154.6 mg of brown paste (30% yield). Analysis by <sup>1</sup>H NMR indicated that both the ester substituents and the polymer backbone were fully hydrolyzed, leading to a urea structure. LC/MS analysis confirmed the anticipated urea structure, as the two most abundant m/z values matched the structure of the protonated urea, 209, and its sodium adduct, 231. <sup>1</sup>H NMR (300 MHz, Acetone-d<sub>6</sub>) δ (ppm) 8.10 (s, br, 1H), 7.48 (d, J = 7.2 Hz, 2H), 7.22 (m, 2H), 6.93 (t, J = 8.0 Hz, 1H), 6.10 (d, br, J = 6.9 Hz, 1H), 4.42 (m, 1H), 1.41 (d, J = 7.2, 3H).

### **Transesterification of a Low Molecular Weight Polycarbodiimide.**

Poly(N-methyl-N'-(L-alanine methyl ester)carbodiimide) (50 mg), synthesized with copper (I) butanethiolate (250:1) at 60 °C, was weighed in a 100 mL round bottom flask. Chloroform (50 mL), 2-methoxyethanol (20 mL), and a magnetic stir bar were added to the flask. A catalytic amount of mercury (II) acetate (1 mg) was added to the flask. Approximately three grams of molecular sieves were suspended in the flask in an improvised holding device designed to expose the reaction solution to the sieves while keeping them from contacting the magnetic stir bar. [See Appendix 3 for instructions on creating an improvised holding device for molecular sieves.] The headspace of the sealed flask was purged with nitrogen for approximately two minutes. Both the chloroform solvent and the residual alcohol were removed four days later by rotovap, followed by high vacuum. The replacement of the methyl ester proton set with the 2-methoxyethyl ester proton sets, coupled with the absence of a corresponding signal for the hydroxyl proton set of 2-methoxyethanol, as shown in Figure 3.4, is consistent with a high degree of transesterification for this low molecular weight batch of polymer.

### 3.10. References

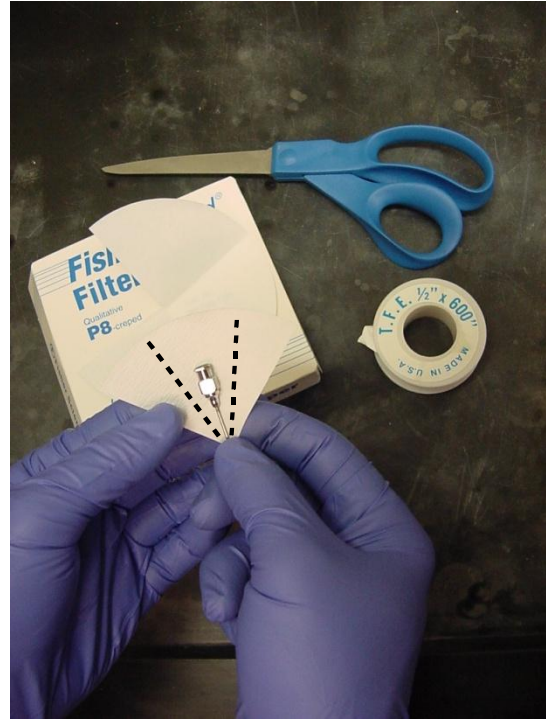
- (1) Padovani, M.; Hilker, I.; Duxbury, C.; Heise, A. *Macromolecules* **2008**, *41*, 2439-2444.
- (2) Otera, J. *Chemical Reviews* **1993**, *93*, 1449-1470.
- (3) Yamaguchi, H.; Fujiwara, Y.; Minoura, Y. *Die Makromolekulare Chemie* **1974**, *175*, 7-16.
- (4) Yuki, H.; Hatada, K.; Nagata, K.; Kajiyama, K. *Bulletin of the Chemical Society of Japan* **1969**, *42*, 3546-3550.
- (5) Birch, A.; Corrie, E.; Macdonald, P.; Rao, G. *Perkin Transactions 1* **1972**, 1186-1193.
- (6) Taber, D.; Amedio, J.; Patel, Y. *Journal of Organic Chemistry* **1985**, *50*, 3618-3619.
- (7) Kim, J., PhD Dissertation, North Carolina State University, 2002.
- (8) Olah, G.; Ho, T. *Synthesis* **1977**, 1977, 417-418.
- (9) Olah, G.; Ho, T. *Angewandte Chemie International Edition in English* **1976**, *15*, 774-775.
- (10) Taylor, E.; Fletcher, S.; Sabb, A. *Synthetic Communications* **1984**, *14*, 921-924.
- (11) Goodwin, A., PhD Dissertation, University of California at Berkley, 1996.
- (12) Schlitzer, D., PhD Dissertation, University of Massachusetts Amherst, 1998.
- (13) Tang, H.; Boyle, P.; Novak, B. *Journal of the American Chemical Society* **2005**, *127*, 2136-2142.
- (14) *Purification of Laboratory Chemicals*; Perrin, D.; Armarego, W., Eds.; Pergamon Press: Oxford, 1988.

## APPENDICES

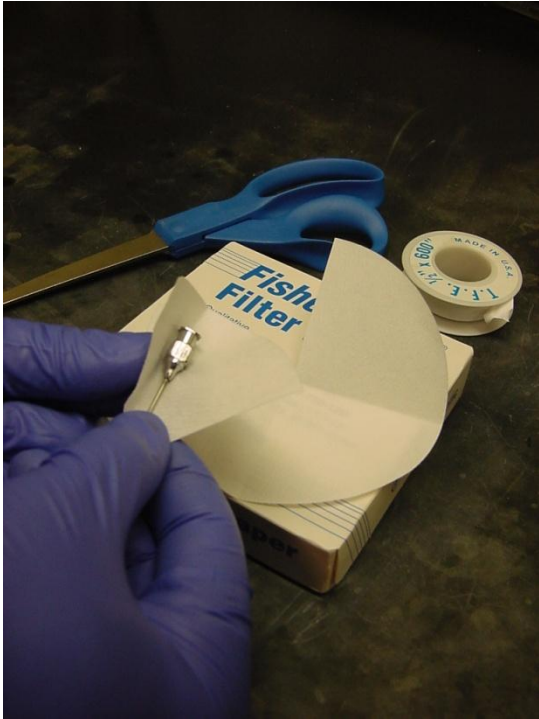
## Appendix 1: Filter Paper-Covered, Vacuum-Needle Assembly Instructions



Step 1: Begin by cutting out a quarter section of 11 cm diameter Qualitative P8-creped Fisherbrand Filter Paper.



Step 2: Position the hilt of a 12 inch, 18-gauge needle at the center of the quarter cut as shown. Folds to be made in Steps 3 and 4 are outlined by the dashed lines.



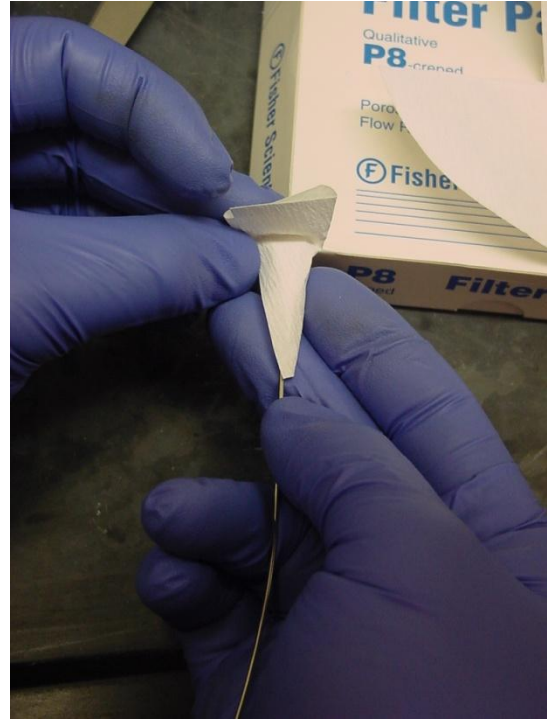
Step 3: Fold the left side of the quarter cut across the top of the needle hilt as illustrated.



Step 4: Fold the right side of the quarter cut, as well as the overlap from the left side fold, back across the top of the needle hilt.



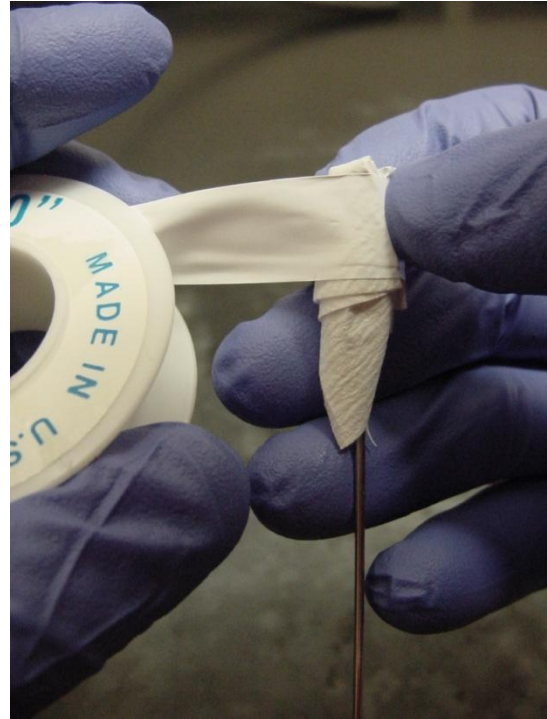
Step 5: At this point, the folds should amount to a cone over the needle hilt. The next fold to be made is outlined by the dashed line.



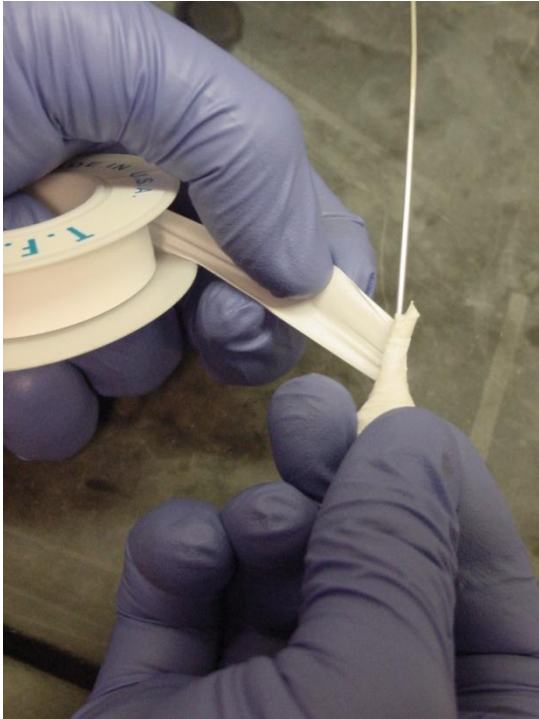
Step 6: Fold the top of the cone down and over the needle hilt until it is flush with the opposite side.



Step 7: Turn the hilt over and pinch the edges of the overfold flush with the sides of the needle as shown.



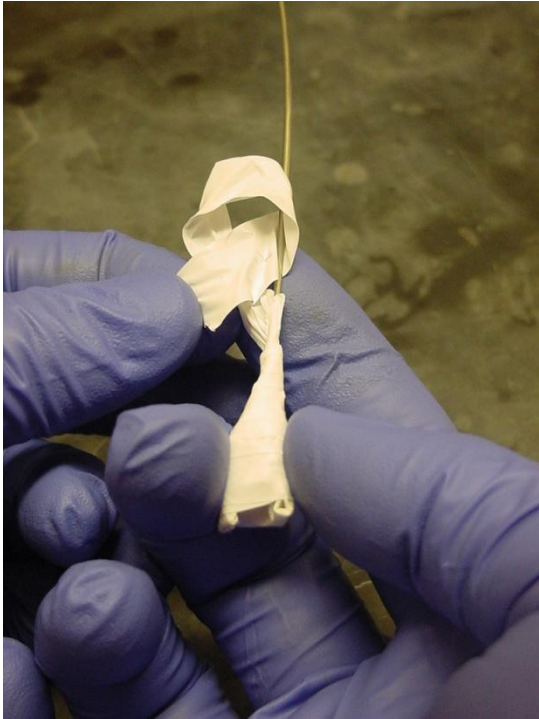
Step 8: Begin securing the filter paper to the needle hilt by wrapping Teflon tape around the top edge of the needle hilt first. Do not wrap the Teflon tape over the end of the hilt: the end should only be covered by the filter paper.



Step 9: Tightly continue the Teflon-tape wrap down the needle until the entire length of folded filter paper is secured.



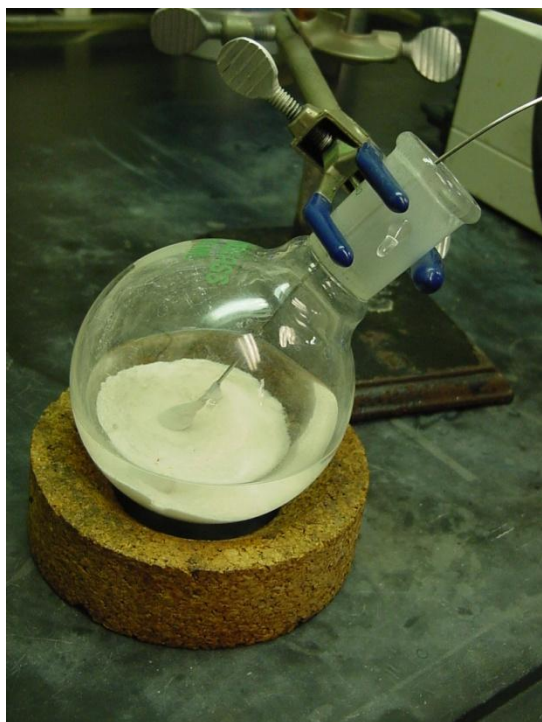
Step 10: Cut the tape from the roll, sparing several inches with which to tie the tape to the needle.



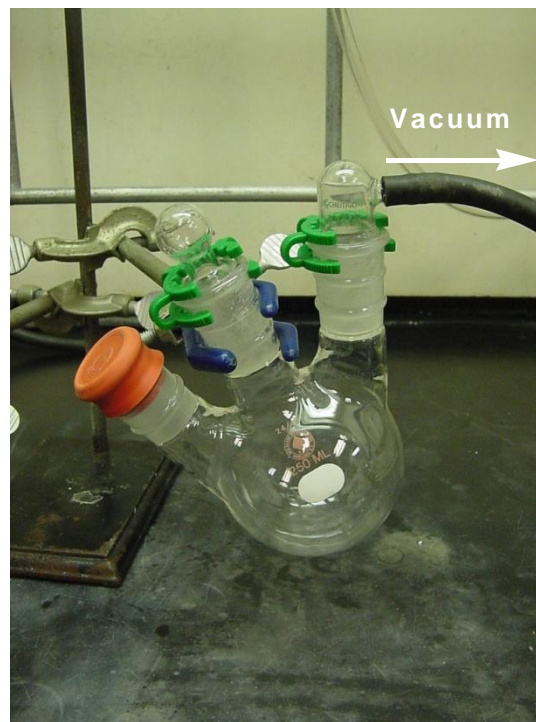
Step 11: Hang the loose end of the tape over the needle, making a loop, and feed it through from underneath to create an overhand knot.



Step 12: Pull the overhand knot tight and cut off the extraneous tape at the loose end.



Step 13: Place the filter paper-covered end of the needle into the flask containing the supernatant to be removed.



Step 14: Assemble a 3-neck flask such that one neck is plugged with a septum, the second is sealed with a glass stopper, and the third is attached to a vacuum source.



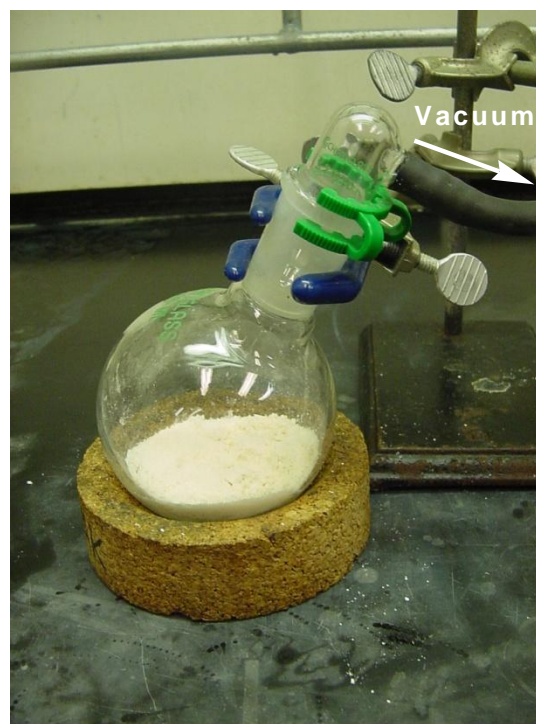
Step 15: Puncher the rubber septum with the sharp end of the needle.



Step 16: The supernatant is sucked from the flask containing the precipitate to the 3-neck flask.



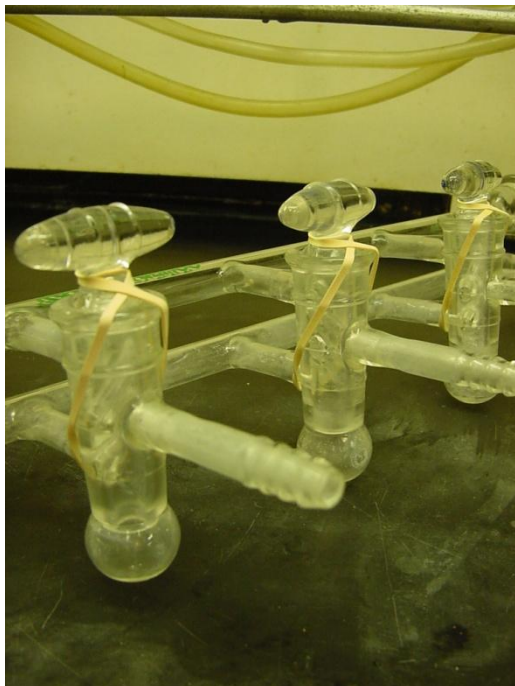
Step 17: Reposition the filter paper-covered needle as needed to suck the last standing remnants of supernatant from the bottom of the flask.



Step 18: Utilize one or more rinses with a non-solvent if an ultra-clean sample is desired. Otherwise, simply remove the needle and attach the flask directly to the vacuum source to evaporate residual supernatant.

## Appendix 2: Guide to Vacuum Manifold Maintenance

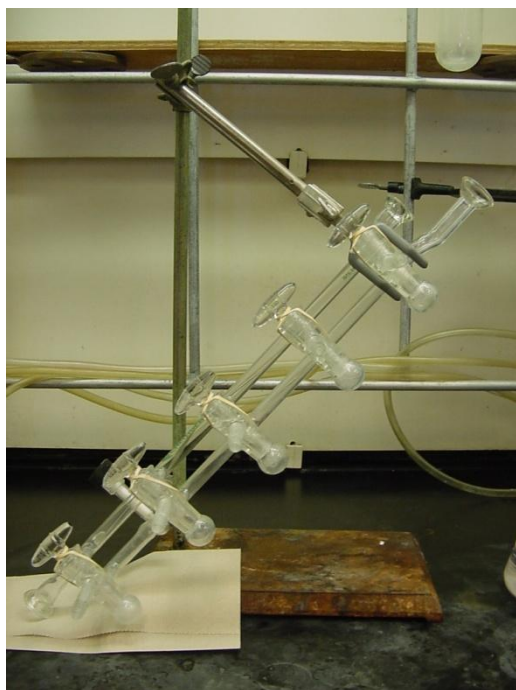
Caution: Take care to avoid contacting the glass surface of stopcocks and vacuum manifold joints with metal or any other abrasive. The slightest scratch may significantly reduce the vacuum capacity of the system.



Step 1: Begin by fastening each stopcock in place with a rubber band wrapped in a figure eight around the stopcock joint. Orient each stopcock so that the valve leading to the air space within the stopcock is open to the vacuum line.



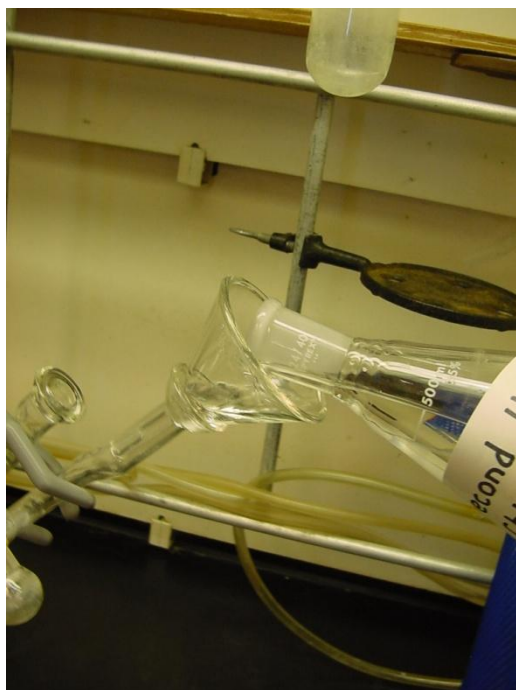
Step 2: Tighten a three-prong clamp on the manifold at the first set of joints from the open end of the vacuum line such that the two-pronged side of the clamp sandwiches the joints leading to the stopcock as illustrated.



Step 3: Secure the clamp holding the manifold to a ring stand at an angle of approximately 45 degrees, with the stopcocks facing up and the open end of the vacuum line at the top. Angling the manifold with the stopcocks up will utilize gravity to hold them in place.



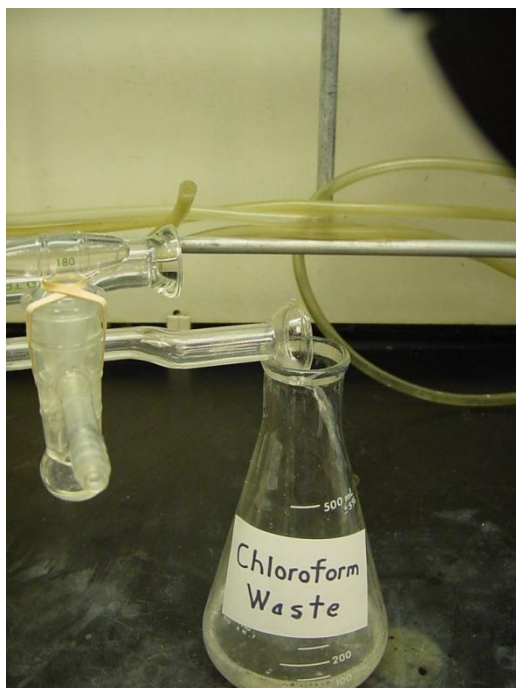
Step 4: Tighten the Teflon stopcock leading to the vacuum gauge joint until closed. [Don't forget to reopen this valve for a vacuum gauge reading upon reassembling the manifold and turning on the vacuum pump.]



Step 5: Fill the vacuum line with solvent (utilize a long-stem funnel to minimize spillage). Halogenated solvents, such as chloroform and methylene chloride, are the most effective at removing old silicon grease deposits. Cleaning a vacuum manifold with rotovap-recovered, halogenated solvents is a more economical practice than doing so with reagent grade solvents.



Step 6: Utilizing a heat gun to reflux the solvent in the vacuum line is a particularly effective way to dissolve large grease deposits. It is especially important that the valve leading to the air space within the stopcock is open to the vacuum line while heating, as vaporization of solvent and expansion of heated air within the stopcock might otherwise lead to a violently blowout.



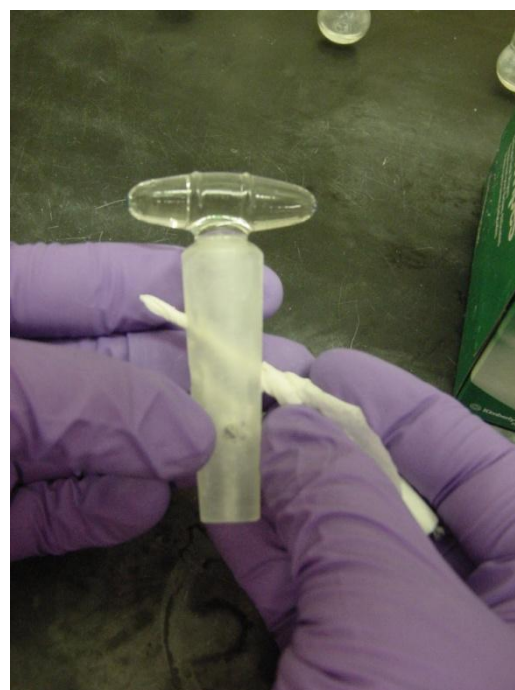
Step 7: Pour the solvent into an appropriately-labeled waste flask for transfer to a halogenated waste container. Repeat steps 5 through 7 with halogenated solvents for heavy grease deposits. Metal deposits are best removed by soaking the line with aqua regia. A base bath of potassium hydroxide in isopropyl alcohol is another useful cleaning alternative when halogenated solvents fail. Note that extended soaking in a base bath will damage manifold glassware.



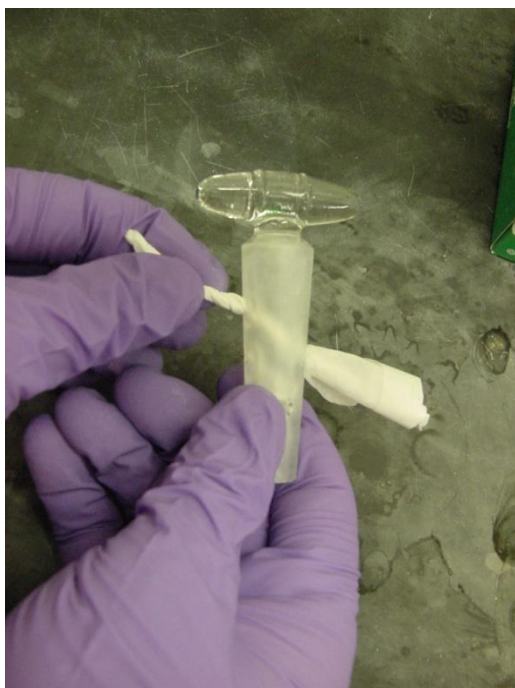
Step 8: Submerge each stopcock, handle down, in a beaker of halogenated solvent. For particularly difficult grease deposits, boil the solvent to facilitate the cleaning process. As with the vacuum line, soaking the stopcocks in aqua regia or a base bath for a few minutes may be advisable alternatives, depending on the contaminants to be removed.



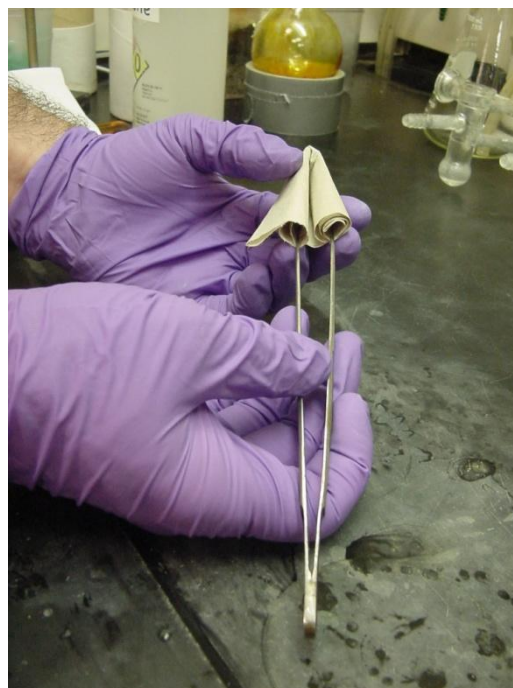
Step 9: Grease-clogged stopcock channels can be cleaned with a Kimwipe. Tear a Kimwipe in half widthwise, roll it, and twist one end of the roll into a tight point.



Step 10: Insert the twisted end of the Kimwipe through the stopcock channel. If the channel is too clogged with grease to do so, unclog it by inserting the narrow end of a glass pipet.



Step 11: Pull the Kimwipe through the stopcock channel. The drag of the untwisted end should leave the channel relatively grease free. Use a clean Kimwipe for each channel.

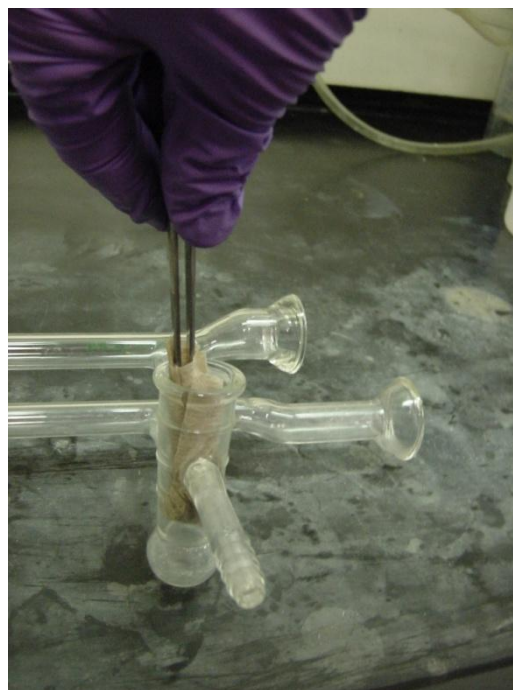


Step 12: The stopcock socket on the manifold is most easily cleaned with a solvent-soaked paper towel. Tear a paper towel in half widthwise, roll it, fold the roll in half, and position the folded roll on a long pair of needle-nose tweezers as illustrated.

Kimwipes can be used for this application, but keep in mind that Kimwipes are thin and easily torn. Scratching a stopcock socket with metal tweezers will assuredly ruin it, so proceed with caution if using Kimwipes.



Step 13: Soak the paper towel with halogenated solvent. Chloroform works well for removing high vacuum silicon grease.



Step 14: Repeatedly insert and withdraw the chloroform-soaked paper towel into the socket with a twisting motion to remove old silicon grease deposits.



Step 15: Apply a fresh coat of silicon grease to each stopcock before returning it to its respectively-numbered joint. Dow Corning high vacuum grease is recommended for mobile joints such as stopcocks.



Step 16: Return each stopcock to its properly-numbered joint. Double check that the joint number matches the stopcock number, as each custom fit maximizes the vacuum capability of the system.



Step 17: Clean the ball and socket ends of each ball-and-socket joint with a solvent-soaked Kimwipe. Hexanes work well for removing Apiezon brand hydrocarbon greases.



Step 18: Apply a fresh coat of hydrocarbon grease to each joint after removing the old grease. Apiezon grease is recommended for stationary connections, such as ball-and-socket joints.



Step 19: Remove the cold traps and clean off the old grease from the contact surfaces.

DO NOT use force when attempting to remove the trap from the manifold. If the trap is frozen or otherwise stuck, twisting with excessive force will break the trap or, worse still, the manifold.

If this joint was previously sealed with hydrocarbon grease, warming with the heat gun will soften the grease, allowing the trap to be removed with minimum shearing force. If previously sealed with silicon grease... good luck!!



Step 20: Apiezon grease is especially recommended for the manifold / trap connection.

Both silicon and hydrocarbon greases harden over time as the volatile components off-gas under vacuum. The difference is that the remaining heavy fraction of hydrocarbon grease can be softened with heat, while the nonvolatile components of silicon-based grease cannot.

Having an especially large contact surface, trap joints are particularly susceptible to becoming stuck when sealed with silicon grease. Apply hydrocarbon grease instead.



Step 21: Cleaning and applying a fresh coat of grease to the manifold / tube connection require removing the tubing from the glass. While taking care not to scratch the glass, cut along the length of the tubing with a razor blade until the glass stem can be pulled free.



Step 22: After trimming off the damaged portion of the tubing, clean the end section of old grease deposits by use a long pair of needle-nose tweezers to insert and withdraw a hexane-soaked paper towel with a twisting motion.



Step 23: Smear Apiezon grease on the thick end of a glass pipet.



Step 24: Use the pipet to apply a fresh coat of grease several inches deep on inside of the rubber tubing.



Step 25: Use a hexane-soaked paper towel to clean the glass stem of the manifold / tube connector.



Step 26: Apply Apiezon grease to the half of the glass stem to be inserted in the rubber tubing.



Step 27: Soften the grease applied to the inside of the rubber tubing by heating briefly with a heat gun. This will make it much easier to insert the glass stem.



Step 28: Insert half the length of the glass stem into the rubber tubing.



Step 29: Secure the connection with a hose clamp.



Step 30: Disconnect the rubber tubing from the vacuum pump and use a hexane-soaked paper towel to clean the vacuum pump, tube connector.



Step 31: Use a hexane-soaked paper towel on a long pair of needle-nose tweezers to remove old grease deposits from the tubing.



Step 32: Drain the old vacuum pump oil into an appropriately-labeled and properly-secured oil waste container.



Step 33: Refill with clean vacuum pump oil to the top oil level mark shown above. Monitor the oil level between changes. If the oil level falls below the bottom mark, the vacuum capability of the pump will drop precipitously.



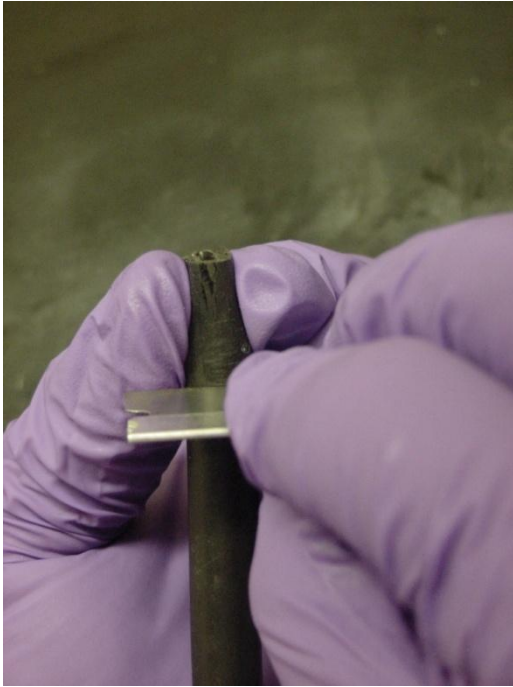
Step 34: Apply a fresh coat of Apiezon grease to the vacuum pump / tube connector and to the inside of the rubber tubing.



Step 35: Attach the tubing to the vacuum pump and secure the connection with the hose clamp as illustrated.



Step 36: Inspect the Teflon plugs. Replace the O-rings if they appear cracked or worn. Applying a very thin coating of Apiezon M grease to each O-ring is recommended, as doing so will allow the O-ring to slide on the glass with less friction.



Step 37: Inspect the rubber tubing to be attached to each stopcock line. Cut off the ends if they appear cracked from previous wear.



Step 38: Clean the manifold stems to which each rubber tube will be attached.



Step 39: Apply a thin coat of high vacuum silicon grease to each stem before attaching each tube.



Step 40: Turn the vacuum pump on. Twist and press each stopcock to uniformly distribute the silicon grease and tighten the seal. Each stopcock should rotate smoothly. If not, remove the stopcock and apply more grease.



Step 41: Gently twist the cold traps back and forth under vacuum to ensure a proper seal. As with the stopcocks, apply more grease if the traps fail to rotate smoothly and easily.



Step 42: Align each ball-and-socket joint. Twist the connection back and forth under vacuum to ensure a uniform coating of grease and a proper seal.

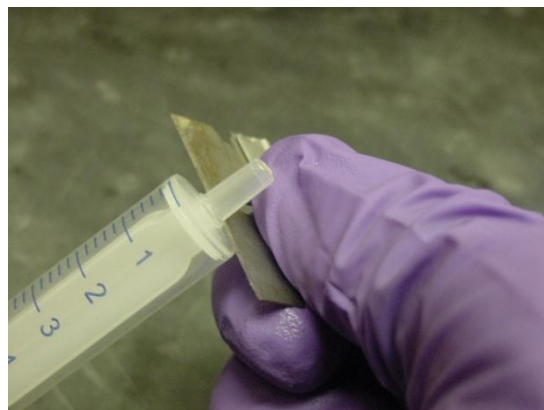


The manifold pressure should quickly fall to less than 100 mtorr. Without the use of liquid nitrogen in the cold traps, it may take several hours to reach maximum vacuum as the volatile components of the Apiezon grease off-gas, creating a virtual leak in the system. The pressure should drop steadily during this time. Once the pressure stabilizes, twist and press each stopcock, each cold trap, and each ball-and-socket joint again to ensure a maximum seal.

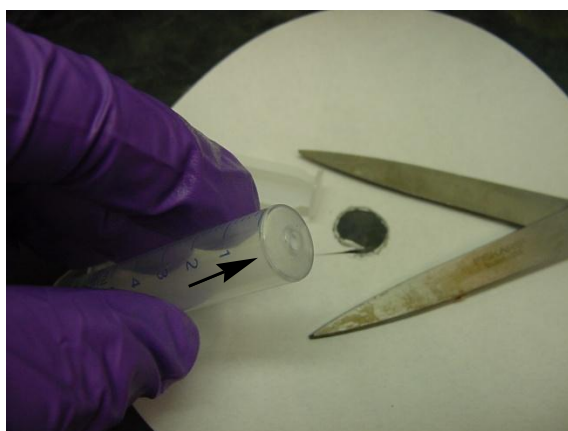
### Appendix 3: Creating an Improved Holding Device for Molecular Sieves



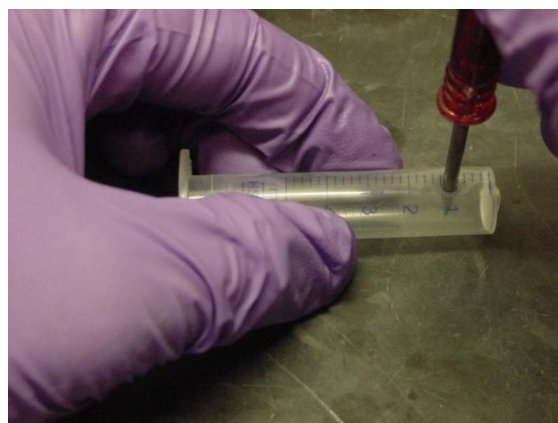
Step 1: Begin with a 5 mL Luer-Slip Plastic Syringe.



Step 2: Cut off the tip.



Step 3: Insert a small, circular cut of filter paper to plug the end of the syringe. Using the plunger to trace a circle on a piece of filter paper will assist in making a cut that will fit appropriately.



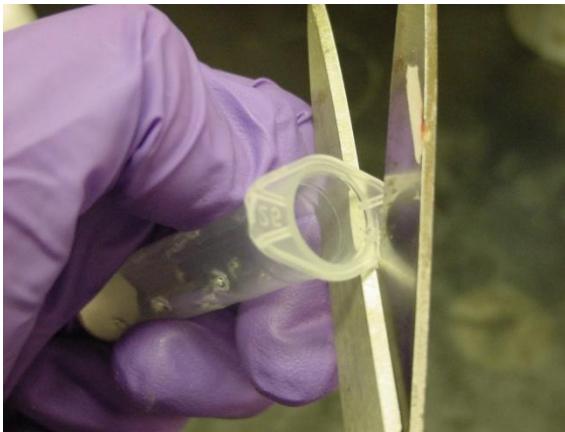
Step 4: Using an ice pick or a similarly shaped tool, puncher the syringe at the 1 mL mark.



Step 5: Make a series of staggered puncher holes at the 2, 3, 4, & 5 mL marks as illustrated.



Step 6: Rotate the syringe 120° and repeat steps 4 & 5 to make a second line of staggered puncher holes. Repeat step 6 again to create a total of 15 puncher holes in the plastic syringe.



Step 7: Trim the edges at the top of the syringe. This will become important later when fitting the syringe through the neck of a round bottom flask.



Step 8: Insert the plunger to the 4 mL mark. Measure and cut the end of the plunger as needed to fit the depth of the flask to be used.



Step 9: Fill the syringe to the 4 mL mark with molecular sieves that have been oven dried overnight at 220 °C and cooled to room temperature in a desiccator.



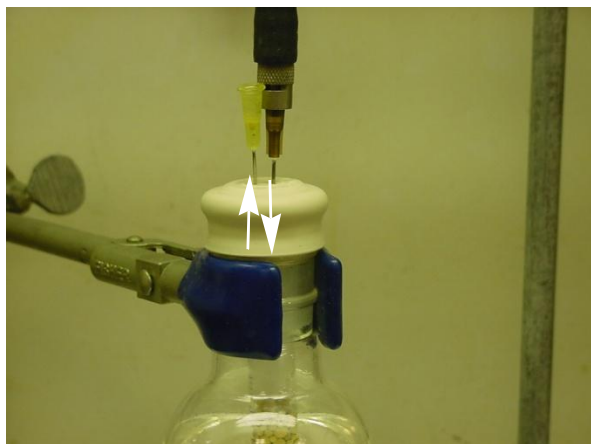
Step 10: Insert the cut end of the plunger into the underside of a Suba-Seal #45 Rubber Septum.



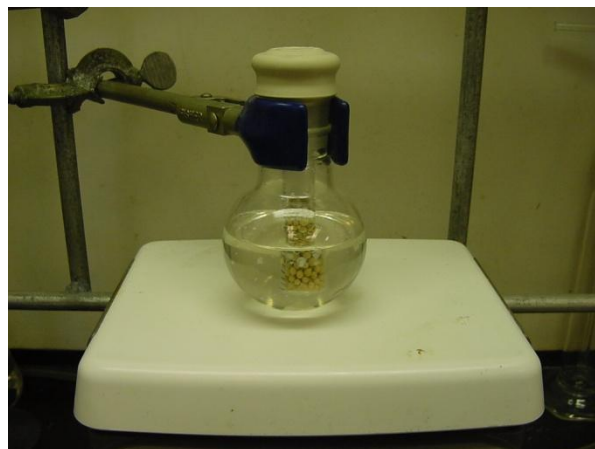
Step 11: Re-insert the plunger into syringe. The three puncher holes at the 5 mL mark will function as tabs to secure the plunger in the syringe.



Step 12: Insert the molecular sieve holding device into the reaction flask and secure the septum.



Step 13: The headspace above the reaction may be purged via inserting two needles through the septum and applying a positive pressure of nitrogen through one needle while venting out the other.



4A molecular sieves are useful for removing equilibrated  $\text{H}_2\text{O}$ ,  $\text{CH}_3\text{OH}$ , or  $\text{CH}_3\text{CH}_2\text{OH}$  reaction byproducts. The improvised molecular sieve holding device is useful for keeping the sieves from contacting the magnetic stir bar.

**North Carolina State University**  
**Department of Chemistry**  
**Varian NMR User's Manual**



by  
**J.B. Clark IV**

Dissertation Edition  
05/21/2010

## Section 1: Essential Operations for Basic 1D Spectra

### Preparing a Sample

To prepare a sample for  $^1\text{H}$  NMR analysis, dissolve 5 to 10 mg of sample in approximately 0.6 mL of deuterated solvent. The ideal concentration for  $^{13}\text{C}$  NMR analysis is higher, such as 50 mg in 0.6 mL deuterated solvent.

### Log In

Consult your Research Group for the username and password with which to log in. Upon logging in, left click on the Varian NMR Icon (6<sup>th</sup> icon from the bottom left of the screen, showing blue peaks on a black background) to bring up the NMR program.

### Loading a Sample

- To eject the standard, type **e** into the keyboard window and hit enter.
- Remove the sample by grabbing the sample tube holder, rather than the sample tube itself, to avoid allowing the holder to slip off and fall down the loading tube.
- If the outside of the sample tube is not clean, wipe it with a Chem Wipe.
- Place the sample tube holder in the sample tube gauge.
- Insert the sample tube into the holder and line the middle of the sample volume up with the prominent black line on the measuring scale or, at the lowest, flush with the bottom of the gauge.
- Set the loaded sample tube holder back in the NMR loading tube.
- Type **i** and hit enter to insert the sample into the NMR.

### Locking onto the Solvent Deuterium Signal

- Type **getshim** and hit enter to load pre-programmed shim parameters that are a good starting point for further adjustment.
- Select **[Acqi]** to enter the acquisition menu.
- Select **[LOCK]** to enter the lock submenu.
- Select **[on]** for the spin. [The spin is customarily set to 20 Hz.]
- Select **[off]** for the lock.
- Begin by setting the **lockpower** and **lockgain** to their maximum value.
- Adjust **Z0** until the resonance line rises sharply from the left and levels off as a plateau. Left or right click on **[-4+]** to decrease or increase by 4 increments respectively. Fine tune with **[-1+]** increment adjustments.
- If the line fails to fully plateau, change the **lockphase** and re-adjust **Z0**.
- Select **[on]** for the lock.
- Set the lock level to ~70% by reducing the **lockpower** and/or **lockgain**.\*
- Adjust the **lockphase** to maximize the lock level.

\* The optimum range for the lockpower will depend on the number of deuterium atoms on the solvent. For solvents that have a weak deuterium signal, such as  $\text{CDCl}_3$ , reduce the lockpower to between 20 and 25 before reducing the lockgain. For stronger solvents, such as  $\text{DMSO-d}_6$  or  $\text{benzene-d}_6$ , reduce the lockpower to between 10 and 20 before reducing the lockgain.

### Shimming the Magnet

- Select **[SHIM]** to enter the shim submenu.
- Alternate **[-1+]** increment adjustments of **z<sub>1c</sub>** and **z<sub>2c</sub>** to maximize the lock level.
- If the lock level reaches 100%, return to the lock submenu and reduce the **lockpower** and / or **lockgain** to lower the lock level for further shimming.
- After maximizing the lock level with the course shims, continue shimming by alternating **[-4+]** increment adjustments of the fine shims, **z<sub>1</sub>** and **z<sub>2</sub>**.
- Readjust the lock level to between 70 and 80% and then select **[CLOSE]** to exit the acquisition menu.

### Collecting a Spectrum

- Select **[Main Menu]**.
- Select **[Setup]**.
- For a sample in chloroform-d, select **[H1, CDCI3]** for proton analysis or **[C13, CDCI3]** for carbon-13 analysis. For other solvents, select **[Nucleus, Solvent]**. Select the nucleus and then the solvent from the subsequent option displays. See *Table 2* for the commands with which to access **[Other]** solvents.
- Type **zg** and hit enter to begin the analysis.
- The spectrum should appear on the screen once data collection is complete. If the spectrum does not appear, type **wft** and hit enter.
- To remove extraneous traces that appear on the display, type **ds** and hit enter.

### Adjusting the Vertical Scale

The command **vsadj** will optimize the vertical scale so that the fit of the most intense peak is maximized on the screen.

### Autophasing

Type **aph** and hit enter to autophase the spectrum. This command automatically adjusts the zero- and first-order phasing. If there is only one peak on the spectrum, utilize **aph0** instead to adjust the zero-order phasing only.

### Manual Phasing

If autophasing proves insufficient, select **[Phase]** and then:

- Left click on a peak on the far right side of the spectrum.
- Click and hold inside the blue region and drag up or down to adjust the zero-order phasing. [Left click for course adjustments, right click for fine adjustments.]
- Repeat the process with a peak on the far left side of the spectrum to adjust the first-order phasing.
- Select **[Box]** or **[Cursor]** to exit the manual phase correction mode.

### Displaying the Scale

Select **[Dscale]** to display the ppm chemical shift scale below the spectrum.

### Zooming Into and Out of a Region

- Left click to the left of the left-most point of the region.
- Right click to the right of the right-most point of the region.
- Select **[Expand]** to zoom in or **[Full]** to zoom back out.

### Referencing the Scale

- Zoom in on the reference peak and left click on the highest point of the peak to mark the position with a vertical red line. [The command **nl** can be used to center the cursor on the top of the nearest signal line.]
- Select **[Ref]**.
- Using the numbers at the top of the keyboard, rather than the number keypad, type the frequency of the reference peak, to two decimal places, and hit enter.

### Adjusting the Slope and Bias

- Select **[Lvl/Tilt]** to enter the slope/bias adjustment mode.
- Select **[No Integral]**, then **[Part Integral]**.
- Click and hold on the right side of the spectrum and move up or down to adjust the slope of the integration line to zero at the left edge of the integral trace. [Left click for course adjustments, right click for fine adjustments.]
- Repeat on the left side of the spectrum to adjust the bias of the integration line so that the slope is as close to zero as possible between peaks.
- Select **[Box]** or **[Cursor]** to exit the slope/bias adjustment mode.

### Integrating the Spectrum (Not viable for routine $^{13}\text{C}$ NMR spectra)

- Left and right click, respectively, on each side of the first region of interest.
- Select **[Expand]** to zoom in.
- Select **[Resets]** to enter the integral reset mode.
- Left click on the left and right side of each peak to cut the integration line.
- Select **[Box]** or **[Cursor]** to exit the integral reset mode.
- Select **[Full]** to zoom out.
- Repeat this process for every region of peaks.

If you wish to re-integrate a specific cut, select **[Reset]**, then right click on the previous cut mark to restore the uncut line, and then left click to cut the integral anew. To start over completely, type **cz** and hit enter to restore the entire, uncut integration line.

### Referencing Integration Ratios

- Left click at the top of the integral you want to set as the reference.
- Select **[Set Int]**.
- Using the numbers at the top of the keyboard, rather than the numeric keypad, type in the reference value to two decimal places and hit enter.

### Setting the Peak Threshold for Print or Display

Select **[Th]** to enter the threshold adjustment mode. Left click and hold on the horizontal threshold line and adjust upward or downward until only the peaks of interest break the threshold. Select **[Th]** again to exit the threshold adjustment mode. The command **dpf** will display the peak frequencies, while **ds** will remove them.

### Printing the Spectrum

There are a variety of print commands that can be utilized to customize the information printed with a spectrum. The two essential commands are **pl**, the command to plot the spectrum, and integrals, if shown, and **page**, which sends preceding plot commands to the printer.

Other commands that can be used in conjunction with these are **pscale**, which plots the frequency scale; **ppf**, which plots the frequency of peaks that break the threshold setting; **pir**, which plots the integration data; and **ppa**, which plots a partial list of the experiment parameters, or **pap**, which plots a complete list of experiment parameters.

There is one other command that must be entered prior to the **pir** command. In order to make room below the spectrum for integration data, the vertical position of the plot must be adjusted 12 mm higher with the command **vp=12**.

A typical print command might read **vp=12 pl pscale pir ppf ppa page** to print the frequency scale, integration data, peak frequency data, and key experimental parameters with the spectrum.

### Creating a Personal Data Storage Directory

- Select **[Main Menu]**.
- Select **[Data]**.
- Use the command format **mkdir('JBClark')** to create a personal directory.

### Saving a Spectrum

- Select **[Main Menu]**.
- Select **[Data]**.
- Left click on the desired directory to highlight it and select **[Set Directory]**.
- Type **svf('xyz')** and hit enter to save the file (as *xyz*) in the current directory.

To return to the default home directory, type **cd** and hit enter prior to selecting **[Data]**.

### Accessing a Saved Spectrum

- Select **[Main Menu]**.
- Select **[Data]**.
- Left click on the folder containing the data file and select **[Set Directory]**.
- Left click on the data file to highlight it and select **[Load]**.
- Type **wft** and hit enter.

### Log Out

- Eject the sample and return the standard.
- Type **exit** and hit enter.
- Right click on the desktop background to access the log out option.
- Right click on **[Log Out]**.
- Select **[OK]**.

## Section 2: Optional Operations for Basic 1D Spectra Enhancement

### Improving the Resolution

Increasing the acquisition time will sharpen the resolution. The acquisition time is directly proportional to the number of data points and inversely proportional to the sweep width. Hence the resolution can be improved by increasing the number of points, decreasing the sweep width, or a combination of both adjustments.

Increasing the number of data points will improve the resolution for a given sweep width. For proton spectra, increasing the number of points to no more than 32,000 is recommended. Use the command format **np=32000** to set the number of points.

Reducing the sweep width will improve the resolution for a given number of points:

- Type **nt=1 zg** and hit enter to collect a rough spectrum.
- Right click 1 ppm to the right of the right-most peak, then left click 1 ppm to the left of the left-most peak. [The selected region must contain all peaks, including those of the solvent and standard.]
- Record the default setting for the number of points (np), which is the fourth parameter listed under ACQUISITION on the display. [The software will automatically reduce the number of points in response to a decrease of the sweep width.]
- Type **movesw** and hit enter to reduce the sweep width to the selected region.
- Reset the number of points to improve the resolution. Type **np=24000** and hit enter to approximate a previous value of 23936 for instance.

If a subsequent command prompts an error message saying "P.S.G. Aborted...", increase the sweep width, from the value listed under the ACQUISITION display, by increments of from 10 to 100 until executing a subsequent command no longer prompts the error message. For instance, type **sw=4020** and hit enter for a sw value listed as 4006.

After collecting the data, resolution can be further enhanced by setting the Fourier number to double the number of points, a process referred to as zero-filling. As an example, use the command **fn=48000 wft** to adjust the Fourier number for a spectra collected with an np setting of 24000.

### Improving the Signal-to-Noise Ratio

Several parameters may be adjusted to improve the signal-to-noise ratio. One commonly applied adjustment is to increase the number of transients. The signal-to-noise ratio is proportional to the square root of the number of transients. The default setting for proton spectra is 16 transients. Use the command **nt=32** or **nt=64** to set 32 or 64 *transients* respectively. Type **time** and hit enter to get a run time estimate with the new setting.

A second parameter that may be adjusted is the pulse width, which may be increased to 90 degrees. Type **pw90?** and hit enter to prompt the display to return the value of a 90 degree pulse. Type **pw=17.5** and hit enter, if the returned value is 17.5 for instance. Increase the delay time as well, as outlined under "Improving the Accuracy of Integration Ratios," to

compensate for the increased pulse width. Again, utilize the **time** command to get a run time estimate with the new settings.

A third parameter adjustment that may be applied, after collecting the data, is line broadening. Line broadening sacrifices resolution to improve the signal-to-noise ratio. Type **lb=1.0 wft** and hit enter to apply line broadening of 1.0 Hz. To calculate the magnitude of line broadening in ppm, divide the value in Hz by the field strength of the spectrometer. For example, on a “400 MHz” spectrometer, 1 Hz / 400 MHz = 0.0025 ppm for <sup>1</sup>H or 1 Hz / 100 MHz = 0.01 ppm for <sup>13</sup>C.

To display the signal-to-noise ratio for a given peak, left click on top of the peak to mark it, type **dsn**, and hit enter. Be aware that the exact value of this ratio is relative to the noise within the region of expansion in which the command is executed.

### Improving the Accuracy of Integration Ratios

Several factors may negatively affect the accuracy of integration ratios, the most common being an insufficient delay time. The default delay time is 1 second. Use the command **d1=5** before re-running the analysis to change the delay time to 5 seconds. If the integration improves but is still not adequate, try **d1=10** or **d1=20**.

Other factors that may negatively affect integration accuracy include poor phasing and baseline drift. Carefully examine the phasing of the spectrum and re-phase manually if autophasing was suboptimal. Type **dc** and hit enter to correct drift. Type **cz**, hit enter, and re-integrate the spectrum to determine whether these adjustments have improved integration accuracy.

### Adding Text to the Spectrum

Use the command format **text('JB Clar\06-16-08')** and hit enter to add lines of customized text for printing. [The \ marks open a new line of text.] Adding the command **ptext** to the print command line, discussed in the previous section, will add the text to the printout. The command **ctext** will clear the previous text entry.

### Additional Print and Display Commands

Using the command **axis='h'** prior to **pscale** changes the scale units to Hertz, while **axis='p'** changes the units back to ppm. The command **pll** can be used to print a peak frequency list having both ppm and Hz. Do not use **ppa** or **pap** when using **pll**.

To display a list of the integrals on the text screen, use the command **dli**. A list of peak frequencies can be displayed on the text screen with the command **dll**. The command **dg** will return the original display of parameters to the text screen.

## Section 3: Glide Program Operations for Advanced 1D & 2D Spectra

### Glide Program Setup

- Lock on the solvent and shim the magnet before entering the Glide Program.
- Select **[Glide]**.
- Select **[Setup]**.
  - Select **[No]** for both **Autolock** and **Autoshim**.
  - Right click on the ▼ button beside **Solvent** and select the solvent from the pull down menu.
  - Right click on the ▼ button beside **Experiment** and select **[H1 and H1 detected Expt]** from the pull down menu for 2D experiments or **[H1 and selective 1D Expt]** for advanced 1D proton experiments.
- Select **[Setup]**.
- Select **[Acquire]**.
  - For **PROTON Spectral Width (ppm):**, select the minimum spectral width that will include all proton signals of the sample, solvent, and standard.
  - Select **[No]** for **Minimize SW?:**
  - Select a setting for **PROTON scans:**
  - Select a setting for **PROTON Relaxation Delay (sec):**
  - Select **[Default]** for **PROTON Pulse Angle:**

Select the desired experiment under “Select Experiments in addition to PROTON:” to access the corresponding popup menu settings described in the following instructions:

### Homonuclear Correlation Spectroscopic Techniques

#### I. [COSY] CORrelation Spectroscopy

- Select **[4]** to **[8]** for **COSY scans per inc:**
- Select **[128]** for **COSY number of inc:**  
[The aforementioned settings are fine for **[gCOSY]** as well.]
- Select **[OK]**.
- Select **[DO]**.
- Upon completion of the run, select **[AutoProcess]**.
- To expand a given region, select **[Box]** and then...
- Left click and drag to set the lower and left limit of the region to expand.
- Right click and drag to set the upper and right limit of the region to expand.
- Select **[Expand]** to zoom in on the region.
- Select **[vs+20%]** or **[vs-20%]** to magnify or reduce the vertical scale respectively.
- Select **[Autoplot]** to plot the screen.
- Select **[Full]** to zoom out.

The file is automatically saved to the group directory in a format displaying the group name followed by the day, month, and year such as **novak\_10Apr2008/** To re-access the COSY spectrum, right click on the file to highlight and select **[Set Directory]**. Right click on **COSY.fid/** to highlight, select **[Load]**, and then select **[AutoProcess]**.

## II. [TOCSY1D] 1D Total Correlation Spectroscopy

1D TOCSY reveals long-range correlations with a proton signal of a selected frequency. After selecting desired parameters and running the 1D analysis, box and **[Expand]** the proton signal of interest. Place the cursor on the center of the signal peak and then select **[Select]**. You may select multiple peaks to set up a series of analyses. After selecting all peaks of interest, select **[Proceed]**. Each of the resulting spectra will reveal the long-range couplings with one of the selected proton signals for the given mixing time.

## III. [TOCSY] 2D Total Correlation Spectroscopy

- Select **[16]** to **[32]** for **TOCSY Scans per inc:**
- Select **[128]** for **TOCSY number of inc:**
- Select from **[30 ms]** to **[80 ms]** for **TOCSY mixing time:**  
**Warning: Selecting a mixing time in excess of 80 ms will damage the probe!**
- Select **[OK]** and then select **[DO]**.
- Processing operations are analogous to those described under [COSY].

## IV. [NOESY1D] 1D Nuclear Overhauser Effect Spectroscopy

1D NOESY reveals through-space  $^1\text{H}$ - $^1\text{H}$  correlations with the proton signal of a selected frequency. For observations of NOE, it is important to deoxygenate the sample prior to analysis. One simple, but crude, deoxygenating method is to begin with a sufficient excess of solvent and bubble nitrogen through the sample for five minutes. The more thorough, recommended method is to utilize several freeze-pump-thaw cycles under  $\text{N}_2$ .

After selecting desired parameters and running the 1D analysis, box and **[Expand]** the proton signal to be analyzed for through-space correlations. Place the cursor on the center of the signal peak and select **[Select]**. You may select multiple peaks to set up a series of analyses. After selecting all peaks of interest, select **[Proceed]**. Each of the resulting spectra will reveal the through-space correlations with one of the selected proton signals for the given mixing time.

## V. [NOESY] 2D Nuclear Overhauser Effect Spectroscopy

- Select **[64]** for **NOESY scans per inc:** to maximize the signal-to-noise ratio.
- Select **[128]** for **NOESY number of inc:**
- The optimum selection for **NOESY mixing time:** will depend on the distance of the spatial interaction one wishes to observe and on the molecular weight of the molecule being analyzed. **[500 ms]** to **[1000 ms]** is typically optimum for molecular weights of up to 2,000, while an initial selection of **[100 ms]** is recommended for studying molecular weights in excess of 2,000.
- Select **[2 sec]** for **NOESY relaxation time:**
- Select **[OK]**.
- Select **[DO]**.
- Processing operations are analogous to those described under [COSY].

## Heteronuclear Correlation Spectroscopic Techniques

### I. [HMQC] Heteronuclear Multiple Quantum Coherence Correlation Spectroscopy

- Select [16] to [32] for **HMQC Scans per inc:**
- Select [128] to [256] for **HMQC number of inc:**  
[The aforementioned settings are fine for [gHMQC] as well.]
- Select the minimum spectral width that will include all carbon peaks.
- Select [OK] and then select [DO].
- Processing operations are analogous to those described under [COSY].

The scale of the carbon and proton spectra, found respectively on the vertical and horizontal axes, can be adjusted by selecting [Proj] followed, respectively, by [V proj(max)] or [H proj(max)]. Use the middle mouse button to adjust the scale and select [Plot] after each respective adjustment. Use the command **pcon** to also plot the 2D contour and **page** to send all of the preceding commands to the printer. The command **dcon** will return the original display.

### II. [HSQC] Heteronuclear Single Quantum Coherence Correlation Spectroscopy

Appropriate settings for [HSQC] and [gHSQC] are the same as the aforementioned ones for [HMQC] and [gHMQC]. Select [No] for the additional setting of **C-H multiplicity edit?** Processing operations are analogous to those listed for [COSY].

## Miscellaneous Techniques

### I. [HOMODEC] HOMONuclear DECoupling

HOMODEC allows decoupling of a selected frequency. After selecting desired parameters and running the 1D analysis, box and **[Expand]** the peak of interest. Place the cursor on the center of the peak to be selectively decoupled. Select **[Select]** and then **[Proceed]** to run a <sup>1</sup>H NMR analysis in which coupling(s) to the signal of the selected proton will be removed.

### II. [DEPT] Distortionless Enhancement Polarization Transfer

Enter the Glide Program Setup as described earlier, again selecting **[No]** for both autolock and autoshim. After selecting the solvent, select **[C13 and DEPT only]** from the experiment submenu.

- Select **[Acquire]**.
- Select **[1]** for **Relaxation delay**.
- Select **[Default]** for **Pulse Angle**.
- Select **[Decoupled + NOE]** for **H1 dec mode**.
- Select **[DO NOT TEST]** for **Carbon S/N Test**.
- The appropriate selection for **DEPT Scans per inc**: will depend on the sample concentration. **[512]** is the minimum for highly concentrated samples, while **[1000]** is more appropriate for a low concentration, such as 20 mg / 0.6 mL.
- Select **[Full Edit]** and then **[Do]**.

The “full edit” printout will display four spectra, one for “all protonated carbons,” a second for “CH carbons,” a third for “CH<sub>2</sub> carbons,” and a fourth for “CH<sub>3</sub> carbons.” In cases where a given signal shows up on the spectrum of two different types of carbons, the correct assignment is the one having the higher signal-to-noise ratio.

To re-access a saved DEPT file, highlight the file, select **[LOAD]** and then **[AutoProcess]**. The four spectra can be printed on the same page by selecting **[Autoplot]**. Each of the four spectra may also be displayed and printed individually. Utilize the command **ds(1)** to display the “all protonated carbons” spectrum. **ds(2)**, **ds(3)**, and **ds(4)** can be utilized to display the “CH carbons,” “CH<sub>2</sub> carbons,” and “CH<sub>3</sub> carbons” spectra, respectively. The command sequence **pl pscale page** can be used to print any spectrum on display.

## Section 4: Manual Setup Operations for Advanced 1D Experiments

### Inverse-Gated Decoupled Carbon-13 Spectroscopy (Quantitative $^{13}\text{C}$ Analysis)

- Go through the normal  $^{13}\text{C}$  NMR analysis setup routine.
- Utilize the command **pw=90?** to determine the length of a  $90^\circ$  pulse width.
- Change the pulse width to  $90^\circ$  with the command format **pw=##.#**
- Type **dm='nny'** and hit enter.
- Type **d1=10** and hit enter to change the delay time to 10 seconds. [A delay of up to 20 seconds may be required for the carbons in some samples.]
- Set **nt=1**, collect a rough spectrum, and adjust the sweep width. [Be sure that the width includes every anticipated peak of the sample, solvent, and standard.]

To maximize the number of transients with the chosen parameters in a given run time, first set the number of transients to some high value, such as **nt=10000**, then type **time** and hit enter to prompt the display to provide a time estimate. Iteratively adjust the number of transients and check the time until finding the maximum number of transients that will fit in the desired run-time frame.

Special Note: If, when checking the run time, the software returns an error message saying "code file already exists PSG Aborted..." increase the sweep width by increments of from 10 to 100 until the error message is no longer returned upon utilizing the **time** command.

Since obtaining a quantitatively-accurate carbon spectrum may take longer than a typical overnight analysis, it becomes vitally important to save the data in case data re-processing becomes necessary. Therefore, saving the data is the highest priority and should be done even before the first processing attempt in order to avoid accidentally forgetting to do so.

The Relaxation Reagent  $\text{Cr}(\text{acac})_3$  may be utilized for samples having long spin-lattice relaxation times,  $T_1$ . Increasing the amount of the reagent results in shortened relaxation times and an increase in line width, usually without affecting chemical shifts. A concentration of 0.1 M is ideal for quantitative work. The highest concentration reported to give reasonable results is 0.4 M, as severe line broadening and difficulty with locking on the solvent signal become problems at higher concentrations.\* Other relaxation reagents include  $\text{Mn}(\text{acac})_2$ ,  $\text{Cu}(\text{acac})_2$ , and  $\text{Gd}(\text{acac})_3$ .

\* Braun, S., H.O. Kalinowski, and S. Berger, *150 and More Basic NMR Experiments*, 1998.

### **Inversion Recovery Experiments for Determining Spin-Lattice Relaxation Times ( $T_1$ )**

Having an approximate idea of the  $T_1$  values within a molecule can be useful when optimizing the delay time for a variety of NMR analyses. Since the speed of relaxation correlates directly with the strength of coupling to other nuclei,  $T_1$  values can also be used for structural assignments. For small organic molecules,  $T_1$  values of 1 to 5 seconds are typical for protons, while those of carbons generally range from 1 second to greater than 10 seconds.

To begin, lock on the solvent and shim the magnet. To measure the  $T_1$  of the protons in the sample, begin by selecting the submenu options that are appropriate for a basic  $^1\text{H}$  analysis. Utilize the commands **nt=1** and **zg** to collect a single-scan spectrum. Type **gain?** and hit enter. A message should appear stating "gain = Not Used (32)." Type **gain='y'** and hit enter. The command **gain?** should now prompt the return message of "gain=32." Use the command **pw90?** to prompt the display to provide the value of a 90 degree pulse width. If the returned value is 17.5, for instance, use the command **pw=17.5** to set the pulse width to 90 degrees. Set p1 to 180 degrees by setting the value to double that of pw (**p1=35** in this case). **d1** should be set to at least five times the longest anticipated  $T_1$ . Set the number of transients, **nt**, to 16 or 32 for proton or to a minimum of 1024 or 2048 for carbon. The command **dot1** will prompt the entry of three parameters "ENTER MINIMUM T1 EXPECTED," "ENTER MAXIMUM T1 EXPECTED," and "ENTER EXPERIMENT TIME (hours)." For protons, 0.1 seconds would be a good starting point for the minimum  $T_1$  estimate, while 2 seconds is a good first guess for the maximum. Following entry of these parameters, utilize the command **go** to initiate the sequence of analyses.

Save the data following acquisition. To analyze the data, select **[Load]**, **[Analyze]**, **[Exponential]**, **[T1 Proc]**, and then **[T1 Analysis]**. The program will display the plots horizontally by default. To view and print a stacked plot of the spectra, begin by selecting **[Main Menu]**, **[Display]**, **[Size]**, and then **[Left]**. Type **vs?** and hit enter to find out the default vertical scale setting. Use the command format **vs=200** to reduce the vertical scale as needed to create an appropriate fit. [Determining the optimum vertical scale for a given number of spectra will be a matter of trial and error.] Type **vp=-10 pscale** and hit enter to set the scale to plot at the bottom of the page. Type **vp=0 dssa** to display the stacked plots and set the first one to print 10 mm above the scale. Use the commands **pl('all')** to plot the stacked spectra and **page** to send the preceding commands to the printer.

### APT (Attached Proton Test)

The appropriate sample concentration for an Attached Proton Test is the same as for a basic  $^{13}\text{C}$  spectrum. Before running an Attached Proton Test, collect and save a good quality, basic  $^{13}\text{C}$  spectrum of the sample. If one is already on file, begin by locking and shimming as always. Next, set up for a basic  $^{13}\text{C}$  analysis and then type the command **apt** and hit enter. Now type **dg** and hit enter to display the group parameters. Check that the parameter **d2** is set to 0.007. [If not, type **d2=0.007** and hit enter.] Set **nt** to half the number needed to collect a basic  $^{13}\text{C}$  spectrum of desirable quality. Type **zg** and hit enter. Save the APT spectrum following acquisition. To phase the APT spectrum, begin by loading and phasing the basic  $^{13}\text{C}$  spectrum. Upon subsequent re-loading, the APT spectrum should be properly phased. If not, manually adjust the phasing of the APT spectrum until all portions of the solvent peak are up. In the resulting spectrum, the signal of carbons attached to one or three protons will be down, while the signal of carbons attached to no protons or two protons will be up.

### Single-Frequency Decoupled Carbon-13 Spectroscopy

- Run a quick,  $^1\text{H}$  NMR analysis of the sample.
- Expand the region of interest and place the cursor on the center of the peak to be selectively decoupled. [The command **nl** can be used to center the cursor on the nearest signal line.]
- Type **movetof** and hit enter. [“tof” stands for transmitter off-set.]
- Write down the **tof** number from the parameter list. [The sign of the number, positive or negative, is a critical detail.]
- Now go through the normal  $^{13}\text{C}$  NMR analysis setup routine.
- Change the decoupler off-set by entering the **tof** number recorded earlier, including the sign, by utilizing the command format **dof=-###.#** to enter the specific **tof** number you copied. [Omit the minus sign from this example format if the tof number was positive rather than negative.]
- Type **dmm='c'** and hit enter.
- Type **dpwr=20** and hit enter. [A decoupler power of up to 25 may be used.]
- Type **zg** and hit enter.

### NOE-Enhanced, Proton-Coupled Carbon-13 Spectroscopy

Go through the normal  $^{13}\text{C}$  analysis setup routine and then use the command **dm='yyn'** to turn the decoupler off during the acquisition period. Since proton-coupled carbon signals will appear as multiplets, achieving a signal-to-noise ratio equivalent to that of a qualitative, decoupled  $^{13}\text{C}$  spectrum may take an analysis of up to 10 times longer.

### Manual Setup for gCOSY (gradient CORrelation Spectroscopy)

Lock on the solvent and shim the magnet as usual. Type **nt=1 zg** and hit enter to collect a single-scan spectrum. Adjust the sweep width and collect a single-scan spectrum again. Type **gain='y'** and hit enter. Change the pulse width to 90 degrees. Record the displayed value of sw, tof, and the other acquisition parameters. Type **gcosy** and hit enter. Check that np is approximately 1000. Set the desired values of d1, nt, and ni. Type **dg** and hit enter to update the parameter display with the new settings. Utilize VT NMR commands to adjust the temperature, if need be, at this point. If the instrument loses the lock signal with the temperature change, it may turn the lock signal off. In this case, turn the lock on before proceeding with the analysis. Use the **go** command to initiate acquisition.

Special Notes: np is the number of points in the  $t_2$  dimension,  $n_1$  is the number of points in the  $t_1$  dimension.

### Manual Setup for DEPT (Distortionless Enhancement Polarization Transfer)

First, setup for a routine carbon-13 experiment, type **nt=1** and **zg** to collect a single-scan spectrum. This will set the receiver gain. Next type **DEPT** and hit enter. Subsequent adjustments of d1 and nt can be applied to the DEPT analysis at this point. Use the **go** command to initiate acquisition.

### Fluorine-19 and Phosphorus-31 NMR Spectroscopy

To prepare a sample for  $^{19}\text{F}$  or  $^{31}\text{P}$  NMR analysis, dissolve 10 to 20 mg of sample in approximately 0.6 mL of deuterated solvent. Perfluorobenzene ( $\text{C}_6\text{F}_6$ ), referenced to Freon 11 ( $\text{CFCl}_3$ ) as -163.0 ppm, is an often used standard for fluorine-19 analyses.  $\text{H}_3\text{PO}_4$ , referenced as zero ppm, is the customary standard for phosphorus-31 analyses.

The simplest means of referencing a compound is to add a trace of the appropriate standard directly to the sample. However, if the standard is not miscible in the analysis solvent, or, if in the case of phosphorus-31 analysis, the compound to be analyzed is acid sensitive, the standard may be isolated in a specially-designed, coaxial insert tube.

After locking and shimming, select **[Nucleus, Solvent]**, select **[F19]** for fluorine-19 or **[P31]** for phosphorus-31, and then select the solvent from the subsequent option display. See *Table 2* for the commands with which to access [Other] solvents. Alter the number of transients, nt, as needed to achieve the desired quality of spectra. The **Time** command can be used to prompt the display to provide a time estimate for a given number of transients.

For [F19] analysis, the command zg will initially prompt an error message stating "P.S.G. Aborted." At the bottom of the screen, the error will read "oversamp \* sw > 100000.000000 Hz". In this case, the default sweep width, which is set at 50000, is problematic. Use the command format **sw=50200** to alter the sweep width by plus or minus 200. A subsequent command of zg should successfully initiate acquisition.

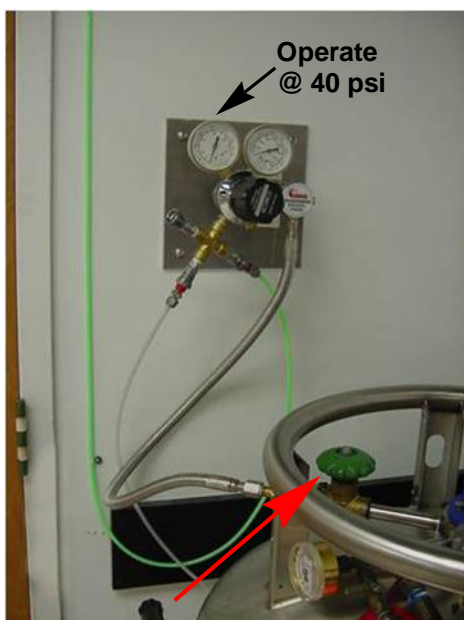
## Section 5: Operations for Collecting Spectra at Variable Temperatures

This guide is a supplement to training, not a substitute. **DO NOT attempt to run Variable Temperature NMR Experiments without training authorized by Dr. Sankar.** Carefully follow instructions and keep a vigilant eye on the instrument status window at all times when operating below or above room temperature. The \$40,000 to \$45,000 NMR probes are fragile and easily damaged. You are responsible for ensuring not only that you do not make a mistake, but also that all components of the system are operating properly. **Notice: Under no circumstance are NMR users allowed to reboot the computer!**

### Low Temperature Analysis

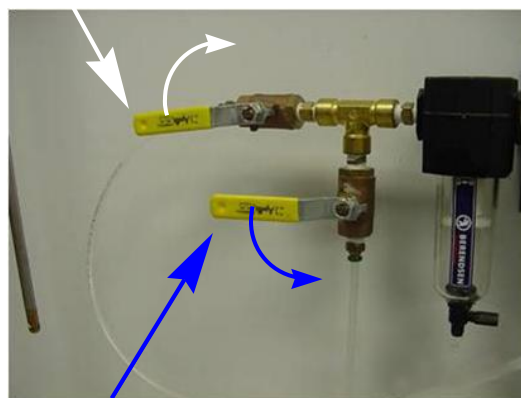
Do not assume nitrogen will be available at all times. Plan ahead! Consult with Dr. Sankar several days in advance if you intend to run low temperature analyses.

- Lock and shim at room temperature. [A lock level setting of 70 to 80% is optimum.]
- Select **[Setup]**.
- Make the appropriate **[Nucleus, Solvent]** selections.
- Switch from air to nitrogen by following the three steps illustrated below:



Step 1: Open the N<sub>2</sub>-tank valve leading to the regulator.

Step 2: Close the air line leading to the coil.



Step 3: Open the N<sub>2</sub> line leading to the coil.

- Type **temp=-20 su** and hit enter to flush the coil with nitrogen. [This simply opens the valve. Because the coil is not yet submerged in liquid nitrogen, the temperature will not change.]
- Flush for a minimum of 20 minutes, longer on a humid day. [The system must be purged with nitrogen to flush moisture from the line before beginning a low temperature experiment. Otherwise, ice may plug the coil, inhibiting the flow of nitrogen, leading to temperature fluctuations.]
- Add liquid nitrogen to the dewar. [For lengthy analyses at -30 to -40 °C, add enough liquid to immerse half the coil. For lengthy analyses at -50 to -80 °C add enough liquid to fully immerse the coil. Failure to properly immerse the coil may result in uncontrollable temperature variability.]
- Once the temperature settles at -20 °C, re-optimize the lock level by adjusting the lockpower and/or lockgain, and then re-shim the magnet.
- Lower the temperature, re-optimize the lock, and re-shim the magnet in increments of 20 °C. [**-80 °C is the low temperature limit: DO NOT set for less than -80 °C!** Also be mindful not to set the temperature below the freezing point of the solvent, listed in *Table 1*. The sample may not spin at very low temperature. If it does not spin, do not re-shim.]
- Wait at least 10 minutes after reaching the desired temperature and then proceed with the analysis.
- To bring the sample back to room temperature, type **temp=25 su** and hit enter.
- Leave the sample loaded until the outside of the line leading from the coil to the probe has completely de-iced. [**DO NOT attempt to manually remove the ice: doing so could easily damage fragile probe components. Instead, patiently wait for the ice to melt.**]
- Once the line has de-iced, type **e** and hit enter to eject the sample. While retaining the sample tube holder, type **i** and hit enter – as if to load a sample, but without doing so – in order to turn off the ejection air flow.
- Very slowly remove the dewar. [**As the nitrogen inside the coil warms and expands, it will vent through the ejection tube, which is why it is imperative that you not insert the sample tube holder with the standard yet.**]
- Wait 10 to 20 minutes until the coil has completely de-iced and then type **temp='n' su** and hit enter to turn VT off.
- Type **e** and hit enter, to turn the ejection air flow on again. Place the sample tube holder, with the standard, back in the loading tube. Type **i** and hit enter to return the standard to the NMR.
- Check the display to make sure VT is off.
- Switch back from nitrogen to air by performing the three steps illustrated on the previous page in reverse.

**Special Note:** The recommended temperature sequence for a series of analyses, spanning a range from below to above room temperature, is from low to high. Unless the nitrogen tank is nearly empty, it is not necessary to switch back from nitrogen to air until you have completed the high temperature analyses as well.

## High Temperature Analysis

**Warning!!** Carefully watch the temperature status reading while operating at high temperature. Going 1 or 2 °C above the target temperature is typical. However, if there is a malfunction, such as the tank running out of nitrogen, the temperature may continue increasing. If the temperature goes 5 °C above the target setting, there is a problem and you must quickly take corrective action to protect the probe. If the command **temp='n' su** fails to stop the temperature from increasing, turn the heater off at the Temperature Control Unit pictured below. Leave the switch in the off position and notify Dr. Sankar of the malfunction.



Open the cabinet. Flip the switch to the off position and leave it there to turn the heater off manually.

### Model L900 Temperature Controller

- Lock and shim at room temperature. [A lock level setting of 70 to 80% is optimum.]
- Select **[Setup]**.
- Make the appropriate **[Nucleus, Solvent]** selections.
- Type **temp=40 su** and hit enter to turn VT on and set the temperature to 40 °C.
- Re-optimize the lock level and re-shim the magnet at 40 °C.
- Increase the temperature, re-optimize the lock, and re-shim the magnet, in increments of 20 °C. **[100 °C is the high temperature limit: DO NOT set for greater than 100 °C! Also take care not to exceed the boiling point of the solvent, listed in Table 1.]**
- Wait at least 10 minutes after reaching the desired temperature and then proceed with the analysis.
- Type **temp='n' su** and hit enter to turn VT off.
- The sample will need to cool to approximately room temperature before the software will allow sample ejection.

**Table 1: Freezing & Boiling Point of Deuterated Solvents**

**Warning: Do not attempt analyses below -80 °C or above 100 °C as such extreme temperatures will damage the probe!**

Solvent	Freezing Point	Boiling Point
Acetic Acid-d <sub>4</sub>	15 °C	> 100 °C
Acetone-d <sub>6</sub>	< -80 °C	55 °C
Acetonitrile-d <sub>3</sub>	-45 °C	80 °C
Benzene-d <sub>6</sub>	7 °C	79 °C
Chloroform-d	-63.5 °C	60 °C
Cyclohexane-d <sub>12</sub>	7 °C	80 °C
Deuterium Oxide	3.8 °C	> 100 °C
1,2-Dichlorobenzene-d <sub>4</sub>	-17 °C	> 100 °C
1,2-Dichloroethane-d <sub>4</sub>	-35 °C	83 °C
Diethyl-d <sub>10</sub> Ether	< -80 °C	34 °C
N,N-Dimethylformamide-d <sub>7</sub>	-61 °C	> 100 °C
Dimethyl Sulfoxide-d <sub>6</sub>	19 °C	> 100 °C
1,4-Dioxane-d <sub>6</sub>	12 °C	99 °C
Ethanol-d <sub>6</sub>	< -80 °C	78 °C
Methanol-d <sub>4</sub>	< -80 °C	64 °C
Methylene Chloride-d <sub>2</sub>	< -80 °C	39 °C
Nitrobenzene-d <sub>5</sub>	6 °C	> 100 °C
Nitromethane-d <sub>3</sub>	-29 °C	100 °C
Pyridine-d <sub>5</sub>	-42 °C	> 100 °C
Tetrahydrofuran-d <sub>8</sub>	< -80 °C	65 °C
Toluene-d <sub>8</sub>	< -80 °C	> 100 °C
Trifluoroacetic Acid-d	-15 °C	75 °C

**Table 2: Commands for Access to Standard Solvent Parameters**

The **[Nucleus, Solvent]** submenu displays selection options from which to access standard parameters for the five most commonly used solvents: **[CDCl<sub>3</sub>]**, **[D<sub>2</sub>O]**, **[Benzene]**, **[DMSO]**, and **[Acetone]**. Standard parameters for all other solvents have to be accessed by selecting **[Other]** and typing in the appropriate solvent command following the "Enter Solvent:" prompt. Some solvents have more than one command with which these parameters can be accessed, as listed below:

Solvent	Command(s)	Solvent	Command(s)
Acetic Acid-d <sub>4</sub>	CD3COOD or Acetic_Acid	Dimethyl Sulfoxide-d <sub>6</sub>	DMSO
Acetone-d <sub>6</sub>	CD3COCD3 or Acetone	1,4-Dioxane-d <sub>8</sub>	Dioxane
Acetonitrile-d <sub>3</sub>	CD3CN or CH3CN	Ethanol-d <sub>6</sub>	CD3CD2OD or Ethanol
Benzene-d <sub>6</sub>	C6D6 or Benzene	Methanol-d <sub>4</sub>	CD3OD or CH3OH or Methyl_Alcohol-d4
Chloroform-d	CDCl3 or Chloroform	Methylene Chloride-d <sub>2</sub>	CD2Cl2 or MethyleneChloride
Cyclohexane-d <sub>12</sub>	C6D12 or Cyclohexane	Nitrobenzene-d <sub>5</sub>	Nitrobenzene
Deuterium Oxide	DeuteriumOxide	Nitromethane-d <sub>3</sub>	CD3NO2
1,2-Dichlorobenzene-d <sub>4</sub>	ODCB	Pyridine-d <sub>5</sub>	Pyridine
1,2-Dichloroethane-d <sub>4</sub>	C2D4Cl2 or CD2ClCD2Cl or Dichloroethane	Tetrahydrofuran-d <sub>8</sub>	THF
Diethyl-d <sub>10</sub> Ether	Ethyl_Ether	Toluene-d <sub>8</sub>	C6D5CD3 or Toluene
N,N-Dimethyl-formamide-d <sub>7</sub>	DMF	Trifluoroacetic Acid-d	TFA

The command `cat('/vnmr/solvents')` will list the solvents recognized by the software.

**Table 3: Comprehensive Reference Chart  
of Solvent Chemical Shifts**

<i>Solvent</i>	$\delta^1\text{H}$ (ppm) (multiplicity)	<i>J</i> <i>H</i> <i>D</i> (Hz)	$\delta$ Carbon-13 (ppm) (multiplicity)	<i>J</i> <i>C</i> <i>D</i> (Hz)	$\delta$ of <i>HOD</i> (ppm)
Acetic Acid-d <sub>4</sub>	11.65 (1) 2.04 (5)	2.2	178.99 (1) 20.0 (7)	20	11.5
Acetone-d <sub>6</sub>	2.05 (5)	2.2	206.68 (1) 29.92 (7)	0.9 19.4	2.8
Acetonitrile-d <sub>3</sub>	1.94 (5)	2.5	118.69 (1) 1.39 (7)	21	2.1
Benzene-d <sub>6</sub>	7.16 (1)		128.39 (3)	24.3	0.4
Chloroform-d	7.24 (1)		77.23 (3)	32.0	1.5
Cyclohexane-d <sub>12</sub>	1.38 (1)		26.43 (5)	19	0.8
Deuterium Oxide	4.80 (DSS) 4.81 (TSP)		NA	NA	4.8
1,2-Dichloroethane-d <sub>4</sub>	3.72 (br)		43.6 (5)	23.5	
Diethyl-d <sub>10</sub> Ether	3.34 (m) 1.07 (m)		65.3 (5) 14.5 (7)	21 19	
N,N-Dimethyl formamide-d <sub>7</sub>	8.03 (1) 2.92 (5) 2.75 (5)	1.9 1.9	163.15 (3) 34.89 (7) 29.76 (7)	29.4 21.0 21.1	3.5
Dimethyl Sulfoxide-d <sub>6</sub>	2.50 (5)	1.9	39.51 (7)	21.0	3.3
1,4-Dioxane-d <sub>8</sub>	3.53 (m)		66.66 (5)	21.9	2.4
Ethanol-d <sub>6</sub>	5.29 (1) 3.56 (1) 1.11 (m)		56.96 (5) 17.31 (7)	22 19	5.3
Methanol-d <sub>4</sub>	4.87 (1) 3.31 (5)	1.7	49.15 (7)	21.4	4.9
Methylene Chloride-d <sub>2</sub>	5.32 (3)	1.1	54.00 (5)	27.2	1.5
Nitrobenzene-d <sub>5</sub>	8.11 (br) 7.67 (br) 7.50 (br)		148.6 (1) 134.8 (3) 129.5 (3) 123.5 (3)	24.5 25 26	
Nitromethane-d <sub>3</sub>	4.33 (5)	2	62.8 (7)	22	
Pyridine-d <sub>5</sub>	8.74 (1) 7.58 (1) 7.22 (1)		150.35 (3) 135.91 (3) 123.87 (5)	27.5 24.5 25	5
Tetrahydrofuran-d <sub>8</sub>	3.58 (1) 1.73 (1)		67.57 (5) 25.37 (5)	22.2 20.2	2.4-2.5
Toluene-d <sub>8</sub>	7.09 (m) 7.00 (1) 6.98 (5) 2.09 (5)	2.3	137.86 (1) 129.24 (3) 128.33 (3) 125.49 (3) 20.4 (7)	23 24 24 19	0.4
Trifluoroacetic Acid-d	11.50 (1)		164.2 (4) 116.6 (4)		11.5

(DSS) denotes chemical shift relative to 2,2-dimethyl- 2-silapentane- 5-sulfonic acid, sodium salt. (TSP) denotes chemical shift relative to 3-(trimethylsilyl)- propionic acid-d<sub>4</sub>, sodium salt. All other chemical shift values are relative to tetramethylsilane (TMS). These values were compiled from the NMR Solvent Tables of **Cambridge Isotope Laboratories** and **Numare Spectralab Inc.**, with deference to the former.

## List of Useful Varian NMR Software Commands

<b>aph</b>	Automatically corrects zero- and first-order phasing
<b>aph0</b>	Corrects zero-order phasing only (use on single-peak spectra)
<b>axis='h'</b>	Changes axis to Hertz
<b>axis='p'</b>	Changes axis to ppm
<b>bs=64</b>	Changes block size to <i>64 transients</i> (data can be transformed every time a block-size increment of transients is reached)
<b>cd</b>	Changes the directory back to the default home directory
<b>ctext</b>	Clears previous text entry
<b>cz</b>	Clears all integral reset points
<b>d1=5</b>	Changes the delay time between scans, to <i>5 seconds</i> for instance
<b>dc</b>	Corrects drift, which occasionally effects the accurate of integrations
<b>dg</b>	Displays the original text screen of group parameters
<b>dli</b>	Displays a list of integrals
<b>dll</b>	Displays a list of peak lines
<b>dpf</b>	Displays the frequency of peaks that are above the Threshold setting
<b>dpir</b>	Displays integrals on the spectrum (must be preceded by <b>vp=12</b> )
<b>ds</b>	Displays spectrum (use to remove traces of previous spectra or to clear the display of peak frequencies, integrals, etc.)
<b>dsn</b>	Displays the signal-to-noise ratio (left click on the peak to mark it with a cursor and use the command <b>nl</b> to center the cursor at the top first)
<b>e</b>	Ejects the sample from loading tube
<b>exit</b>	Exits the Varian NMR software program
<b>ft</b>	Fourier transforms the data (no weighing function)
<b>fn=48000</b>	Sets the fourier number, to <i>48,000</i> in this case (must be followed by <b>wft</b> )
<b>getshim</b>	Loads pre-programmed shim parameters that are a good starting point for further adjustment
<b>i</b>	Inserts the sample into the loading tube
<b>lb=1</b>	Applies line broadening of <i>1 Hertz</i> for instance (must be followed by <b>wft</b> )

<b>movesw</b>	Adjusts the sweep width to the region enclosed by cursor lines (for improved resolution, re-adjust the number of points ( <b>np</b> ) afterwards)
<b>nl</b>	Centers the cursor on top of the nearest peak
<b>np=24000</b>	Sets the number of points, to <i>24,000</i> for instance (record np from the parameter list before adjusting the sweep width and use approximately that figure as the reset value for the number of points)
<b>nt=32</b>	Sets the number of transients to <i>32</i>
<b>page</b>	Sends all preceding plot commands to the printer
<b>pap</b>	Plots all parameters
<b>pir</b>	Plots integral regions (must be preceded by <b>vp=12</b> )
<b>pl</b>	Plots spectrum
<b>pll</b>	Plots line list in ppm and Hertz (use <b>pll page</b> to plot a peak frequency list)
<b>pltext</b>	Plots text (the commands <b>pap</b> or <b>ppa</b> plot the text automatically)
<b>ppa</b>	Plots a partial list of parameters
<b>ppf</b>	Plots frequency of peaks that are above the Threshold setting
<b>pscale</b>	Plots the axis scale
<b>pw=90?</b>	Displays the value of a 90 degree pulse width
<b>pw= 17.5</b>	Sets the pulse width, to <i>17.5 microseconds</i> as an example
<b>svf('XYZ')</b>	Saves data in a file, named <i>XYZ</i> for instance
<b>sw= 1200</b>	Sets sweep width, to <i>1200</i> for instance
<b>text</b>	Creates lines of customized text (use the format <b>text('Novak Group\Project 7')</b> to add two lines of text)
<b>time</b>	Displays an estimate of run time given the current parameter settings
<b>vp= 12</b>	Moves the vertical position of the plot up by <i>12 mm</i> (must precede <b>pir</b> or <b>dpir</b> commands to create space below the plot for integral values)
<b>vs= 160</b>	Sets the vertical scale, to <i>160</i> as an example (the default setting is 200)
<b>vsadj</b>	Optimizes the vertical scale to the maximum value that will fit the most intense peak on the display
<b>wft</b>	Fourier transforms the data with weighing
<b>zg</b>	Zero and go (begins the experiment)
<b>zg wexp('svf('XYZ'))</b>	Begins experiment and saves data to any pre-[Set Directory]